

City Research Online

City St George's, University of London

Citation: Charlwood, F. J. (1971). The development of a systems engineering design method, and its application to a nuclear reactor. (Unpublished Doctoral thesis, The City University)

This is the accepted version of the paper.

This version of the publication may differ from the final published version. To cite this item please consult the publisher's version.

Permanent repository link: https://openaccess.city.ac.uk/id/eprint/38575/

Copyright and Reuse: Copyright and Moral Rights remain with the author(s) and/or copyright holders. Copies of full items can be used for personal research or study, educational, or not-for-profit purposes without prior permission or charge, unless otherwise indicated, provided that the authors, title and full bibliographic details are credited, a hyperlink and/or URL is given for the original metadata page and the content is not changed in any way. For full details of reuse please refer to City Research Online policy.

City Research Online: http://openaccess.city.ac.uk/ publications@citystgeorges.ac.uk

THE CITY UNIVERSITY, LONDON

DEPARTMENT OF SYSTEMS AND AUTOMATION

The Development of a Systems Engineering Design Method, and its Application to a Nuclear Reactor.

A report submitted for the degree of Doctor of Philosophy.

THE CITY UNIVERSITY LIBRARY
ST. JOHN STREET, LONDON, E.C.1.

F. J. CHARLWOOD

SEPTEMBER 1971

65768

SUMMARY

The development of a design method for systems which must attempt to satisfy a variety of possibly conflicting objectives relating to different aspects of performance at different stages in the life cycle is described. A review of the development of systems engineering (the basis of the design method), a statement of the systems engineering concept and definitions of the terminology are given as an introduction.

A specific problem is used in the development of the method, termed the design-control problem, in which the system must aim at objectives based on the construction cost, dynamic performance and static performance. A specific application is also used, the optimal design of a nuclear power station, this being of the size and complexity of problems encountered in practice.

The problem and design objectives are defined, mathematical models of the system which are used in the design optimisation and their means of solution are described. An outline of the techniques used in combining the various design objectives to form an overall design utility function, precedes the derivation of the utility function for the reactor problem. The utility function is related to the design parameters via the models, and the procedure used to maximise the expected utility by adjustment of parameters is described.

Finally, the results of the optimisation are presented and discussed, and in conclusion an analysis of the design method, its merits and shortcomings is made, with suggestions as to how improvements and additions could be effected.

CONTENTS

		Page
NOTES ON LAYOUT AND NOTATION		3
1.	INTRODUCTION	
1.1	The Development of Systems Engineering	5
1.2	The Systems Engineering Method	7
1.3	Aims of the Present Work	10
2.	THE PROBLEM	
2.1	The General Design-Control Problem	13
2.2	The Nuclear Reactor Problem	14
3.	DESCRIPTION OF THE REACTOR	
3.1	Nuclear Physics	20
3.2	The S.G.H.W.R.	28
3.3	Reactor Controls	33
4.	PLANT MODELS, THEIR SIMULATION AND SOLUTION	
4.1	Dynamic Model	39
4.2	Static Model	54
4.3	Cost Model	63
5.	FORMULATION OF UTILITY FUNCTIONS AND CONSTRAINTS	
5.1	General Principles	65
5.2	Constraints	70
5.3	Utility Functions for the Reactor	72
6.	OPTIMISATION PROCEDURE	
6.1	Principles of Optimisation	87
6.2	The Procedure Adopted	90
7.	RESULTS	
7.1	Presentation of Results	96
7.2	Discussion of Results	109
8.	CONCLUSIONS	114
ACKNOWLEDGEMENTS		122
REFERENCES		123
APPENDICES		
1.	S.G.H.W.R. System Parameters	127
2.	S.G.H.W.R. System Variables	130

Page

APPENDICES (continued)

3.	S.G.H.W.R. Non-linear Dynamic Model	132
4.	S.G.H.W.R. Linear Dynamic Model	137
5.	S.G.H.W.R. Static Model (Additional Equations)	150
6.	S.G.H.W.R. Cost Model	153
7.	Sensitivity Chart	154
8.	Computer Programmes	156
9.	Optimal Controller Design for the S.G.H.W.R.	164
10.	Analog Computer Patching Diagram and Potentiometer Coefficients	174
11.	Limits on the Use of Sensitivity Coefficients in the Assessment of Pole or Zero Locations	182
12.	Nuclear Properties of Materials used in the S.G.H.W.R.	186

Notes on Layout and Notation

1.	References.	References are indicated by two numbers separated by a stop within parenthesis, thus - (1.1).
2.	Figures.	Figures are contained on separate sheets, text on these sheets refers to the figure only.
3.	Notation.	A list of symbols used in the text follows. These do not include the design parameters and variables of the nuclear reactor which are listed in Appendix 1 & 2, or the gains of the linear dynamic model listed in Appendix 4, Prefixes, subscripts and super-scripts do not appear in the list, but are defined in the text as they occur. Some duplication of symbols occurs, the symbol is then re-defined in the text before it is used.

Notation

A, B, C, D.	matrices defining the general linear dynamic model.
$\underline{c}$	system constants
c	velocity of light
e	fuel enrichment
E	kinetic energy
f	thermal neutron utilisation factor
G	gains
k , K	constants or gains
K_{eff}, δk	effective and excess reactivity
l	neutron escape rate
M	mass
N	numbers of atoms
n, m	integers defining dimensionality of system
$\underline{o}$	system objectives
$\underline{p}$	the system parameters
p	resonance escape probability, probability in general
P	system poles

Notation (continued)

$\underline{P}$	system performances
s	surface area
S	Laplace operator, sensitivity coefficients
T	temperature, final time
t	time
U	overall utility
u	category utilities
$\underline{u}$	system inputs
V	volume
v	system values
w	within category weightings
W	between category weightings
x	proportion of S.G.H.W.Rs. in the plant mix
$\underline{x}$	system variables
Z	system zeroes
δ, Δ	increments
ζ	damping ratio
ε	fast fission factor
η	neutron multiplication factor
λ, μ	functions used in estimating resonance escape probability
ξ	logarithmic energy decrement per collision
σ Σ	microscopic and macroscopic cross sections
τ	time constants
ω_n, ω_d	natural and damped natural frequencies

1. INTRODUCTION

1.1 The Development of Systems Engineering

The concept of total system design is not new, Bertalanffy (1.1) traces the history of such ideas and shows that by the 1920's several authors had laid down the fundamentals of systems theory. It was not until the Second World War, however, that application of the theories in the engineering field began, and systems engineering was born. During this period of rapid advancement of weapon technology, great urgency and economic pressure, the traditional 'free enterprise' method of weapon development by individual companies proved inadequate. The production of competitive designs from which the services could take their pick was far too extravagent. It became necessary for the services to be aware of exactly what was required, and for the manufacturers to gear themselves for its development and production, in a situation where materials and manpower were at a premium. A good example of this is the way the Merlin aero engine was produced in plants throughout the country, and used in all types of aircraft, from Spitfire to Mosquito to Lancaster.

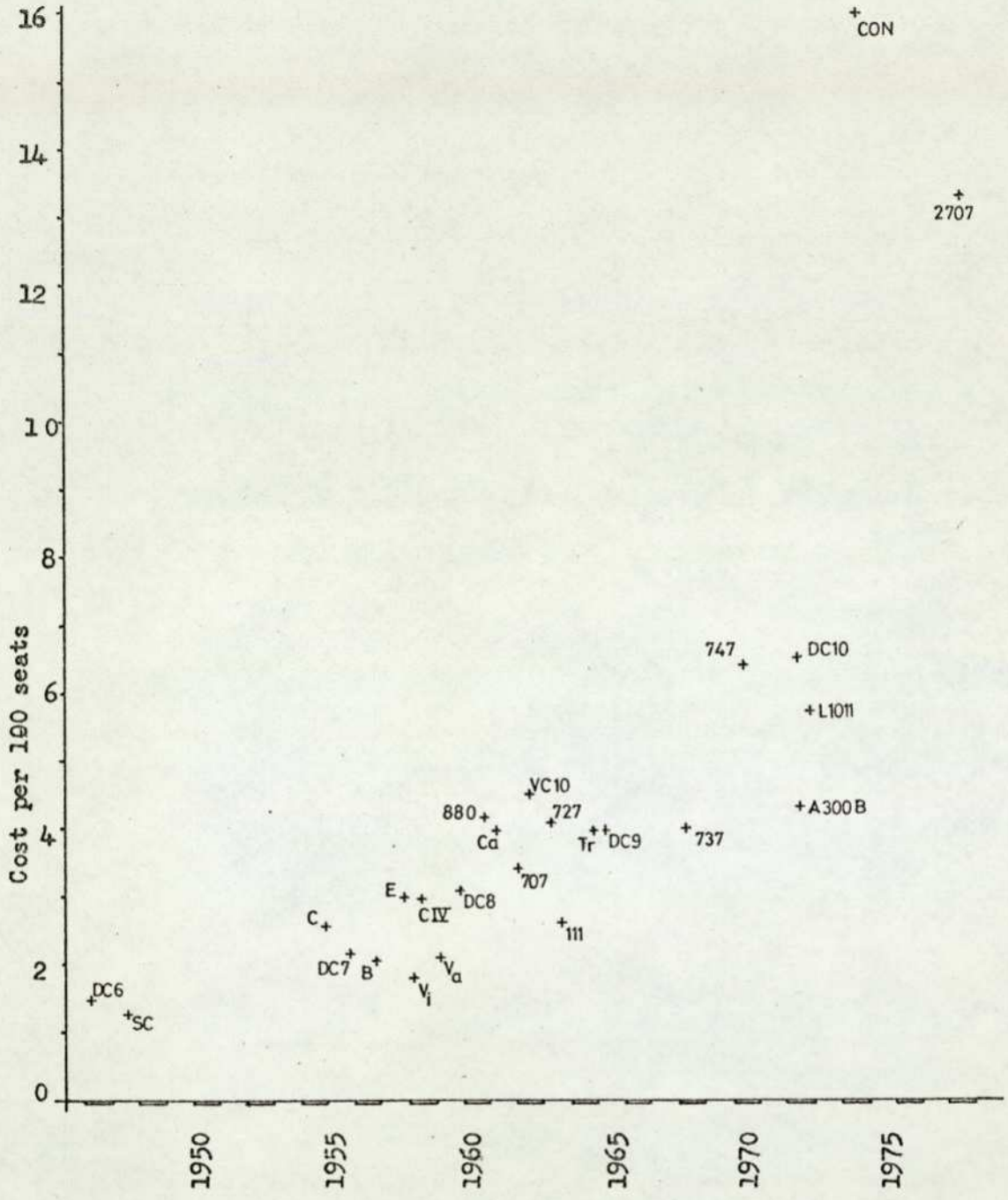
The integrating policy went beyond just hardware, for as this became more complex and the cost of 'backup' increased, the need for a more closely controlled spares, servicing and training facility was apparent. Maintenance schedules had to be arranged to give maximum utilisation of equipment. Recruitment and training had to be planned, to ensure that a complement of men were available to operate the new weapons.

The war, however, was by no means a division between ignorance and knowledge of the systems approach, indeed, the majority of those involved at the time were probably ignorant of the term. After the war much remained of the old methods, the 'V' bombers and the Hunter and Swift fighters were developed competitively for service orders. Increasing application of advanced technology and the consequent rise in development costs, however, soon made it apparent in the military field, and later the civil field, that a careful analysis of requirments and formulation of a specification were necessary before embarking on any new major project. Figure 1.1 illustrates the effect on cost of the continual application of advanced technology. The purchase price of civil aircraft per 100 passenger seats is shown for types produced or proposed between 1945 and 1980. Escalation effects are cancelled to some extent by the larger sizes which should keep the cost per seat down. (This data

7 →

Figure 1.1

Purchase price of civil aircraft in millions of dollars per 100 seats, plotted against date of introduction.



Types

SC Stratocruiser	E Electra
C Constellation	CIV Comet 4
B Britannia	Ca Caravelle
Vi Viscount	Tr Trident
Va Vanguard	Con Concorde

and the histories of Concorde and Tristar are powerful evidence for the need of a systems study.)

A spur to the development of systems engineering came in the 1960's when powerful digital computers became generally available. Where previously the analysis of a proposed system could only be undertaken in a cursory manner, now the computer could be used for a thorough and detailed analysis. Reliable and accurate predictions of system performance could be made, whereas previously only a guide could be established. Use of computers was not, however, without its problems; systems had to be described in a way the computer could understand, and more precisely than was necessary for manual analysis. Techniques had to be developed, and have still to be, which enable computers to take decisions which a man can take from experience, intuition or hunch. To a large extent these techniques are based on algorithms or theories known for many years, but which were inapplicable or restricted before the computer, linear programming is a typical example.

Problem analysis no longer being the limitation it once was, the barriers to the wider application of systems engineering are the education of the designers of the future in the systems method and its tools, and the breakdown of the old design procedures. Interest is spreading from the areas where systems engineering was first applied and has a foothold, predominantly in the military and aerospace fields, to the more conservative areas of industry.

1.2 The Systems Engineering Method

The preceding section outlined the development of systems engineering without actually defining it, except to say that it was based on a philosophy of looking at a problem in the broadest possible terms. Before describing the systems engineering method, it is appropriate to define a system and systems engineering. There are variations in the definition of a system (1.1 - 1.5) but the following is representative

> System - A set of interacting units within a stated boundary assembled to perform some definite function.

The manner in which the units are assembled is defined by the system structure, the dimensions and other physical properties of the units are defined by the system parameters ($\underline{p}$) and the state of the system is defined by the system variables ($\underline{x}$), pressures,

temperatures, etc. Mathematical equations based on the conservancy of mass, energy and momentum defining the relationships between the system variables are the system models. The structure of the equations is determined by the system structure, and their coefficients are functions of the system parameters. An open system exists within an environment which may be defined as -

Environment - All that is external to the system and which affects the system or is affected by it.

It is the environment which initially creates the need for a system, and which supplies the system objectives (o) and inputs (u). It is on the basis of benefit to the environment (meeting the objectives) that the system's worth will be judged. The environment determines system constants (c) which are functions of nature, and will also place certain constraints upon the system parameters and variables, again a result of nature.

The system and environment, having been defined, it now remains to define systems engineering -

Systems Engineering - The design of complete systems so that the system's performance, over its life cycle, is most effective in meeting stated objectives.

To analyse a system over its entire life cycle, it is necessary to include at the very minimum the research, design, development, manufacture, operation and disposal stages. It is convenient to sub-divide the objectives into categories, each containing one or more objectives. Each of the stages outlined above will be associated with objectives in one or more categories. The system performances (P) are functions of the variables which are used as a measure of the system in meeting the objectives. There will be a performance associated with each objective. The values (v) are scalers which define the merit of the performances in meeting the objectives. Values summed within objective categories are category values. System utility (U) is the weighted sum of all category values, and it is this which is maximised to produce an optimum system design by adjustment of the parameters (and more generally the system structure). Utility may be referenced to a monetary scale, but it is more usual to use an arbitrary dimensionless scale in the formulation of the utility function.

To be more specific about objectives, performance and value, consider the manufacturing stage of the system life cycle. Here

the objectives will be a function of the total cost and completion date, and the performances relating to these are construction cost (forming a part only of the total cost) and construction time. Values will be functions of these performances, perhaps a straight negation in the case of cost, and a zero value for time until a certain date is approached then a sharp cut off. During the operational stage the objectives will be concerned with static performance (efficiency, product quality, etc.), dynamic performance (response, stability, etc.) and running and maintenance costs. The life cycle may include a commissioning stage in which debugging and personnel training would contribute to utility (negatively). Finally, there are the less tangible contributions to utility, such as penalties for waste discharge or use of farmland, and a value for flexibility in case of a specification change in the future.

In calculating the weighting factors used in combining the values for each objective category to form overall utility some common reference is needed. This is normally financial (money is merely a convenient scale on which to relate values of otherwise imcomparable objects), and in estimating weighting factors values must be combined on a present worth basis to allow for interest on borrowed capital and inflationary tendencies on the prices of raw materials and products.

Utility as defined will be a function of the performances of the system, that is (effectively) a function of the variables. The design is optimised by adjustment of the parameters and it remains therefore to define the variables in terms of the parameters, which is achieved by the formulation and solution of the system models. There will be a number of models for each system, their relative importance depending upon the type of system and the formulation of the utility function. For example, in an aircraft the dynamic and reliability models are of high importance, whereas in a chemical plant the static performance model is of greater significance. The required model accuracies will be determined by the relative contributions made by the solution of the various models to overall utility.

Summarising, the systems engineering method may be considered in four stages -

(a) Define the problem, select the objectives and formulate the utility function.

(b) Synthesise the system and formulate models.

(c) Analyse and solve the models to relate utility to the system parameters.

(d) Optimise the system by adjustment of the parameters.

In practice it is not possible to express utility explicitly in terms of the parameters as suggested by the list, and an iterative optimising procedure has to be adopted. This is illustrated by the flow diagram shown in Figure 1.2. Variations of this diagram appear in the literature but basically they express the same ideas (1.3, 1.6, 1.7).

In implementing a systems engineering design mathematical tools are borrowed from other disciplines; decision theory, reliability theory, linear and non-linear optimisation methods and other O.R. techniques. (O.R. may, in fact, be considered a subset of systems engineering as it optimises the operation of an existing system.) The conventional methods of static and dynamic analysis of engineering systems are required, and finally some statistical theory is needed as the utility functions will contain many terms based on predicted future events about which there is considerable uncertainty. An expected value of utility is then used in design optimisation.

1.3 Aims of the Present Work

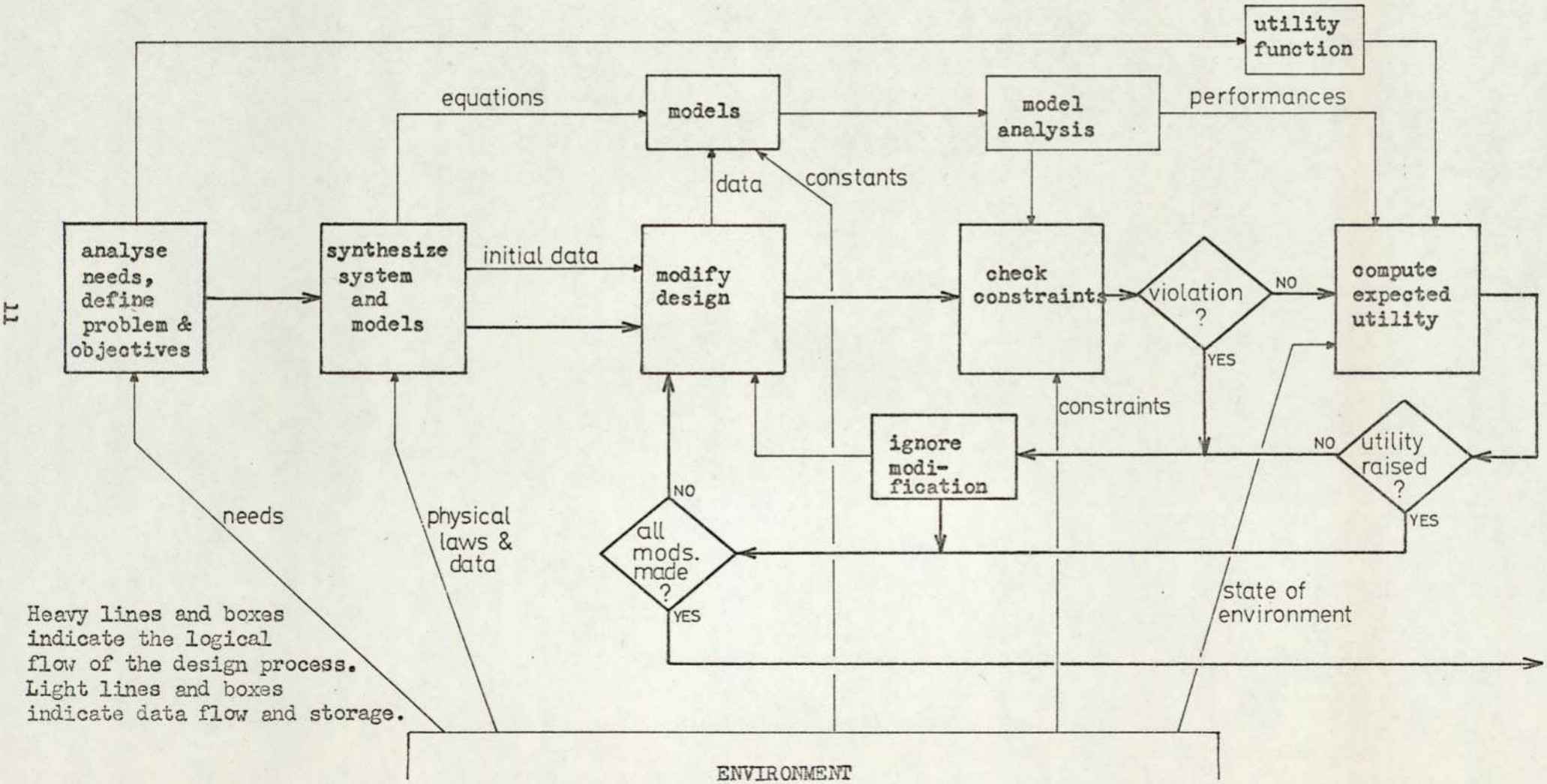
The present research aims to develop a systems based design method for a class of problem, termed the design-control problem, which arises in all sizes of system from instrumentation to chemical plant. It concerns the design of any system which has design objectives under the static performance, dynamic performance and cost categories, with normally more than one objective in each category. The problem is somewhat restricted in that it concerns only the manufacture and operation stages of the system life cycle, and only three of many possible objective categories. It is proposed, however, to formulate the design method in a general manner, so that it may be used as a 'package' for any problem, the user supplying certain blocks defining the system and the utility functions. The method will also be flexible so that other categories of system objective may be added at a later date, e.g. to cover startup or reliability criteria.

The aim is to show that the various design criteria can be assigned values and related to each other in a meaningful way; that uncertainties concerning future events may be included in the design evaluation, and that computer techniques may replace the design optimisation process which has previously been largely intuitive. Not least is the aim to show that the criteria traditionally adopted to design optimal control systems, mainly for reasons of ease of

12 →

Figure 1.2

The systems engineering design process.



solution, can be replaced by more meaningful criteria, which may also be related to the other design objectives.

The work is the first stage of the implementation of the systems design procedures described by Professor M'Pherson (1.6 & 1.7). It is a prerequisite that the implementation should be applicable to real systems. To ensure this the problem chosen to develop the method is of a size and complexity representative of that met in practical situations.

The following five sections follow broadly the steps outlined in section 1.2 (page 9) as the stages of a systems engineering study. The problem and the objectives are described in section 2, although formulation of the utility functions is delayed until section 5 after a description of the plant and models. Section 3 describes the system, it having already been synthesised, and section 4 describes the system models and their solution. The optimisation procedure is described in section 6.

2. THE PROBLEM

2.1 The Plant Design - Control Problem

Despite statements made above that a systems design method should be all embracing, it was necessary to be a little more restrictive choosing a problem for the development of the method. The problem selected was the optimal design of a plant and its controllers with respect to the many and various criteria relating to its cost and performance (in its widest sense). This has been called the Plant Design - Control Problem, although Plant Design - Dynamics Problem might be more accurate. Too much stress should not be placed on 'plant' as the method will be equally applicable to instrument systems. This particular sub unit of the total system design was selected because of the control interest of the Department of Systems and Automation, and because analysis and evaluation of dynamics and controller design will be one of the most difficult areas in the total system design of a multivariable plant.

It has been common practice in designing control systems for process plant to represent the plant as a fixed unit, designed to meet specified static operating conditions and engineering constraints. In this case the control engineer is required to conceive a control system which enables the plant to be operated with stability at the required conditions, and to respond satisfactorily to any changes demanded of it. There are obvious limitations to this procedure, because unfavourable dynamic characteristics may be designed into the plant, and these are difficult or impossible to overcome by control action. The result could be a final plant with poor stability or response, or a complicated and expensive control system to compensate for inherently poor dynamics, or both. A slow corrective feedback exists, based on experience of previous similar plants, and in the chemical and petroleum industries codes were compiled for the sizing of pressure vessels and other components affecting plant dynamics on this basis.

In areas where there is a high interaction between static and dynamic ability, as in aircraft and other high performance vehicles, the division between static and dynamic design broke down as the slow feedback based on experience of previous types proved inadequate. Increasingly this is becoming the case in the process and power generation industries, with their increasing rate of innovation and trends towards larger and integrated - and hence more interactive - plants. These, in addition to higher costs, demands for higher quality or waste control and better dynamic capability, are forcing

an integrated design philosophy into the process industries.

In general terms the preceding paragraphs demonstrate the need for a systems design method for the Plant Design - Control Problem in which the static performance (efficiency, product quality, etc.,) and dynamics (stability, response, etc.,) are considered together in the design stage. It is necessary also to consider plant cost in the design, as a plant optimised on purely technical merits could be economically unviable. The problem used for developing the method has now been defined and the general flow diagram of Figure 1.2 may be simplified and made more specific as Figure 2.1. Three system models may now be identified: the static, dynamic and cost models correspond to the three categories of design objective under consideration. The flow diagram is arranged in such a way that the optimisation loop (heavy lines) calls for data from (and sends it to) the model and analysis blocks. This is done to make the design method as flexible as possible so that alterations to the models or the utility function can be made easily.

2.2 The Nuclear Power Station Problem

Nuclear power plants currently in operation and under construction in the U.K. are designed as base load stations, fluctuations in power demand being met by the conventional fossil fired or hydro-electric stations. The reasons for this policy were both economic and technical: the high capital cost of nuclear stations meant that they could only produce power economically if operated on a full power full time basis, and in applying the new nuclear technology it was much simpler, cheaper and safer to build a static rather than a dynamic plant. This policy was possible while the fraction of nuclear power was relatively small (at present a little over 10% of the installed generating capacity is nuclear, but as these are base load stations they supply nearer 15% of demand). However, world energy supplies and generating economics dictate that nuclear power must play an ever larger part in meeting the country's electricity demand. Figure 2.2 shows the predicted total and nuclear capacities of power stations in the U.K. until 2000 A.D. (2.1)

Present nuclear plant then was designed for fundamentally static operation, and could therefore employ intermediate coolant loops for safety (in view of the uncertainties of the new technology) and energy storage could be cut to a minimum to reduce construction costs. Typically a nuclear station today has about one third the available thermal energy storage of a conventional station (10 full

17 →

Figure 2.1

Systems design procedure for the design-control problem.
Needs analysis, problem definition and system synthesis stages are as in Figure 1.2.

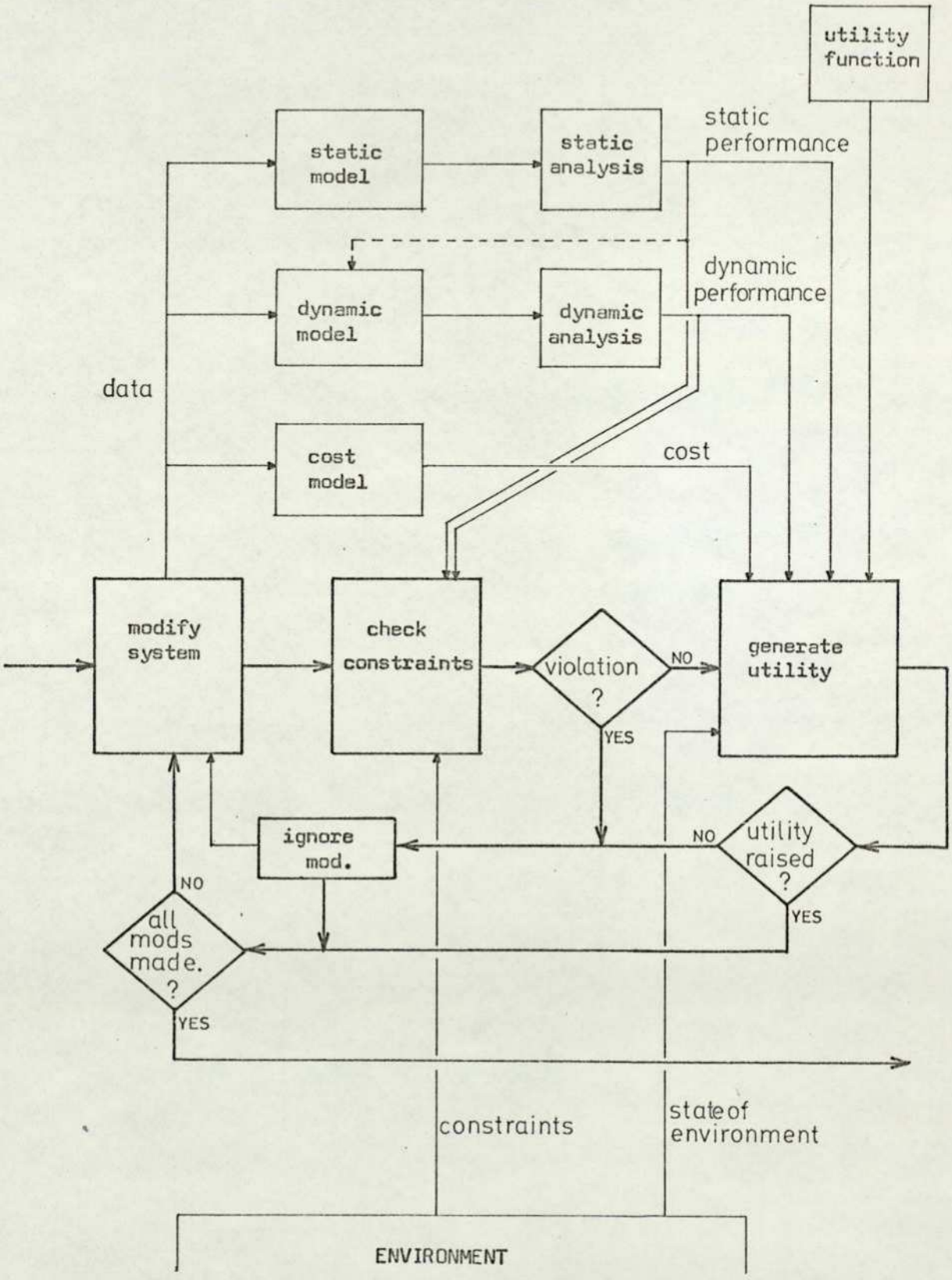


Figure 2.2

Estimated generating capacity in the U.K. to 2000 A.D.

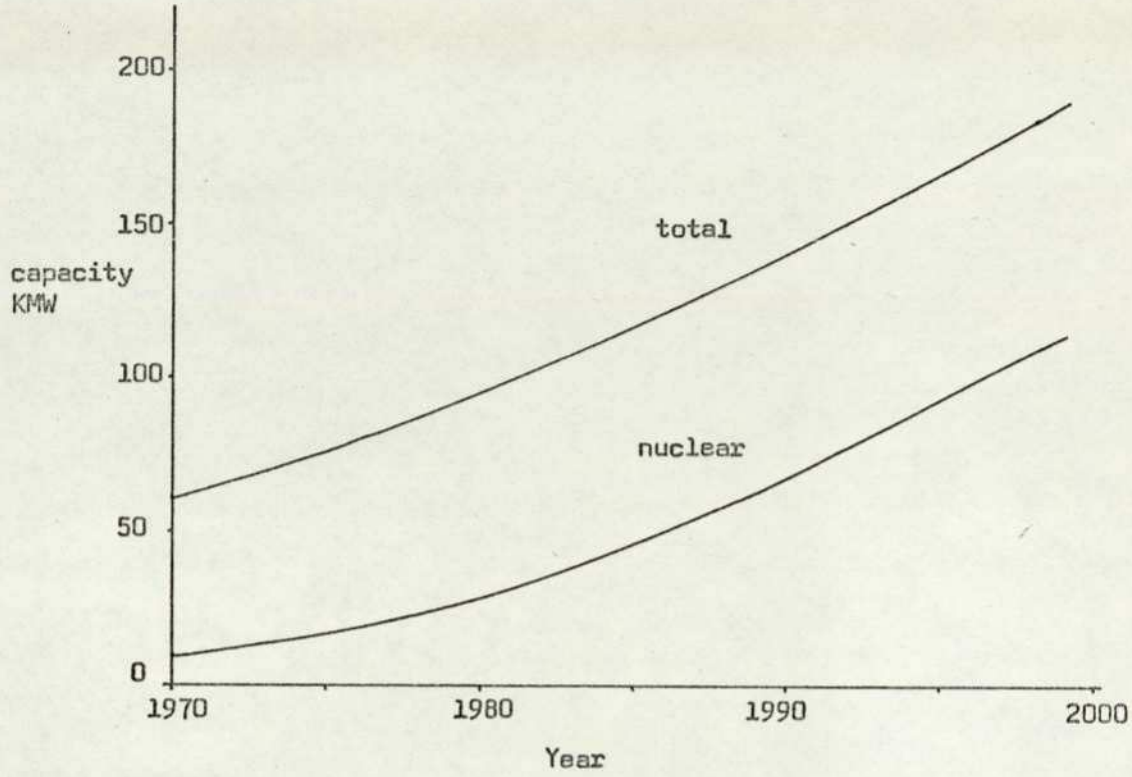
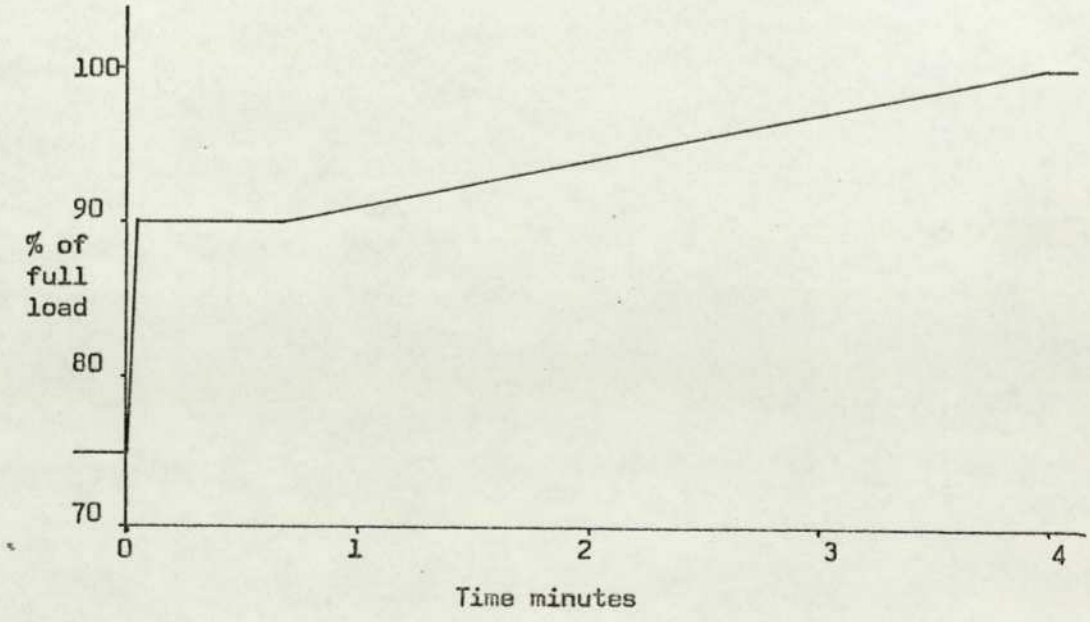


Figure 2.3

Idealised power response required of future nuclear reactors to cope with demand fluctuations.



power seconds against 30). Intermediate coolant loops and low energy storage do not make for good dynamic performance, and clearly a change in design philosophy is needed for the next generation of nuclear power stations.

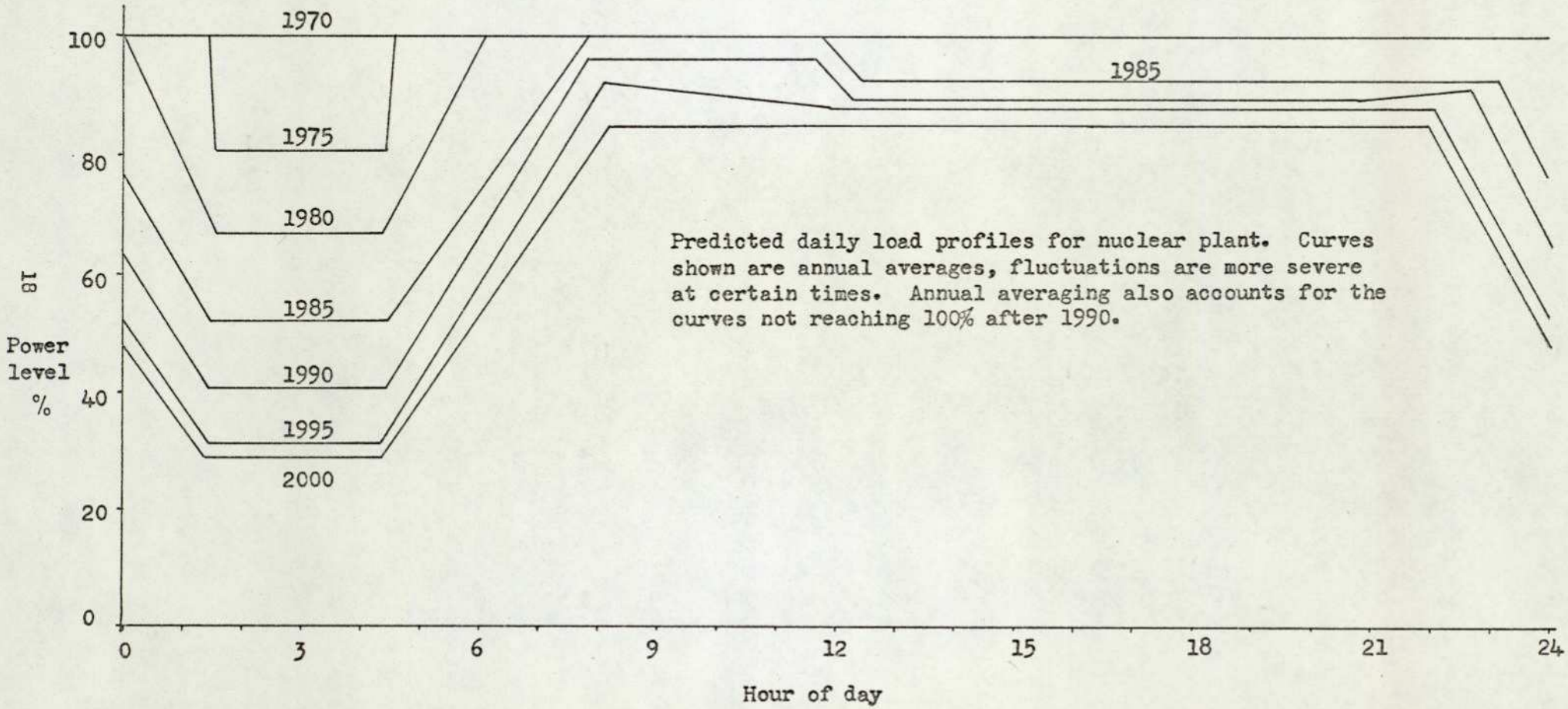
There are other basic changes in the electricity supply system taking place concurrently with the increasing proportion of nuclear power. The most significant is the trend, again for economic reasons (2.5) towards larger power generating stations and generating sets (turbo alternators). In addition total power demand is increasing and so too is the ratio between daily and annual maximum and minimum demand (2.2, 2.3). At present the largest stations are of 2000 M.W. and the largest generating sets 650 M.W. Stations of 3000 M.W. and sets of 1000 M.W. are under construction, and economic pressure will be for still larger sizes. The implication of larger stations is that the system will have to sustain larger power deficiencies, in both absolute and relative terms, following a reactor or transmission line fault. Similarly a fault in a larger turbo-alternator will result in a bigger power deficiency, but a more significant effect of larger set sizes is their lower mechanical inertia per unit output. Typically mechanical energy storage is 4 megawatt seconds per megawatt for a 500 M.W. machine and twice that for a 120 M.W. machine. As larger sets are installed the grid 'inertia' per unit output will decrease and the response of grid frequency to a power surplus or deficit will be faster.

The policy of the C.E.G.B. is to maintain grid frequency to within $\pm$ 0.2 c/s of the nominal 50 c/s under all circumstances. If this standard is to be maintained, the dynamic capability of the nuclear station of the future must be considerably superior to that of today's conventional station, due to the larger step inputs to be expected (following faults in other parts of the system) and the faster grid response. Even in normal circumstances severe load following demands will be made of the plants, as the predicted daily power profiles of Figure 2.4 show. Work by the C.E.G.B. has shown that power responses of nuclear stations must be of the form shown in Figure 2.3 if grid security is to be maintained when the majority of power is nuclear produced in 20 years' time (2.4).

Designing a nuclear station with a dynamic capability adds a new dimension to the design problem, and to design assessment. The various design criteria, static performance, dynamic performance, cost, are highly interactive and must be traded off against one another to produce an optimum design. In fact the nuclear reactor is

19 →

Figure 2.4



Predicted daily load profiles for nuclear plant. Curves shown are annual averages, fluctuations are more severe at certain times. Annual averaging also accounts for the curves not reaching 100% after 1990.

a typical example of the Plant Design - Control Problem. Also it is of a size and complexity common in real problems, and a design method which tackles the reactor would be applicable to a fair range of problems. The reactor design is then an ideal problem to use for the development of a systems based design method.

Stated in the broadest possible terms the design objectives in three categories being considered are -

(a) Static Performance. The reactor should produce power at a specified rate, and its total energy output for a given quantity of fuel should be a maximum.

(b) Dynamic Performance. The reactor should be able to follow any load changes demanded of it.

(c) Cost. The reactor should be built at minimum cost.

These are obviously conflicting requirements.

Studies have been carried out in the C.E.G.B. along the lines indicated above for Advanced Gas Cooled Reactors (AGRs) (2.6). The studies, however, do not use a computer model of the whole problem to optimise the design, but use predictions of the various aspects of station performance to aid a 'manual' optimisation.

3. DESCRIPTION OF THE PLANT

3.1 Reactor Physics

Before describing in detail the reactor to be used for the development of the design method, it is as well to consider the principles of nuclear reactors as this will be necessary for an understanding of the plant models to be discussed later. For a more detailed account of the principles of reactors see (3.1 & 3.2)

3.1.1 The Fission Process

The properties of the three fundamental particles of which atoms are formed may be summarised as follows -

Particle	Charge	Mass	
		a.m.u.	grams
Electron	- 1	.00055	9.106×10^{-28}
Neutron	0	1.00898	1.675×10^{-24}
Proton	+ 1	1.00759	1.673×10^{-24}

Light atoms have equal numbers of neutrons and protons, but heavier atoms have an increasing proportion of neutrons to protons, see Figure 3.1. If the total mass of electrons, protons and neutrons in an atom is calculated, it is found that this exceeds the mass of the atom. The difference is the mass equivalent of the energy required to 'dismantle' the atom into its fundamental particles, and is termed the binding energy. It is usually expressed in terms of binding energy per nucleon (protons + neutrons), and if plotted against mass number gives the curve shown in Figure 3.2. Energies are expressed in electron volts (ev) with an appropriate prefix, i.e. Kev or Mev. One electron volt is equivalent to 1.6×10^{-19} joules. It may be seen that binding energy is a maximum for atoms with an atomic mass in the range 40 - 80. If heavy atoms can be split into fragments of atomic mass 40 - 80 an energy release will be obtained, this is the fission process. A much larger energy release per nucleon is available if light atoms can be combined to form heavier atoms, this is the fusion process.

Present power generating nuclear reactors make use of the fission process, and in the main use uranium as a fuel. Under suitable conditions fission will occur spontaneously in the uranium isotope U_{235} which constitutes about 0.7% of natural uranium, the remainder being mostly U_{238}. Reactors may be designed to operate on natural uranium or fuel enriched in U_{235}. Fragments of the uranium atoms (fission products) are distributed over a range of atomic weights

22 →

Figure 3.1

Proton-Neutron combinations in stable isotopes

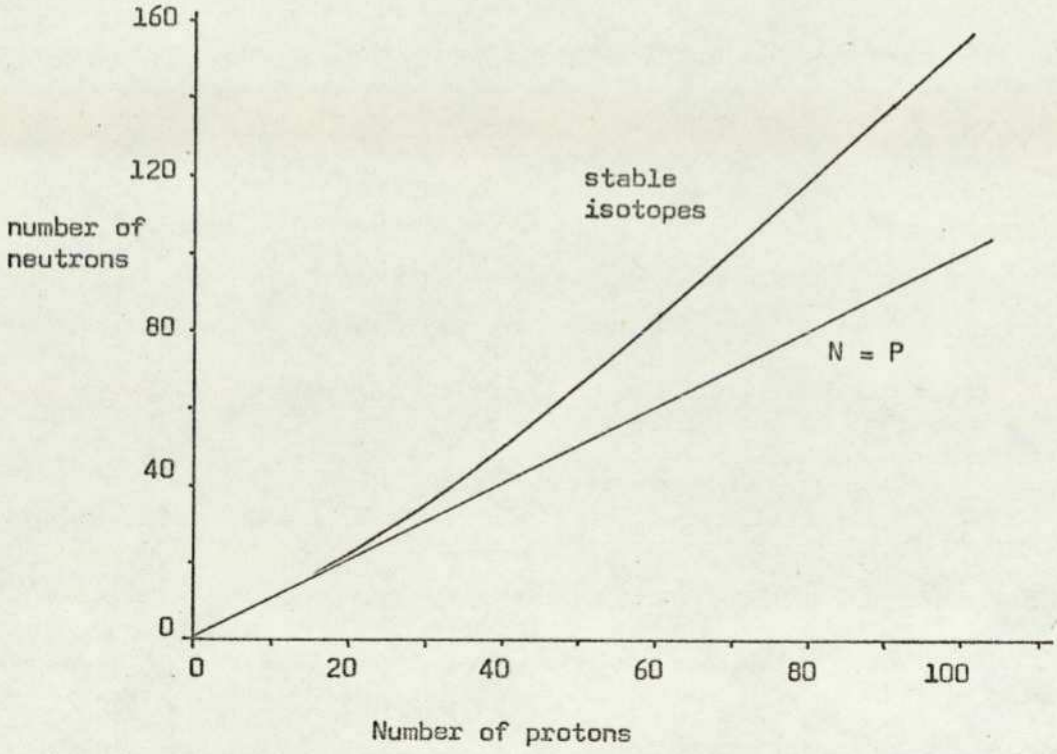
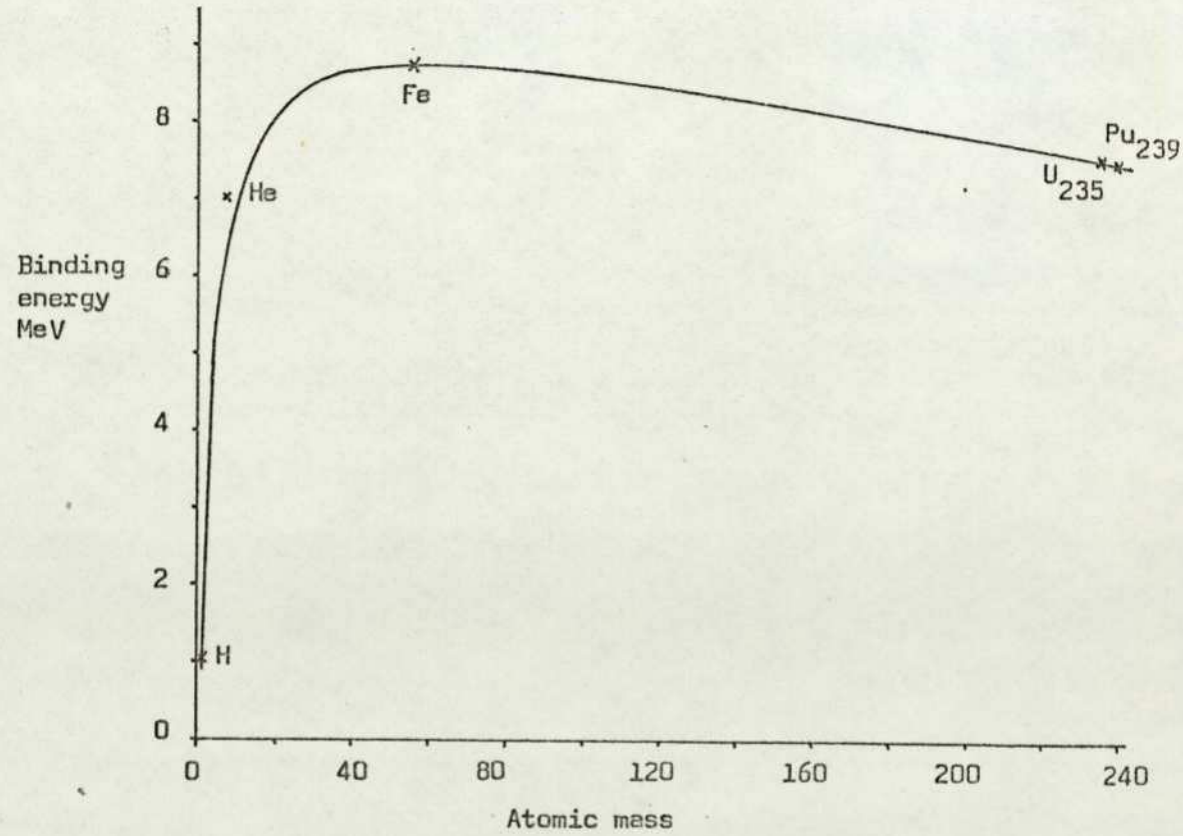


Figure 3.2

Binding energies of stable isotopes



as illustrated in Figure 3.3. The fragments lie mainly in the ranges 85 - 105 and 130 - 150, energy release is therefore less than the theoretical maximum, however this is a natural process over which there is no control. Nuclear fission in U_{235} is initiated by the capture of a neutron, and as a result of the fission in addition to the fragments two or three neutrons are ejected and energy released. Individual fission reactions vary, but on average 2.46 neutrons and 200 Mev of energy are released for each U_{235} fission. The energy release is equivalent to 3.1×10^{10} fissions per joule (watt second).

3.1.2 Neutron Properties

Neutrons are ejected at high velocity v and may be classified by their energy in Mev using the relationship -

$$E_k = \frac{M_o v^2}{2} \times 6.25 \times 10^5 \text{ Mev} \qquad 3.1$$

where M_o is the rest mass of the neutron i.e.

$$E_k = 5.24 \times 10^{-19} v^2 \text{ Mev} \qquad 3.2$$

This applies so long as the velocity is small relative to that of light c, if not we have -

$$E_k = M_o c^2 \left\{ \frac{1}{(1-(\frac{v}{c})^2)^{\frac{1}{2}}} - 1 \right\} \times 6.25 \times 10^5 \text{ Mev} \qquad 3.3$$

A distribution of the neutron energies resulting from fission is shown in Figure 3.4. When a neutron has an energy such that it is in equilibrium with the temperature of the matter in which it exists, it is called a thermal neutron. The energy at which equilibrium will occur is given by kinetic theory as -

$$E = KT \qquad 3.4$$

where T is the absolute temperature and K is the Boltzmann constant = 1.37×10^{-16} erg/°K. At 20°c therefore a neutron would be in thermal equilibrium with its surroundings if its energy were 0.025 ev.

Fission may be initiated by either the high energy (fast) neutrons, or by thermal neutrons, and reactors are classified as fast or thermal reactors depending upon which process is employed. Fast reactors have not yet been built commercially and it is the thermal reactors which are of interest here. As each U_{235} fission is initiated by the capture of neutron and ejects on average 2.46 neutrons, there

24 →

Figure 3.3

Distribution of fission fragments.

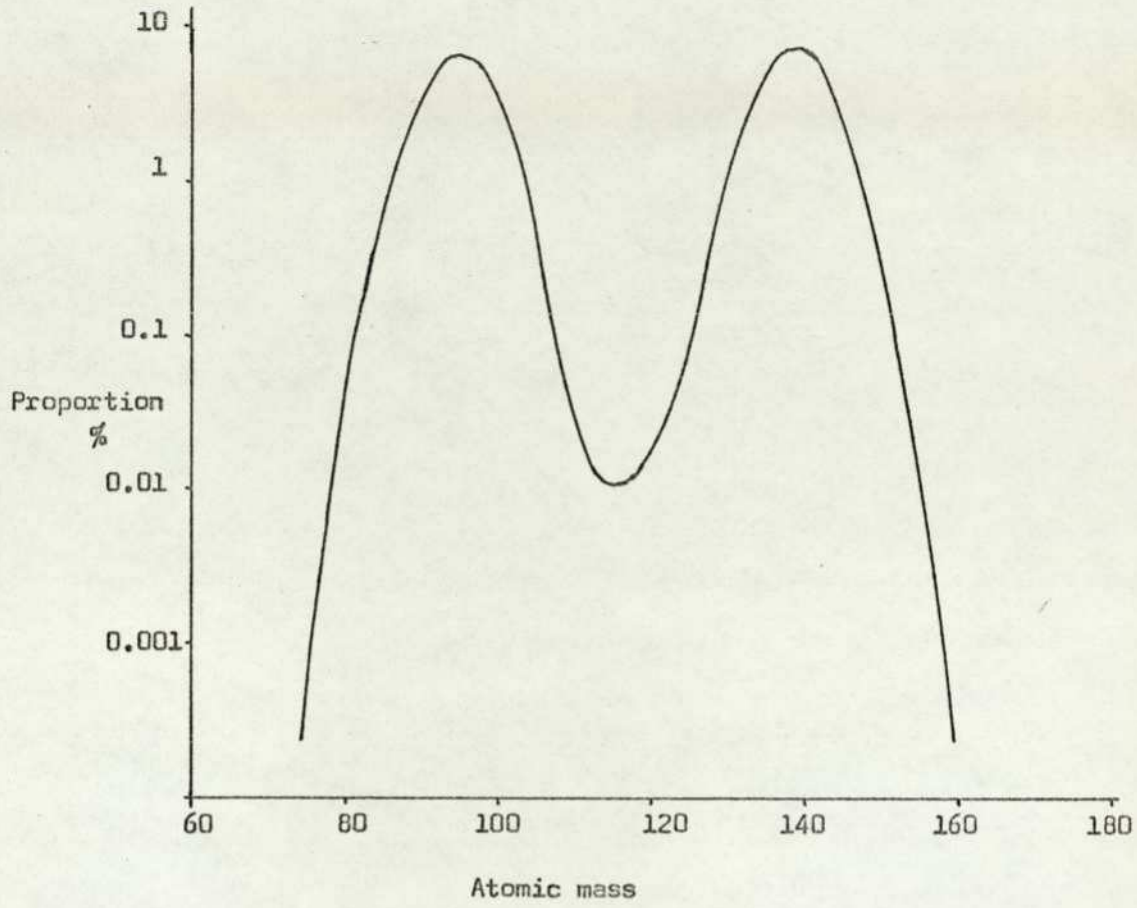
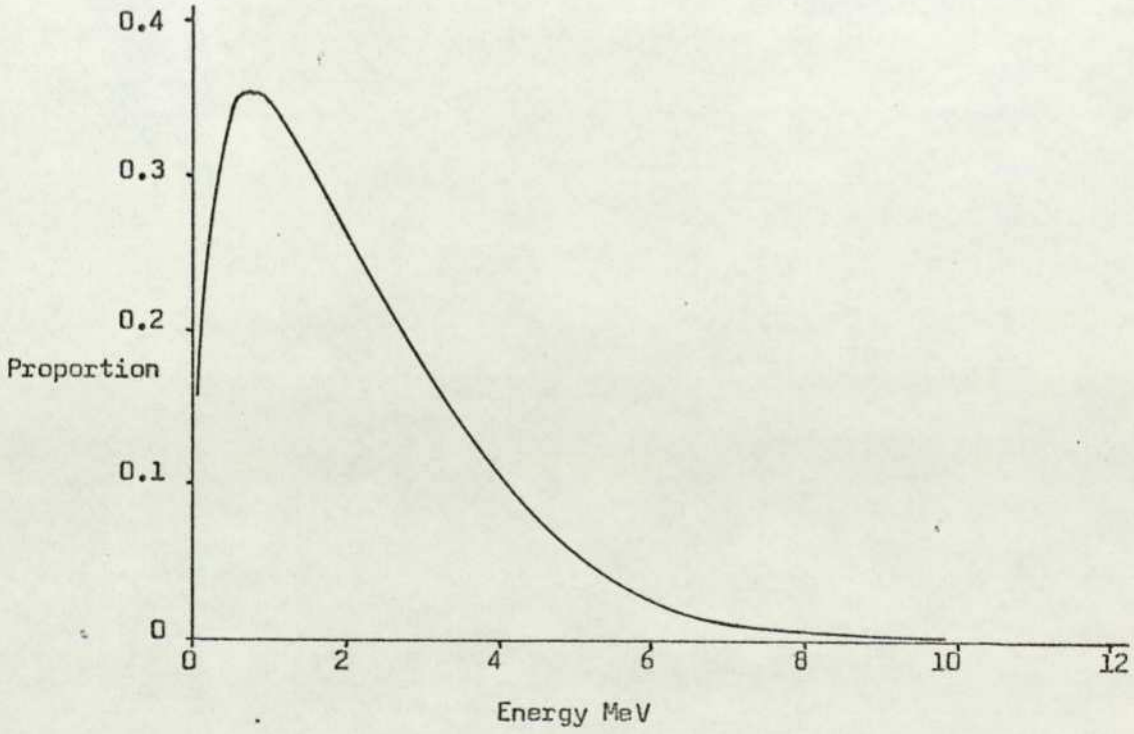


Figure 3.4

Distribution of fission neutron energies.



is a gain of 1.46 neutrons per fission. If a steady fusion process is to be maintained therefore 1.46 neutrons must be removed from the reactor for every fission that occurs. The mechanisms of neutron loss are to be discussed later, but basically it depends upon the ratio of neutrons absorbed by the fuel, to those absorbed by other reactor materials. A measure of the capacity of a material to absorb neutrons is given by its microscopic absorption cross section σ_a measured in barns, one barn being 10^{-24} cm.^{2} The product of the number of atoms and the cross section is a measure of the total neutron absorbing capacity. If this product is summed for all the reactor material, then the total absorbing power of the reactor is obtained. Absorbing capacity may alternatively be expressed in terms of the microscopic absorption cross section Σ_a, which is the product of the microscopic cross section and the number of atoms per cubic centimeter. A similar property called the fission cross section σ_f gives a measure of the ability of an atom to capture a neutron which will cause a fission. Using these quantities the proportion of neutrons absorbed by the fuel may be estimated. Both the fission and absorption cross sections vary with neutron energy, exhibiting sharp 'resonant' peaks at certain energies. The fission cross section for U_{235} is plotted against neutron energy in Figure 3.5. Nuclear cross sections of materials used in the S.G.H.W.R. are tabulated in Appendix 12.

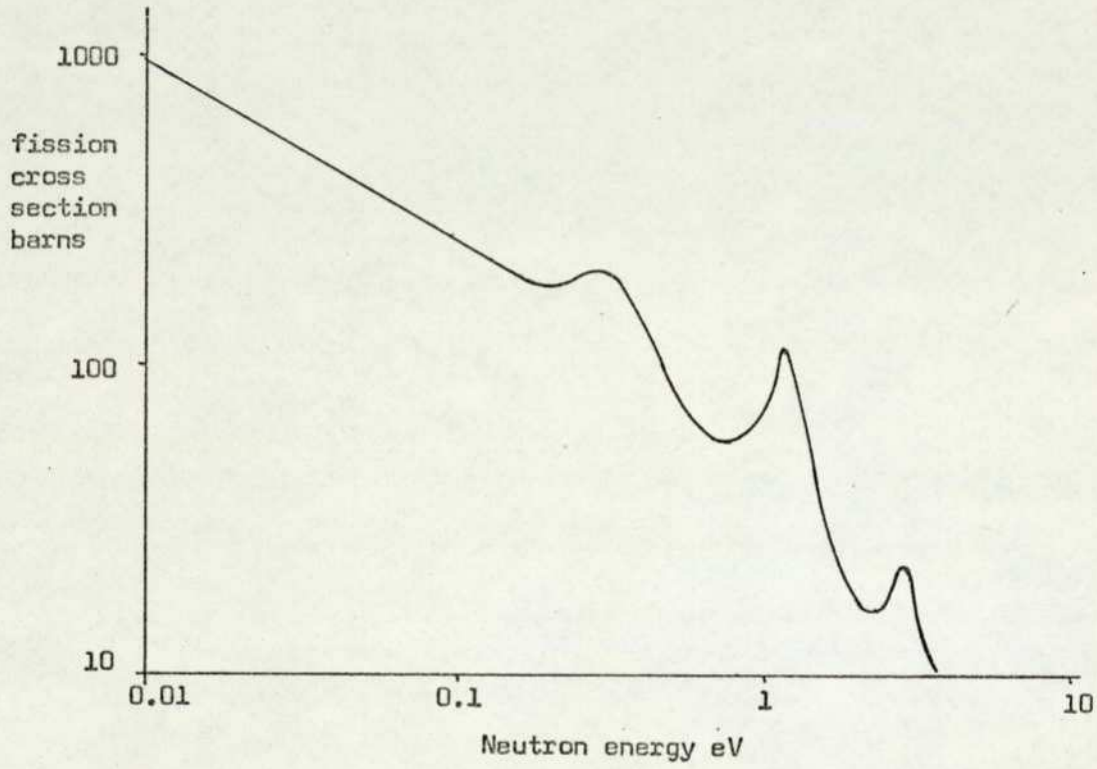
3.1.3. The Chain Reaction.

As stated previously thermal reactors use neutrons in the 0 - 3 ev region to initiate fission, but neutrons are released in the Mev range. These neutrons must therefore be slowed, this is achieved by the introduction of a moderator which slows the neutrons by elastic collisions with the moderator atoms. The properties of a moderator are determined by its scattering and absorbing cross sections σ_s and σ_a and the average logarithmic energy decrement per collision ξ. The energy decrement is a function only of the atomic mass of the moderator atoms, light atoms have higher decrements per collision as a larger proportion of the neutron energy is transferred to the atom. These quantities are combined to give the moderating ratio $\xi \frac{\sigma_s}{\sigma_a}$ (for an element, for a compound the cross sections must be summed for all elements). The mechanisms of neutron loss may now be examined. If there are n_o neutrons at time t_o, then in the next generation of neutrons (after fission) these will be ηn_o neutrons where η is the multiplication factor = 2.46 for U_{235} i.e.

26 →

Figure 3.5

Fission cross-section of U_{235}.



$$n_t = \eta n_o \qquad 3.5$$

Before these are slowed down some cause fast fission in the fuel, slightly increasing the number of neutrons by a factor ε, which is about 1.03 for natural or slightly enriched uranium fuel. The number of fast neutrons is therefore -

$$n_t = \varepsilon\eta\, n_o \qquad 3.6$$

While the neutrons are slowed to thermal energies by the moderator some are captured, mainly by U_{238}. The probability of avoiding capture is p, the number of thermal neutrons is therefore -

$$n_t = p\varepsilon\eta\, n_o \qquad 3.7$$

The proportion of thermal neutrons entering the fuel is the thermal utilisation factor f. The remainder are absorbed by the reactor structure or are lost into the shielding. Thermal neutrons entering the fuel are -

$$n_t = fp\varepsilon\eta\, n_o \qquad 3.8$$

Finally, not all the neutrons entering the fuel cause fission, some are absorbed, η is therefore replaced by η_e the effective multiplication factor, therefore -

$$n_t = fp\varepsilon\eta_e n_o \qquad 3.9$$

The ratio of neutron flux from one generation to the next is the effective reactivity denoted by K_{eff} and is given by -

$$K_{eff} = p\varepsilon f\eta_e \qquad 3.10$$

for a steady reaction $K_{eff} = 1$. Excess reactivity denoted by δK is given by -

$$\delta K = \frac{K_{eff} - 1}{K_{eff}} \qquad 3.11$$

The time between a neutron being ejected and being absorbed to cause another fission is the mean neutron lifetime l, and is of the order of 10^{-3} to 10^{-4} seconds. Neutron flux would, if all neutrons were ejected, immediately after fission be given by -

$$n = n_o K_{eff}^{\,t/l} \qquad 3.12$$

Fortunately this is not the case as neutron flux (and therefore power output) would be extremely sensitive to small changes in reactivity and reactors would be virtually uncontrollable. Most neutrons are ejected within 10^{-12} sec. (prompt neutrons) of fission, but about 0.755% are delayed and may be represented by six groups. Each group provides a definite proportion of the delayed neutrons β_i, and they are released according to an exponential distribution with

time constant $\frac{1}{\lambda_i}$. The sum of the proportions is $(\sum \beta_i)$ 0.00755 and the time constants vary from 0.07 to 80 seconds. Providing then that excess reactivity does not exceed 0.00755 therefore, the rapid power variations predicted by 3.12 will not occur. When $K_{eff} = 1.00755$ sufficient prompt neutrons are released to support the chain reaction and the reactor is said to be prompt critical, a dangerous situation which is never intentionally created.

3.1.4. Inherent and External Reactivity Control.

The mechanisms of neutron absorption have now been described, and it has been shown how absorption affects the effective reactivity K_{eff}. Reactivity may be controlled by varying the moderator to absorber ratio and this may be achieved by varying the quantity of either. Control rods of a highly absorbent material (high absorption cross section) are a common control mechanism. Reactivity is also dependent on various effects within the reactor which can lead to inherent stability or instability of the design. It was shown in Figure 3.5 that the fission cross section of U_{235} has a decreasing trend as neutron energy increases. As the core temperature rises so does the energy of the equilibrium neutron and there is less probability of it causing fission. This then is a temperature stabilising effect, known as the doppler feedback effect. More marked effects occur in reactors with a liquid or gaseous coolant, for as temperatures vary so does the mass of coolant in the reactor. Depending upon whether the absorbing or moderating effect of the coolant is dominant the reactivity may increase or decrease with temperature, although for safety reasons the latter is usually aimed at. For gas cooled reactors pressure changes have a similar effect, and if a liquid moderator is used its quantity is again temperature dependent. Where the coolant is an evaporating liquid large variations in the mass of coolant in the core can occur depending upon the liquid-vapour ratio or voidage. The effects of variables on reactivity are expressed by reactivity coefficients, e.g.

$$\delta k = K_T \delta T \qquad 3.13$$

3.1.5. Fission Product Poisoning.

Finally there are some points to be made concerning the effects of fission products. Some of these, notably Xenon (Xe_{135}) have very high neutron absorption cross sections, and are referred to as poisons, (although this term is also used for absorbers deliberately introduced for control or shutdown purposes). Xenon is formed several hours

after fission due to radioactive decay of an unstable isotope of Iodine (I_{135}) formed as a fission fragment. It is itself unstable and decays with a half life of 9.13 hours, but the main cause of elimination is by neutron absorption, also called burnup. During steady reactor operation the production and burnup and decay rates of Xe_{135} form a balance. At startup (after a prolonged shutdown) however, there will be a low level of Xe_{135} and some alternative absorber must be provided to remove excess neutrons from the reactor until the Xenon level stabilises. After shutdown the production of Xe_{135} continues, but as neutrons are no longer available for burning the level will rise until the supply of I_{135} is depleted. The concentration then falls as Xenon is destroyed by radioactive decay. The peak levels of Xenon built up after shutdown are such that it is impracticable to provide sufficient reactivity override to counter its absorbent effect. Following shutdown then it is necessary to restart quickly or to wait until Xenon has decayed naturally before restart is possible. In large reactors Xe_{135} can lead to a spatial oscillation in the power distribution throughout the reactor. Being gaseous Xenon also causes pressure buildup within the fuel.

3.2. The S.G.H.W.R.

The reactor used in developing the design method is a new type known as the Steam Generating Heavy Water (moderated) Reactor, or S.G.H.W.R. A 100 MW(E) prototype has been built at Winfrith in Dorset, and this is currently undergoing trials. Commercial designs of the S.G.H.W.R. have been prepared and are under consideration for application in the U.K. and overseas. A brief description of the reactor follows, for a more detailed account see (3.3).

The reactor configuration is basically a conventional recirculating boiler system with the fired heater replaced by a nuclear heater, the configuration is illustrated schematically in Figure 3.6 and Figure 3.7 shows a perspective detail of the reactor core and coolant system. The reactor core is contained within an aluminium vessel 12 feet in diameter and 13 feet high called the calandria, this vessel contains the heavy water moderator which is essentially at atmospheric temperature and pressure. Through the calandria pass 104, 6" OD pressure tubes, each containing a cluster of 36 fuel pins as illustrated in Figure 3.8. A feature of the reactor is that pressure is contained within these tubes and large pressure vessel is avoided. Light water coolant enters the bottom of the tubes and partially evaporates as it passes over

32 →

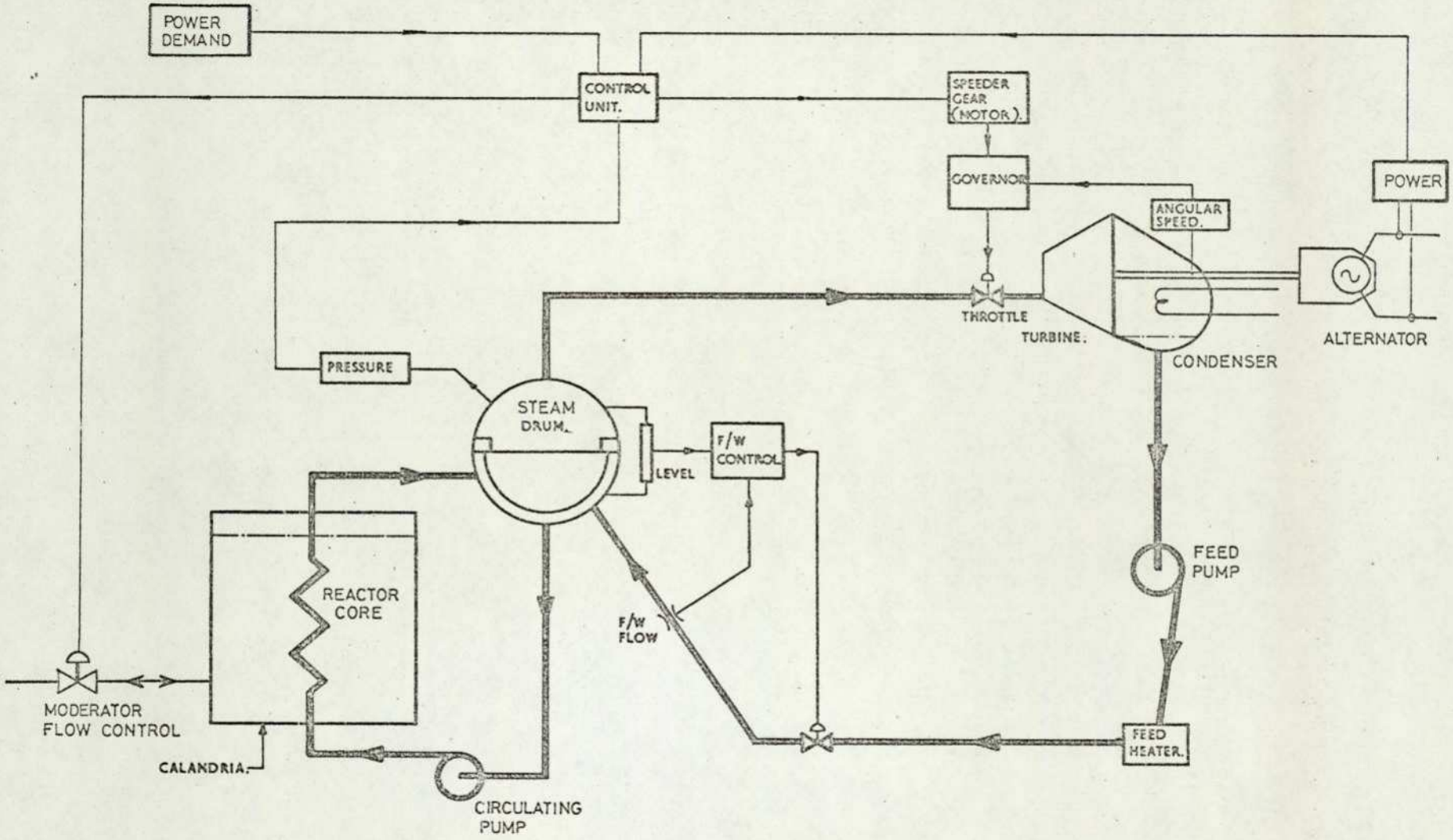


Figure 3.6 Schematic of the S.G.H.W.R. circuit

Figure 3.7

S.G.H.W.R. PRIMARY CIRCUIT

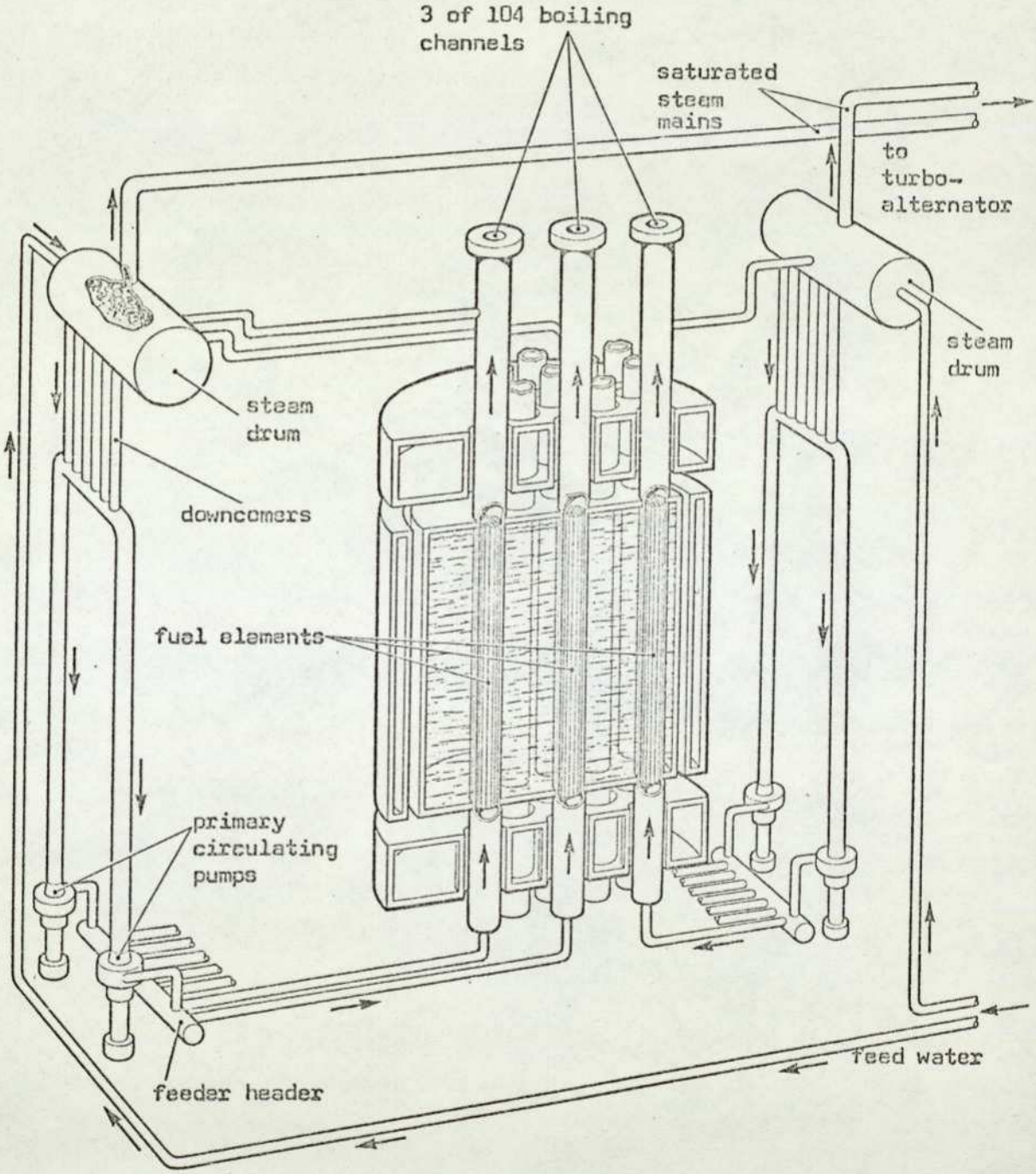
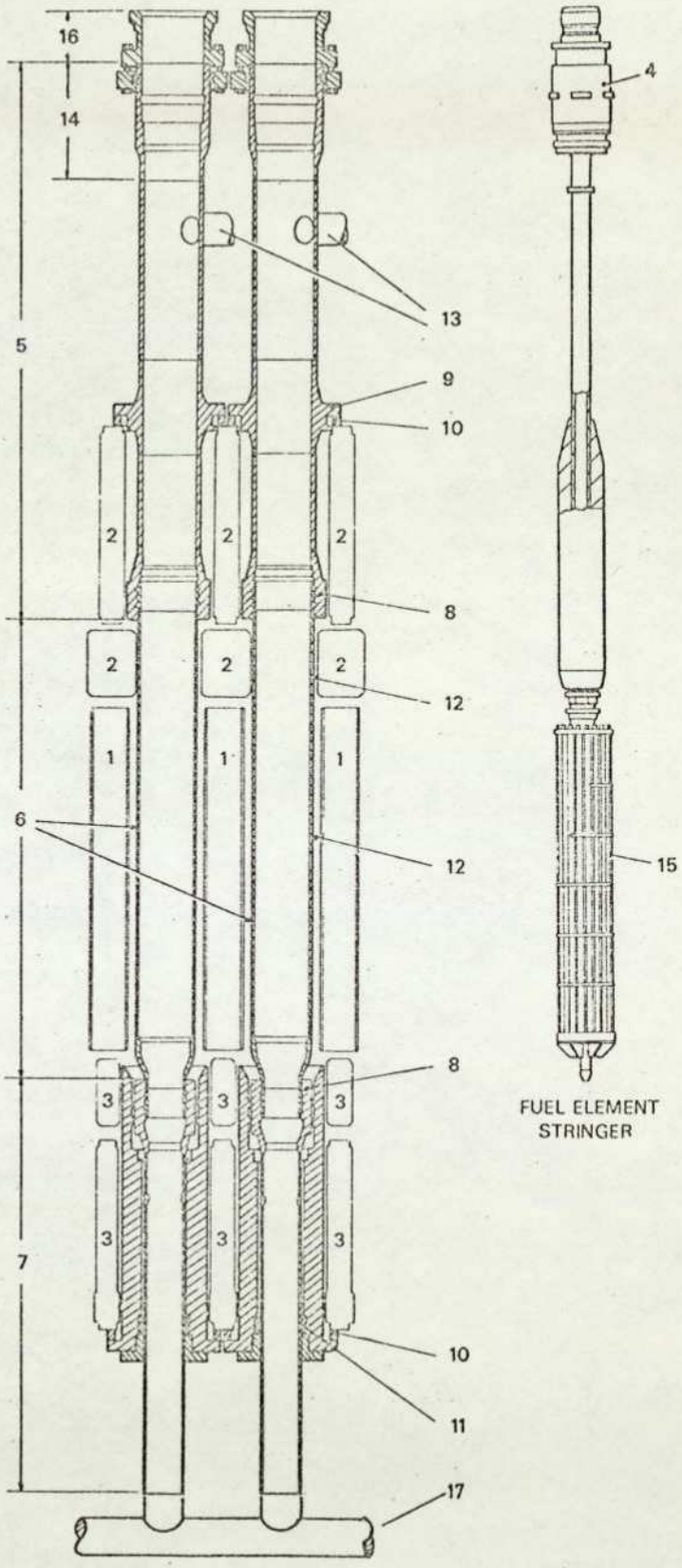


Figure 3.8

Detail of the S.G.H.W.R. boiling channels and fuel pins.



1. CALANDRIA
2. UPPER NEUTRON SHIELDS
3. LOWER NEUTRON SHIELDS
4. SEAL PLUG
5. STEEL STANDPIPE
6. ZIRCONIUM PRESSURE TUBE
7. STEEL TAIL PIPE
8. EXPANDED JOINT
9. CHANNEL SUPPORT FLANGE (BOLTED TO NEUTRON SHIELD)
10. THERMAL INSULATION BLOCK
11. SEALING BUSH
12. GAS INSULATION GAP
13. COOLANT OFFTAKE PIPE(RISER)
14. SEAL PLUG HOUSING
15. FUEL ELEMENT (36 PIN CLUSTER)
16. REFUELLING MACHINE CONNECTION PIECE
17. COOLANT INLET MANIFOLD

the fuel which is uranium oxide enriched to 2% in U_{235}. About 3 MW of thermal energy is generated in each pressure tube.

In the prototype the steam water mixture from each pressure tube is carried through individual risers to one of two steam drums. In some of the commercial designs several pressure tubes are linked to headers and transfer lines which carry coolant from several pressure tubes to the drums. Liquid separation takes place in the steam drums, and dry steam from each is fed to the turbine. Superheating is not employed as the startup of superheater tubes in this type of reactor would create problems. Exhaust steam from the turbine is condensed and pumped back into the drum via feed heaters. Water from the drum is recirculated to the reactor core, there are two recirculating pumps per drum.

Turbine power is controlled conventionally by the turbine stop valve. Reactor power is controlled in the short term by adjusting the height of moderator in the calandria, and in the long term by the much slower control of neutron absorber dissolved in the moderator. Emergency shutdown is effected by injecting under gas pressure a boric acid solution into special tubes through the calandria (boron has a high absorption cross section). Control schemes are discussed in the following subsection.

Important features of the design are the lack of an intermediate coolant circuit, and the relatively small mass at high temperature in the reactor core, i.e. the fuel, pressure tubes and a fairly small amount of coolant. Direct cooling of the reactor leads to a close coupling between the reactor and turbine, suggesting the possibility of a good inherent load following capability. The low thermal inertia gives a fast thermal time response in the core, again giving the prospect of a dynamic capability considerably in advance of existing commercial reactors. For reasons explained in the previous section the pressure, temperature and degree of evaporation of the coolant have significant effects on the excess reactivity. As all of the variables mentioned will change during a load following transient the degree to which they affect the neutron balance is important in determining the overall load following capability.

In developing the design method the 100 MW prototype was used as a reference case from which the optimisation procedure could begin. A list of the plant parameters is given in Appendix 1, with the reference (prototype) values. A list of the system variables and their reference values is given in Appendix 2.

3.3. Reactor Controls

It was stated in the previous section that the primary controls on the reactor were the turbine stop valve position and the moderator level. The control of boron dissolved in the moderator is a long term action and is of no interest for controlling reactor response to load changes. A control is also required on the feedwater flow to maintain the drum water level. Although this control has little effect on the overall power response, it has some significance on the drum water level excursion on which there is a limit.

In practical terms, considering the time scale of power responses, the turbine stop valve position is capable of an instantaneous or step change. The rate at which moderator level may be changed is limited by the pump capacity to the equivalent of a reactivity change of 3×10^{-5} per second. The limit is imposed by the maximum safe rate of reactivity rise during startup of the reactor.

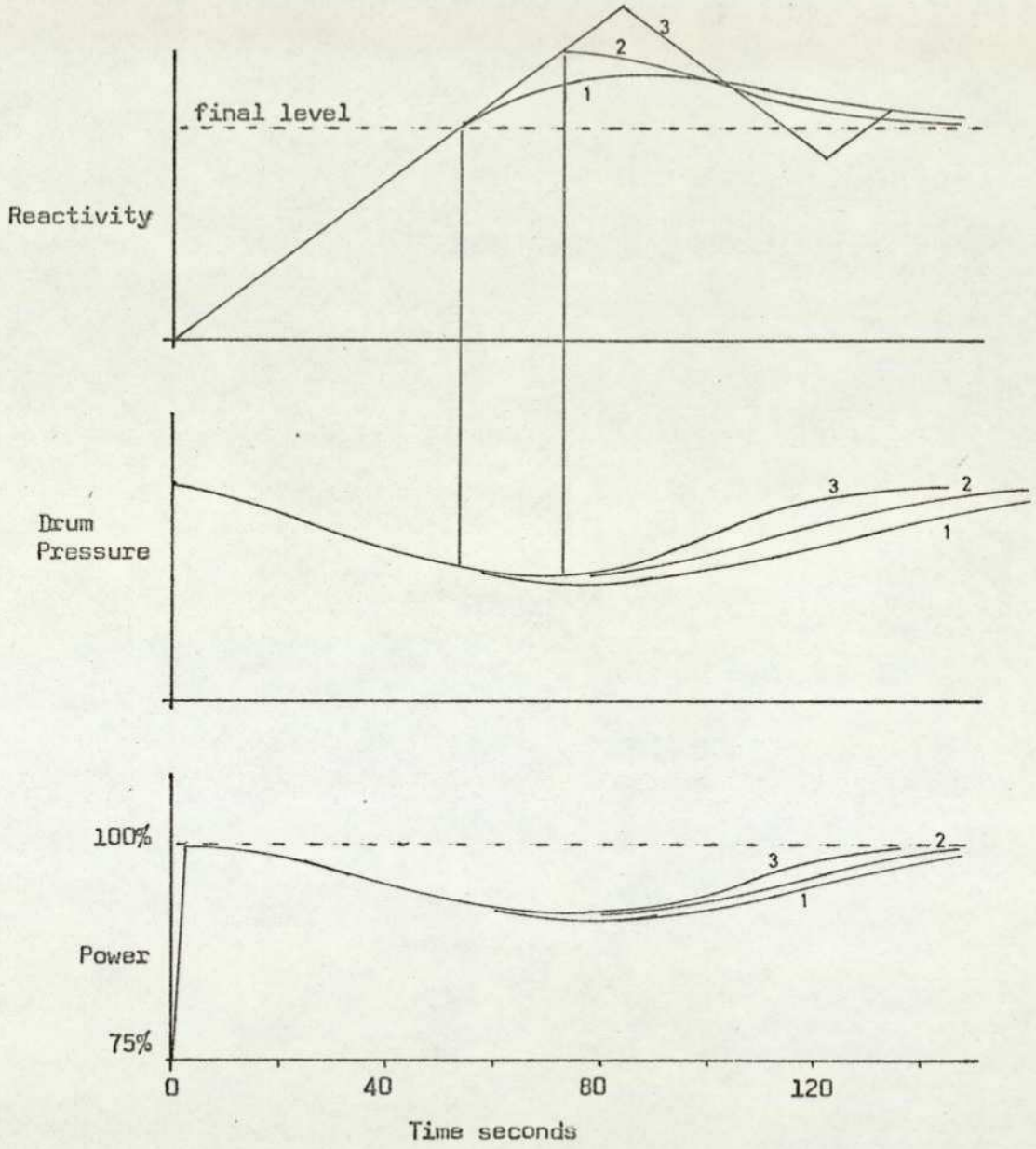
The prime interest in optimising the reactor control system (in the present context) is to enable the power output to follow, as closely as possible, step changes in demand resulting from faults elsewhere in the system. When the power requirement is raised to 100% the best possible power response is obtained initially using a control strategy outlined in (3.4), in which the turbine stop valve is opened immediately to 100%, and reactivity is inserted at the maximum rate. Responses of some of the system variables with this control scheme are shown in Figure 3.9. Reactivity is increased until either drum pressure begins to recover, or until the reactivity level is compatible with the final steady state level when the control mode is changed to stabilise the system and trim the final state power and drum pressure levels. It may be demonstrated, using a much simplified model, that this control strategy is that prescribed initially by a Pontryagin analysis using a conventional performance criterion, see Appendix 9. The Pontryagin analysis also suggests that an improvement in the power response after pressure recovery may be effected by increasing reactivity still further at the maximum rate, and then switching to a reactivity reduction at maximum rate. Subsequently reactivity rate is switched between maximum positive and negative levels, see Figure 3.9. This leads to only small improvement over the mode switching scheme mentioned earlier and delays the settling of the system. Actual switching points depend upon the time at which the error function is to be minimised.

If a power increase to less than 100% is demanded an improved response may be obtained by controlling steam flow on the stop valve

35 →

Figure 3.9

Responses of the S.G.H.W.R. to step inputs of power, with various reactivity control strategies.



Curves refer to control actions as follows -

1. Control mode switched at final level reactivity.
2. Control mode switched at drum pressure recovery.
3. Pontryagin's control of reactivity.

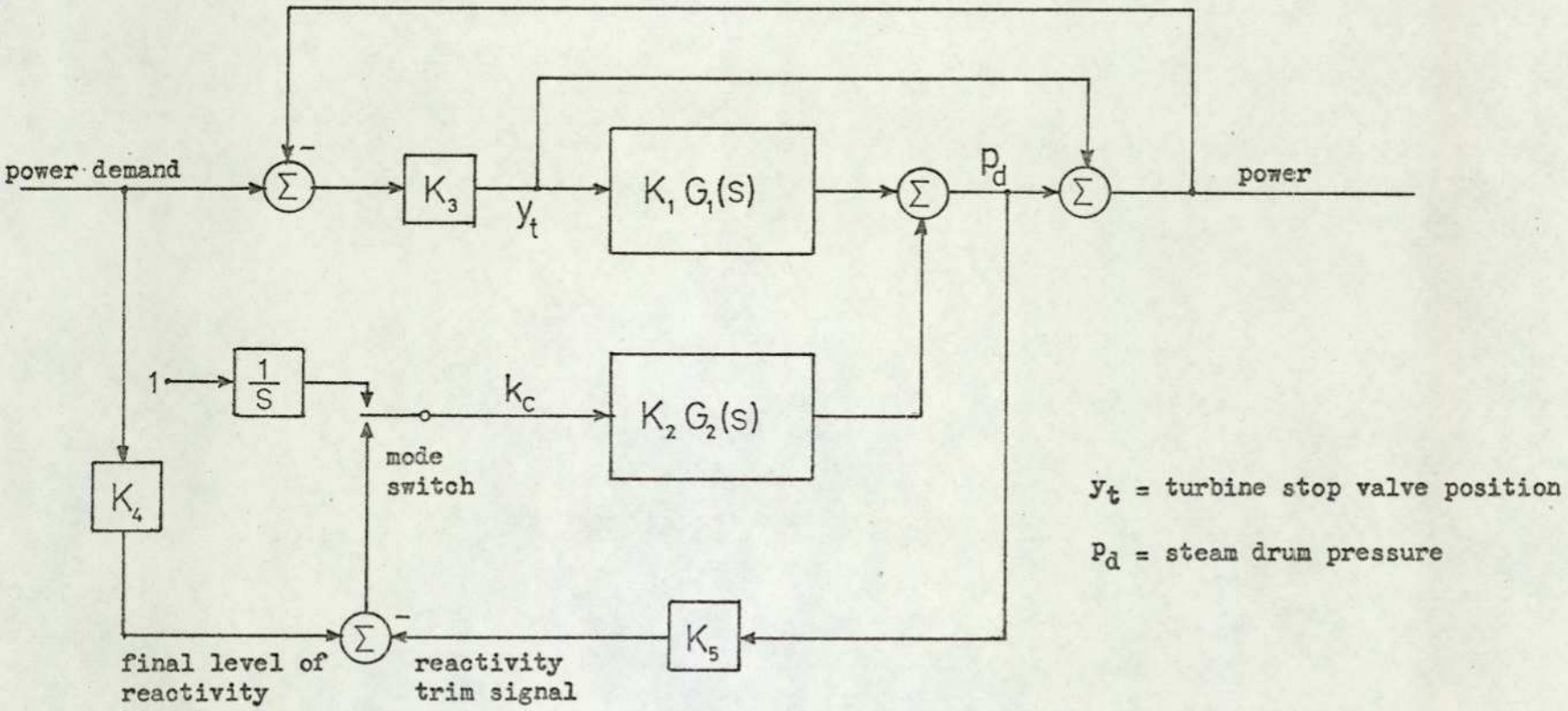
to a value equivalent to the power requirement. This control is fast (time constant of the order of 2 seconds) and therefore virtually any power profile can be followed until the stop valve saturates. Reactivity is then input at the maximum rate initially, as before, with switching to a stabilising and trimming mode at some point. A block diagram of this scheme is shown in Figure 3.10, if the controller gain K_3 is large then power output follows the demand. The normalised stop valve to drum pressure transfer function gain K_1 is negative, and in the reference design is slightly greater than one, which means that in the initial control mode (reactivity rate = $\pm$ 1) the system is unstable (K_1 = 1 for marginal stability). Responses of the reactor with this control scheme are shown in Figure 3.11 for a case where the stop valve saturates (power increase to 95%) and where it does not (power increase to 90%). For the case of a demanded power increase to 100% the latter scheme is equivalent to that discussed earlier. Drum pressure drop will be larger using the steam controlled scheme for input demands to less than 100%.

In the non saturating case the reactivity level after pressure recovery begins is not too important as at this point the increased power demand has been satisfied, although for other reasons it is desirable to effect pressure stabilisation quickly. For the saturating case pressure recovery must be as fast as possible to reduce power error. A Pontryagin analysis similar to that of Appendix 9 again indicates that reactivity should be input at maximum rate until considerably after pressure recovery before reversing. (The Pontryagin analysis uses the simplified model of Appendix 9 in the block diagram of Figure 3.10 to give a new pair of system poles, which are now both real making the work simpler. Pressure error is used instead of power error). The reactivity control strategy adopted is sub optimal; reactivity is increased at the maximum rate until it intersects a reactivity control curve proportional to pressure error and about the predicted final state reactivity level, at which point control is switched to the curve. Figure 3.12 illustrates the strategy and the responses obtained, the switching point may be altered by setting the proportional gain, which will be in the range $0.25\text{-}1.5\times10^{-5}$. A final state trimming action (long trim constant integrator) would be needed in a practical realisation of this controller.

A proportional plus integral feedwater controller was adopted for the steam drum level (feedwater) control. This is slightly simpler than the controller on the S.G.H.W.R. prototype.

39 →

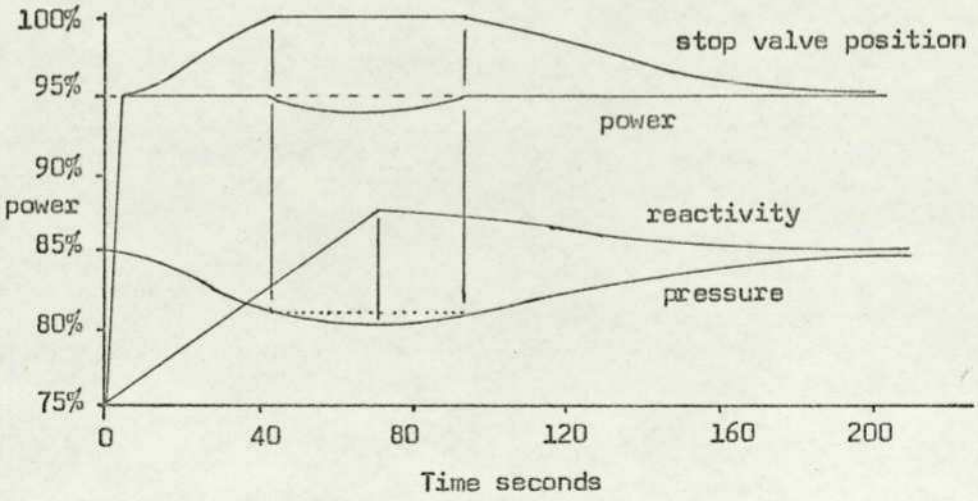
Figure 3.10



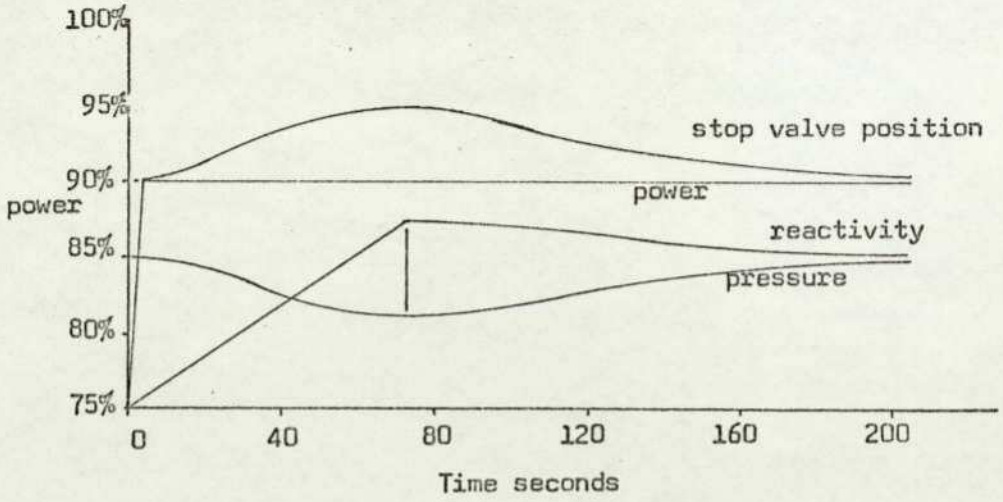
Block diagram of the S.G.H.W.R. controller.

Figure 3.11

Responses of the S.G.H.W.R. to step inputs of power with the controller illustrated in Figure 3.10.

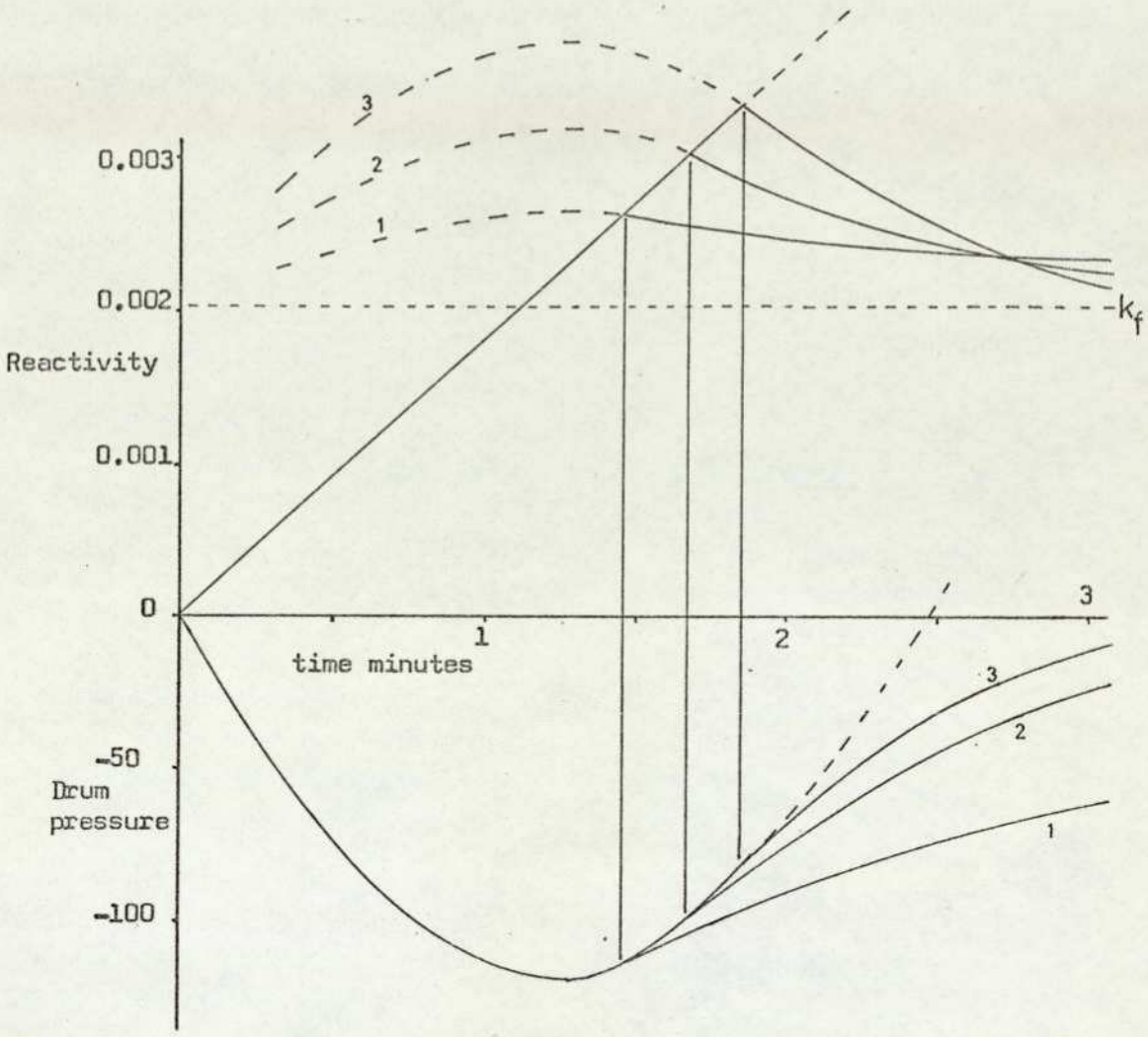


(a) Power increase to 95% causing saturation of turbine stop valve.



(b) Power increase to 90%.

Figure 3.12



Responses of the prototype S.G.H.W.R. with the adopted control scheme. Curves show reactivity input and drum pressure response for a reactor operating at 75% full load when subject to a 15% step increase. Reactivity levels of the trimming control are shown broken before switching occurs, the curves refer to controller gains (K_5 of Figure 3.10) as follows -

1. $K_5 = 0.5 \times 10^{-5}$
2. $K_5 = 1.0 \times 10^{-5}$
3. $K_5 = 1.5 \times 10^{-5}$

Trimming control curves are defined by -

$$k = k_f - K_5 \times p_d$$

Switching occurs when the reactivity level(initially increased at the maximum rate) intersects these curves.

4. PLANT MODELS, THEIR SIMULATION AND SOLUTION

4.1. The Dynamic Model

4.1.1 Dynamic Models Generally

It is appropriate to consider the dynamic model of the plant before the static model, as the latter consists largely of the dynamic model with all time derivatives of the variables set to zero. The dynamic model defines the relationships between the system variables (including outputs) and inputs during non steady state or transient conditions. It is used to determine the system's dynamic characteristics and performance, and to relate these to the design parameters. The normal state representation is used i.e.

$$\dot{\underline{x}} = f(\underline{x}, \underline{u}, t) \qquad 4.1$$

a series of first order differential equations, non linear and time varying in the general case. It is not normally possible to formulate the dynamic model directly in the form of 4.1, and it is more usual to represent the model in the form -

$$\dot{\underline{x}}_i = f_i(\underline{x}, \underline{u}, t) \qquad i = 1, m \qquad 4.2$$

$$\underline{x}_j = f_j(\underline{x}, \underline{u}, t) \qquad j = m + 1, n \qquad 4.3$$

for a system of n variables of order m. Equations 4.2 and 4.3 are a combination of non linear first order differential equations and non linear algebraic equations including transcendental equations. In the linear case 4.3 may be substituted into 4.2 to give 4.1, but for the non linear case it is not always possible to express $\underline{x}_j$ in 4.3 explicitly. For a linear system of order m with n variables equations 4.2 and 4.3 may be written in Matrix form -

$$\dot{\underline{x}}_i = A\underline{x} + B\underline{u} \qquad i = 1, m \qquad 4.4$$

$$0 = C\underline{x} + D\underline{u} \qquad 4.5$$

Where if there are r inputs the matrices A, B, C, D are of size -

$$A = m \times n$$

$$B = m \times r$$

$$C = (n - m) \times n$$

$$D = (n - m) \times r$$

the matrices A and C may be partitioned to give -

$$\dot{\underline{x}}_i = A_1 \underline{x}_i + A_2 \underline{x}_j + B\underline{u} \qquad i = 1, m \qquad 4.6$$

$$0 = C_1 \underline{x}_i + C_2 \underline{x}_j + D\underline{u} \qquad j = m + 1, n \qquad 4.7$$

Multiplying 4.7 by the inverse of C_2 eliminates $\underline{x}_j$ from 4.6 to give -

$$\dot{\underline{x}}_i = [A_1 - A_2 C_2^{-1} C_1]\, \underline{x}_i + [B - A_2 C^{-1} D]\, \underline{u} \qquad 4.8$$

which is the linear form of equation 4.1.

This may be solved by inversion in the normal way to give -

$$\underline{x_i} = \left[SI - \left[A_1 - A_2C_2^{-1}C_1\right]\right]^{-1} \left[B - A_2C^{-1}D\right]\underline{u} \qquad 4.9$$

where S is the Laplace operator.

With the remainder of the variables being found by substitution into 4.7. Solution of 4.9 will give a series of transfer functions between inputs and variables in the form -

$$\frac{x_i}{u_j} = \frac{Z_{ij}(S)}{P(S)} \qquad \begin{matrix} i = 1, m \\ j = 1, r \end{matrix} \qquad 4.10$$

where $Z_{ij}(S)$ and $P(S)$ are polynomials in S.

For a non linear system a formal solution of equations 4.2 and 4.3 is not normally possible and the system has to be simulated (by analog or numerical means) or linearised to determine the input-output relationships.

4.1.2 The S.G.H.W.R. Model

A dynamic model of the S.G.H.W.R. was based on the equations presented in (4.1), but these proved inadequate in some respects (as discussed below) and were supplemented from (4.2), a report describing a model of the S.G.H.W.R. used for a training simulator. For convenience the model is divided into six sub systems as follows -

(a) Neutronics and Reactivity
(b) Fuel Element Thermal
(c) Coolant Evaporation
(d) Recirculation Hydraulics
(e) Steam Drum
(f) Turbine Power Output

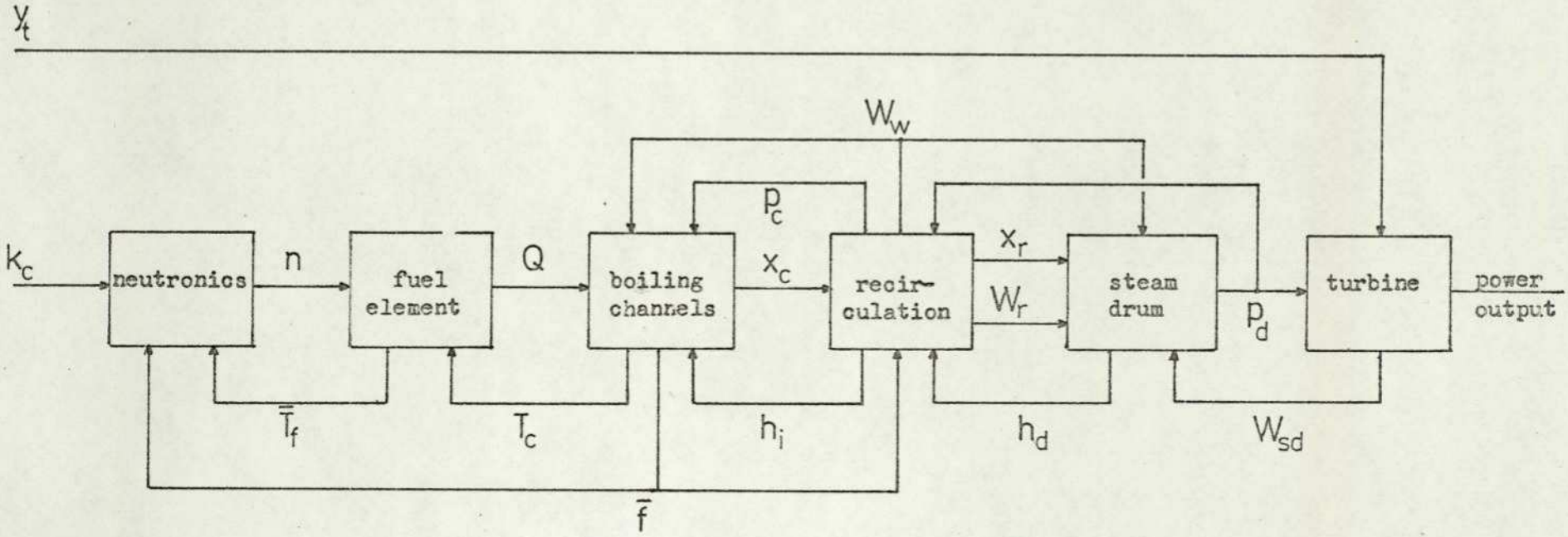
Interactions between these subsystems are shown in Figure 4.1. The condensing and feedheating subsystems are not modelled.

Each subsystem is considered in turn below, the relationships expressed by the dynamic model equations and the assumptions made in their formulation are discussed. A rigorous derivation of the equations is given in (4.2). The equations are listed in Appendix 3.

(a) Neutronics and Reactivity. Equations in this subsystem define the neutron flux level in the reactor. The flux is considered uniform throughout the reactor (i.e. as a point reactor), although it in fact falls both radially and axially towards the reactor boundaries. Originally reactivity changes due to fuel temperature and average channel voidage were modelled, but a coolant temperature reactivity coefficient was introduced

42 →

Figure 4.1



Interactions between subsystems of the S.G.H.W.R.

as it was found to be significant. Delayed neutrons are represented by two groups (of 6) with 'effective' concentration and decay coefficients.

(b) Fuel Element Thermal. Equations define the average fuel temperature and energy output. Fuel pins are represented by two zones of equal mass, an inner zone of circular section and an outer annular zone (4.5). At any instant the inner and outer zone temperatures are considered constant throughout the length of the fuel pins, and all pins are assumed to operate under identical conditions. Power output from all pins is, therefore, equal and uniformly distributed axially, which is consistent with the uniform neutron flux assumption (which also implies that power generation is uniform radially within pins). Thermal resistance between the fuel zones and between the outer zone and coolant determine the dynamics of the fuel pins.

(c) Coolant Evaporation. Equations for this subsystem define the coolant temperature, average channel voidage and the dryness fraction of steam leaving the boiling channels. To be consistent with the uniform power and temperature distributions in the fuel pins a constant fuel to coolant heat transfer coefficient and coolant temperature are required; the latter is taken as the saturation temperature at average channel pressure. Two regions are used in the analysis of the boiling process, a subcooled region and a boiling region, latent enthalpy in the latter is that corresponding to average channel pressure. Instantaneous equilibrium is assumed to exist between the boiling coolant and fuel during reactor transients.

(d) Recirculation Hydraulics. Equations define the circulatory flow rates and pressure drops in the pipework between the reactor core and steam drum. They also define the dryness fraction of steam entering the drum and the enthalpy of coolant entering the boiling channels. Two phase fluid friction theory assuming a constant slip is used to calculate pressure drops in the channels and risers (4.6). Initially no allowance was made in the model for the pressure drop resulting from the acceleration of the fluid in the boiling channels, where liquid partially evaporates in a constant section tube and its velocity increases appreciably; the model was altered to include this effect. A relationship between water density and temperature was also included as

this had a significant effect on the pressure drop in the liquid part of the circuit (downcomers). Flow was considered to be equally divided between all channels (and therefore risers), and between the four circulating pumps. Pump characteristics were represented by a quadratic function, and an instantaneous equilibrium assumed between the pump pressure rise and circuit pressure drop, i.e. fluid inertia is neglected. In fact the hydraulic loop has a time constant of a little over 0.1 seconds. Some coefficients of the recirculation subsystem equations were given as constants in the source documents, and for the present purpose have to be related to the design parameters. These are the friction factors for the risers, channels and downcomers, the riser and downcomer transport delays, and the volume of the riser pipework. The relationships are given in Appendix 3 (after the model equations) and are straightforward except for the friction factors, which are based on the D'Arcy postulate that the force required to drive liquid through a pipe is proportional to the product wetted area (wetted perimeter x length) and the velocity squared.

(e) Steam Drum. Drum model equations define the drum pressure, drum water enthalpy and the mass of liquid in the drum. Modelling of the steam drum presents little problem except for the evaporation-condensation exchange between the saturated liquid and saturated vapour; as pressure drops liquid evaporates, and as pressure rises some vapour condenses. The rates of evaporation or condensation are modelled by assuming that a layer of water exists in the drum which is in equilibrium with the vapour, mass exchange rates are then determined by an enthalpy balance (4.8). The proportion of drum water considered to be in equilibrium with the vapour does not have a very significant effect on drum pressure transients (4.1), this is because a large proportion of the liquid in the drum is suspended in the vapour space prior to separation. There are many effects not accounted for in this representation (droplet falling time and bubble rise time, for example) but in practice it is satisfactory if pressure changes are not too violent. The remainder of the drum model consists of a hydraulic mixing process and wet steam capacitance both represented as first order. Vapour-liquid separation is deemed perfect at all times. The prototype S.G.H.W.R. has, in fact,

two steam drums, these are considered in combination.

(f) Turbine Power Output. Power output of the turbine is related very closely to the steam consumed since the available energy (via Willans line) is not affected greatly by supply (i.e. drum) pressure (4.2). There is a lag between flow increase and power increase, this is approximately first order with a time constant of a little under 0.5 seconds and is ignored. Steam flow is proportional to the product of drum pressure and stop valve position, the flow is supercritical and is therefore unaffected by back pressure.

The assumptions made in formulating the model appear quite sweeping, especially the uniformity of neutron flux, power fuel temperature and coolant temperature in the reactor core and the over-simplified drum model. Justification of the assumptions is made to a certain extent in (4.1 & 4.2) and is based on experience gained on previous models when compared with real plant or rigs, or on the comparison of responses generated from complete (relatively) and simple models of the same plant. Earlier models of the S.G.H.W.R. split the channel boiling region into a number of zones and represented boiling dynamics (4.7); this approach was abandoned in later models as it was found to make little difference to predicted transients and considerably increased the model size. A direct comparison of the model and S.G.H.W.R. prototype responses was not possible since prototype transients were not available.

4.1.3 Solving the Dynamic Model.

Generating dynamic responses from non-linear equations is very time consuming, and since the responses would be required many times during the optimisation procedure it was necessary to use a faster method to analyse plant dynamics even if this meant losing some accuracy. A two stage linearisation process was devised to achieve this aim. The dynamic model equations were first linearised and solved in the manner indicated in section 4.1.1 to give the system poles, and zeroes of selected transfer functions. These poles and zeroes (the roots of the polynomials of equation 4.10) were then related by sensitivity coefficients to the design parameters, this being the second linearisation stage. A normalised sensitivity matrix S (normalised Jacobian) was formed whose elements were -

$$S_{ij} = \frac{\partial P_i}{\partial p_j} \cdot \frac{p_{jo}}{P_{io}} \qquad 4.11$$

Where P_{io} is the reference value of the i^{th} pole (or zero) and p_{jo} the reference value of the j^{th} design parameter. The normalised form is used because the figures produced are more meaningful. If P_i is complex then S_{ij} is also complex.

Assuming that the effects of design parameter changes may be linearly superimposed, the shift of a system pole is given by -

$$\frac{\delta P_i}{P_{io}} = \sum_{j=1}^{n} S_{ij} \cdot \frac{\delta p_j}{p_{jo}} \qquad 4.12$$

where there are n parameters. For all poles -

$$\left(\frac{\delta P}{P_o}\right) = [S]\left(\frac{\delta p}{p_o}\right) \qquad 4.13$$

where $\left(\frac{\delta P}{P_o}\right)$ is the normalised vector of pole shifts and $\left(\frac{\delta p}{p_o}\right)$ the normalised vector of parameter changes.

The position of a pole is given by -

$$P_j = P_{jo}\left(1 + \frac{\delta P_i}{P_{jo}}\right) \qquad 4.14$$

or for all poles -

$$\underline{P} = [P_o]\left(\underline{u} + \left(\frac{\delta P}{P_o}\right)\right) \qquad 4.15$$

where $\underline{u}$ is the unit vector, and $[P_o]$ is a matrix with the reference poles on the diagonal.

Equations 4.13 and 4.15 relate the system poles and zeroes (and therefore system dynamics) to the design parameters using standard matrix algebra. There are obviously limits to the departure from the starting point which can be made using this method before excessive errors result. This topic is discussed when considering constraints in section 5.

The linearised dynamic model equations and signal flow graphs for the S.G.H.W.R. are listed in Appendix 4, the linearisation is quite straightforward except that the riser transport delay has been represented by a first order lag and the downcomer delay by a second order Pade approximation. A first order lag was considered adequate for the riser delay because slip and turbulence effects tend to spread the delaying action (4.1). The validity of the linearised dynamic model in representing the dynamic behaviour of the plant was verified using an analog simulation of the linearised model and comparing responses with those of the training simulator at

Winfrith (4.3). It was during these tests that the inadequacies of the original model (see section 4.1.2) were observed and rectified. The results indicated a satisfactory degree of correlation between the linearised and non-linear models, Figure 4.2, and also that for the type of inputs experienced the second order approximation to downcomer delay gave a very good representation. Details of the analog configuration are given in Appendix 10.

Calculation of the sensitivity matrix was in three stages -

(a) Calculate the linear model coefficients after changing a design parameter.

(b) Calculate the modified poles and zeroes.

(c) Using the reference and modified poles and zeroes and the change in design parameter calculate the sensitivity coefficient.

The first stage was carried out at The City University (T.C.U.). Coefficients of the linear dynamic model are functions of the design parameters and the steady state variables (see Appendix 4). On changing a design parameter then, the steady state model had to be re-solved (see section 4.2) before the coefficients could be calculated. Parameters were varied by $\pm$ 10% and the effects on the coefficients averaged.

Coefficients of the reference and modified models were processed by the U.K.A.E.A. Winfrith programme ZIP (4.4) to solve the system poles and zeroes. This is a powerful programme which executes the procedure outlined in section 4.1.1 of eliminating the algebraic equations from a mixed algebraic, differential set, and then effectively factorising the polynomials of equation 4.10.

The final stage of the matrix calculation was carried out at T.C.U. The resulting sensitivity chart is shown in Appendix 7, this includes sensitivity coefficients for the static and dynamic gains of the system, zero sensitivities are not shown as they are not meaningful directly. Reference condition poles and zeroes for some transfer functions are shown in Figures 4.3 to 4.7.

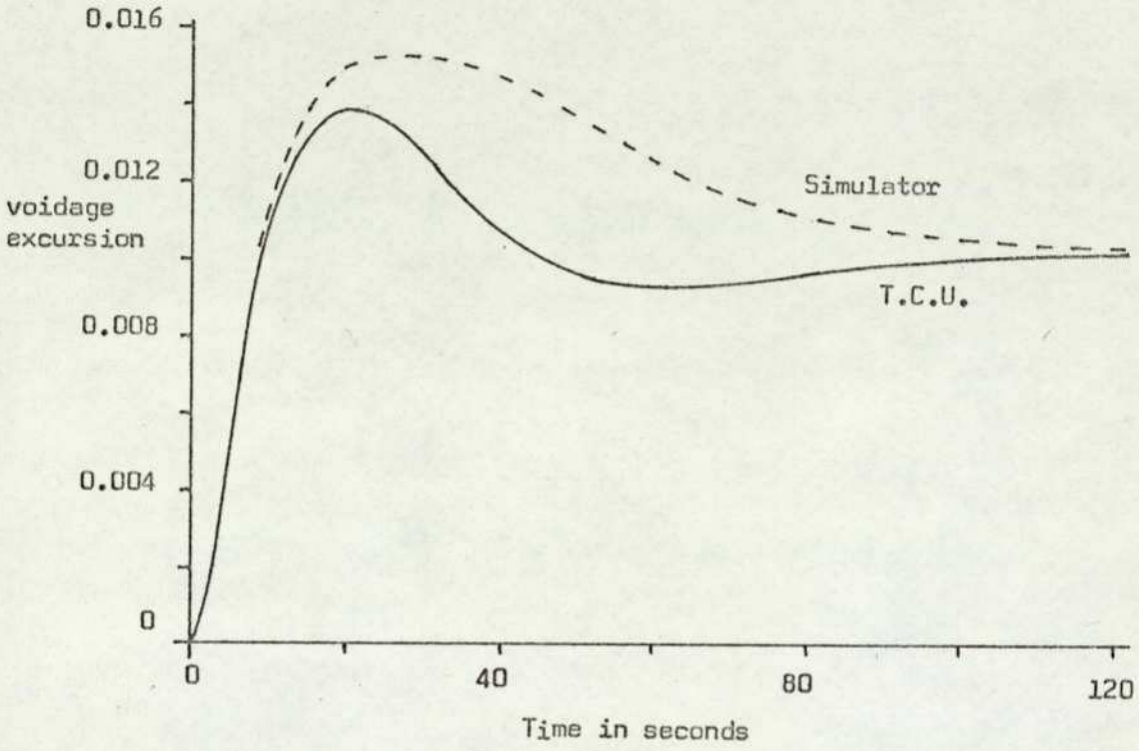
A direct method of calculating sensitivity coefficients by repeated factoring of the numerator and denominator polynomials or matrices was adopted because of the availability of ZIP. There are methods for determining the sensitivity of an eigenvalue to a change in the matrix without re-solving the matrix (4.9 - 4.11). To employ these methods the algebraic equations of the set must be eliminated, and certain manipulations carried out to create the zero (numerator) matrices, both these procedures are contained in ZIP. Also ZIP is a

54 →

Figure 4.2

Comparison of responses of the S.G.H.W.R. simulator and the T.C.U. linear model. Transients are due to a 5% opening of the turbine stop valve in 5 seconds.

(a) Channel average voidage $\bar{f}$



(b) Fuel to coolant heat flux Q.

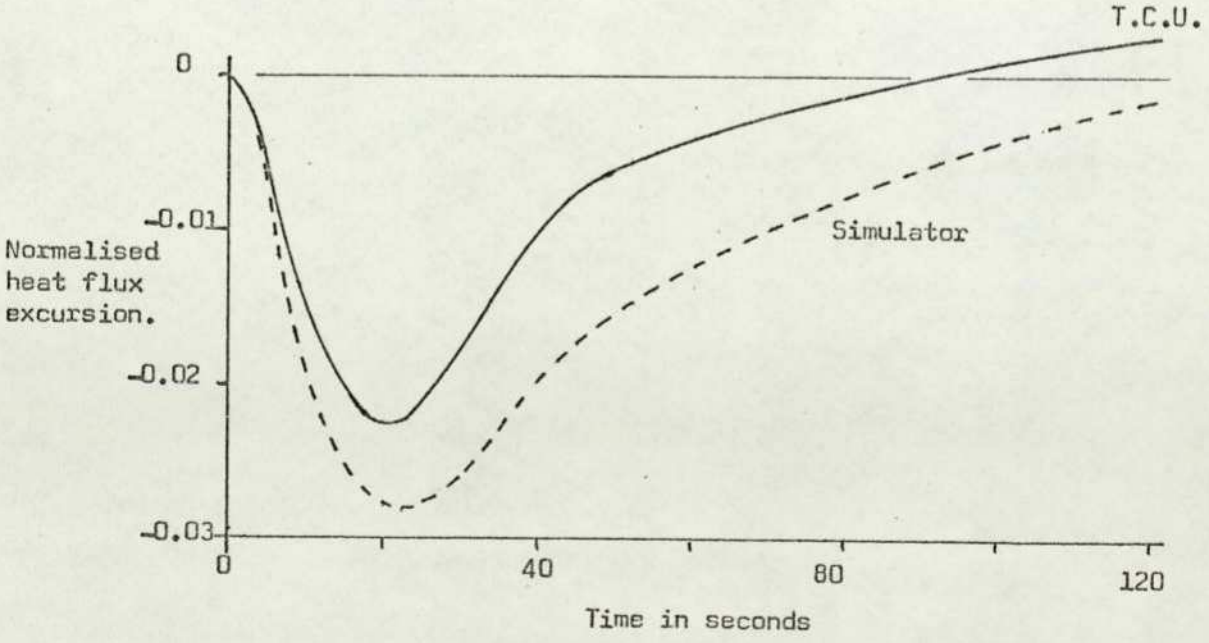


Figure 4.2 (continued)

Curves (a) and (b) above represent the worst case of comparison between the simulator and T.C.U. models. The error in voidage fraction is due more to the different values of slip coefficient used in the two models than to error produced in linearisation. For the simulator channel slip = 1.275 at exit while 1.6 is used in the T.C.U. model. The voidage error is transferred via the voidage reactivity coefficient to neutron flux and reactor power (heat flux).

(c) Drum exit and channel inlet enthalpy responses illustrating the adequacy of the second order approximation to downcomer delay. Delay = 6 seconds.

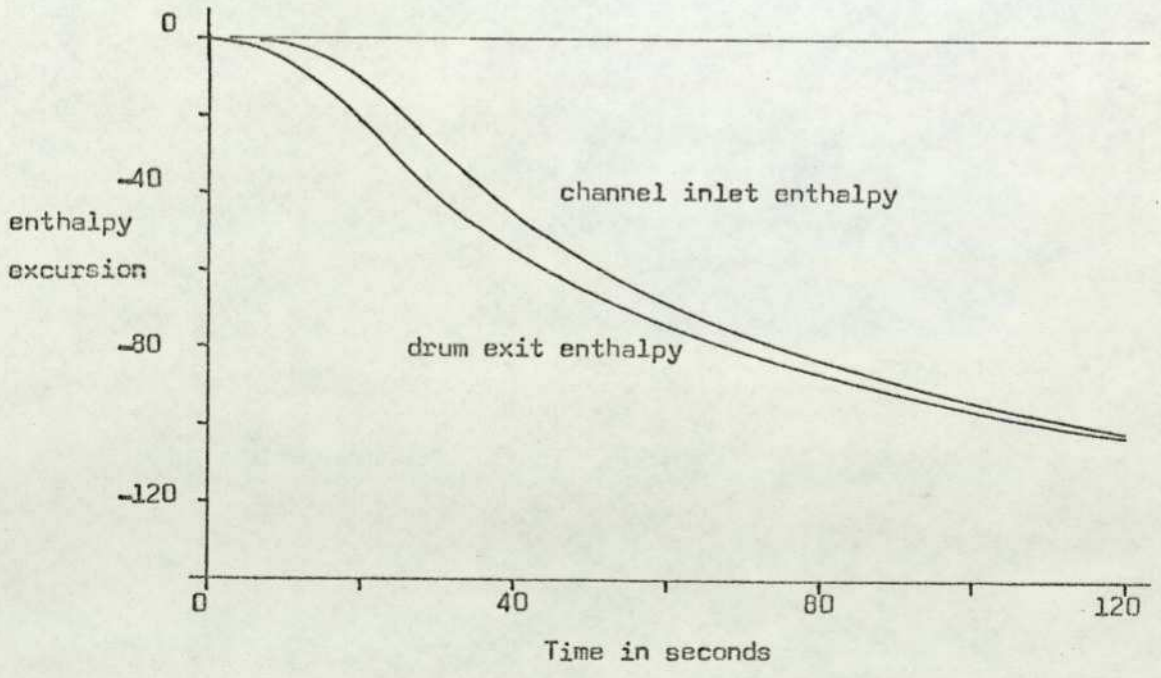
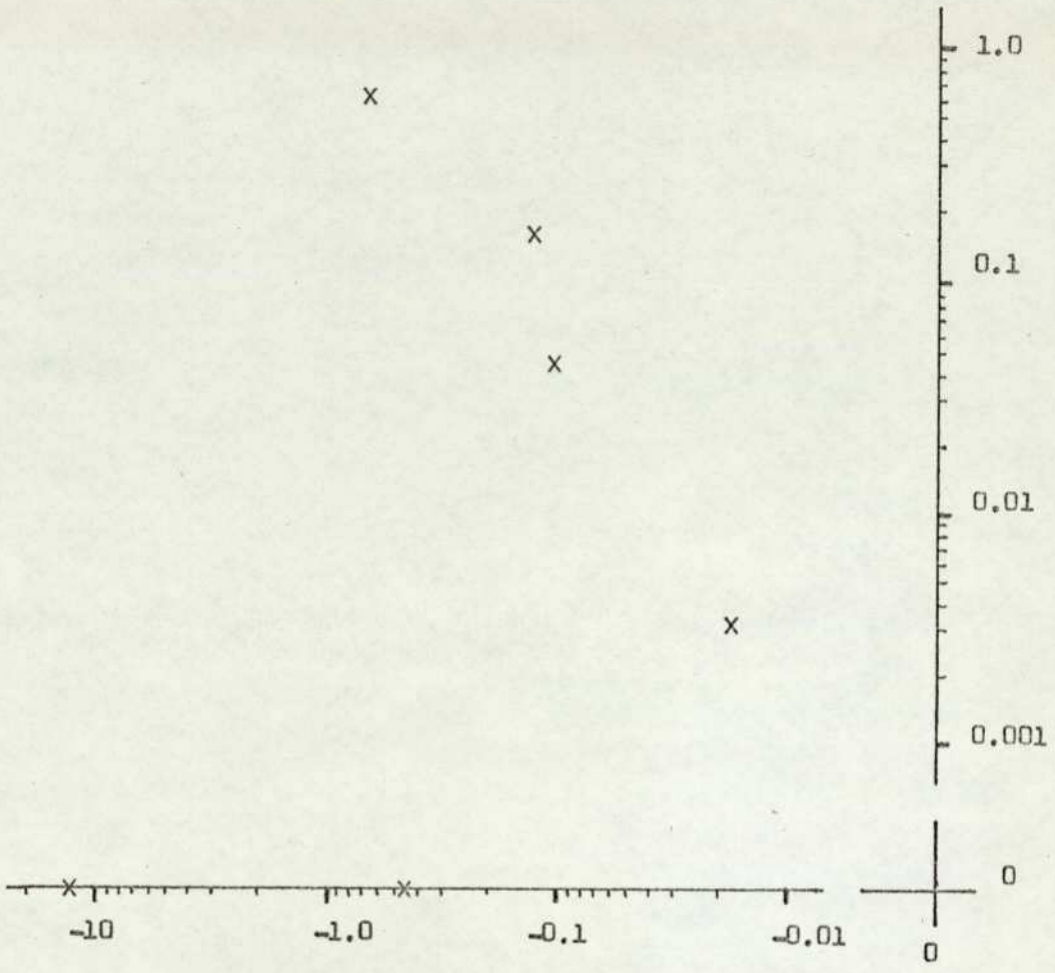


Figure 4.3

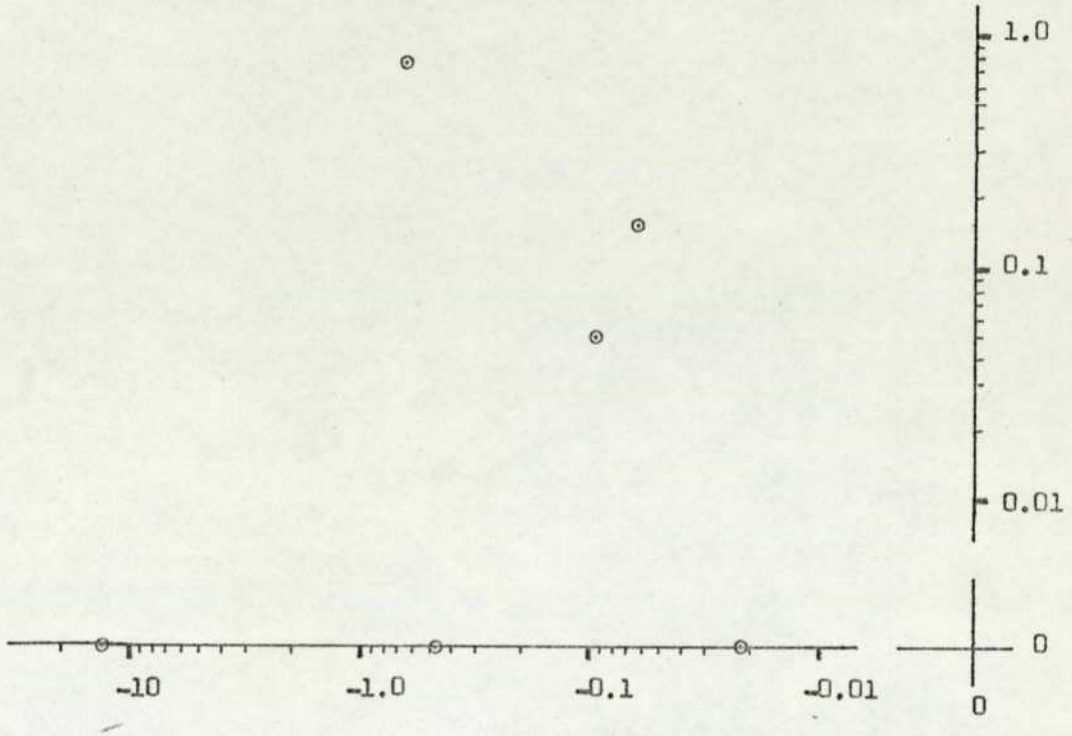
Poles of the S.G.H.W.R. reference design dynamic model.



-0.01871	±	0.003147 j
-0.10154	±	0.04902 j
-0.12180	±	0.15126 j
-0.48896		
-0.64254	±	0.63488 j
-12.774		

Figure 4.4

Zeroes of the turbine stop valve to drum pressure transfer function for the reference design S.G.H.W.R.



-0.02089

-0.06519 ± 0.15105 j

-0.09291 ± 0.04927 j

-0.48432

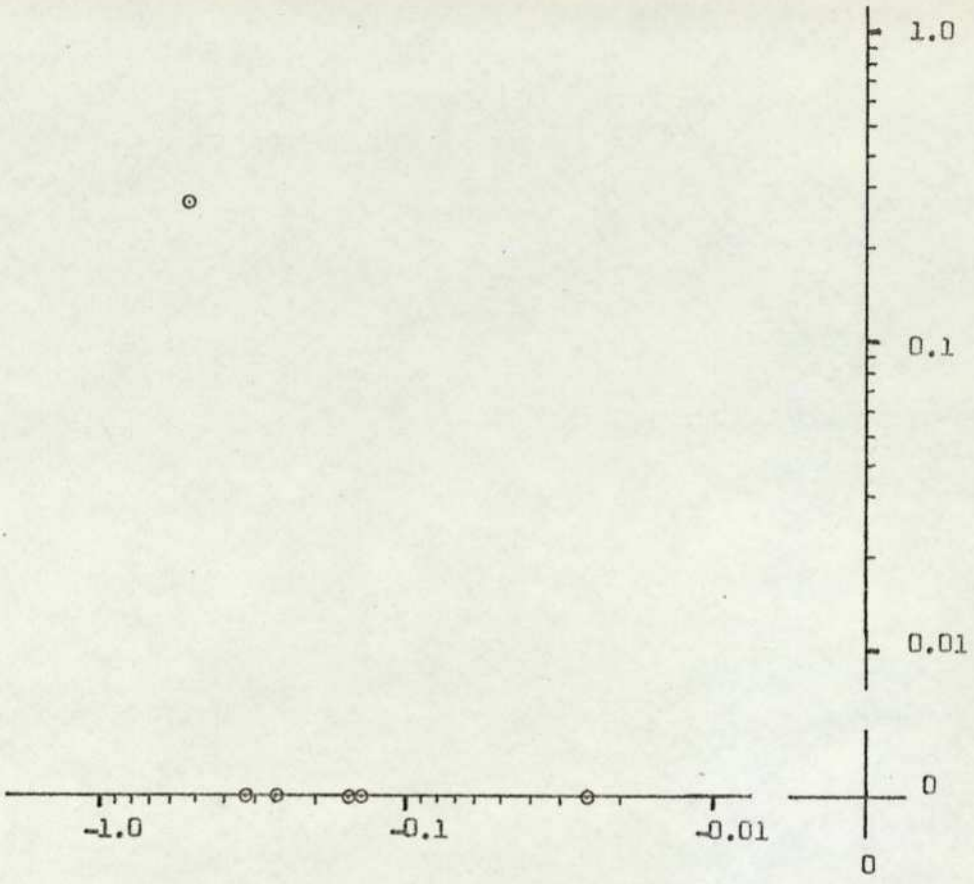
-0.60935 ± 0.76405 j

-12.78

static gain of transfer function = 1194.7

Figure 4.5

Zeroes of the control reactivity to drum pressure transfer function for the reference design S.G.H.W.R.

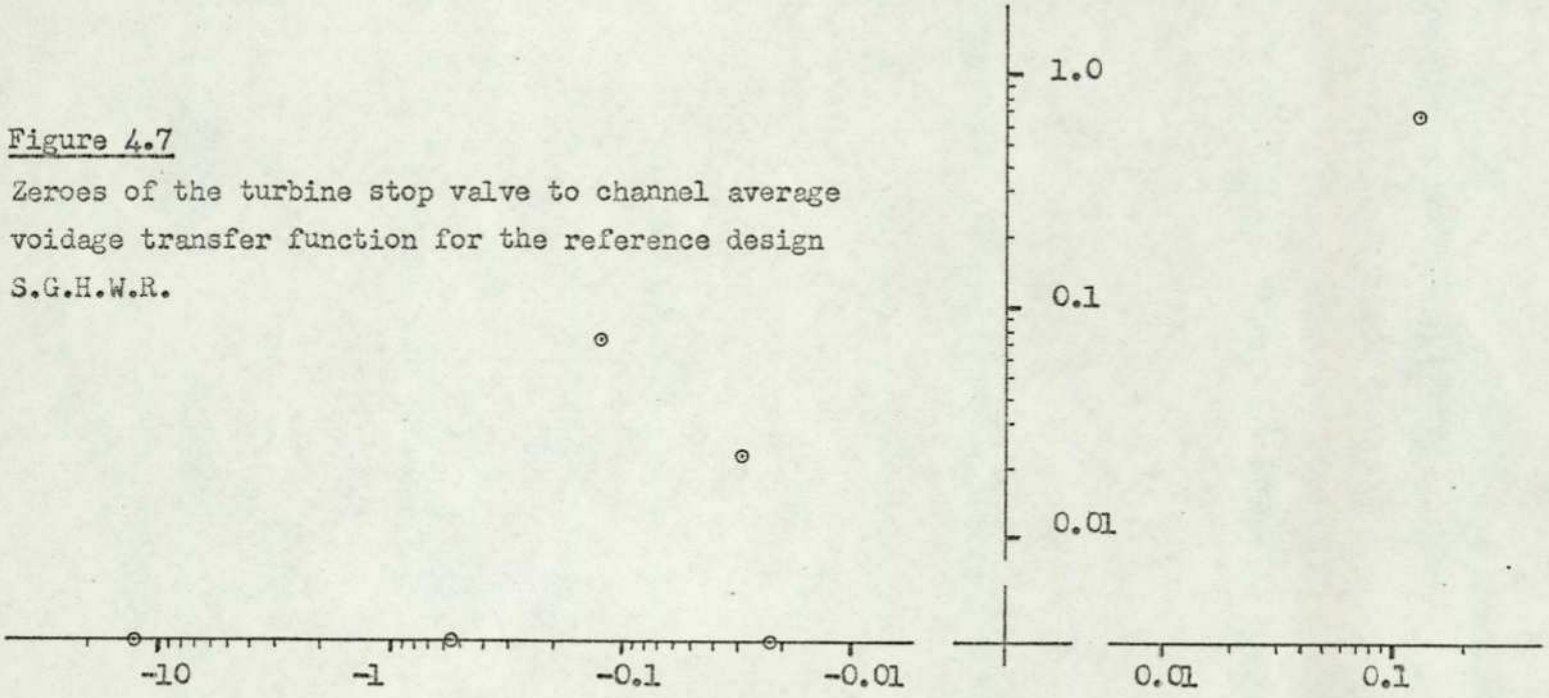


-0.0240
-0.13991
-0.15000
-0.25699
-0.31904
-0.47391 ± 0.26869 j

static gain of transfer function = 88420.2

Figure 4.7

Zeroes of the turbine stop valve to channel average voidage transfer function for the reference design S.G.H.W.R.

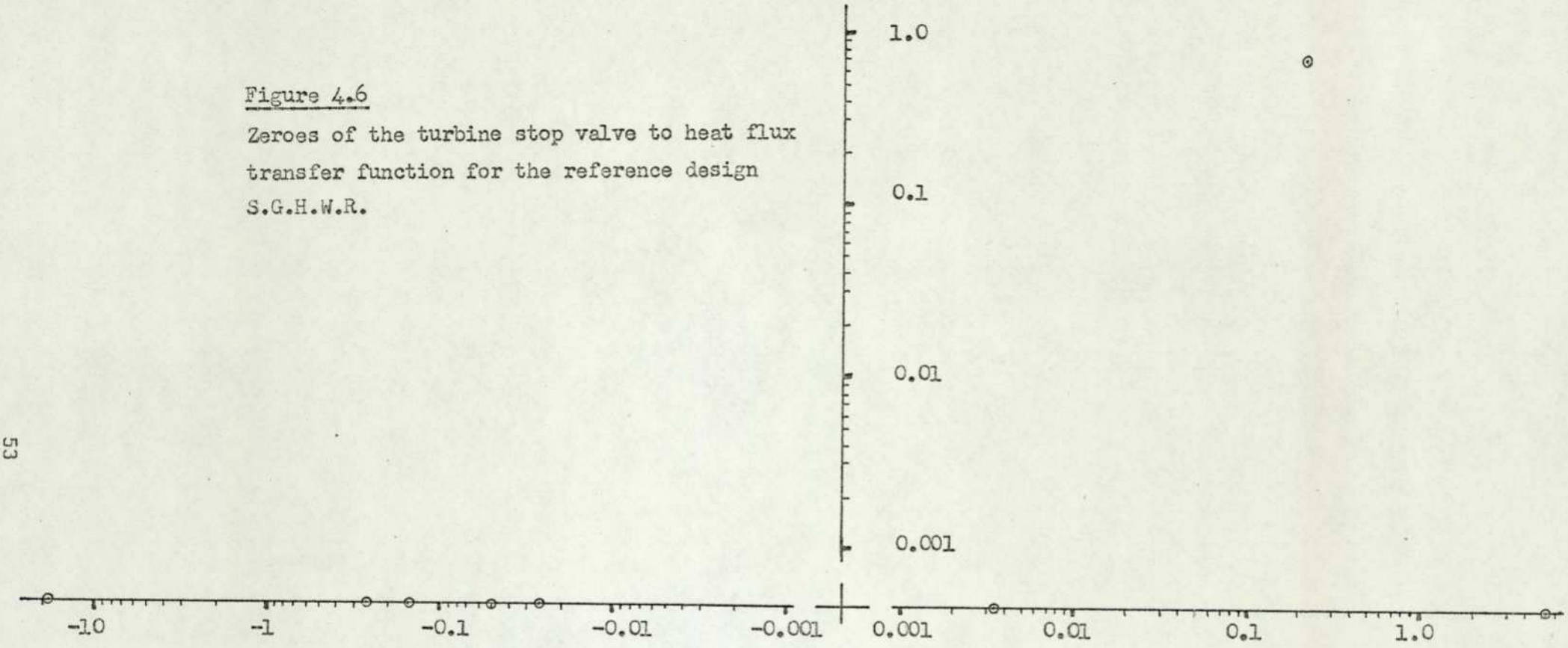


$0.12755 \pm 0.68052\ j$
-0.021725
$-0.029267 \pm 0.022315\ j$
$-0.116716 \pm 0.07283\ j$
-0.54933
-12.966

Static gain of transfer function = 0.2472

Figure 4.6

Zeroes of the turbine stop valve to heat flux transfer function for the reference design S.G.H.W.R.



5.1608
0.21173 ± 0.71004j
0.003678
-0.02451
-0.04995
-0.14596
-0.256988
-19.500

Static gain of transfer function = 178124.2

well proven programme, whereas the use of an indirect sensitivity calculating method although theoretically faster would have involved the development of a new programme.

Pole - zero sensitivity methods have been used in power system analysis, both for stability and controller design (4.12) and for studying the effects of parameter variations (4.13).

4.2. Static Models

4.2.1 Static Models Generally.

Static models of the system define the relationships between the system variables and inputs when the system is operating in the steady state. In general the model will be a set of non-linear algebraic equations, whose coefficients are functions of the system parameters, and whose form depends upon the system structure. A subset of the static model is obtained by setting all the time derivatives in the dynamic model to zero, this will not be the complete model however as there will usually be some variables of interest in the steady state but not transiently. For instance, operational efficiency will often be of importance only in the steady state if transient conditions exist only for short periods during the system's life, in such cases an expression for efficiency would not be included in the dynamic model. Equations will therefore be needed in addition to the zero time derivative dynamic model to complete the static model.

The static model is used in relating those parts of the utility function or constraints formulated in terms of static performance (steady state variables) to the design parameters. Also if, as in the present study, a linearised dynamic model is used to generate system transients the solution of the static model is required to calculate the dynamic model coefficients.

4.2.2 Static Model for the S.G.H.W.R.

The majority of the static model was obtained as described above from the non-linear dynamic model with time derivatives set to zero. The equations are not therefore presented separately (the non-linear dynamic model is presented in Appendix 3). Additional equations were required to define the reactivity change resulting from the alteration of some design parameters. The use made of this information is described when the formulation of the utility functions is dealt with in section 5, but it determines the total energy output available from a given quantity of fuel and is therefore somewhat analogous to the operating efficiency equation for a conventional power station.

Two effects contribute to the reactivity surplus or deficit resulting from the change of a design parameter. Firstly, when a parameter change is made the steady state equilibrium conditions of the reactor are altered including the fuel and coolant temperatures and the average channel voidage. These changes acting through the reactivity coefficients cause a reactivity change from the reactivity equation (equation 4, Appendix 3) -

$$\delta k = K_v \delta \bar{f} + K_T \delta \bar{T}_f + K_{Tc} \delta T_c \qquad 4.16$$

where $\delta \bar{f}$ etc. represent the changes in the steady state value of $\bar{f}$ etc. due to a parameter change. This effect is quite straightforward and relies only upon the solution of the steady state model. The second effect is more difficult to represent as it concerns the relative quantities of fuel, absorber and moderator in the reactor and the relative neutron escape rate. Equation 3.10 expressed the effective reactivity as -

$$K_{eff} = pf\eta_e\varepsilon(1-l) \qquad 4.17$$

The reference values of the factors in this equation may be determined from the neutron absorption data presented in Table 4.1. This data refers to the S.G.H.W.R. prototype operating at full power, and was obtained from Winfrith (4.14). The proportional absorption of total and thermal neutrons by the fuel, moderator, coolant and the various structural materials are shown. Figures are average values for all boiling channels.

The five factors of equation 4.17 depend upon the reactor configuration and material balance in quite complex ways and an exact representation is beyond the scope of this project. Described below are approximate relationships between the factors and the design parameters, the assumptions made are indicated and where possible an assessment of the accuracy expected is given.

Fast fission factor ε depends chiefly on fuel enrichment, but it is only slightly greater than unity (1.03) and for the range of enrichment under consideration remains essentially constant.

Resonance escape probability p is a function of the fuel (or fast neutron absorber) to moderator ratio and may be expressed as -

$$p = e^{\frac{-A^1}{\Sigma_s N_m \xi}} \qquad 4.18$$

where A^1 is the resonance escape integral, Σ_s the macroscopic scattering cross section of the moderator, ξ the logarithmic energy decrement of the moderator and N_m the molecular ratio of moderator to fuel. Moderating effects of fuel, coolant and other materials

57 →

Table 4.1

Neutron absorption data for the S.G.H.W.R. prototype at full power.

Region	Material	Description	Proportion of all Neutrons absorbed	Thermal Neutrons absorbed
1	H_2O		0.000709	0.000652
2	Zr	Inner row of six	0.000363	0.000190
3	H_2O		0.000663	0.000607
4	UO_2	fuel pins.	0.110193	0.073906
5	Zr		0.001085	0.000519
6	H_2O	Middle row of	0.002425	0.002175
7	UO_2	twelve fuel pins.	0.247668	0.174836
8	Zr		0.002365	0.001226
9	H_2O	Outer row of	0.010040	0.009302
10	UO_2	eighteen fuel pins.	0.483457	0.364672
11	Zr		0.004374	0.002555
12	H_2O	Support pin.	0.017388	0.016430
13	H_2O		0.007932	0.007595
14	Zr	Pressure tube.	0.021385	0.014837
15		Gap between 14 & 16		
16	Al	Calandria tube	0.023536	0.021936
17	D_2O	Moderator	0.041876	0.040691
18	Al	Displacer tube	0.010941	0.010322
19	D_2O	Moderator	0.013641	0.013266
Total for fuel			0.8413	0.6134
Total			1.0	0.7556

The difference between the final two columns is the proportion of fast neutrons absorbed in each region.

should be considered for completeness, but these are dominated by the moderator proper. For heavy water $\Sigma_S = 10.7$ and $\xi = 0.51$, 4.18 therefore becomes -

$$p = e^{\frac{-A^1}{5.457 N_m}} \qquad 4.19$$

For heterogeneous reactors A^1 may be estimated by an equation of the form (4.15) -

$$A^1 = A\left(1 - \frac{\frac{\mu}{A}}{\frac{M}{S} + \lambda_o}\right) \qquad 4.20$$

where $$\lambda_o = \frac{\mu}{A_\infty - A} \qquad 4.21$$

and $\frac{M}{S}$ is the mass to surface area ratio of the fuel. A_∞ is the value of the resonance escape integral for an infinite moderator to fuel ratio (= 290 for U_{238}), and A and μ are functions of the scattering cross section per atom of fuel within the fuel (as opposed to moderator scattering which is external to the fuel). In the S.G.H.W.R. the internal scattering is provided by the uranium itself and the oxygen atoms in the UO_2 fuel. Figure 4.8 is a plot of the functions A and $\frac{\mu}{A}$ for diluted U_{238} (4.15). Using this data equations 4.20 and 4.21 reduce to -

$$A^1 = 11.5\left(1 + \frac{2.1}{\frac{M}{S} + .0826}\right) \qquad 4.22$$

In this equation $\frac{M}{S}$ is required in g/cm^2 and for the S.G.H.W.R. fuel pin design is a function of pin diameter only, for a fuel density of 10.5 g/cm^3 -

$$\frac{M}{S} = 2.625\ d \qquad 4.23$$

For the reference condition -

$$A^1 = 17.74 \text{ barns} \qquad 4.24$$

which when substituted into 4.19 gives -

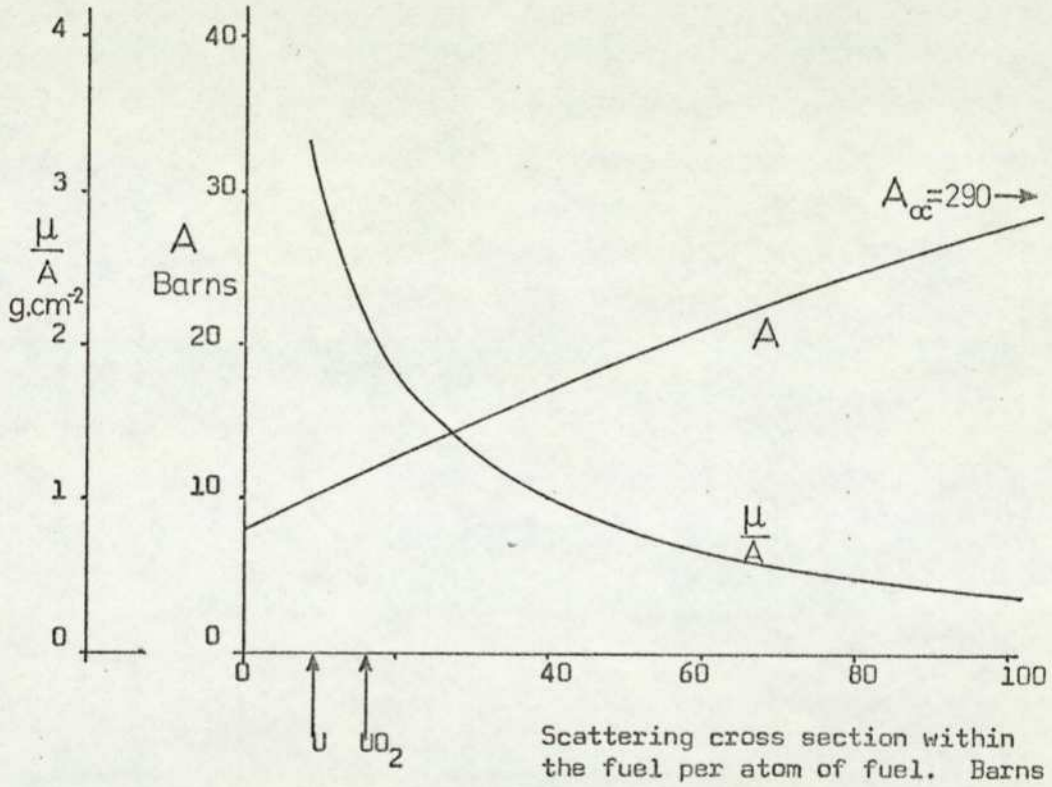
$$p = e^{\frac{-3.252}{N_m}} \qquad 4.25$$

Table 4.1 indicates that 0.7556 of all neutrons absorbed reach thermal energies before absorption. The reference value of p is therefore 0.7556, giving a reference value of 11.59 for N_m corresponding to a quantity of moderator which would be contained within a cylinder of 10.7 ft. diameter around the reactor core, i.e. a cylinder just clearing the outer boiling channels. Moderator quantity would be

59 →

Figure 4.8

Coefficients used in equation 4.20 for estimating the resonance escape integral in heterogeneous reactors.



reduced very slightly if the moderating effect of other materials was considered. The value of p given by equation 4.25 considers variations of fast neutron absorption by the fuel only, these comprise 0.935 of all fast neutrons absorbed. Some precision is also lost in averaging absorption over all fuel rods, in fact the inner fuel rods absorb relatively more high energy neutrons. This effect will be present in all modified designs and little inaccuracy results.

To estimate N_m the volumes of moderator and fuel must be related to the design parameters, relative values are -

$$V_f = l_c n_b N_b d^2 \times 0.00992 \qquad 4.26$$

$$V_m = l_c N_b (1 - 2.5 d_c^2) \times 0.001381 \qquad 4.27$$

In 4 .27 it is assumed that the calandria area is proportional to the number of boiling channels. This leads to an expression for N_m -

$$N_m = \frac{(1 - 2.5 d_c^2)}{n_b d^2} \times 1.617 \qquad 4.28$$

Equations 4.19, 4.22, 4.23 and 4.28 enable p to be related to the design parameters.

Thermal utilisation factor f is the ratio of thermal neutrons captured by the fuel to those captured by all other reactor materials including coolant and moderator. For a uniform neutron flux it may be expressed in terms of the macroscopic absorption cross sections -

$$f = \frac{\Sigma_f}{\Sigma_f + \sum \Sigma_a} \qquad 4.29$$

For the reference condition the distribution of thermal neutron absorption is shown in Table 4.1. Using these figures as a basis an expression for f based on the volumes of fuel and absorber relative to the reference design may be formulated -

$$f = \frac{.61342 V_f}{.61342 V_f + .03226 V_{al} + .01933 V_{zr} + .03686 V_c + .05396 V_m} \qquad 4.30$$

where V_f, V_m, V_{zr}, V_{al}, V_c are the relative volumes of fuel, moderator, zirconium, aluminium and coolant. V_f and V_m are defined by equations 4.26 and 4.27, the remainder may be expressed in terms of the design parameters as -

$$V_{zr} = 0.00487 d_c^2 N_b l_c \qquad 4.31$$

$$V_{al} = 0.00199 d_c N_b l_c \qquad 4.32$$

$$V_c = 0.00985\, N_b (d_c^2 - (n_b + 1)d^2)\, l_c \qquad 4.33$$

It is assumed in 4.31 that the pressure tube thickness is proportional to its diameter to maintain stress levels. In 4.32 the thickness of the aluminium calandria tube is assumed constant. In 4.33 voidage coefficient is assumed constant, voidage changes are accounted for by equation 4.16. The coefficient of V_f in equation 4.30 will vary slightly with fuel enrichment but the effect is small for the range of enrichment of interest, and is further reduced as the denominator of 4.30 is dominated by the coefficient of V_f.

The multiplication factor η_e is a function of fuel enrichment, represented in the present study by fuel rating (R) or the amount of power produced by a given neutron flux in a given quantity of fuel (which is proportional to enrichment). On average 2.46 neutrons are ejected per U_{235} fission, therefore η_e will be 2.46 times the proportion of neutrons within the fuel which cause thermal fission in U_{235}. The proportion causing fission is a function of the absorption and fission cross sections; thus -

$$\eta_e = \frac{N_{235}\,\sigma_f \times 2.46}{N_{235}(\sigma_a + \sigma_f)_{235} + N_{238}\,\sigma_{a238} + \sum N_a \sigma_a} \qquad 4.34$$

where N_{235}, N_{238} and N_a are the relative number of atoms of U_{235}, U_{238} and absorbers in the fuel, and σ_a and σ_f are their absorption or fission microscopic cross sections.

If e is the enrichment in atoms of U_{235} to atoms of $U_{235} + U_{238}$ this reduces to -

$$\eta_e = 2.46\, \frac{e\,\sigma_f}{e\,(\sigma_f + \sigma_a)_{235} + (1 - e)\sigma_{a238} + \sum \frac{N_a}{N_{238}} \sigma_a} \qquad 4.35$$

where $\sum \frac{N_a}{N_{238}} \sigma_a$ represents the contribution of the fission product poisons and other fuel dilutants. For the reference design $\eta_e = 1.63$, (calculated from equation 4.17 when all other factors are known) which when substituted in equation 4.35 with the values of cross sections and reference enrichment (2%) the value of $\sum \frac{N_a}{N_{238}} \sigma_a$ is given as 0.93. If the poison and dilutant contributions are assumed constant (which is reasonable) and the cross section values are substituted; equation 4.35 becomes -

$$\eta_e = \frac{2.46 \times 582 \times e}{694_e + 2.73(1 - e) + .93} \qquad 4.36$$

This is the equation used for multiplication factor, the enrichment being related to fuel rating by -

$$e = 0.003705R \qquad 4.37$$

Finally the neutron escape or leakage factor l must be considered. For a given neutron flux the total neutron population depends upon the reactor volume, and the leakage on the surface area. Leakage factor then is a constant times the ratio of area (A) to volume (V) -

$$l = K \frac{A}{V} \qquad 4.38$$

where K depends upon the reflector and shielding characteristics. Taking the areas and volume relative to the reference design which has a 4% leakage -

$$l = 0.04 \frac{A}{V} \qquad 4.39$$

Relative area and volume may be expressed in terms of the design parameters as follows -

$$A = (2N_b + 3.67\, l_c \sqrt{N_b}) \times 0.001532 \qquad 4.40$$

$$V = N_b\, l_c \times 0.00081 \qquad 4.41$$

where in 4.40 reactor area is assumed proportional to the number of boiling channels.

An assessment of the accuracy of this relatively crude method of estimating leakage factor may be seen by examining the effect of moderator height on reactivity in the prototype. Here increasing moderator height increases the active reactor volume proportionally but has no effect on the leakage area and fuel to moderator or fuel to absorber ratios (assuming as usual an homogeneous uniform flux reactor). Reactivity increase then is mainly a function of leakage factor and a comparison of that calculated by 4.39 and by accurate methods is shown in Figure 4.9, the accurate curve is from (4.2).

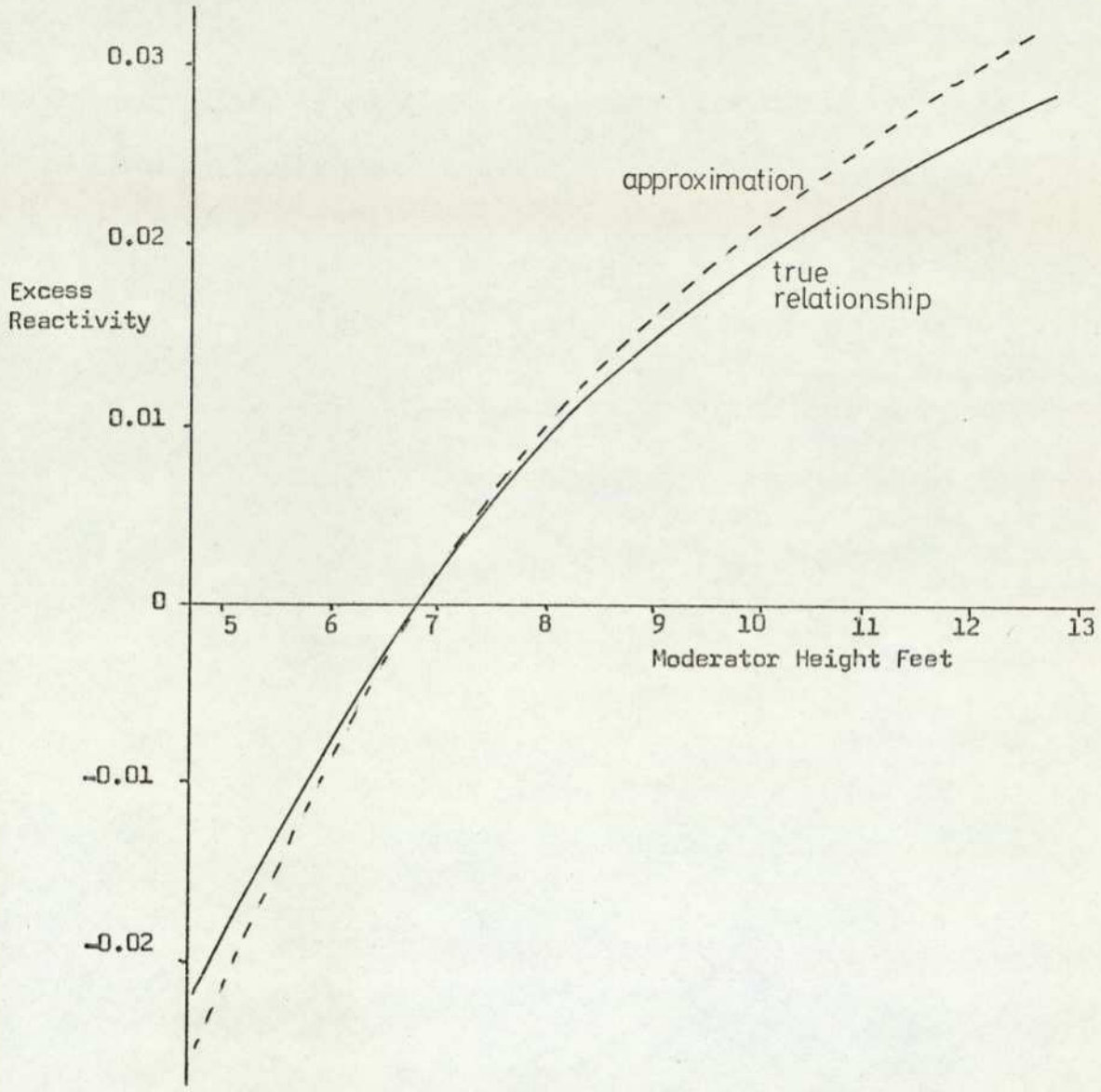
Equations 4.16 to 4.41 enable the reactivity deficit or surplus resulting from parameter change to be estimated. Apart from 4.16 the equations are explicit in the design parameters and do not depend upon the solution of the part of the static model derived from the dynamic model. A summary of the reactivity balance equations is listed in Appendix 5.

4.2.3 Solution of the Static Model.

Solution of the non-linear static model was by a multivariable Newton-Rapheson method, using the reference conditions as a starting point for the solution. The programme called NONLIN2 is described in Appendix 8. Some of the coefficients of the model were functions of the steam pressure-temperature, pressure-enthalpy or pressure-

63 →

Figure 4.9



Comparison of exact and approximate representation of reactivity changes due to changes in moderator level. In the approximate representation neutron leakage is assumed proportional to reactor surface area, and neutron population proportional to reactor volume. For the curve shown reactor area is constant and volume is proportional to moderator height, leakage rate l is inversely proportional to height and reactivity is proportional to $(1 - l)$. The approximate curve is based on zero excess reactivity at a height of 6.85 ft. to correspond with the exact curve from (4.2), and a leakage of 4% at a reactor height of 12 ft.

i.e. $k_{eff} = 1.075 \left(1 - \frac{0.48}{h}\right)$

density relationships and their derivatives. These relationships were represented by 20 element arrays of values taken from steam tables and a Bessel interpolation and derivative interpolation routine used to extract the required values, see subroutine INTERP Appendix 8.

In solving the static model reactor power was normalised to 100MW by assuming sufficient reactivity was inserted or taken out, this is discussed further in section 5 on utility function formulation. Coefficients of the linear dynamic model were calculated as a part of the static model solution.

It was convenient to relate the static values of the plant variables in equation 4.16 to the design parameters by sensitivity coefficients, in the same way as dynamic characteristics were. This precluded solving static model during the optimisation process, the actual relationships between reactivity and design parameters (the contribution from 4.16 only) and the linear approximations used are shown in Figures 4.10 and 4.11. The equations resulting from the use of sensitivity coefficients on 4.16 are listed in Appendix 5.

4.3 The Cost Model

The cost model of a system is a set of equations which define the cost of purchasing, manufacturing and erecting the system in terms of the system parameters. Cost can usually be expressed explicity. In many cases it is much easier to express marginal costs as a function of the parameters, rather than absolute costs, which is all that is required. Also the only part of the total cost which is of interest is that part affected by the parameters under consideration. Technically there are few problems in formulating the cost model, the problems are in the area of information gathering. Once available the data is easily put into tabular or equation form.

Data for the formulation of the S.G.H.W.R. cost model was supplied by U.K.A.E.A. Risley (4.16) and was based on estimates made for commercial designs of the S.G.H.W.R. Additional information concerning structural details of the commercial design was supplied by U.K.A.E.A. Winfrith (4.17). The data gave the marginal costs of altering the relevant design parameters, and the relative contributions of certain subsystems to the total station cost, e.g. steam drum and reactor core. Marginal costs could be expressed explicitly using the data supplied, the cost model equations being presented in Appendix 6.

65 →

Figure 4.10

Changes in reactivity caused by changes in steady state due to parameter alterations. The four most non-linear cases are shown.

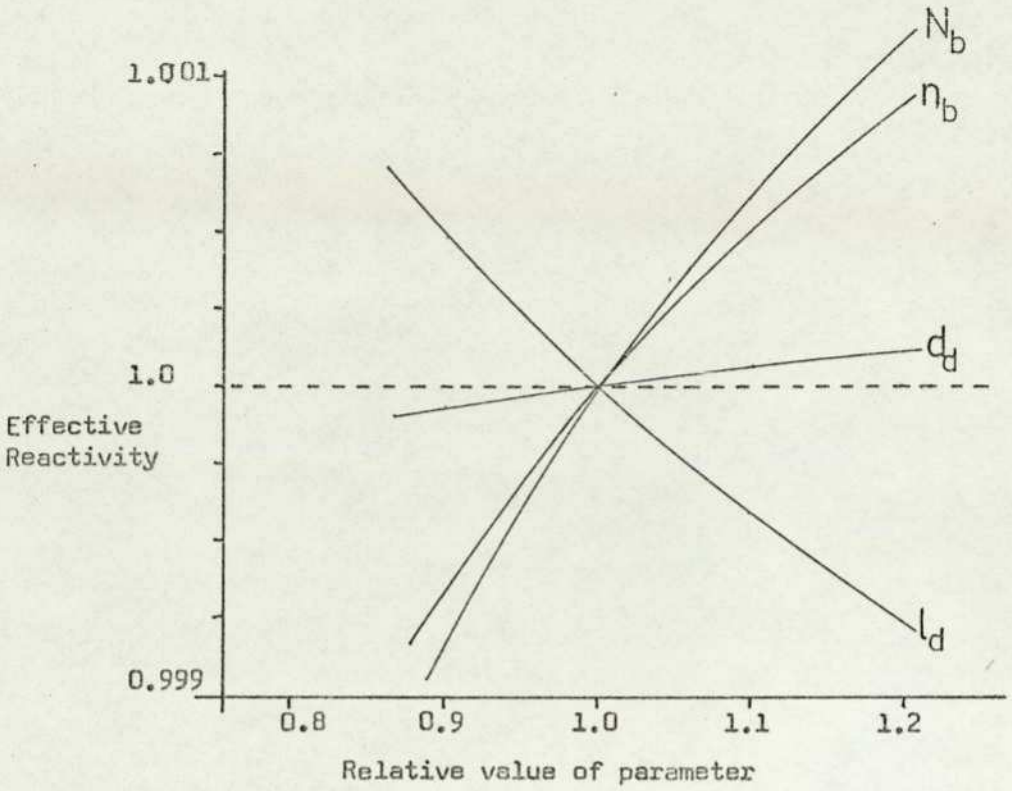
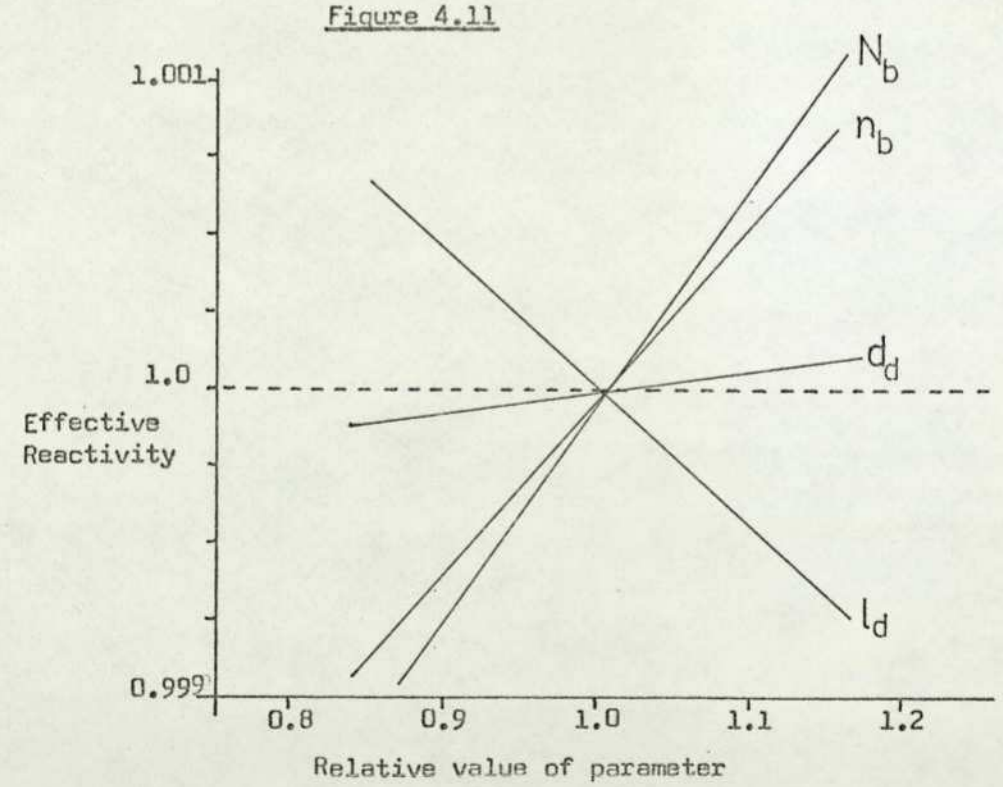


Figure 4.11



Approximate reactivity - parameter relationships from Figure 4.10 used in estimating reactivity changes via sensitivy coefficients.

5. FORMULATION OF UTILITY FUNCTIONS AND CONSTRAINTS

5.1 Principles of Utility Functions

The utility function represents on an arbitrary scale the overall worth, value or effectiveness of the system which is to be maximised during the optimisation procedure. When there are several categories of design objectives utility may be expressed as -

$$U = \sum_{i=1}^{n} W_i u_i \qquad 5.1$$

Where u_i is the utility of the system in respect of the i^{th} category of design objective and W_i is a weighting factor between categories. There will, in general, be more than one objective in each category, therefore -

$$u_i = \sum_{j=1}^{m} w_j v_j(P_j) \qquad 5.2$$

Where v_j is the value or merit of the system in meeting the j^{th} objective in the i^{th} category and is a function of performance P_j. w_j is a weighting factor within categories. In a typical case the categories may be static performance, dynamic performance, cost and reliability, and in the static performance category there may be objectives relating to efficiency, power to weight ratio, maximum speed and range. Performances P_j of equation 5.2 will be functions of the system parameters and variables, in the latter case the solution of the system models is required to relate P_j to the parameters.

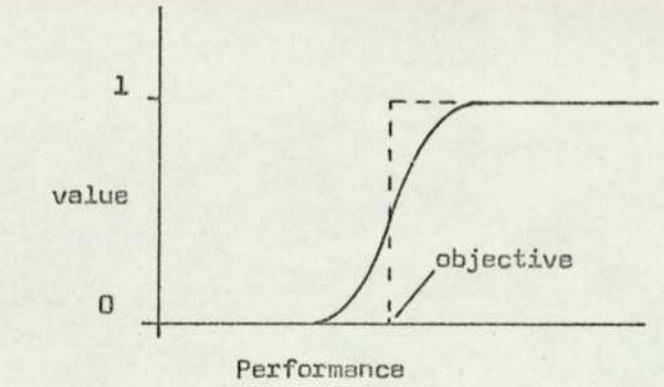
Typically the relationship between value v_j performance P_j will be of the form shown in Figure 5.1a on an arbitrary 0 to 1 scale. There may be a sharp cut off to zero value if the objective is not met, or a transition as shown by the solid line. There may be upper and lower bounds as shown in Figure 5.1b, as in grid frequency control for example. In other instances the value may be proportional or inversely proportional to performance, system cost will be of this type. The cut offs in Figures 5.1a & b are due in many cases to a system constraint, in which case it is often convenient to assign a value zero when the constraint is not violated and -1 or minus infinity when it is.

From the optimising viewpoint the discontinuities of Figure 5.1a and the zero slope areas of Figures 5.1a & b would create difficulties, although the zero slope problem would be largely eliminated when the performances were expressed in terms of the parameters (p). It is advisable, however, to avoid discontinuities and use instead fairly

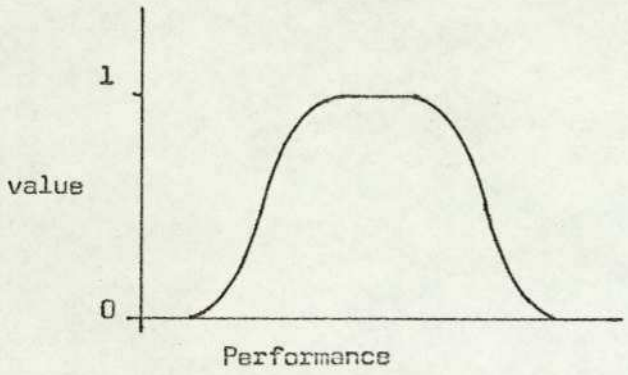
67 →

Figure 5.1

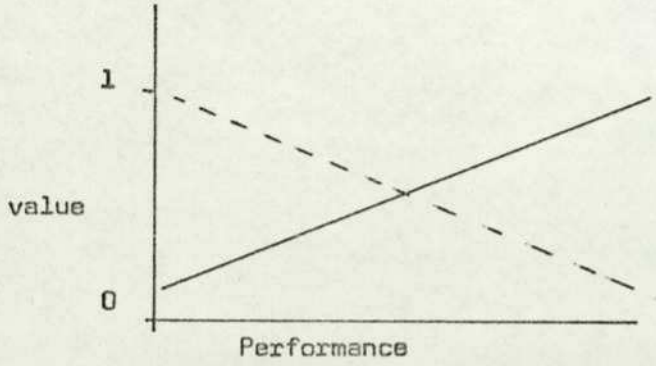
Typical performance - value relationships.



(a) Performance either satisfactory or not so, with hard (broken line) or soft transition.



(b) Performance is satisfactory within a range.



(c) Value proportional to performance.

sharp barrier or penalty functions. Zero slope areas should be avoided except at level 1 (or level zero in the case of constraints), this can be achieved formally by substituting either -

$$v_j = 1 + \log v_j \qquad 5.3$$

$$\text{or} \quad v_j = v_j - \frac{k}{v_j} \qquad 5.4$$

where K is very small. It is as easy in practice to merely redraw the graphs of v_j against P_j with the zero value replaced by $-\infty$, Figure 5.1b would then become Figure 5.2. The use of logarithmic value functions is also useful in certain circumstances in reducing the range of or differences between values. This is the basis of Bernoulli's theory of value in which the ratio of gain to present value is used as a criteria instead of gain directly (5.1).

Uncertainties will exist about the values of some design parameters, and about the objectives since these depend upon predictions of future events or states of nature. Uncertainties in design parameters are transformed through the system models to uncertainties in the system preformances P_j, which may then be expressed as a probability distribution about an expected value P_{je} -

$$p(P_j) = f(P_{je} - P_j) \qquad 5.5$$

which may typically be of the form shown in Figure 5.3. Referring to this figure the probability of P_j being in the range P_{j1} to $P_{j1} + \delta P_j$ is -

$$\delta P_j \cdot p(P_{j1}) = f(P_{je} - P_{j1})\,\delta P_j \qquad 5.6$$

and this is also the probability of the value function v_j being $v_j(P_{j1})$ if the expected value of P_j is P_{je}. The expected value v_{je} is therefore given by -

$$v_{je} = \int_{-\infty}^{\infty} f(P_{je} - P_{j1})\, v_j(P_{j1})\, dP_{j1} \qquad 5.7$$

This integral may be solved formally for specific value functions and probability distributions, but it does not serve any purpose here. The effect is illustrated in Figures 5.4a & b for some typical functions and distributions. It may be seen that the effect of uncertainty is to soften the value function, discontinuities are removed or made less sharp and peaks are less severe. This averaging effect of uncertainty has the expected effect of making the optimal design less clearcut.

As far as possible the value-performance functions are formulated objectively, although this is not always possible. If some subjective judgement is used at this stage it is pertinent to ask why it cannot be used at a higher level thereby avoiding much analysis and work.

70 ⟶

Figure 5.2

Lower value of $-\infty$ used instead of 0 to avoid problems during optimisation.

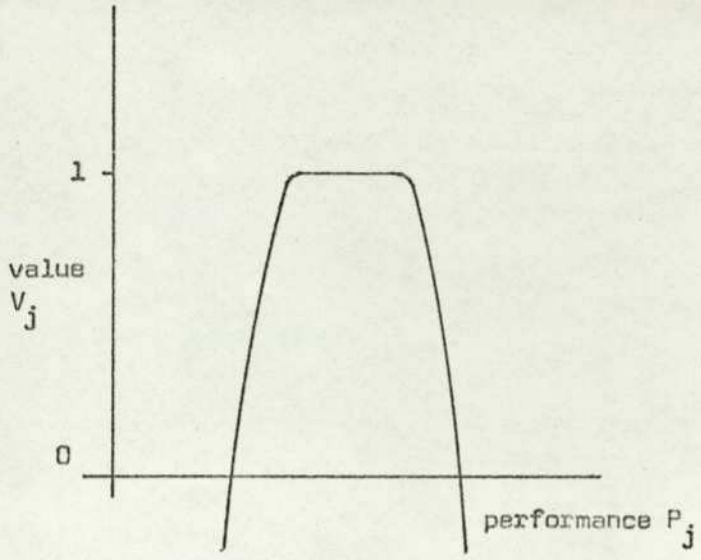


Figure 5.3

Uncertainty of performance expressed as a function of expected performance P_{je}

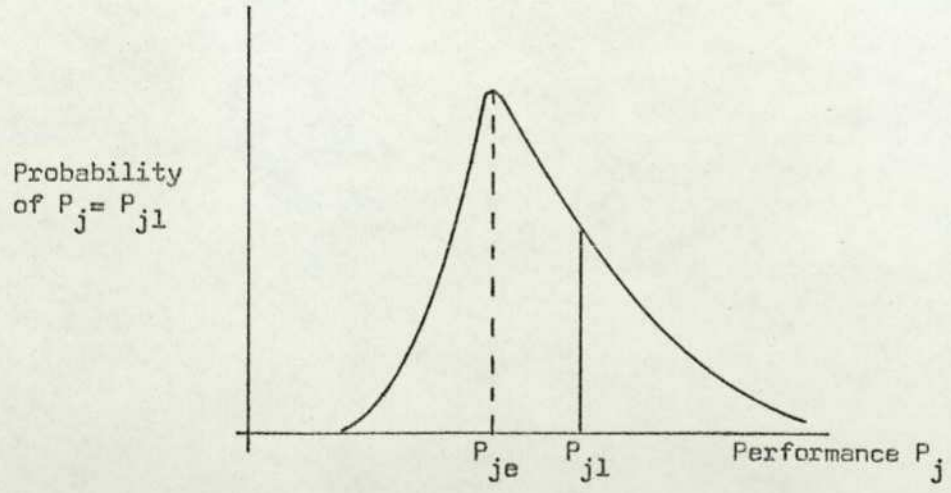
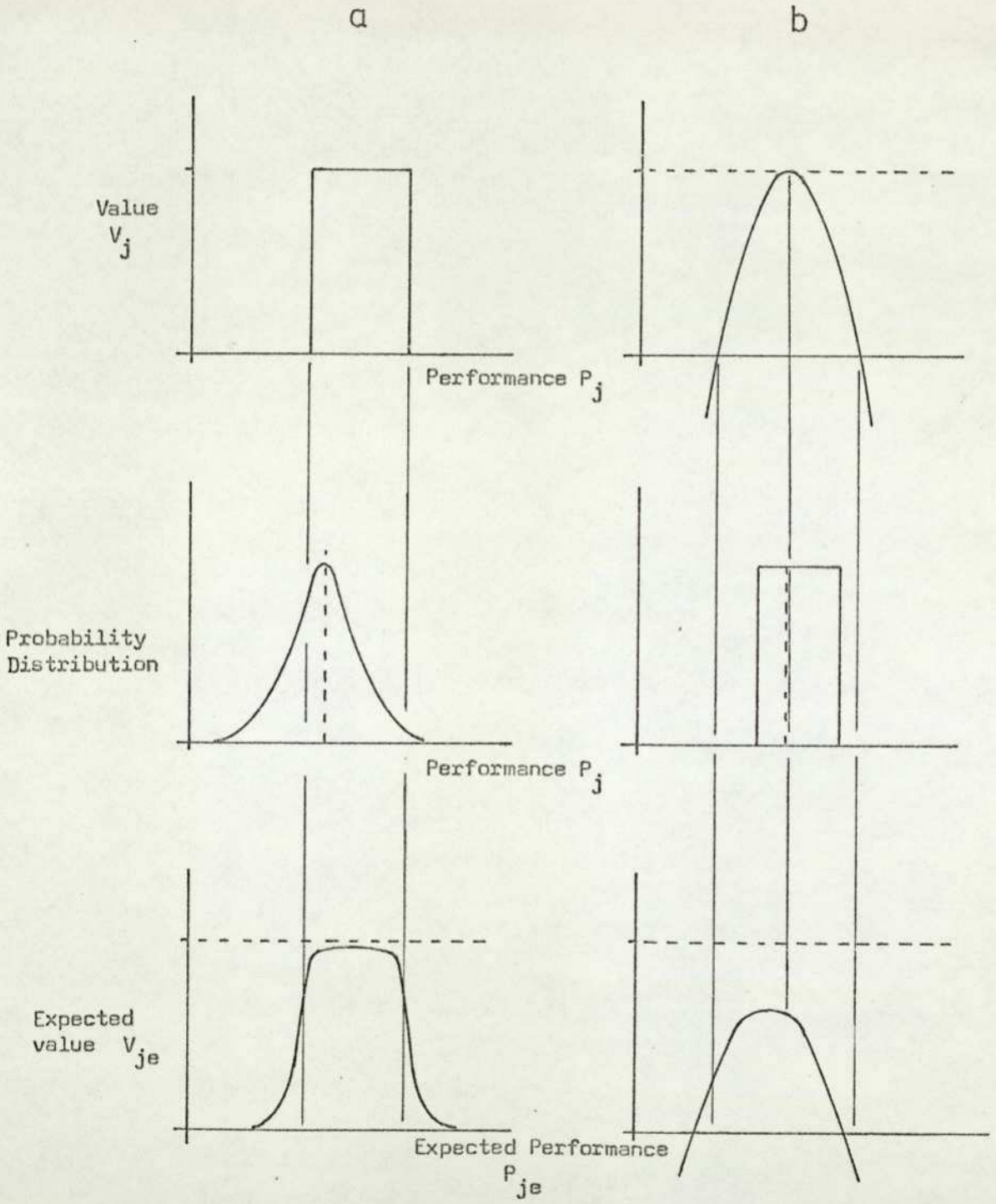


Figure 5.4

Effect of uncertainty of performance on value-performance relationships.



Note that in the second case position of the peak is shifted, this generally occurs with skew probability distributions.

It has been demonstrated, however, that the combination of many low level 'guesses' gives better results than a few at high level (5.2).

The weighting factors within categories w_j and between categories W_i are determined by assessing the relative worths of the category utilities U_i and objective values v_j over the system life cycle. Within category weightings for values assigned on a constraint violation basis are, however, fairly arbitrary. In assessing the weights account must be taken of depreciation, interest on capital investment, inflation and other related factors. All benefits and costs must effectively be reduced to a present worth value. In making estimations of the weightings uncertainty will be an important consideration, and it will often be necessary to determine a weighting distribution or range as opposed to a specific value.

5.2 Constraints

When discussing value-performance relationships in the previous section, cutoff due to constraint violation was mentioned. Constraints on the parameters arise from a variety of sources; these are discussed below in general terms before utility functions for the S.G.H.W.R. are developed in the following section. Types of constraint are as follows -

(a) Geometric Constraints. Where parts of the system have to be assembled it is necessary to ensure that it is physically possible for this to be done. For example, in the S.G.H.W.R. there is a limit to the number of fuel pins which can be fitted into a boiling channel or to the number of risers which may be connected to the steam drum. Both the above examples give rise to an inequality constraint involving several of the design parameters. Also in the geometric category is the need to ensure that certain design parameters remain positive. Geometric constraints are usually obvious intuitively, but it is often not until an inconsistent optimal solution has been obtained that it is realised that they must be stated formally.

(b) Engineering Constraints. Stress levels in the system components will be a function of the system variables (pressures, forces, etc.) and the system parameters (dimensions and mass) for a given system structure. Stress limits are also a function of the system variables, operating temperature for example. The engineering constraints ensure that stress levels are not exceeded, and will be inequalities in the system parameters and variables. Although in theory the

engineering constraints should be based on peak values of variables during transients, the steady state values are often adequate for this purpose. In systems such as the S.G.H.W.R. or process plant engineering constraints play a much less significant role than would at first be expected. This is because there are usually parameters which do not significantly affect dynamic or static performance (they do not appear in the coefficients of the static or dynamic models) and which can be adjusted to maintain stress levels. These parameters will usually contribute to the cost model however. Such parameters in the S.G.H.W.R. are the riser or steam drum thicknesses. This is by no means always the case, in a heat exchanger for example tube thickness affects performance, cost and stress. In other types of system the engineering constraints may dominate the problem, as in mechanism or vehicle design. Stress based engineering constraints do not enter into the formulation of utility functions for the S.G.H.W.R., but equation 4.31 was formulated assuming a constant stress level in the pressure tube. Although the majority of engineering constraints will be stress based there are others, for instance, in the S.G.H.W.R. it is necessary to prevent cavitation of the recirculating pumps which places a constraint on the sub-cooling of water leaving the drum.

In conclusion, it should be noted that engineering constraints arise because of restrictions in the scope and detail of the system models. If the discontinuities arising from metal yield or fluid cavitation were modelled and system objectives and performances amended accordingly engineering constraints would be unnecessary. It is a matter of convenience to use them.

(c) Safety Constraints. Related in many respects to the engineering constraints, the safety constraints are concerned with the peak levels of system variables during transients. If some variables exceed limits laid down in advance a dangerous situation occurs and an emergency shutdown or other control action is initiated. Limits are commonly placed on such variables as temperature, pressure, speed and level in mechanical systems and voltage or current in electrical systems. In specific types of plant other variables may be limited, in the S.G.H.W.R. there is a limit on neutron flux.

The safety constraints will be inequality constraints in the system variables only. The relevance of this category of constraints is very dependent on the system, some instrument systems may have no safety constraints.

(d) Linearity Constraints. The constraints considered above all relate to the system, the final category of constraints relates to the method adopted for solution of the dynamic model. It will be recalled from section 4.1 that sensitivity coefficients were used to relate the shift in pole-zero positions to changes in design parameters, and that the effects of changing several design parameters was obtained by linear superimposition of the sensitivity effects, equations 4.13 and 4.15. The limits to which this process could be taken had to be established before optimisation began to ensure that results would be valid. An acceptable error in a pole or zero position depends very much on its position in the S plane, generally speaking poles of large magnitude (relatively) contribute little to the overall response of the system, and a large error can therefore be tolerated in these. Poles closer to the origin are required more precisely. Tests were carried out to compare the positions of the system poles estimated from the sensitivity coefficients and those recalculated from the dynamic model for the same parameter changes. Results for the poles of smallest magnitude are shown in Figure 5.5. It is difficult to assess analytically the probable error in a pole position estimated by the sensitivity coefficients for large systems. Appendix 11 is an analysis which gives a guide to the extent to which a parameter or group of parameters may be altered without introducing undue error in the positions of poles of low order systems. As a result of the tests and analysis it was concluded that pole or zero shifts of $\pm 50\%$ from the reference values could be safely made. Linearity constraints are not dealt with by introducing penalties, but directly in the optimising routine.

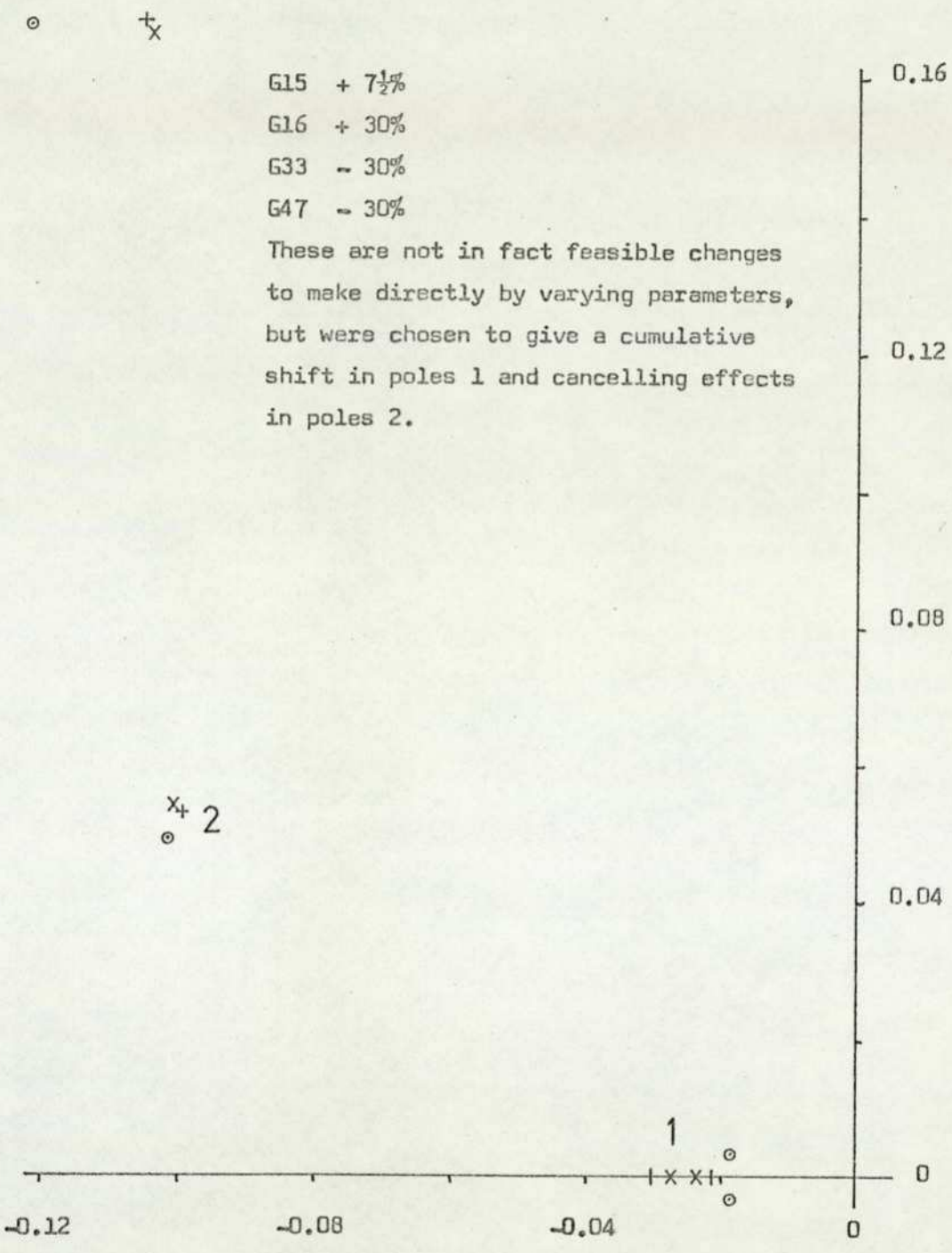
5.3 Utility Functions for the S.G.H.W.R.

Development of the utility functions for the three categories of design objective are discussed under separate headings below. This is followed by the arguments leading to a selection of the weighting factors used in equation 5.1 to generate total system utility.

74 ⟶

Figure 5.5

Results of a superimposition test on system poles. The shifts of the six poles nearest the origin are shown due to the following changes in the linear dynamic model coefficients (Appendix 4).



⊙ Original poles

× Poles calculated by sensitivity coefficients

\+ Poles calculated by re-solution of model.

5.3.1 Static Performance.

The objectives of the S.G.H.W.R. in the static performance category are firstly to produce power at a maximum rate of 100 MW, and secondly to produce as much total energy as possible from a given quantity and enrichment of fuel. The two conditions are related in that by adjusting reactivity any configuration of design parameters can produce 100 MW if constraints on the variables are ignored. This fact is used in assessing the value of static performance by ensuring that whenever a design parameter is altered sufficient reactivity is added or withdrawn to maintain the power output. The reactivity required for this purpose is defined by the equations developed in section 4.2.

When the reactor is brought on line after refuelling there is a surplus of reactivity available which is held down by boron poison dissolved in the moderator, (this is in addition to that required to overcome fission product poisoning). As fuel is consumed the effective reactivity will fall, and this is made up by reducing the quantity of boron in the moderator. When the boron level is reduced to its minimum the reactor must be refuelled. In the S.G.H.W.R. prototype with fresh fuel $2\frac{1}{2}\%$ reactivity is held down by poison, this is sufficient for 150 full power days of operation. When a design change is made the available reactivity reserve will be altered due to the effects previously described, and the time between refuelling will alter correspondingly. Time between refuelling may be expressed as -

$$T = \frac{150(2.5 + \delta k)}{2.5} \qquad 5.8$$

The value to the system is the negative inverse of refuelling period, since refuelling rate determines the annual (and life) cost to the system. As there is only the single design objective in this category (power output having been dealt with by other means) no within category weights are required and static performance utility is given by -

$$U_s = -\frac{1}{60(2.5 + \delta k)} \qquad 5.9$$

or normalised to -1 at the reference condition -

$$U_s^1 = \frac{-2.5}{2.5 + \delta k} \qquad 5.10$$

This relationship is plotted in Figure 5.6.

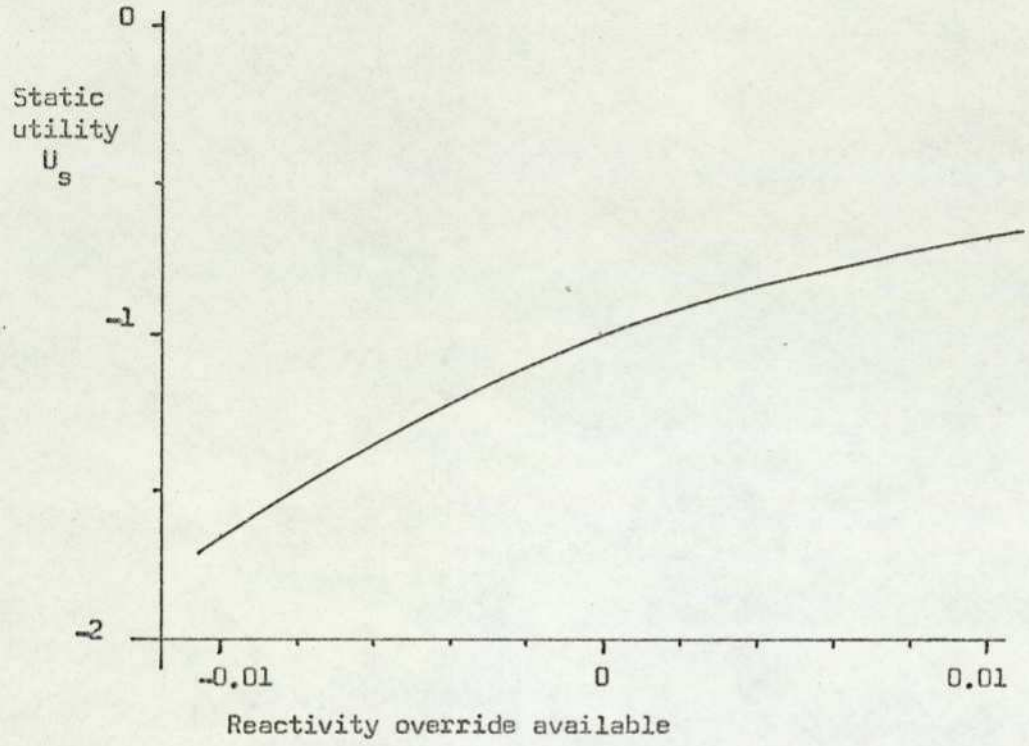
5.3.2 Dynamic Performance.

The dynamic performance objective of the reactor is that it should respond satisfactorily to step power demands which may be asked of it

76 →

Figure 5.6

Static utility as a function of reactivity override available.



without causing violation of any of the constraints on the system variables. To determine what is a satisfactory response, the effect of sudden load deficits on the grid system must be analysed.

The kinetic energy stored in the grid system is proportional to the square of grid frequency -

$$E_s = K f^2 \qquad 5.11$$

where k is a constant determined by the inertia of the generating sets and rotating machinery driven from the grid. The rate of change of stored energy is the difference between the power input and power output to the system -

$$\frac{dE_s}{dt} = P_i - P_o \qquad 5.12$$

Under steady conditions $P_i = P_o$ and the energy storage is proportional to P_o, i.e. the number of sets and pieces of machinery in operation. In the existing grid energy storage is a little less than 10 MW seconds per MW of output, but as mentioned in section 2.2 this figure is decreasing. The figure includes an allowance for energy stored in rotational driven machinery. This means in effect that if all supplies to the grid are cut off stored energy begins to drop at 10% per second, and frequency or speed at 5% per second. Starting from initial steady operating conditions then energy storage may be represented as -

$$E_s = 10P_o - \int (P_i - P_o)\, dt \qquad 5.13$$

If a fault occurs in a station a step decrease in P_i occurs initiating a step demand for more power from the remaining stations, assuming P_o remains unchanged. The integral of equation 5.13 then becomes the integral of power error summed for all stations feeding the grid system -

$$E_s = 10P_o - \sum \int P_e\, dt \qquad 5.14$$

and the fractional stored energy deficit is -

$$\frac{\Delta E_s}{E_s} = \frac{\sum \int P_e\, dt}{10P_o} \qquad 5.15$$

This may be converted using 5.11 to a fractional frequency change; for small changes in frequency -

$$\frac{\Delta_f}{f} = \frac{0.5 \sum \int P_e\, dt}{10P_o} \qquad 5.16$$

To progress further it is necessary to make some assumptions about the operation of stations feeding power to the grid. Two groups of stations are assumed, one group operating at full capacity supplying $(1 - x)P_o$ of the total power, and a second operating below full capacity

supplying xP_o of the total power. The first group will have no capability to supply increased demands, and the second group is assumed to have uniform dynamic characteristics (a number of S.G.H.W.R.s in fact). This is obviously a gross simplification and could be modified by relating the dynamic performance of other stations to the S.G.H.W.R.s. With this assumption in mind 5.16 may be re-written -

$$\frac{\Delta f}{f} = \frac{.05x\sum\int P_e dt}{xP_o} \qquad 5.17$$

All demands for extra power will be made of the S.G.H.W.R.s, and the summation and integral signs apply to these stations only. As their dynamic characteristics are uniform the integrals will all be of the same form, therefore -

$$\frac{\Delta f}{f} = .05x\left\{\frac{\int P_e^1 dt}{xP_o}\right\} \qquad 5.18$$

where P_e^1 is the total power error for all the S.G.H.W.R.s. The part of 5.18 within brackets is the integral of relative power error P_e for all the S.G.H.W.R.s and hence -

$$\frac{\Delta f}{f} = .05x \int p_e dt \qquad 5.19$$

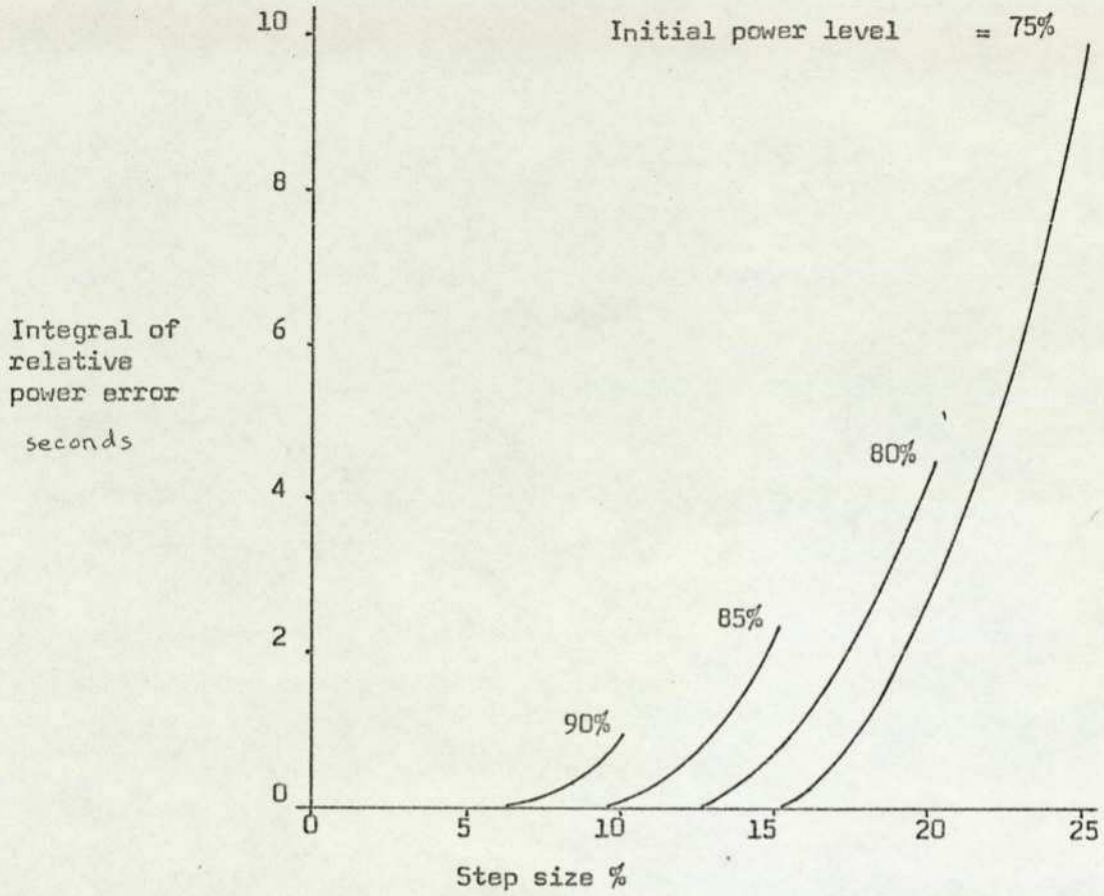
For a grid system power deficit of ΔP, the relative step demand p_d made of each S.G.H.W.R. will be -

$$p_d = \frac{\Delta P}{xP_o} \qquad 5.20$$

In discussing controllers for the S.G.H.W.R. in section 3.3 it was shown how the integral of 5.19 could be maintained at essentially zero until step inputs were large enough to cause saturation of the turbine stop valve travel. For the adopted control system the integral is plotted in Figure 5.7 for a reactor operating at 75% - 90% load with step inputs in the range 0 - 25%. As previously stated the C.E.G.B. policy is to maintain the grid frequency to within $\pm$0.2 c/s of nominal (0.4%), and shedding of load occurs when frequency drops 2 c/s below nominal (4%). Using the curve of Figure 5.7 and equations 5.19 and 5.20 the largest amplitude of step input that the grid system can withstand subject to the above limits can be related to the proportion of S.G.H.W.R.s. The relationships are shown in Figure 5.8 for reactors operating at 75% full load. The fact that the lines of Figure 5.8 are close and almost straight indicates that once a power error occurs (i.e. after steam valve saturation) the frequency error given by equation 5.19 rapidly exceeds the limits. In such circumstances p_d

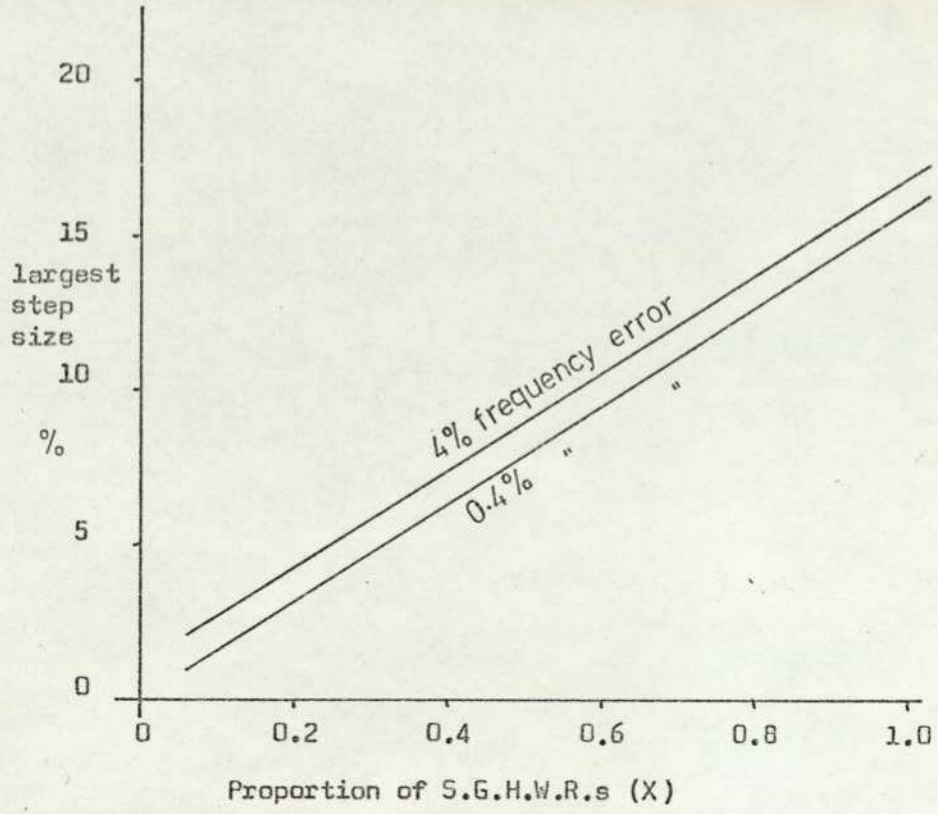
80 ⟶

Figure 5.7



Integral of relative power error for the S.G.H.W.R. prototype with the control strategy defined by Figure 3.10. Integral is plotted against step demand size for reactors operating at various initial power levels.

Figure 5.8



Largest step sizes which can be accommodated by a grid system as a function of the proportion of S.G.H.W.Rs. in the plant mix. S.G.H.W.Rs are assumed to be operating at 75% capacity when the demand is made. The acceptable proportional power error integral for the S.G.H.W.Rs. is given by the equation 5.19 as -

$$\int P_e dt = \frac{\Delta f}{0.05\ f\ x}$$

From Figure 5.7 the acceptable step size for the S.G.H.W.R.s is obtained. The acceptable step size to the grid system is this multiplied by x.

of equation 5.20 is limited to the value which the S.G.H.W.R.S can just follow, which implies that limiting power step inputs to the grid are proportional to x, hence the straight lines of Figure 5.8.

Having established the maximum size of step the grid system can withstand, it is necessary to estimate the number of steps greater than this that the system can expect. Figure 5.9 shows the distribution of step sizes expected per annum (2.4, 5.3), these may occur randomly throughout the day or year (5.3), although data is too scant for the annual distributions to be certain. Figures given are the absolute step demands expected, while it is the relative step size which determines whether the demand can be satisfied. Daily power profiles for typical summer and winter days are shown in Figure 5.10, and the annual power profile in Figure 5.11 (5.4), data refer to 1969-70. From these curves the average annual power distribution of Figure 5.12 may be obtained, this shows the number of hours per year a given power output is supplied.

The data in Figures 5.8, 5.9 and 5.12 enable the power demands which the system fails to meet to be estimated. For example the system supplies power at the rate of 10 - 15 KMW for 1872 hours per year (Figure 5.12). During the year 8.6 faults in the 400 - 500 MW range can be expected (Figure 5.9); the number of these which are likely to occur while the system is supplying 10 - 15 KMW is -

$$\frac{8.6 \times 1872}{24 \times 365} = 1.84 \qquad 5.21$$

and the average relative size of these faults will be -

$$\frac{.45}{12.5} \times 100 = 3.6\% \qquad 5.22$$

If the system is assumed to include 20% of the reference design S.G.H.W.R.s ($x = 0.2$) operating at 75% full power, then a step power demand of 3% can be accommodated (Figure 5.8). On average the demand which cannot be met is -

$$\frac{(3.6 - 3.0)}{100} \times 12.5 \times 1.84 = 0.138 \text{ KMW/year} \qquad 5.23$$

Summed for all power and fault levels the above procedure gives the total annual unmet power demands, the value to the system is the negative of the unmet demands. For the reference design under the conditions assumed above 203 MW/year are not met.

The remaining contributions to the dynamic utility concern constraints on the variables of the system. The constraints are -

(a) Fuel temperature is limited to 2000°F.

(b) Neutron flux level is limited to a value equivalent to the thermal power level demanded plus 40 MW.

84 →

Figure 5.9

Distribution of step fault sizes.

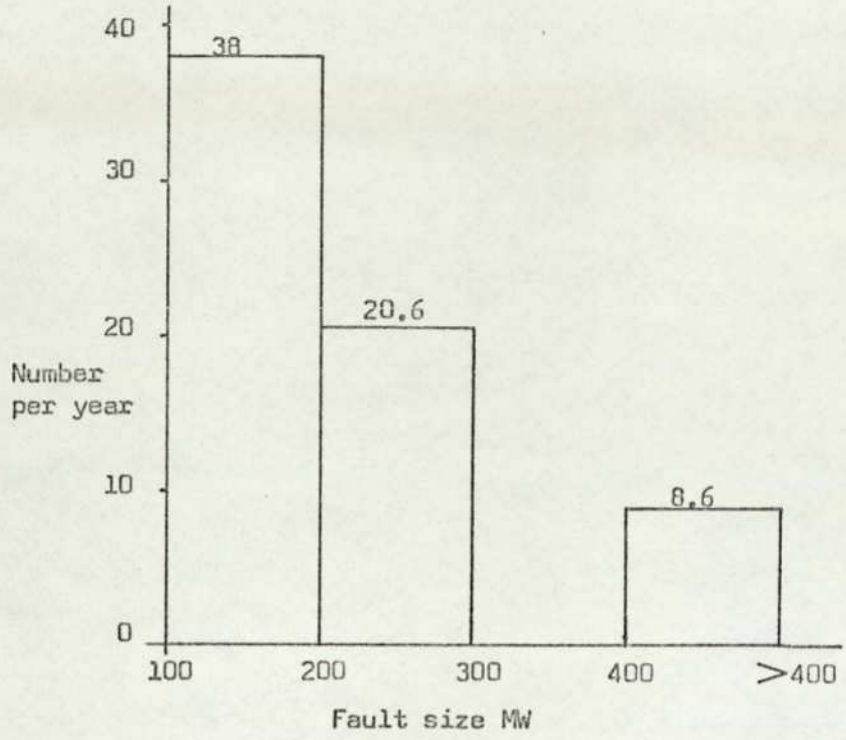


Figure 5.12

Distribution of grid system output.

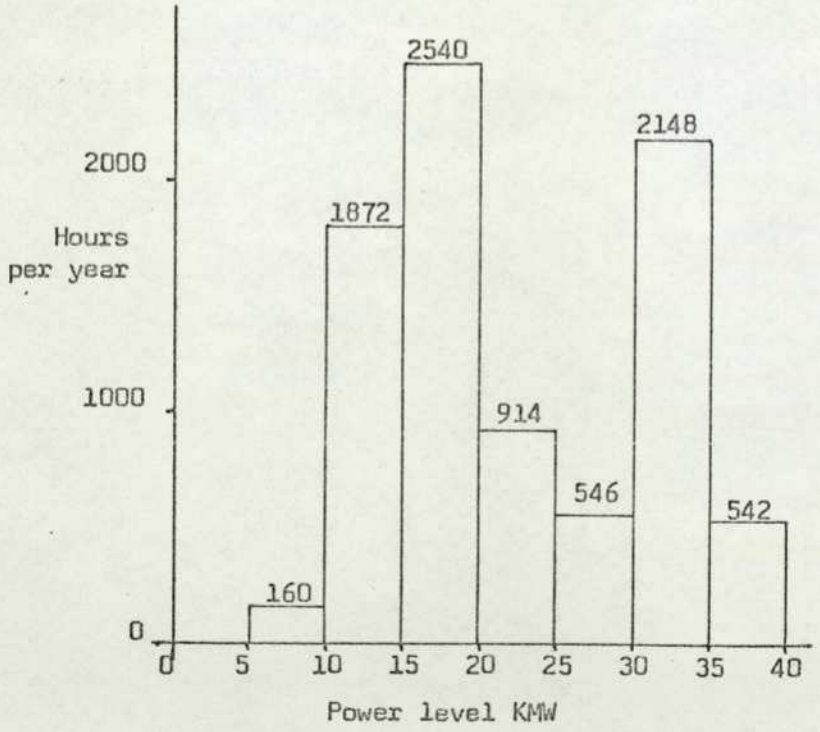


Figure 5.10

Daily power profile of grid system output.

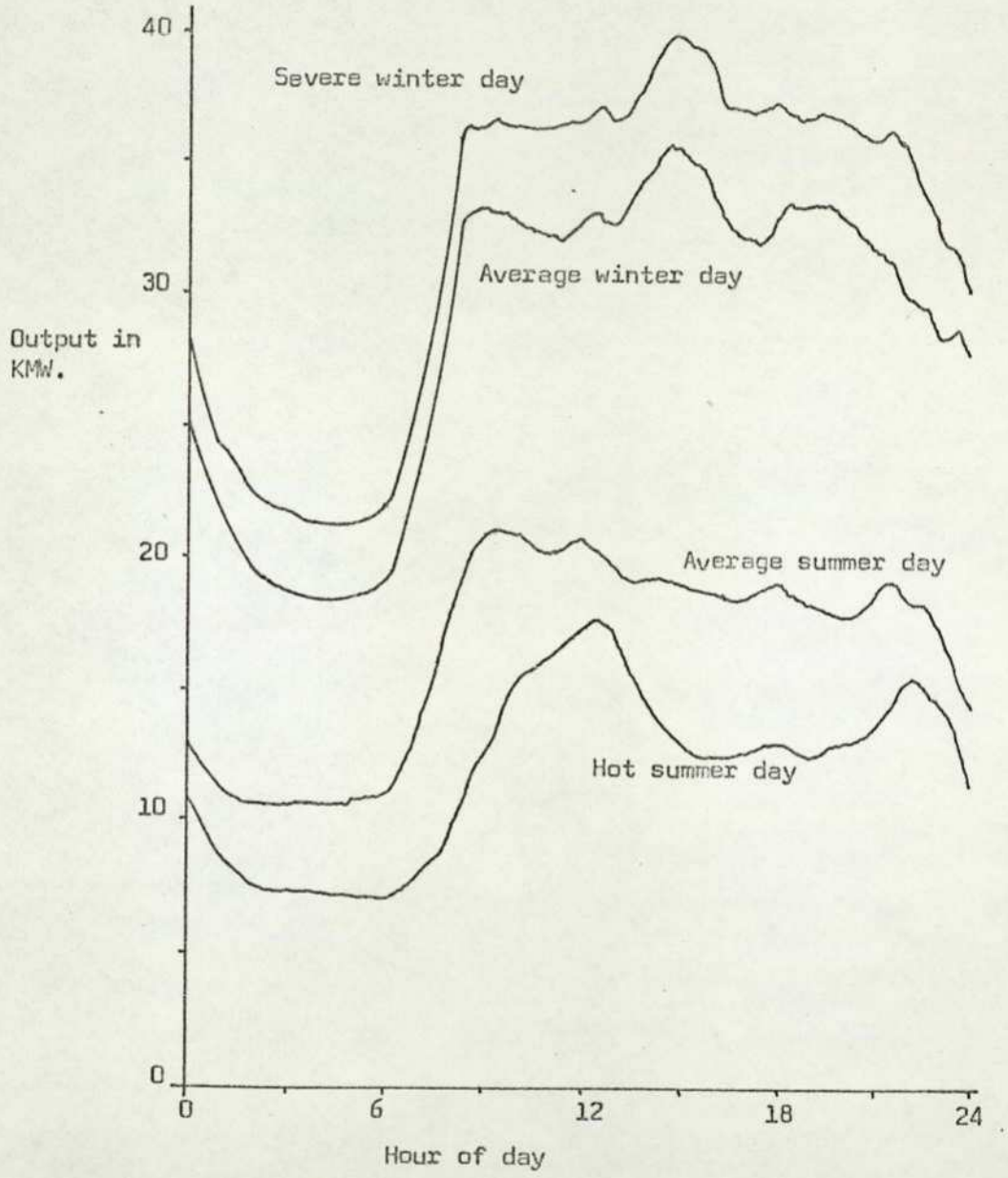
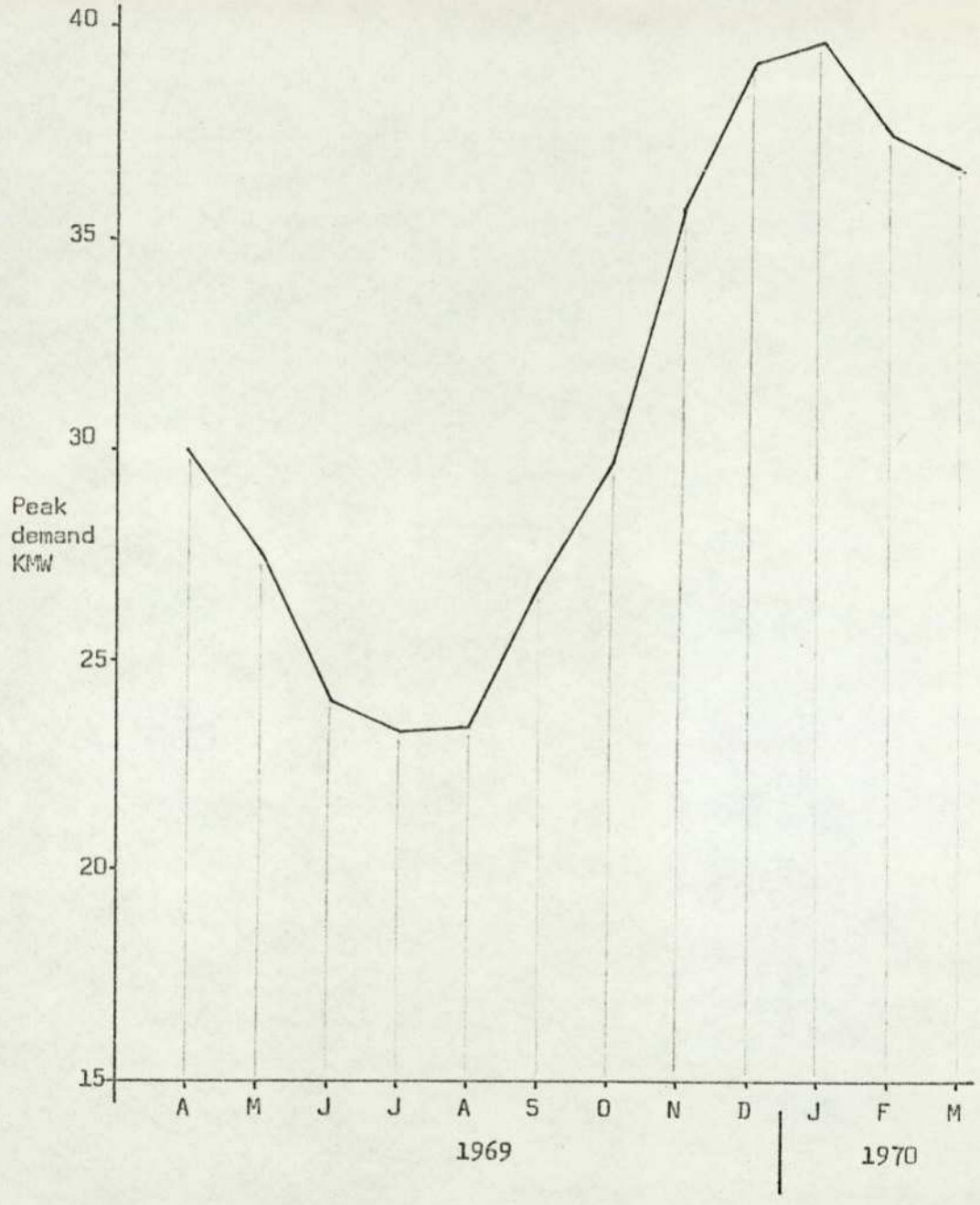


Figure 5.11

Annual power profile of grid system output (peak demands).



(c) Fuel to coolant heat transfer rate is limited by burnout considerations to a value equivalent to a channel power of 6 MW.

(d) Drum water level is limited to within ± 4" of nominal.

(e) Water enthalpy at drum exit must always be below a level which would cause the circulating pumps to cavitate, i.e. it does not saturate.

These constraints are dealt with by penalty functions as indicated in section 5.1. They are weighted equally with the dynamic value within the dynamic performance objective category, i.e. the w_j of equation 5.2 are all unity. Dynamic utility of the system is expressed in normalised form by dividing by the absolute reference value of power demands not met.

5.3.3 Cost.

The marginal cost of the reactor defined by the equations of Appendix 6 is taken as the system performance in the cost category. This is normalised to zero for the reference design (actual cost normalised to unity). The cost utility of the system is merely the negative of normalised marginal cost.

5.3.4 Weighting Factors.

The utilities in the cost, static performance and dynamic performance categories (U_c, U_s and U_D) have been expressed in normalised form relative to the reference design. Weighting factors W_c, W_s and W_D are used to combine the category utilities to form overall system utility, the estimation of the weightings based on the life cost to the system follows.

Total cost of the S.G.H.W.R. prototype was £50M, of this about £8M is affected by the parameters being adjusted in the present work. This is the basis for the cost weighting factor, no adjustment for present worth is required as this money would be invested at the start of the project, i.e.

$$W_c = 8 \times 10^6 \qquad 5.24$$

Static performance utility was defined by 5.9. If a reactor working life of 25 years is assumed, the number of refuellings required is -

$$N = -U_s \times 25 \times 365 \qquad 5.25$$

Each refuelling costs £0.25M, the life cost in the static performance category is therefore -

$$£2280 \times 10^6 \times -U_s \qquad 5.26$$

or in terms of normalised static utility -

$$£15.2 \times 10^6 \times -U_s' \qquad 5.27$$

In effect this means that £15.2M is spent on refuelling the reference design during its working life. As this is spent over a period of 25 years it must be reduced to a present worth (or present cost)value. Assuming an amortisation rate of 5% (interest rates being offset by rising fuel and labour costs) the static performance weighting factor is given as -

$$W_s = 10.5 \times 10^6 \qquad 5.28$$

Dynamic performance utility was defined as the negative of the total Megawatts of step demands not met per annum. Putting a value to this is not easy, annual loss of income to the area boards assuming the power deficit lasts for h hours and charging at £.01 per KWH is -

$$-U_D \times P_r \times h \times .01 \times 1000 \qquad 5.29$$

where P_r is the MW of step demands unmet by the reference design per annum.

This is, however, small compared to the real cost of a supply failure which is in the inconvenience and loss of production to consumers and in the effort required within the supply authority to re-establish supplies. Factors to be applied to the cost given by 5.29 to give an estimate of the real cost have been estimated as follows (5.5) -

Commercial consumers	70
Industrial consumers	60
Domestic consumers	15

An average figure would be 55, giving a life cost due to supply failures over 25 years as -

$$-U_d \times P_r \times h \times 550 \times 25 \qquad 5.30$$

Using the assumptions made previously regarding plant mix and S.G.H.W.R. operating level P_r = 203 MW, and assuming that it takes 2 hours to restore power deficiencies the dynamic weighting factor is given as -

$$W_D = 5.6 \times 10^6 \qquad 5.31$$

Finally all weightings may be made relative to W_c as utility is on an arbitrary scale. This gives the overall utility as -

$$U = U_c + 1.26U_s + 0.71U_D \qquad 5.32$$

It is as well to recall at this stage that the weightings are dependent on assumptions made in their estimation, in particular the life of the plant, the ratio of S.G.H.W.R. to other stations and the power level of the S.G.H.W.R. before an increase in power is demanded.

The factors are also based on present day information (Figures 5.9 and 5.10 and equation 5.13 for example), this will change as time progresses. The development leading to the values in equation 5.32 is mainly illustrative, during the optimising procedure variations in weightings were used.

6. OPTIMISATION PROCEDURE.

6.1. Principles of Optimisation.

The optimisation procedure is the centre of the design method, it is this which calls upon the system models and utility function as it requires them. The heavy line loop in Figure 2.1 indicates the function of the optimising procedure; which includes the formulation of a strategy for making design alterations, assessing the results of alterations and deciding when an optimum has been achieved. In the present context a design configuration leading to maximum utility is desired, the discussion which follows is therefore oriented to peak seeking or hill climbing rather than to minimum seeking which is more commonly referred to in the general literature on the subject. Figure 6.1 defines convex and concave functions.

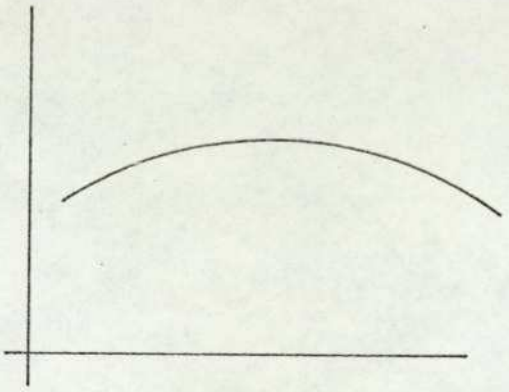
The choice of an optimising algorithm called for some care, a balance had to be struck between the number of iterations needed to reach the peak and the number of estimations of the utility function required at each iteration. Where a complex utility function is employed, as in the present case, it is the total number of estimations of utility which will determine the time taken to optimise the system. The logical and decision-making processes within the programme are fairly fast relative to utility estimation time. The dimensionality of the problem precluded the use of random or patterned search techniques, n parameters divided into a grid of 10 values each needs 10^n utility evaluations and a finer grid would be needed to obtain the required accuracy. Such methods have an advantage over the faster methods to be discussed where discontinuous or multi peak functions are involved. One parameter at a time (univariate) searches involve fewer evaluations, but are still slow and often give rise to convergence problems.

First or second order gradient methods can be used to reduce the number of utility estimations, most common of the first order are the steepest ascent algorithms. Calculation of the direction of steepest ascent can be made with n + 1 utility evaluations using forward or backward differences or 2n + 1 using central differences (which are more accurate but hardly necessary). Steepest ascent algorithms are not very rapidly converging either in the ridge following or travel to peak mode, the latter mode requires further function evaluations to determine the peak along the search vector, and the former demands that only small shifts can be made before reassessing the direction of steepest ascent. Modified algorithms can reduce the number of iterations required for certain types of functions (notably ridges), that of Booth (6.5) for example suggests moving only 90% of the way to

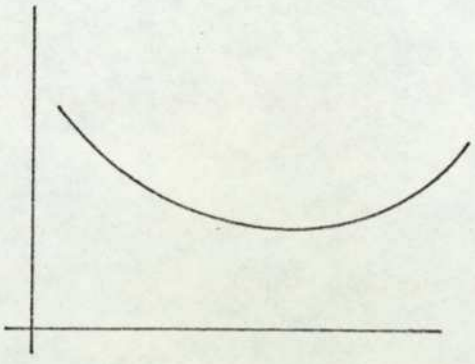
89 ⟶

Figure 6.1

Concave and convex functions defined.



concave



convex

the peak along the search direction at each iteration.

Better search directions can be estimated using the second order gradient methods which fit a second order surface to the function and predict the position of the peak of this surface. This having been done it is better to search in the direction of the peak rather than to take the peak as the starting point for the next iteration. The second order surface may be defined by a multivariable Taylor series expansion of the utility function to the second derivatives. The quadratic approximation to the surface is then defined in terms of the gradient vector $\nabla f(\underline{x})$ and the Hessian Matrix $H(\underline{x})$. The gradient of the quadratic surface at any point $\underline{x}_1$ is given by -

$$\nabla f(\underline{x}_1) = \nabla f(\underline{x}) + H(\underline{x})\,(\underline{x}_1 - \underline{x}) \qquad 6.1$$

The gradient is zero at the peak of the quadratic function and $(\underline{x}_1 - \underline{x})$ (which defines the search direction) is given by the solution of n simultaneous linear equations defined by 6.1. Calculation of the Hessian requires $1 + \frac{n^2}{2} + \frac{3n}{2}$ estimations of the utility function. However, by making certain assumptions about the surface, the pseudo-inverse of the Hessian may be found using only $1 + 2n$ estimations of the value function. There are various techniques for finding the pseudo-inverse, but they in most cases amount to fitting a quadratic to the surface in each of the principal directions (or in a set of conjugate directions) and determining the distance of the peak in each of these (6.1, 6.2). The distances are then combined to form a search direction. For quadratic utility functions solution of equation 6.1 for $\nabla f(\underline{x}_1) = 0$ will lead to the peak directly, use of a pseudo-inverse Hessian will not have this property. However, it can be shown that for many pseudo-inverse methods the peak of a quadratic function will be reached in less than n iterations.

Second order gradient methods using the pseudo-inverse of the Hessian require a little under twice the utility estimations per iteration of the steepest ascent methods; $1 + 2n + S$ compared with $1 + n + S$, where S evaluations are required during a search. For most applications second order gradient methods will converge to a peak in less than half the iterations needed by first order gradient methods, the former are therefore more efficient.

Gradient methods have severe limitations where the utility function is discontinuous (not twice differentiable), noisy or partially convex. In such cases the direct search methods of Powell (6.3) or Rosenbrock (6.4) and other similar methods are valuable, indeed it is debatable

whether the gradient methods have any advantage over direct search methods for 'smooth' functions. The direct search methods make a series of linear searches along directions based upon the results of previous searches, the first search is usually made along the direction of steepest ascent.

Constraints may be handled in several ways, equality constraints by Lagrange multipliers, linear constraints by projecting the search vector onto the constraint. Penalty and barrier functions as discussed in section 5 are more generally applicable.

All the methods discussed above have one major drawback, they cannot guarantee to find the global maxima of a multi-peak function. The only exception to this would be the patterned (Gausian) search, but as explained previously this is not viable for large order systems. In practice all that can be done is to start the optimisation from several points and see if all solutions converge to the same maxima, or at least several to the greatest maxima. For large order systems finding several feasible starting points can be a problem.

6.2. The procedure adopted.

A second order gradient method was adopted as the noise problem was not present and care was taken to ensure that the utility function was continuous. Figure 6.2 shows a flow diagram for the optimising procedure. The programme is written in two segments, one determines a search direction (CHIC) and the second makes a linear search and determines the peak location along the search vector (LINSEARCH). Both segments refer to the function (CF) which defines the utility to be maximised, and this in turn refers to the system models and model solutions (sensitivity matrices).

A search direction is found by fitting a quadratic approximation to the utility surface at the starting point, using $2n + 1$ function evaluations along n principal directions. The procedure is that described by Mugele (6.6). Modifications to the basic procedure were made when -

(a) The increment of a parameter used in evaluating derivatives was too small to allow accurate peak distance prediction, the increment was increased.

(b) If the predicted distance to the peak in any of the principal directions was such that the linear superimposition constraints were violated, the distance in that direction which would just satisfy the constraint was substituted.

(c) If the surface in any principal direction was convex the

95 ⟶

Figure 6.2 Flow chart of the optimising procedure.

(a) Subroutine CHIC

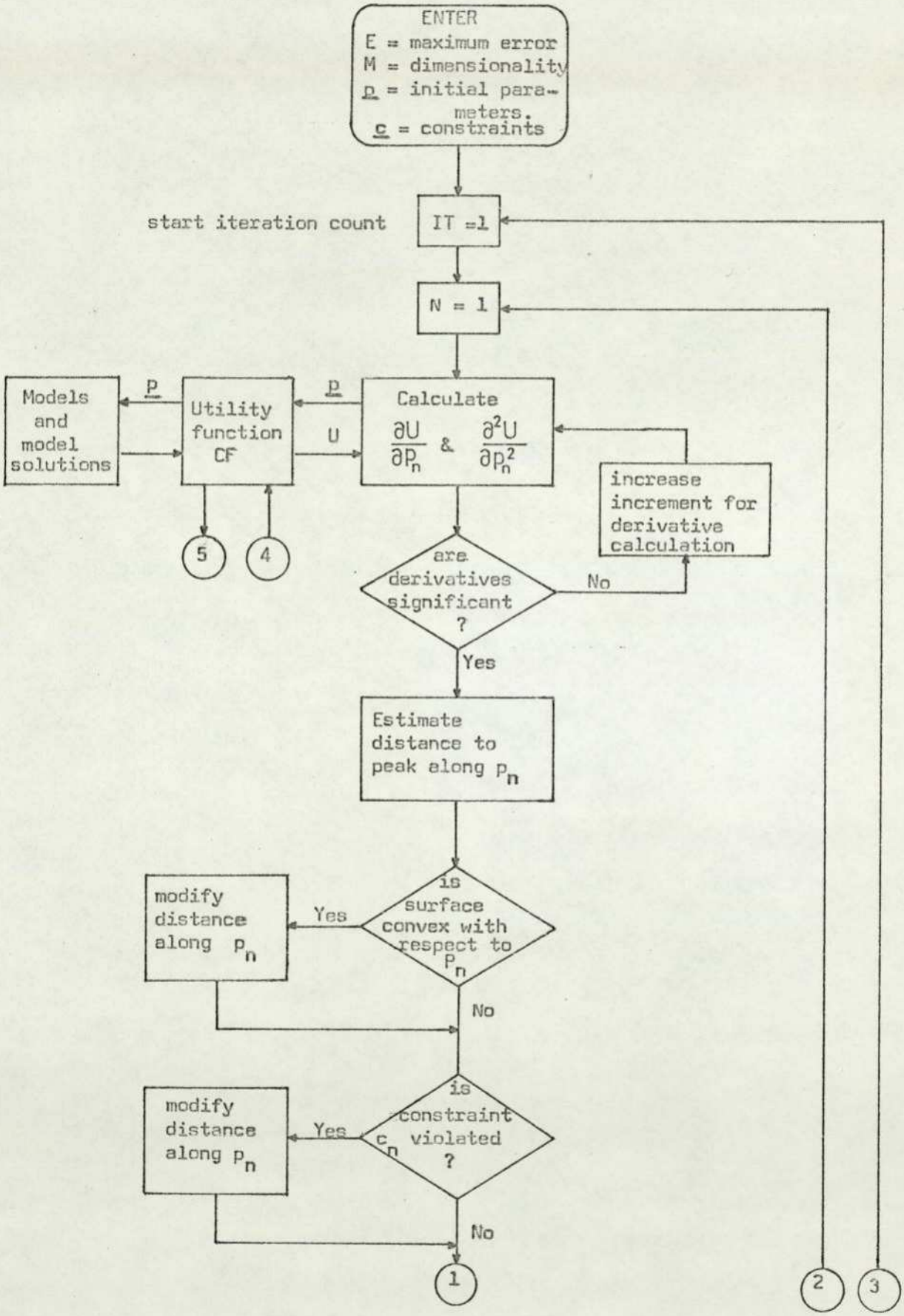


Figure 6.2 continued

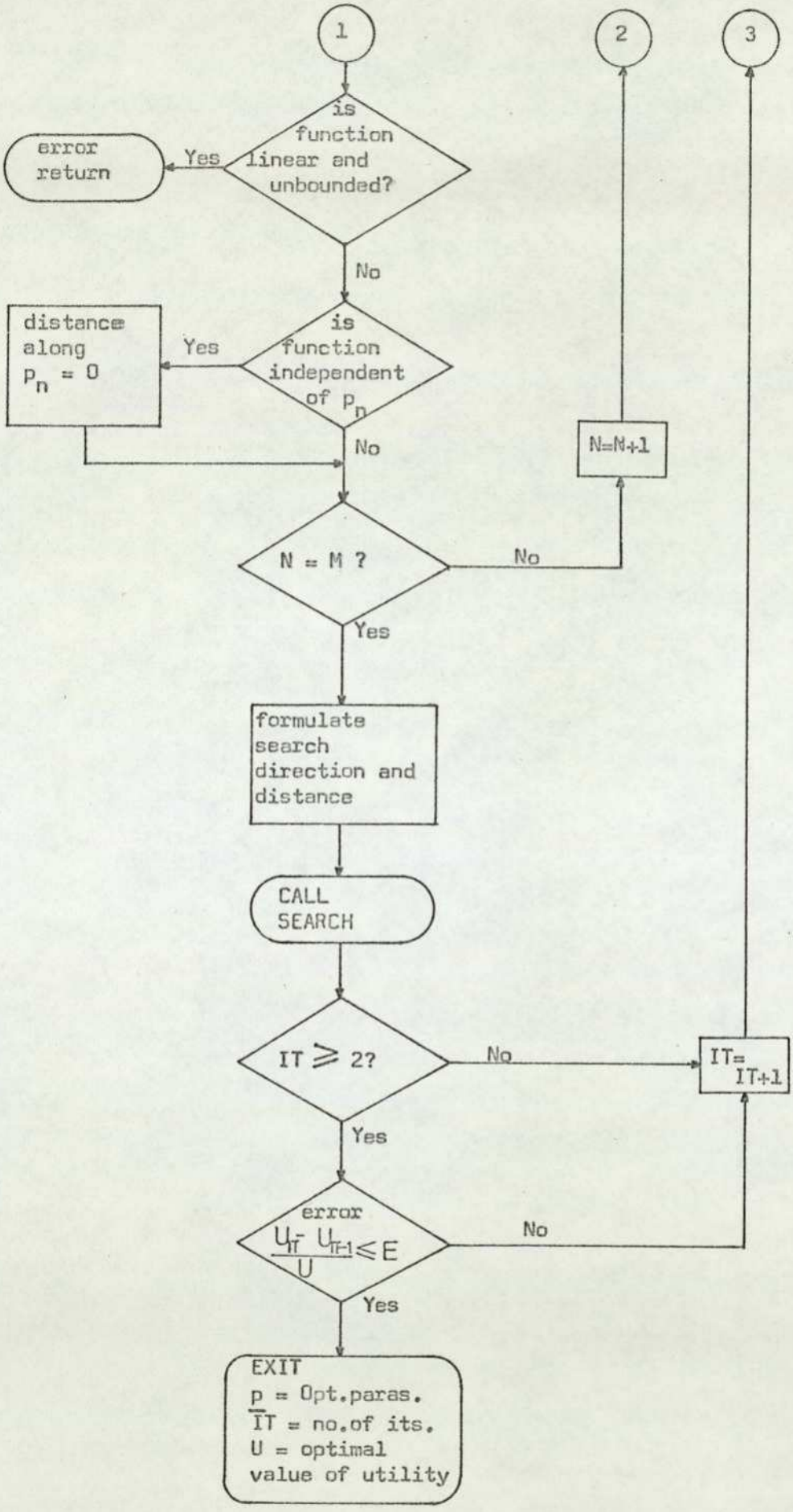


Figure 6.2 continued

(b) Subroutine SEARCH.

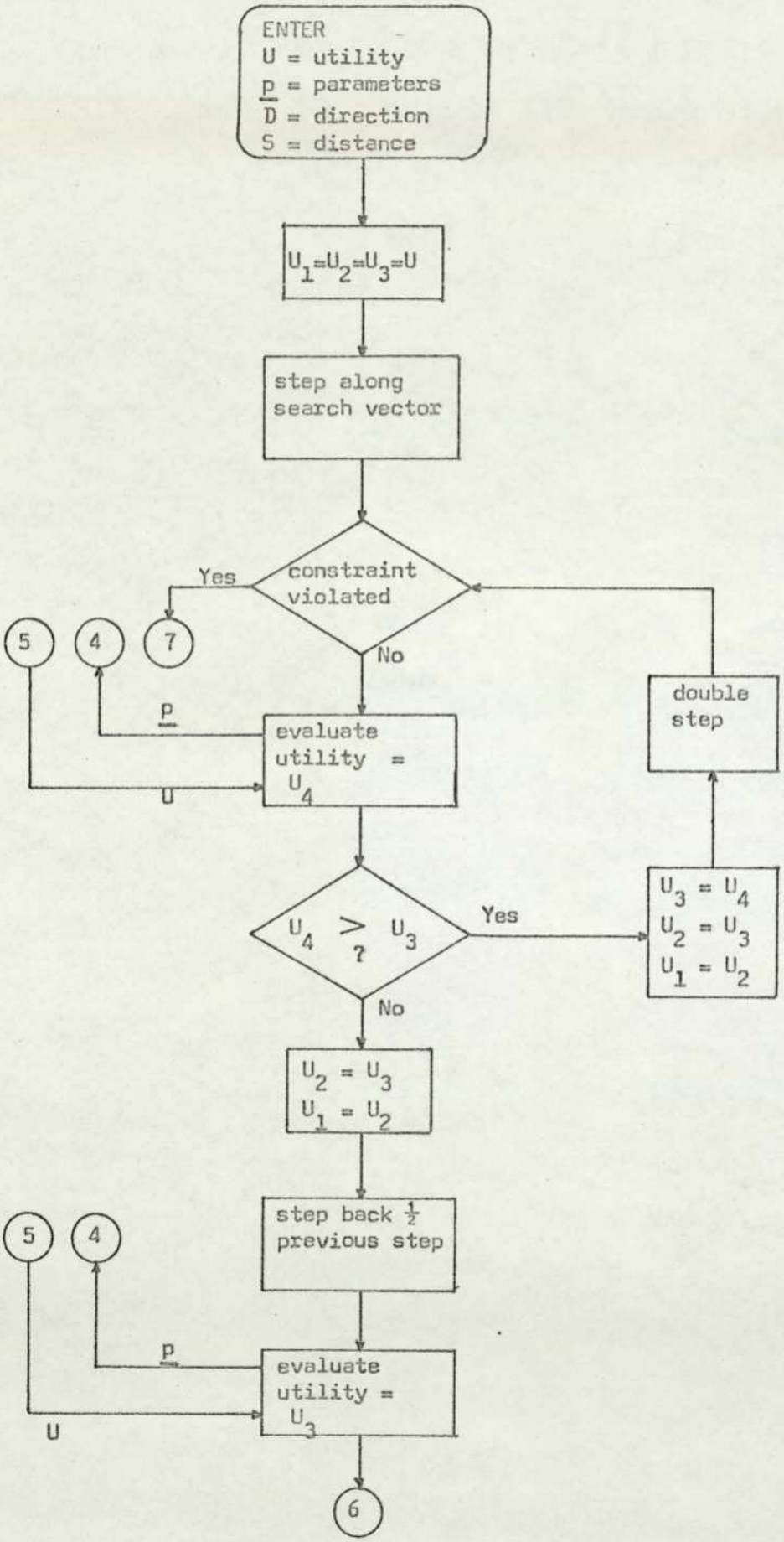
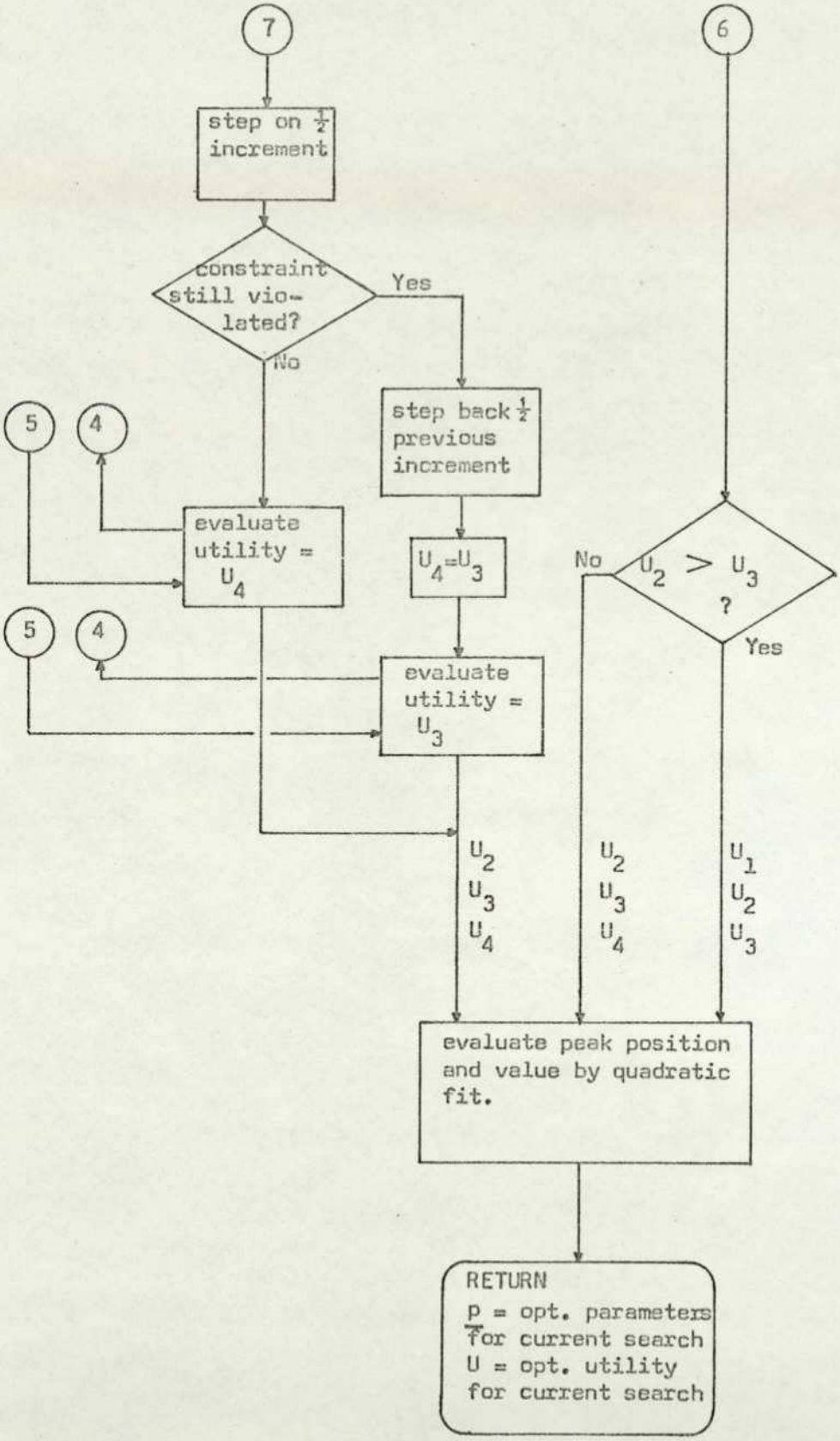


Figure 6.2 continued



The distance to the minimum was calculated and the distance to the 'peak' taken as -1.5 times this, subject to (b) above.

The final action is rather arbitrary, but is not too important as it gives only a small error in overall search direction. The alternative, a search in the offending direction until a constraint or concave surface was found, it was felt would not be justified.

The search subroutine evaluates the utility function at points along the search direction determined by CHIC. Increments are doubled or halved until the peak is straddled, a step back of half an increment is then made giving three equi-spaced points. These are used in a quadratic fit to determine the peak position. Linear superimposition constraints encountered during the search are dealt with by projecting the search direction vector along the constraint and continuing the search until a peak is found or the direction is totally constrained. Other constraints are dealt with by penalty functions and are introduced via the utility function CF.

The procedure is terminated when two successive optima along search vectors are within a prescribed limit. On exit the optimal values of parameters, the value of the utility and the number of iterations needed to find the peak are output.

The search direction and searching segments of the programme are written in general terms suitable for any problem. The user must supply a segment to define the function to be maximised.

7. RESULTS

7.1. Presentation of Results

Results are presented in tabular and graphical form. Table 7.1 lists the optimal values of design parameters for a range of dynamic weightings (WD of equation 5.32), the weighting range is centred on the value 0.71 derived in section 5. Also shown are the parameters for the reactor optimised in respect of dynamic criteria only (WD = ∞) and in respect of static and cost criteria only (WD = 0). Parameters not listed were held constant during the optimisation procedure (by eliminating their component from the search direction vector). Parameters held were those over which the designer has no direct control; heat transfer coefficients, liquid-vapour phase slip ratios, and the delayed neutron decay and concentration coefficients, more is said of this in discussion of the results in section 7.2. Listed in Table 7.2 are the more important properties of the optimal reactors; static transfer function gains, static operating conditions, reactor cost, initial reactivity override available, and the maximum step demand that the design can meet from an initial 75% full power.

Figure 7.1 shows the positions of the dominant poles and zero in the drum pressure (and power) response for the various optimal designs. Figures 7.2 and 7.3 show how two of the parameters, voidage reactivity coefficient and mass of water in the drum, approach the optimal values from the initial reference value. Transients of the reference and optimal reactors resulting from the maximum step input which the reactor can meet when operating at 75% full load are shown in Figures 7.4 - 7.9. Responses are for reactors with the controller adapted for the present study (section 3.3, Figure 3.10) with a trimming mode controller gain of 1.0×10^{-5} (k_5 of Figure 3.10). Riser and channel exit dryness responses are similar to the voidage fraction response but the relative excursions are less, and fuel temperature and heat flux responses are similar to the neutron flux response, but again in the case of temperatures the excursions are less. Excursions in the circulatory flow rates and pressure drops are small.

Positions of all poles for the WD = 0.71 optimal design are compared with the reference poles in Figure 7.10.

109 →

Table 7.1. Optimal Values of the S.G.H.W.R. Design Parameters

Parameter	Symbol	Reference Value	Optimal Values, Dynamic Weighting WD =				
			0	0.568	0.71	0.852	∞
1	K_v	-0.02	0.027	-0.00888	-0.00887	-0.00879	-0.00529
2	K_t	-0.00001	0.00001386	-0.00000559	-0.00000560	-0.00000555	-0.00000517
3	R	5.4	9.21	6.289	6.29	6.353	6.576
6	d	0.0475	0.0351	0.0406	0.0406	0.0406	0.0380
9	n_b	36	35	35	35	35	36
10	N_b	103	72	106	106	104	115
13	P_1	84.3	84.3	87.5	87.5	87.0	88.5
14	P_2	0.1448	0.1448	0.1532	0.1533	0.1539	0.1560
15	P_3	0.00476	0.00476	0.00434	0.00434	0.00435	0.00420
18	h_f	365.0	365.0	346.6	346.5	347.0	339.3

Table 7.1 continued

Parameter	Symbol	Reference Value	Optimal Values, Dynamic Weighting WD=				
			0	0.568	0.71	0.852	∞
19	l_c	12.0	7.23	10.89	10.89	10.88	10.53
20	d_c	0.407	0.271	0.425	0.425	0.424	0.475
21	l_r	1.0	0.8	1.04	1.041	1.037	1.29
22	d_r	1.0	0.8	1.04	1.041	1.037	1.29
23	l_d	1.0	0.8	0.777	0.777	0.762	0.706
24	d_d	1.0	0.8	1.04	1.041	1.003	1.29
25	l_{rv}	20.2	20.2	23.98	23.98	23.91	25.2
26	K_{TC}	-0.0000278	0.00005792	-0.0000289	-0.0000289	-0.0000288	-0.0000368
32	V_{sat}	1350.0	345.0	1365.0	1365.4	1351.0	1460.0
33	M_{wd}	32900.0	26872.0	38306.0	38327.5	37782.0	45472.8
34	z	0.2	0.2	0.228	0.228	0.227	0.237

Table 7.2 Characteristics of Optimal S.G.H.W.Rs.

		Reference Value	Optimal Values, Dynamic Weighting WD =				
			0	0.568	0.71	0.852	∞
Static gain p_d/y_t		-1194.2	-484.6	-720.6	-721.4	-731.7	-324.1
Static gain p_d/k_c		88420.2	206310.0	101322.0	101291.0	101280.9	98632.0
Static variables	$\bar{f}$	0.204	0.278	0.167	0.168	0.169	0.116
at 75% power	W_w	4174.0	4005.0	5016.0	5012.0	5009.0	6460.0
	$\bar{T}_f$	1234.0	1508.0	1229.0	1246.0	1260.0	1178.0
	n	1.0	2.56	1.29	1.30	1.31	1.31
	x_c	0.0723	0.0745	0.0609	0.0610	0.0611	0.0475
	x_r	0.0801	0.0829	0.0670	0.0671	0.0672	0.0522
Maximum step		14.1%	-	19.2%	19.3%	19.4%	23.2%
Cost		1.0	0.915	0.975	0.975	0.975	0.986
Reactivity Override		2.5%	12.3%	1.6%	1.6%	1.6%	-6.6%

Figure 7.1

Shifts of the poles and zero dominant in the pressure response.

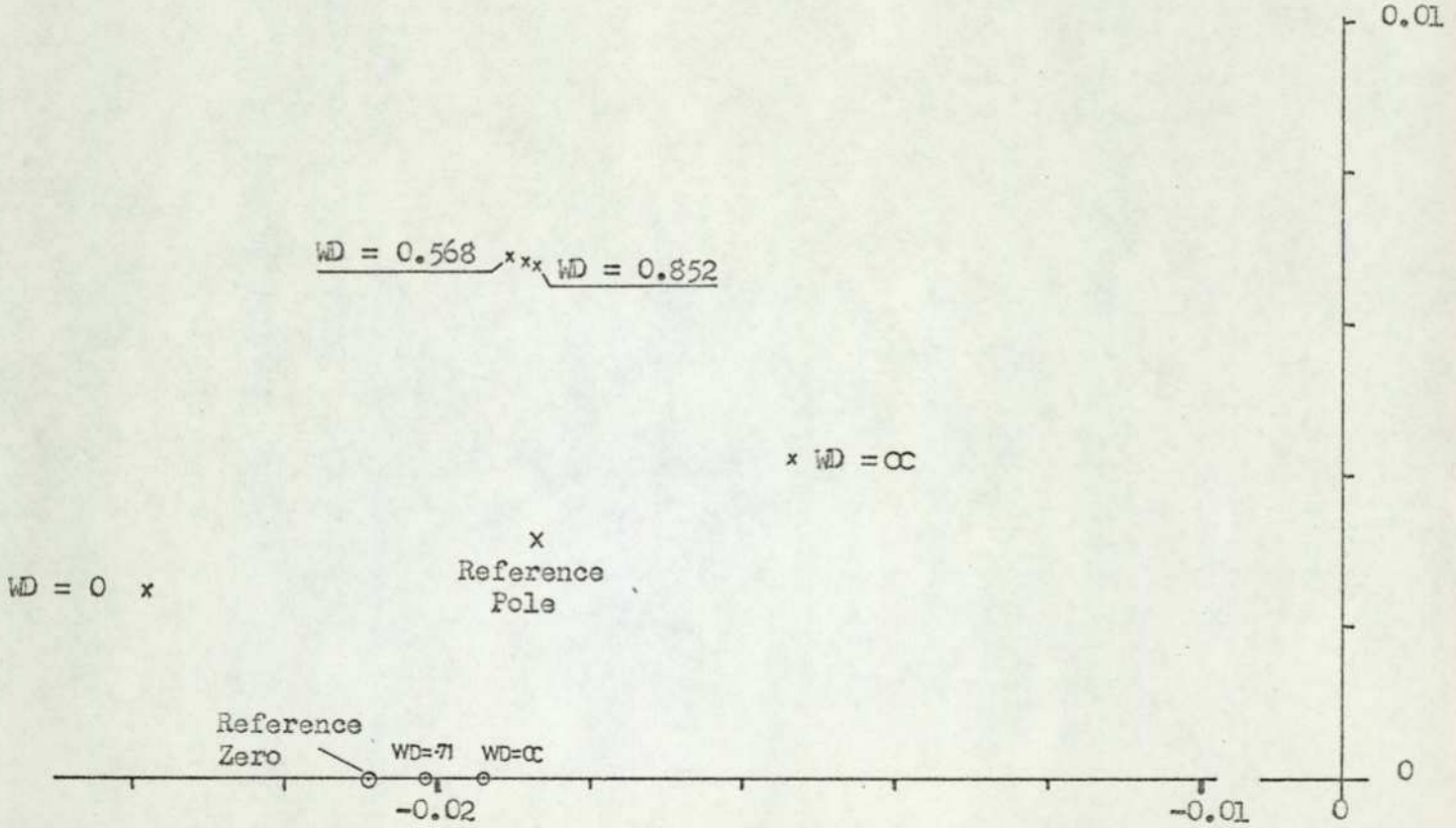


Figure 7.2

Drum volume approach to optimum.

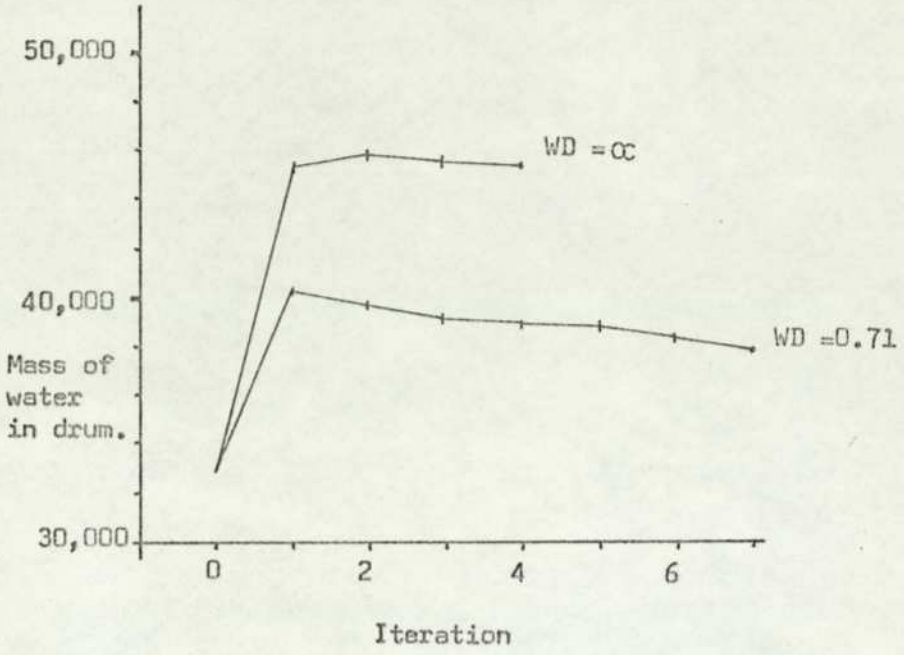


Figure 7.3

Voidage reactivity coefficient approach to optimum.

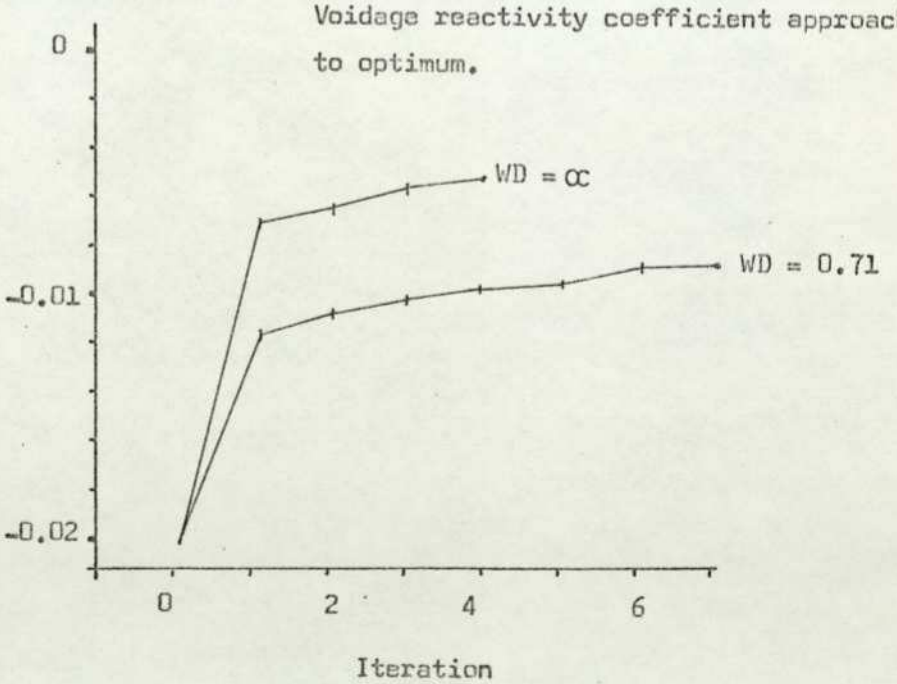


Figure 7.4 Drum pressure response of the reference and optimal reactors.

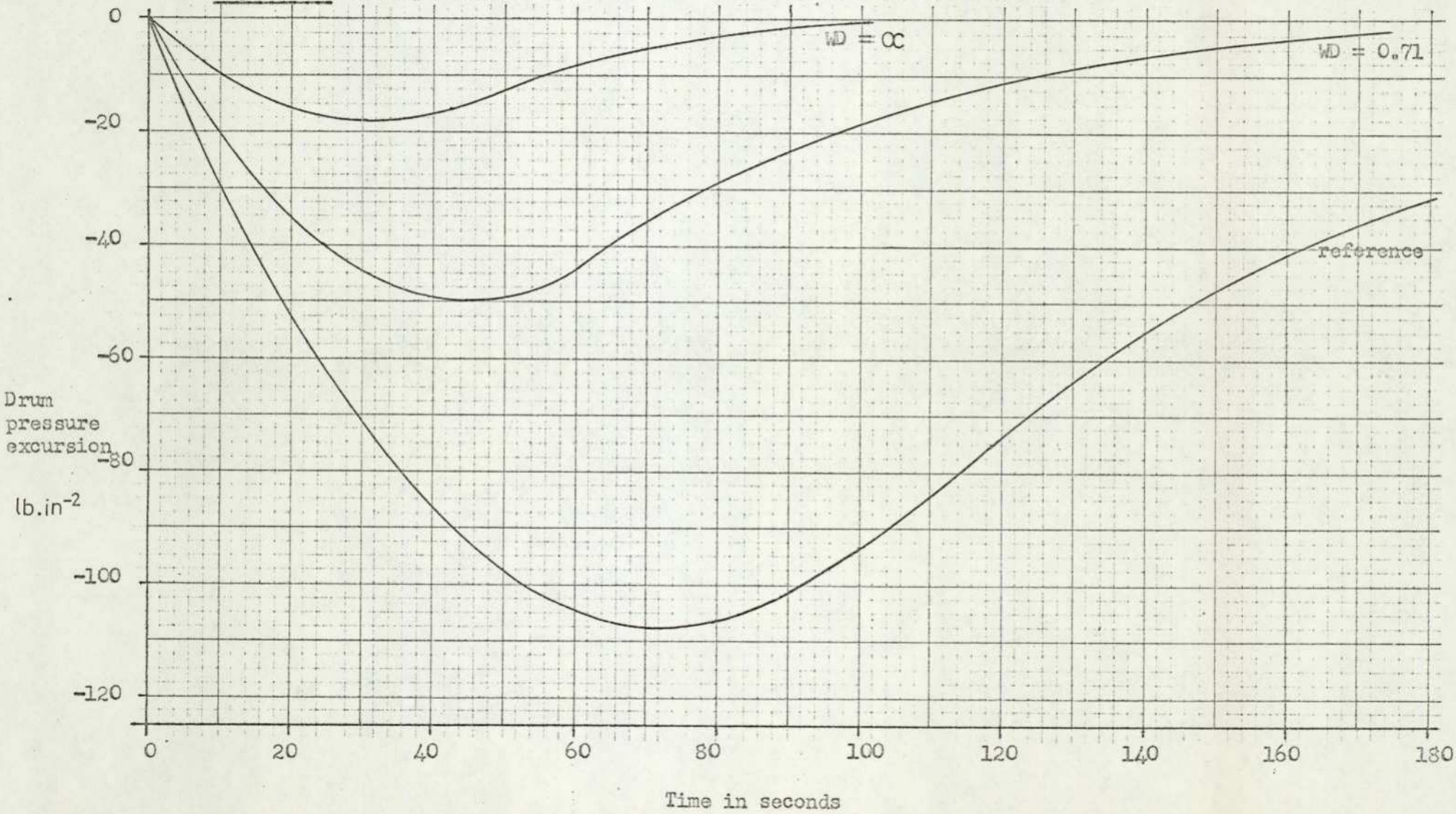


Figure 7.5 Turbine stop valve transients for the reference and optimal reactors.

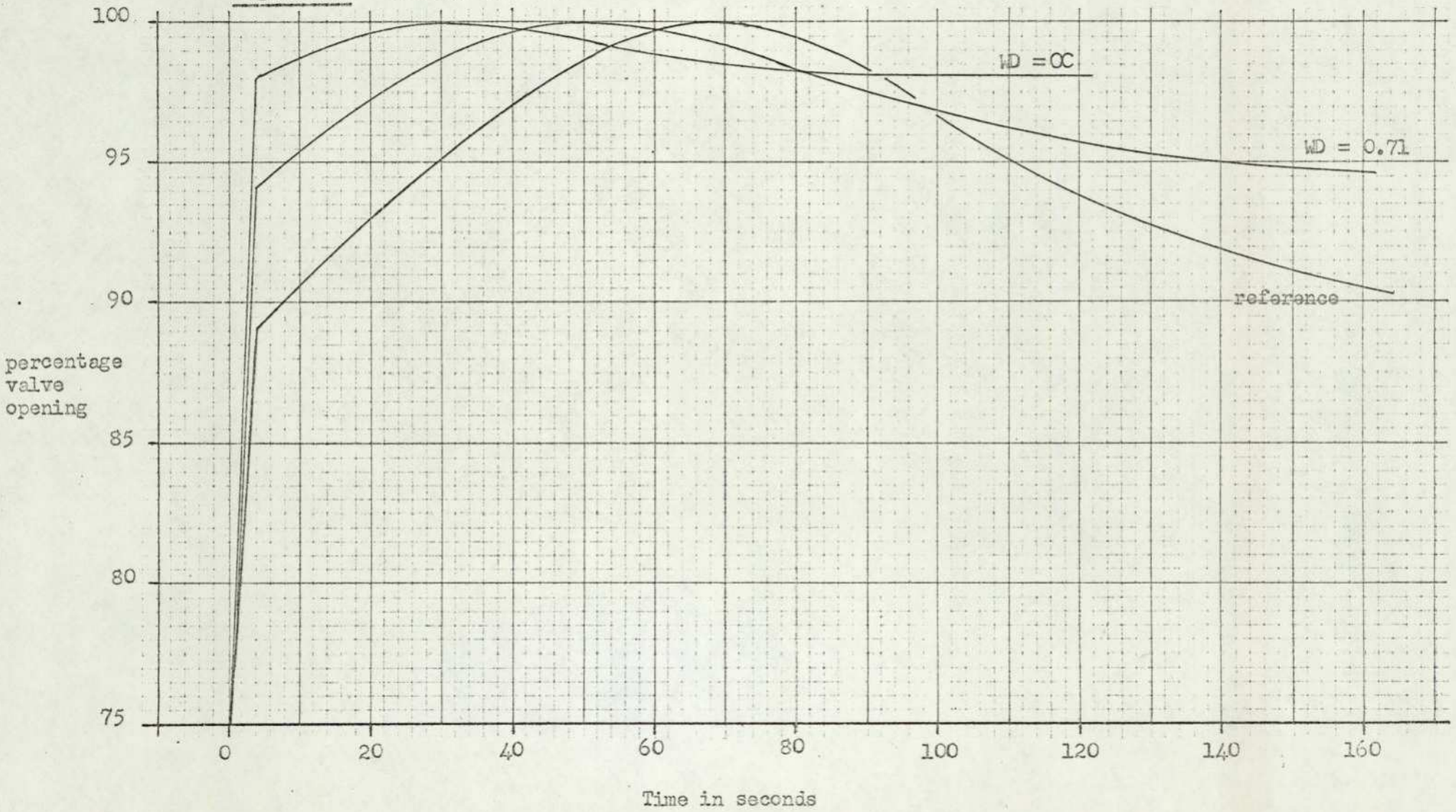


Figure 7.6 Control reactivity responses for the reference and optimal reactors.

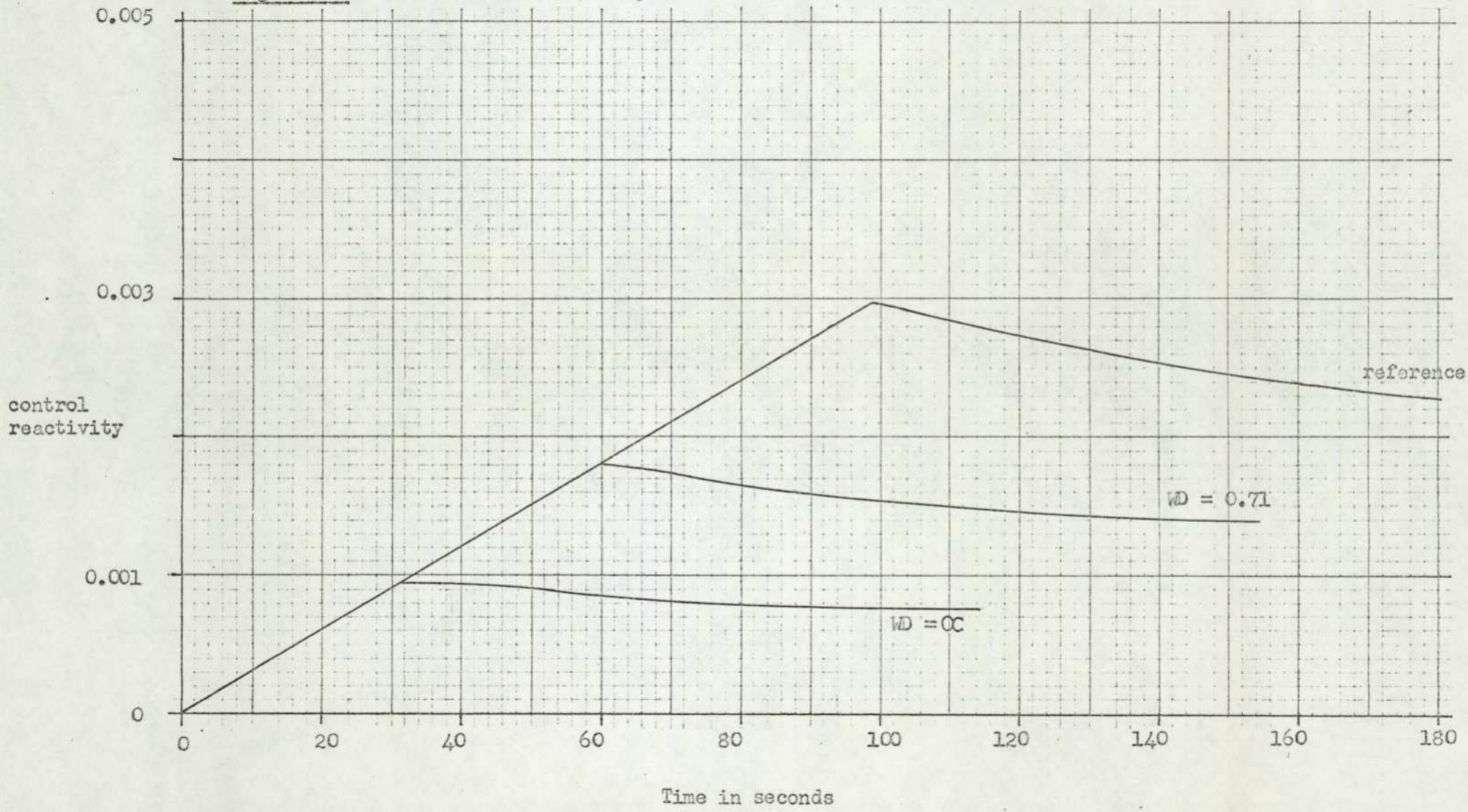


Figure 7.7 Reactivity responses of the reference and optimal reactors.

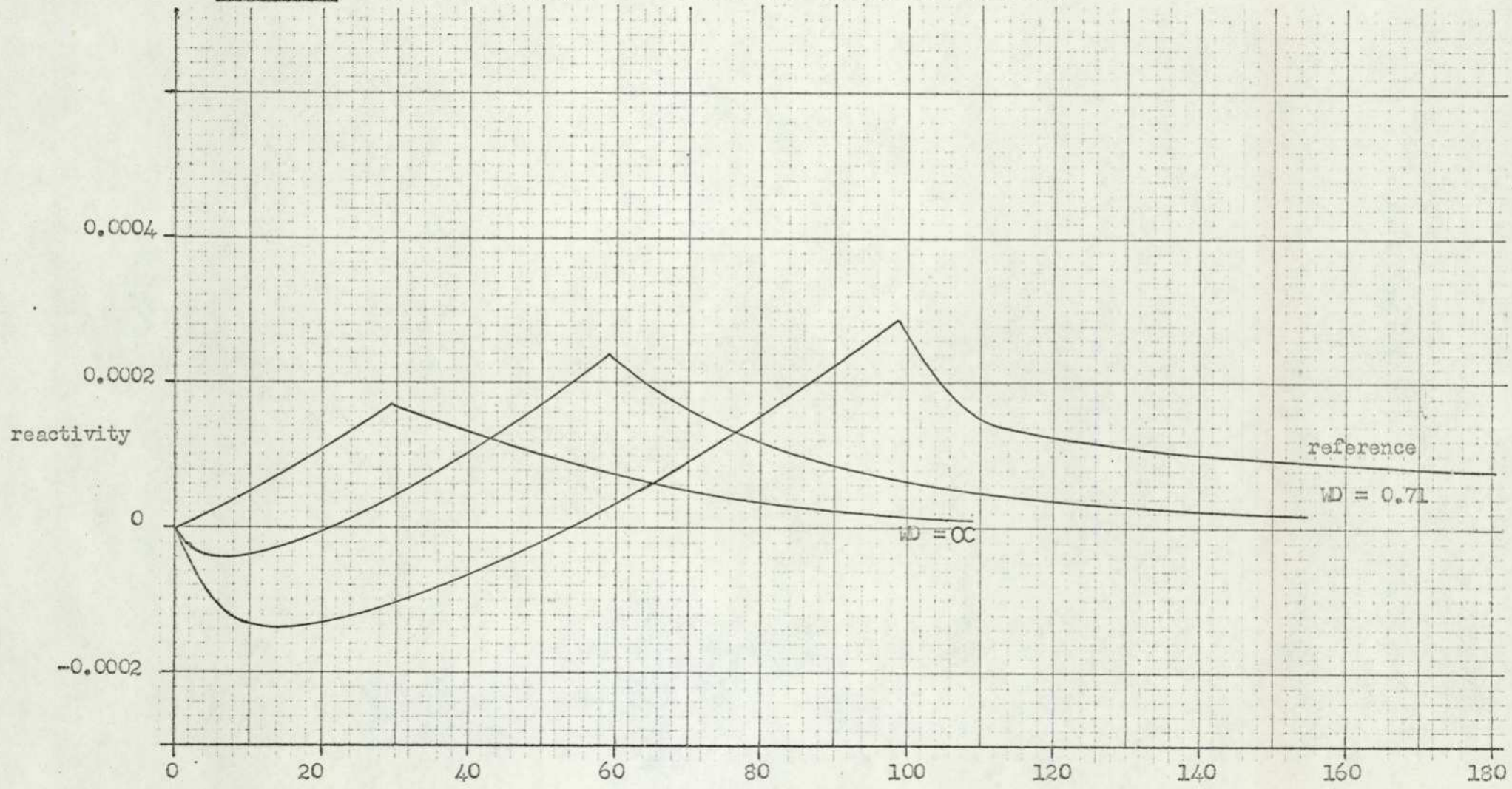


Figure 7.8 Neutron flux responses of the reference and optimal reactors.

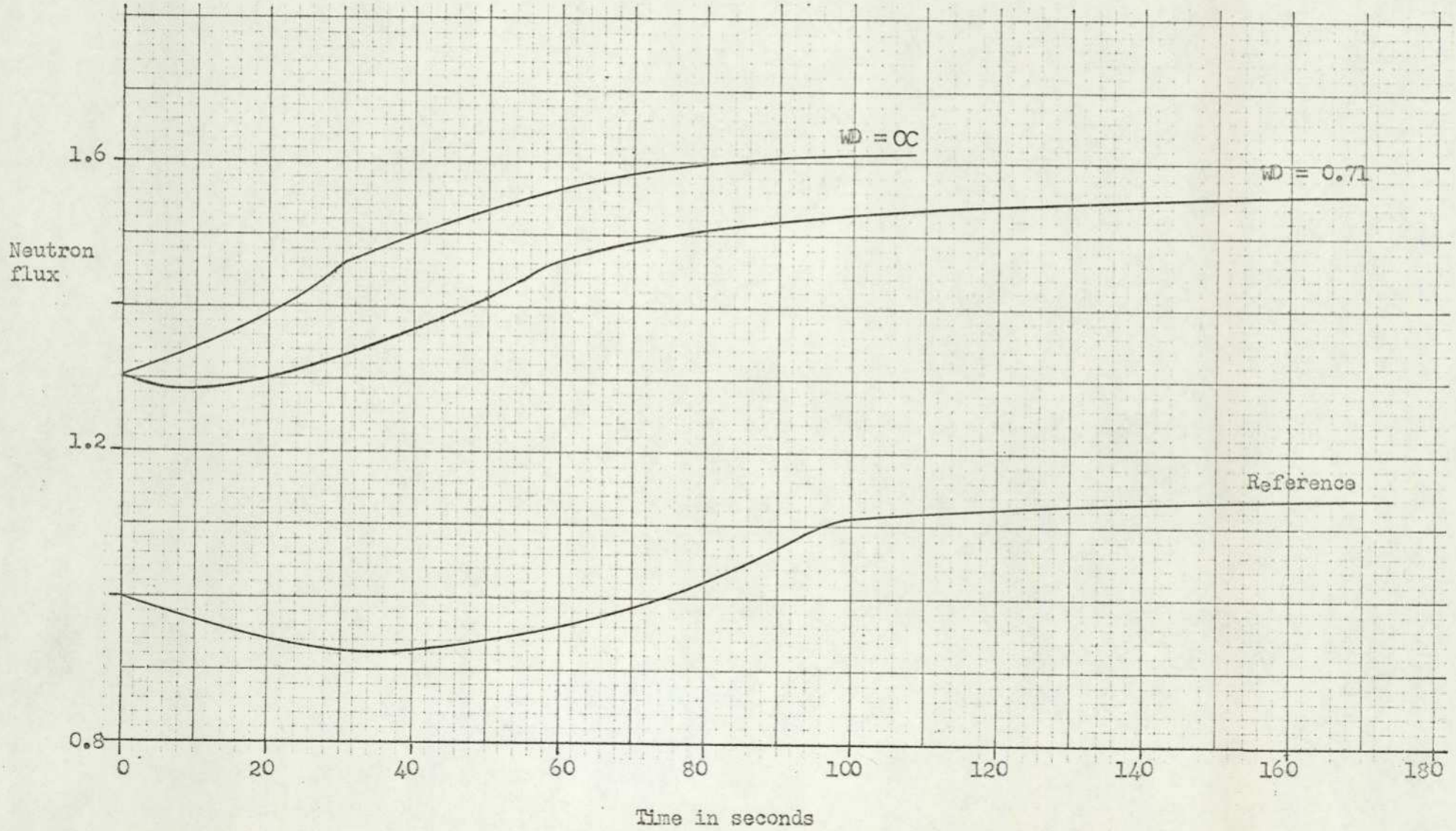


Figure 7.9 Voidage fraction responses of the reference and optimal reactors.

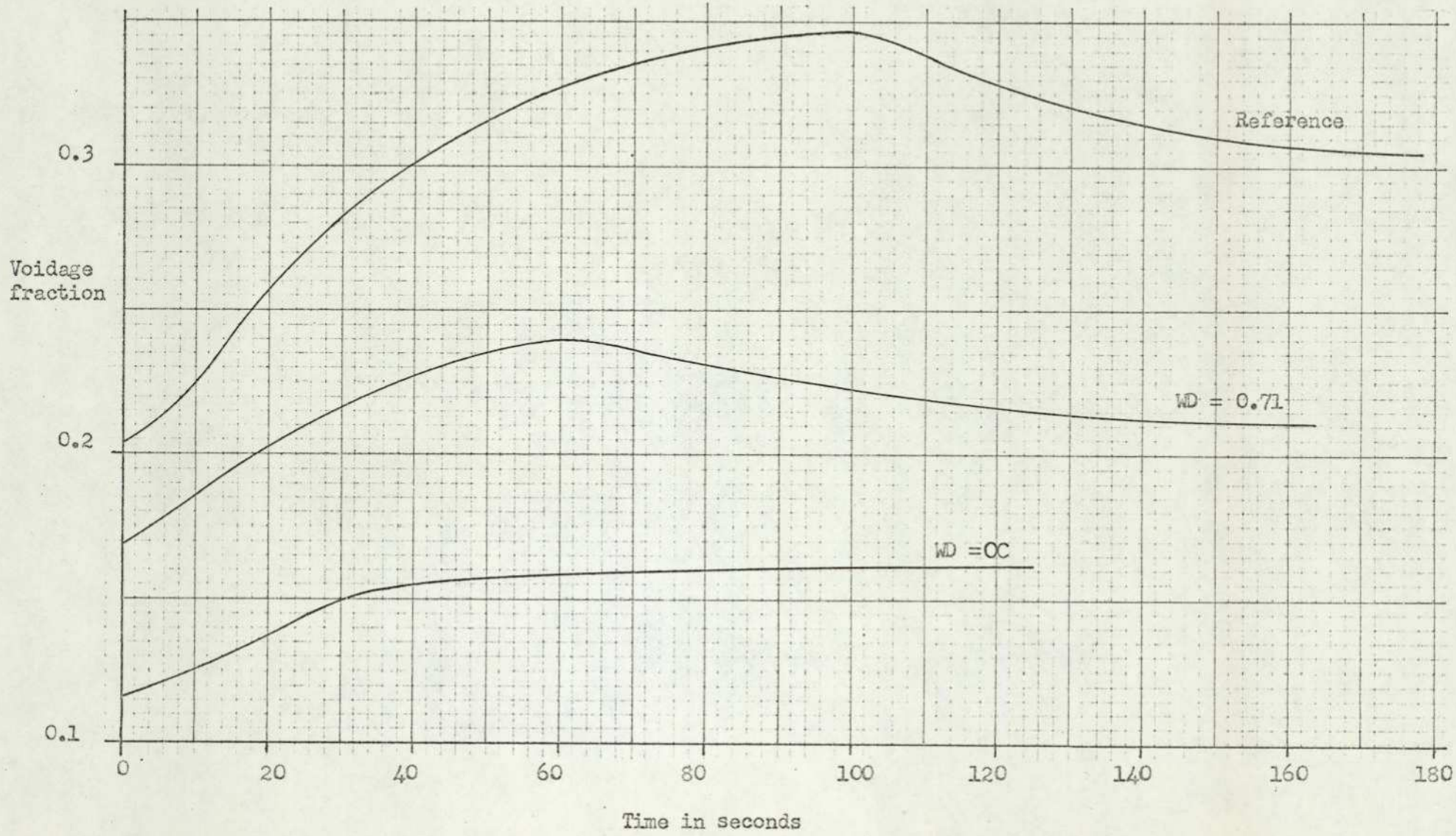
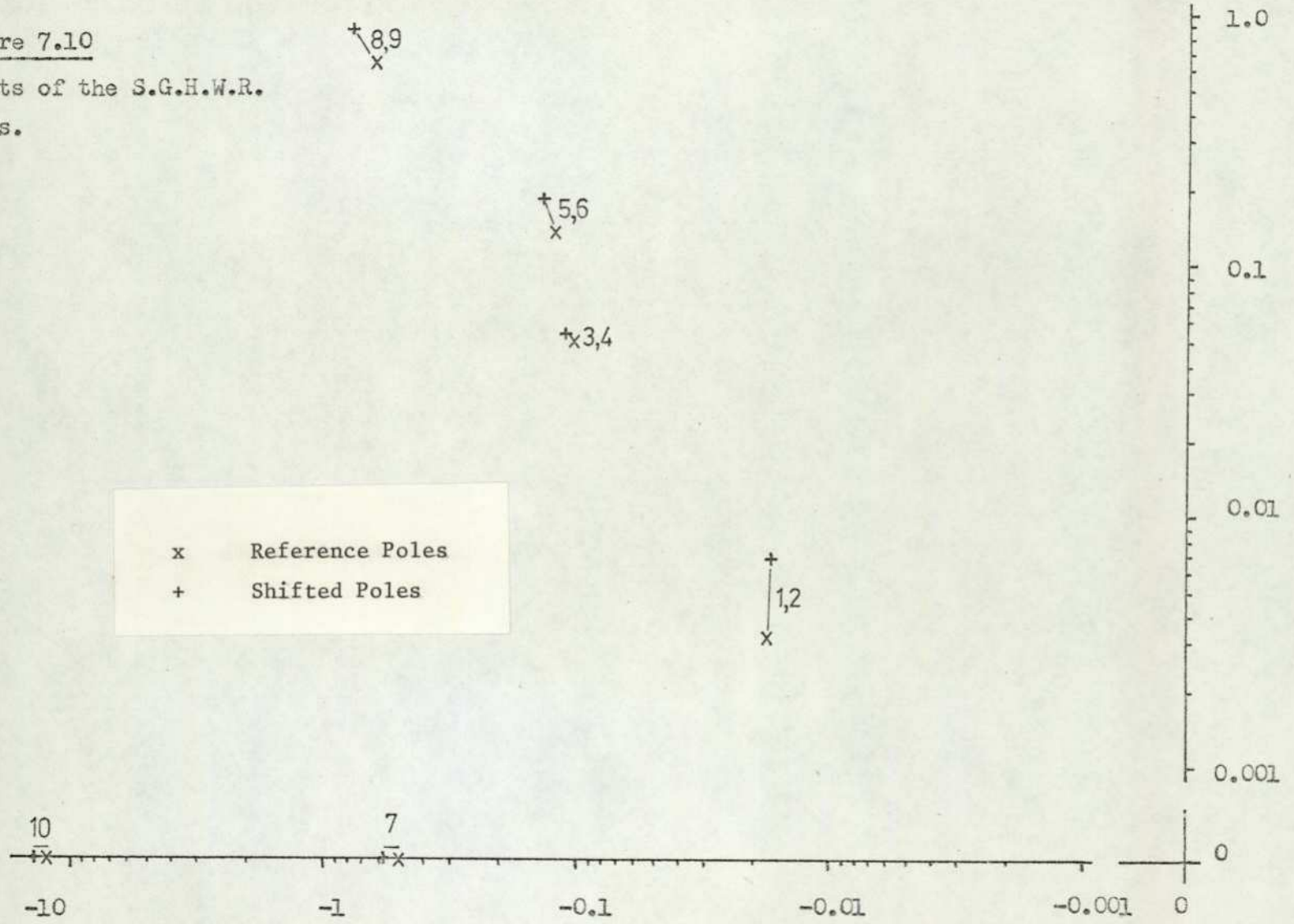


Figure 7.10

Shifts of the S.G.H.W.R. poles.



7.2. Discussion of Results

The optimal reactors for the dynamic weighting range 0.568 to 0.852 show an increased dynamic capability and a rather poorer static performance when compared to the reference reactor. Improved dynamics are achieved almost entirely by influencing the static transfer function gains between the inputs and drum pressure, that from control reactivity being increased and that from turbine stop valve being reduced. Referring to Figure 3.10 (page 36) this means K_1 is reduced (in magnitude - it is negative) and K_2 increased. The effect of reducing K_1 (when the stop valve feed forward and power feedback loops are reduced) is to shift the closed loop poles to the left thereby speeding up the controlled system. The dominant reduced poles are -

reference design	+ 0.0040	, -0.0203
optimal design WD = 0.71	- 0.01096	, -0.01398

as stated previously the reference design is unstable without reactivity feedback control since the normalised K_1 is greater than unity. Increasing K_2 makes the drum pressure more sensitive to reactivity input and since this is rate limited the higher gain leads to a faster pressure recovery rate. The open loop dynamics are only slightly affected during the optimisation as the pole and zero positions of Figure 7.1 indicate. For the WD = 0.71 case the poles dominant in the drum pressure response indicate a lower damping of the dominant mode and a slightly higher natural frequency, both these effects are detrimental to dynamic performance initially as the drum pressure response to a power demand is faster. Response to reactivity control action is also faster, but in the absence of any gain changes a slower open loop response is better. The reasons for the slightly faster response are not clear since both steam drum and riser volumes are increased in the optimal design, which would tend to slow down pressure response. It is possible that superimposition errors are responsible for this paradox, which is in any case of little consequence.

The reactor optimised for dynamic performance alone shows an increased trend towards the reduced stop valve to drum pressure static gain, and also towards the larger drum and riser volumes which this time result as expected in a 'slower' dominant pole. The trend towards larger riser length and diameter in the optimal designs indicates that the increased storage is more beneficial than the closer drum-core coupling and reduced transport delay which would result from smaller risers. Logically it would seem that if increased steam storage was required to improve dynamics it should be added

either to the risers or the drum depending upon which was cheaper as defined in the cost model (drum and riser dimensions do not affect static performance). The reason why this does not occur is that within the limits of pole-zero superimposition it appears better to the optimising process to increase both drum and riser volumes to improve dynamics, since dynamics dominate cost in the utility function. Only when the dynamics were near perfect would the cost term come into play and drum and riser volumes would be traded off.

Optimal designs for WD = 0.568 - 0.852 are very similar, the reasons for this are twofold. Firstly cost is fairly insensitive to the changes made in the design parameters, Table 7.2 shows that a cost saving of only 2.5% is made in the optimisation. The second reason concerns the evaluation of dynamic performance. Referring to Figures 5.9 and 5.12 (page 81) and using a plant mix containing 20% S.G.H.W.Rs., the step size which the S.G.H.W.Rs. must be able to meet to cope with the faults occurring while the grid is supplying 10-15 KMW is -

$$\frac{450}{12500 \times 0.2} \times 100 = 18\% \qquad 7.1$$

Reactors which can cope with step demands greater than 18% can make savings only in the periods when the grid is supplying 5 - 10 KMW, i.e. only 160 hours a year (Figure 5.12). Reactors which cope with less than 18% cannot meet some demands made while the grid is supplying 10 - 15 KMW, a much more significant 1872 hours per year. A discontinuity occurs in dynamic utility at an 18% step capability and the optimum tends to settle here as static utility decline exceeds the dynamic utility improvement for capabilities beyond 18%. A more precise annual power distribution would lessen the discontinuity, but only slightly as the drop in dynamic value in this region is very real. The discontinuity was smoothed considerably (by subdividing the fault levels into 50 MW bands) to avoid problems in derivative estimation during optimisation. This accounts for the optimal reactor for WD = 0.71 being able to meet step demands of 19.1%, rather higher than the 18% of equation 7.1. Dynamic performance is obtained at the expense of static performance, the optimal design has an initial reactivity surplus of 1.6% as opposed to the 2.5% of the reference design. Refuelling would be necessary every 3.8 months.

Optimal designs for WD = 0 or WD = ∞ are not viable, which confirms the inadequacy of maximising with respect to a single criteria without examining the wider implications. The optimal design with respect to dynamic performance only could meet nearly all the power

demands made of it, but has a massive reactivity deficit of 6.6% and could never be started. The static performance plus cost optimal design (WD = 0) has a 12.3% reactivity surplus with fresh fuel (refuelling every 2 years) and its cost is only 91% of the reference design. The positive voidage, fuel temperature and coolant temperature reactivity coefficients make the reactor virtually uncontrollable.

In improving overall dynamics considerable changes have resulted in the core operating conditions. The overall effect is to reduce the total mass of fuel, but increase the enrichment and the static flux level to maintain power output. Despite the higher rating average fuel temperatures have remained fairly constant, there are a number of reasons for this. Smaller fuel pins as well as improving core response time have a larger surface to mass ratio and less internal to external (inner to outer zone) thermal resistance. Circuit pressure drop is lower and therefore channel pressure and evaporation temperature are lower, and mass circulation rates are higher. The higher circulation rates also lead to the lower dryness and voidage fractions of the optimal designs, although the effects are offset to a certain extent by the lower subcooling at channel inlet (due to lower channel pressure and a smaller proportion of subcooled feedwater).

By far the largest relative pole shifts occur in the pair which dominate the power response, poles 1 & 2 in Figure 7.10, the parameter changes which cause shifts in these poles were outlined above. Significant shifts also occur in the pole pairs 5 & 6 and 8 & 9. Both these pairs are particularly sensitive to parameter changes which affect circulatory pressure drops and flow rates (see Appendix 7); the effects are indirect and too obscured by model complexity for any conclusion to be drawn. The modes due to the pole pairs are significant only in the reactor core and therefore do not affect dynamic utility, except when a constraint violation occurs.

During the optimisation certain parameters were held constant; the fuel thermal conductivity, specific heat and density, channel and riser slip ratios, and fuel to coolant heat transfer coefficient. These should be related to design parameters in the same way that the friction coefficients were, they are much less sensitive to parameters than were friction coefficients and little was lost in holding them constant. What is more significant is that the various reactivity coefficients are functions of parameters. As the static gains which were altered during optimisation to improve dynamics were mainly influenced by the reactivity coefficients, it is important for the designer to know how reactivity coefficients are affected by design

changes. The relationships are extremely complicated (7.1.), computer programmes are available to make the necessary calculations (7.2) and could be used to relate reactivity to parameters by sensitivity coefficients. The tools were not available for this to be undertaken in the present study however.

Two conditions which apply to the reference design have been carried through to the optimal designs, this may not be entirely valid and the optimal parameter values would be affected slightly if different conditions were defined. The first concerns the acceptable reactivity input rate which is limited in the reference case to 3.0×10^{-5} sec $^{-1}$, this is assumed constant but should possibly be related to the static gain of the control reactivity - drum pressure transfer function. The limit is due to safety considerations at startup, changing the limit would affect dynamic performance of the optimal designs. The second condition affects the fresh fuel reactivity override to refuelling interval relationship, i.e. static performance. No account is taken of the higher neutron flux levels in estimating the refuelling intervals for the optimal designs. Refuelling would take place more frequently than estimated. There is reason then to believe that both static and dynamic performances of the optimal reactors are a little below those indicated.

Optimising the reactor in respect of cost, static and dynamic performance has been achieved, but this is not the whole story. Criteria based on safety, reliability, (creep and fatigue problems have received much attention) startup and shutdown considerations should ideally be added to the utility function. Nor is the picture complete in the static and dynamic performance categories. Dynamic performance is based on the ability of the plant to meet step demands (the most severe case), performance in following the normal daily load profile or other types of disturbance (e.g. T.V. peaks) has not been covered. Indeed the controller adopted would be unsuitable for normal operation and would have to be initiated from grid control when required. Fault timing is also relevant, if a fault occurs at a time of normal rapid load increase it is more difficult to recover than if it occurs when power is generally declining. Scope for adding to the static performance category lies in the operations and maintenance fields. Finally it should be noted that the optimal designs are based on present day data on power and fault levels and not on predicted levels for some future date.

The system boundary was drawn around the S.G.H.W.R. which led to limitations, although it was necessary to contain the size of the

problem. Assumptions had to be made concerning the proportion of S.G.H.W.R.s in the plant mix and their quiescent operation level. A larger systems study can be envisaged which would include these factors as parameters to be optimised along with the rest, and where the costs of 'static' and 'dynamic' stations would be balanced against power losses. Reliability analysis could be used to relate fault patterns to the system parameters, and beyond this the problems of overall energy and water supply would arise. The problem soon becomes unmanageable.

8 . CONCLUSIONS

Conclusions specific to the S.G.H.W.R. problem have been covered in section 7.2., this section is confined to discussion of the systems design method.

The reactor application has demonstrated that design control problem can be formulated and solved for plants of a size and complexity commonly encountered; this was the primary aim of the work. Cost and static performance have been treated as rigorously as the data available would allow, but the means of analysing dynamic performance - via sensitivity coefficients - is far from rigorous.

In justifying the use of pole-zero sensitivity coefficients two considerations are dominant, errors introduced in the linearisation and superimposition processes, and the time taken to estimate dynamic performance in the optimisation procedure. The error problem has been discussed in sections 4 and 5, where it was demonstrated that for restricted amplitude inputs (small perturbations) and pole shifts the method was satisfactory. However, to justify the errors introduced a substantial time saving in dynamic assessment must result. Alternative methods of generating dynamics would be to solve the linear dynamic model for poles and zeroes each time it was required, or to simulate the system via either the linear or non linear dynamic models. For the S.G.H.W.R. problem reducing the linear model to pole-zero matrices for four transfer functions and determining their eigenvalues using ZIP takes about 40 seconds, (actual ZIP runs were about 2 minutes but this includes data input-output and sorting). Thirty-five runs were required to extract the data for pole-zero sensitivity coefficients plus some time to calculate the coefficients, say 1500 seconds in all. Estimating shifted pole and zero positions and transient evaluation for the four transfer functions took 1.1 seconds approximately and was done about 80 times during a hill climbing iteration. Typically seven iterations were required to achieve an optimum, given a total computing time for dynamics of -

$$1500 + 80 \times 1.1 \times 7 = 2116 \text{ seconds} \qquad 8.1$$

Solving the linear model for poles and zeroes as required for seven iterations and 80 estimations per iteration would use -

$$80 \times 40 \times 7 = 22400 \text{ seconds} \qquad 8.2$$

Digital simulation of the linear dynamic model to produce transients takes over 200 seconds, and for the conditions assumed the total time would be -

$$80 \times 200 \times 7 = 112000 \text{ seconds} \qquad 8.3$$

Simulating the non-linear model digitally would easily double this

time. Using a hybrid computer, analog simulation would reduce the time of equation 8.3 considerably, but the 560 estimations of dynamic performance only just exceed the breakeven point for hybrid optimisation which is around 500 runs (8.1). Hybrid computers are also not available as readily as large digital machines. The sensitivity method then has a clear advantage in dynamic analysis time, an advantage which increases with the order of the model. If the zeroes of more transfer functions are required the advantage over simulation decreases, since the simulation covers all variables. There is scope for reducing the time required to calculate sensitivity coefficients, either by using the reference condition poles and zeroes as starting points in the iterations for the shifted values, or by using one of the indirect methods of eigenvalue sensitivity calculation (4.10, 4.11). Improvements would be slight as the ZIP eigenvalue routine is very fast and solves the five matrices (pole + 4 zeroes) in under 9 seconds. Time savings could also be effected by defining dynamic performance in terms of pole and zero positions directly via Parseval's theorem, thus avoiding the need to generate transient responses. This is not always possible and depends upon the system's dynamic objectives and performance.

The limitation of the sensitivity method is the constraint arising from linear superimposition error, timing advantage is such that coefficients can be re-calculated and the system re-optimised several times and still be faster than the alternatives. This could not be done on the S.G.H.W.R. because ZIP was not available at T.C.U. (a situation which is being rectified), but the technique was tried on a fourth order servo system. A position control system with a flexible drive between motor and load was used, with position and velocity feedback from both motor and load. Seven parameters could be varied, the four feedback gains, armature and field resistances and the damping on the load. To optimise the response it was attempted to move the system poles on to the 0.5 critical damping line, and as far from the origin as possible, a criteria chosen for simplicity rather than reality. Figure 8.1 shows the paths followed by the poles, sensitivity coefficients were re-calculated at each numbered point. Pole positions estimated from the sensitivity coefficients and re-calculated from the system model are shown. Initially shifts were constrained (out of caution) which resulted in virtually no error in the predicted pole positions, later shifts were of greater relative size. Figure 8.2 shows the effects of changing individual design parameters by +10% at the starting point and after 2 and 4 iterations, the changes in sensitivity coefficients are demonstrated and are not dramatic.

118 →

Figure 8.1

Servo problem - successive pole positions.

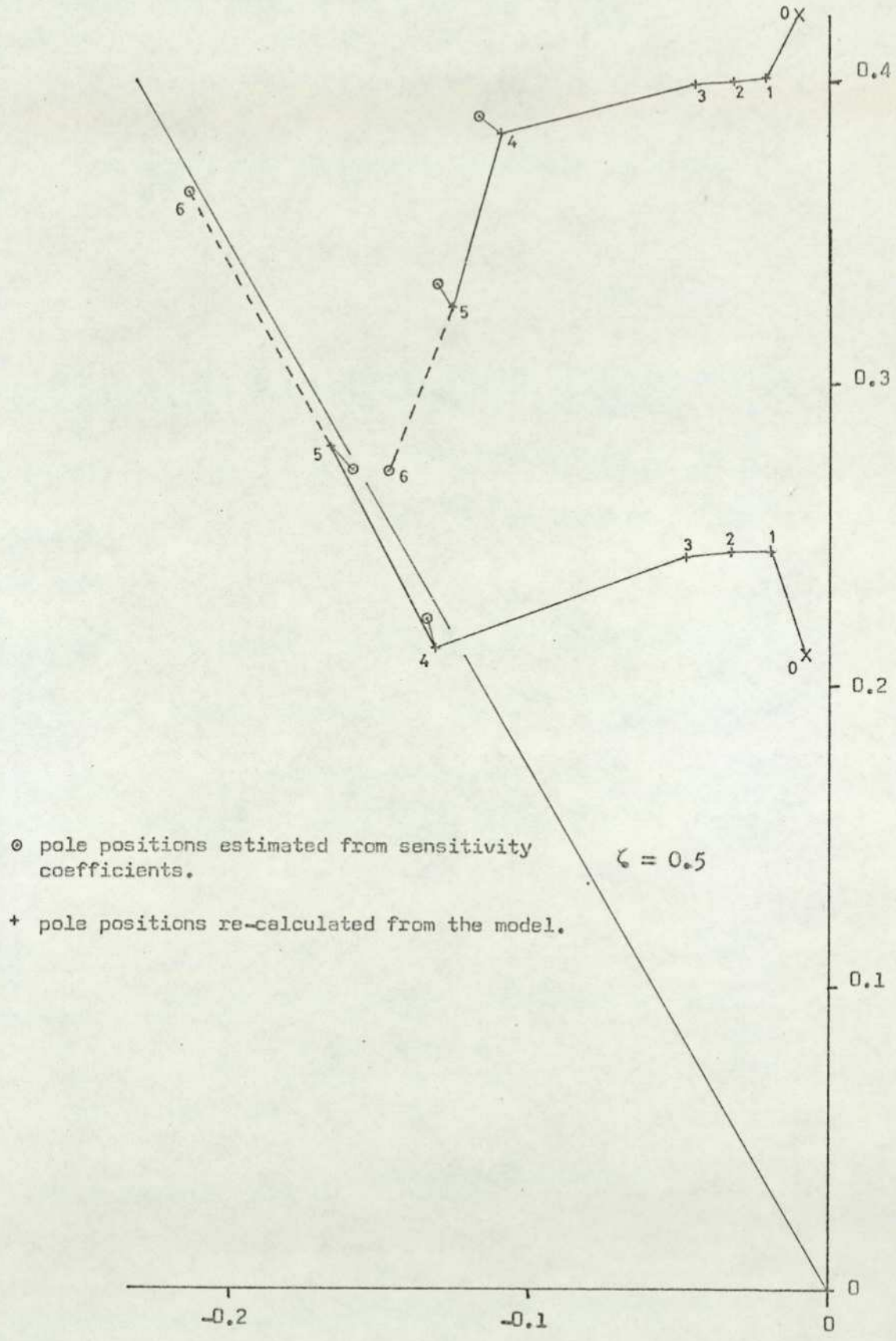
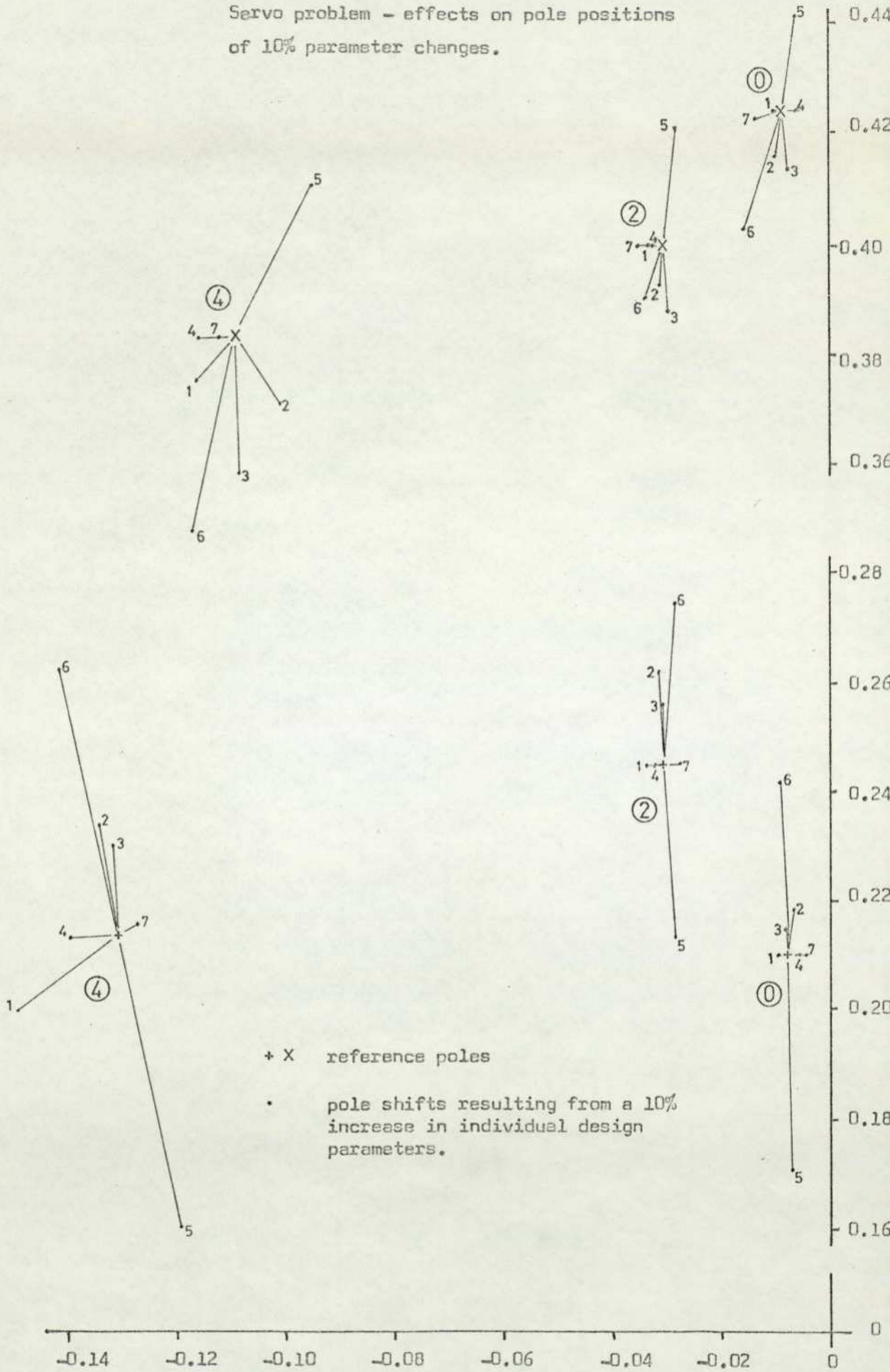


Figure 8.2

Servo problem - effects on pole positions of 10% parameter changes.



As an incidental advantage of the sensitivity method, the value of sensitivity coefficients to the designer as a means of man-computer interfacing should not be overlooked.

The absence of ZIP at TCU has already been referred to, this placed some restriction on the optimisation procedure since open loop sensitivity coefficients were obtained from the Winfrith runs, which were completed before the control strategy had been finalised. During the optimisation process the closed loop responses had to be derived from the open loop shifted poles, which therefore increased the time taken considerably. In addition the zero sensitivities of some transfer functions relating core variables to inputs were not available. Transients of these variables were required for constraint violation checks, and had to be calculated by simulation. These violation checks were made only after each complete iteration and not during each derivative calculation because of the time involved. Availability of ZIP would solve these problems, and until this is the case the sensitivity calculation part of design method cannot be integrated into the scheme. Perhaps a $\frac{1}{2}$ programmer year of effort is required to complete this task. Figure 8.3 shows a flow chart of the programmes making up the design method, indicating those parts which are incomplete, and those parts which the user must supply. Descriptions of the programmes are given in Appendix 8. It will be noted on Figure 8.3 that the decision concerning the adequacy of pole positions and sensitivity coefficients (i.e. the decision to re-calculate) is left to the user as considerations will be very problem dependent.

It is not difficult to see areas where the scope of the design method could be extended, reliability analysis has been mentioned on several occasions and it is along this line that development is expected to proceed. Such extensions would enter the problem via the user supplied segments in the same way as the dynamics analysis package does and would not entail re-structuring of the basic procedure. There are other areas where the structure would be disturbed, where mixed continuous and discrete parameters must be dealt with for example. This occurred in the S.G.H.W.R. problem when considering the number of fuel pins per channel and the number of channels, but in each case the integer involved was relatively large and these parameters were in fact considered continuous and rounded after optimisation, a doubtful practice which cannot be applied if the integers involved are small, e.g. the 'more control - less operators' problem. The alternative material problem, where a whole series of properties affecting many of the model equations will have different discrete values depending

121 →

Figure 8.3

Organisation of programmes forming the Systems Design Method

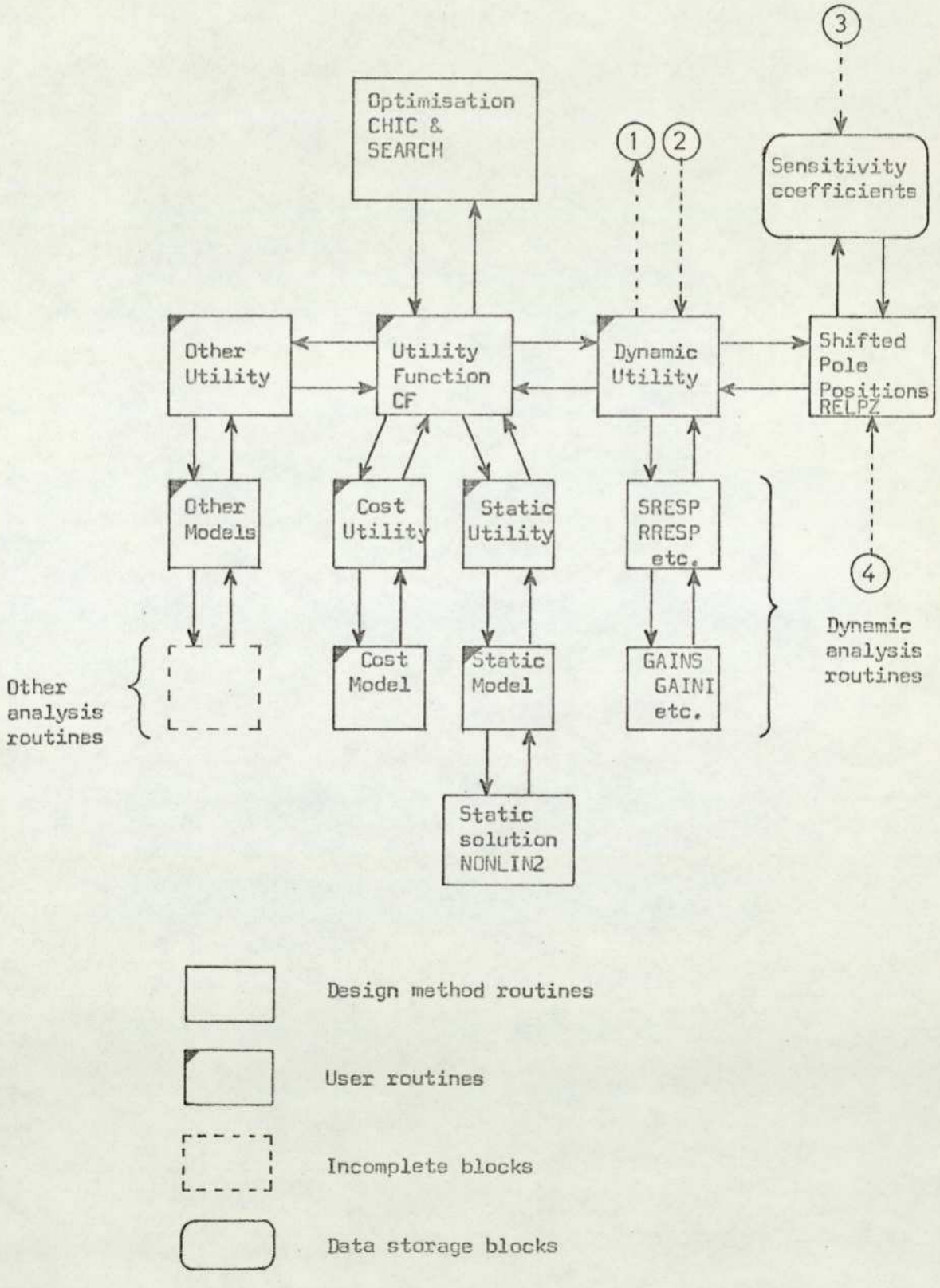
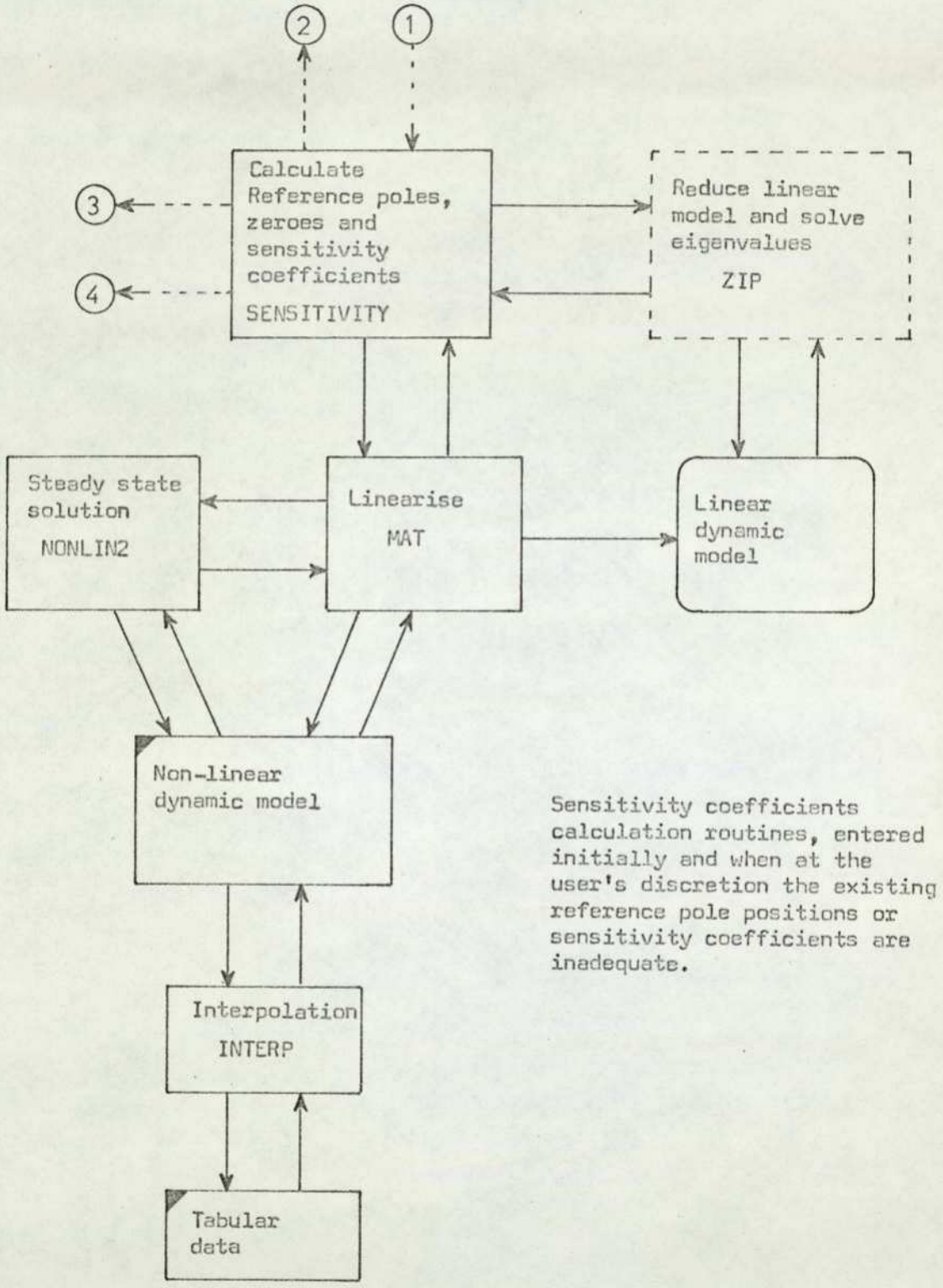


Figure 8.3 (continued)



upon the material selected is important in practice, but is of the type where computers alone are not yet adept and close man-machine interaction is required. The 'alternatives' problem goes farther; electronic or pneumatic control? or electric motor or gas turbine? but the material problem because of the number of possible combinations and the many effects of a single change is one of the most difficult to deal with.

Acknowledgements

The author wishes to express his thanks to the United Kingdom Atomic Energy Authority for their sponsorship of the work contained in this report, and to [redacted] and [redacted] of the Atomic Energy Establishment Winfrith for their co-operation in supplying technical data and valuable discussion on the S.G.H.W.R. Particular thanks are due to [redacted] who organised the simulator runs against which the T.C.U. model of the S.G.H.W.R. was verified, the ZIP runs which were used in estimating sensitivity coefficients, and who obtained the neutron absorption data and cost data on which the static and cost models were based.

Thanks are due to [redacted] who edited sections 1 and 2 of the manuscript, and to [redacted] who typed the whole.

Finally, thanks are due to Professor P.K. M'Pherson who proved to be the ideal supervisor.

REFERENCES

1.1 von Bertalanffy, L. General System Theory, George Braziller, New York 1968.

1.2 Hall, A.D. A Methodology for systems engineering, van Nostrand, New Jersey 1968.

1.3 Chestnut, H. Systems engineering methods, John Wiley, New York 1967.

1.4 De Greene, K.B. System psychology, McGraw Hill, New York 1970.

1.5 Morley English, J. Cost effectiveness, John Wiley, New York 1968.

1.6 M'Pherson, P.K. & Finkelstein, L. Information machines and systems engineering, research memorandum of T.C.U., Feb. 1970.

1.7 M'Pherson, P.K. & Charlwood, F.J. A systems engineering approach to the design of multivariable systems. (To be published at the 2nd. IFAC symposium on multivariable control systems, Dusseldorf 1971).

2.1 Wills, G., Ashton, D. & Taylor, B. Technological Forecasting, Bradford University Press, 1969.

2.2 Whitmarsh-Everiss, M.J. Dynamic design criteria for nuclear plant. C.E.G.B. internal report No. RKR/NPD/243, March 1968.

2.3 Whitmarsh-Everiss, M.J. & Kershaw, Miss J.M. Plant inflexibility, its effect on power cycling histories and system costs. C.E.G.B. internal report No. RKR/SN/12, Nov. 1969.

2.4 Whitmarsh-Everiss, M.J. The design of nuclear plant to dynamic criteria. C.E.G.B. internal report No. RKR/NPD/240, Jan. 1968.

2.5 Palo, G.P. et al. Units of 500 MW and larger found to yield savings. Elect. World (U.S.A.), vol. 171 No. 13 p. 30 - 7, March 1969.

2.6 Whitmarsh-Everiss M.J. Design and control of a generating station. Vacation school on systems engineering, Lancaster 8 - 12 Sept. 1969. IEE 1969 33 pp.

3.1 Stephenson, R. Introduction to nuclear engineering, McGraw Hill, New York 2nd. ed. 1958.

3.2 Littler, D.J. & Raffle, J.F. An introduction to reactor physics. Pergamon 2nd ed. 1957.

3.3 Moore, R.V. & Holmes, J.E.R. The S.G.H.W.R. system. British nuclear energy society, conference on steam generating and other heavy water reactors, Paper 1, May 1968.

3.4 Wray, D., Butterfield, M.H. & McMillan R.N.H. Control of S.G.H.W.Rs. ibid (3.3) Paper 6.

4.1 Taylor, E. A study of the Dynamics and control of an S.G.H.W.R. by Pole-Zero analysis. Report TNPG No. 605, Oct. 1967, Restricted.

4.2 Guppy, C.B. A systems analysis of the S.G.H.W.R. Dynamics and its application to the operations simulator. AEEW Report R501, 1967, Restricted.

4.3 Responses of the S.G.H.W.R. simulator to step inputs of turbine stop valve, private communication, from Dr. Cummins Sept. 1968.

4.4 Sumner, H.M. ZIP Mark 2; A Fortran code for calculating the eigenvalues (poles and zeroes) and frequency responses of large sets of linear equations representing complex dynamic systems. AEEW - R543 1969.

4.5 Randles, J. Heat diffusion in cylindrical fuel elements of water cooled reactors. AEEW R 96, 1961.

4.6 Martinelli, R.C. & Nelson, D.B. Prediction of pressure drop during forced circulation boiling of water. Trans A.S.M.E. Vol. 70, Aug. 1948.

4.7 M'Pherson, P.K. et al. Dynamic analysis of a nuclear boiler. Proc. I. Mech. Eng. Vol. 180, part 1, No. 17, 1966.

4.8 Macrae, G & Taylor, E. Representation of the dynamic behaviour of the S.G.H.W.R. at low pressures. TNPG report 455, March 1964. Restricted.

4.9 Morgan, B.S. Sensitivities of large multiloop control systems. IEEE Trans, vol. AC10 pp 308-315, July 1965.

4.10 Rosenbrock, H.H. Sensitivity of an eigenvalue to a change in the matrix. Electronics letters, vol. 1 p. 278. Dec. 1965.

4.11 Morgan, B.S. Computational procedure for the sensitivity of an eigenvalue. Electronics letters vol. 2, p. 197, June 1966.

4.12 Kasturi, R. & Doraju, P. Sensitivity analysis of power systems. IEEE Trans, Vol. pas. 88, No. 10 pp 1921-9, Oct. 1969.

4.13 Teichgraeber, R.D. et al. A dynamic sensitivity analysis of a power system using a digital computer. 21st Annual S.W. IEEE conference, 1969.

4.14 Neutron absorption data for the S.G.H.W.R. prototype. Private communication from Dr. Cummins, March 1971.

4.15 Etherington, H. Nuclear engineering handbook. McGraw Hill, 1958.

4.16 Constructional cost data for commercial S.G.H.W.R. Private communication from UKAEA Risley, March 1971.

4.17 Dimensional data for commercial S.G.H.W.R. Private communication from Dr. Cummins, March 1971.

5.1 Fishburn, P.C. Decision and value theory. Wiley, New York 1964.

5.2 Edwards, W. Non-conservative probalistic information processing systems. U.S.A.F. Report ESD-TR-66-464, 1966.

5.3 Whitmarsh-Everiss, M.J. Loss of grid generation leading to a step change in grid frequency. C.E.G.B. Report RKR/NPD/255, May 1968, Restricted.

5.4 C.E.G.B. Annual report and accounts 1969-70. H.M.S.O. London.

5.5. Sheppard, H.J. The economics of reliability and supply-distribution. IEE conference on reliability and supply Oct. 1967, pp 248-266.

6.1 Beveridge, G.S.G. & Schechter, R.S. Optimisation: theory and practice. McGraw Hill 1970.

6.2 Zangwill, W.J. Non-linear programming: a unified approach, Prentice Hall 1969.

6.3 Optimisation techniques in circuit and control applications, IEE conference 29-30th June, 1970. IEE conference publication No. 66.

6.4 Rosenbrock, H.H. An automatic method for finding the greatest or least value of a function. Computer Journal; 3, 175-184, 1960.

6.5 Booth, A.D. Numerical methods, academic press, New York 1955.

6.6 Mugele, R.A. A non-linear digital optimising programme for process control systems. IBM systems Journal 1 : 2.

7.1 Hicks, D., Johnstone, I., O'Dell, F.P. Nuclear design of S.G.H.W.Rs. B.N.E.S. conference on steam generating and other heavy water reactors, May 1968, Paper 4.

7.2 Brinkworth, M.J., Griffiths, J.A. Methuselah II - a Fortran programme and nuclear data library for the physics assessment of liquid moderated reactors.

8.1 Optimisation techniques in circuit and control applications, IEE conference 29-30th June, 1970. IEE conference publication No. 66.

APPENDIX 1 (1)

List of the S.G.H.W.R. design parameters. The number in the first column is the subscript which identifies the parameter in the parameter arrays of the computer programs.

No.	Symbol	Description	Ref. value	Units
1	K_v	voidage reactivity coefficient	-0.02	
2	K_t	fuel temperature reactivity coefficient	-10^{-5}	$°F^{-1}$
3	R	fuel rating	5.4	Btu/lb.s
4	C_f	fuel specific heat	0.075	Btu/lb.°F
5	K_f	fuel conductivity	1.59	Btu/hr.ft.°F
6	d	fuel pin diameter	0.0475	ft
7	ρ_f	fuel density	650	lb/ft^3
8	h	fuel to coolant heat transfer coeft.	1140	Btu/hr.°F
9	n_b	no. of fuel pins per channel	36	
10	N_b	no. of channels	103	
11	γ_c	slip ratio in channels	1.6	
12	γ_r	slip ratio in risers	1.6	
13	P_1	coefficients defining characteristics of the circulating pumps	84.3	lb/in^2
14	P_2		0.1448	$(lb/in^2)/(ft^3/s)$
15	P_3		0.0048	$(lb/in^2)/(ft^3/s)^2$
16	g_c	feedwater controller gain	0.1	
17	τ_c	feedwater controller time constant	100	s
18	h_f	feedwater enthalpy	365	Btu/lb
19	l_c	length of channel	12	ft
20	d_c	diameter of channel	0.407	ft

APPENDIX 1 (2)

S.G.H.W.R. design parameters

No.	Symbol	Description	Ref. value	Units
21	l_r	relative length of riser	1	
22	d_r	relative diameter of riser	1	
23	l_d	relative length of downcomer	1	
24	d_d	relative diameter of downcomer	1	
25	l_{rv}	vertical length of riser	20.2	ft
26	K_{tc}	coolant temperature reactivity coeft.	-2.78×10^{-5}	$°F^{-1}$
27	l	average neutron lifetime	0.0004	s
28	β_1	first group delayed neutron fraction	.00156	
29	λ_1	decay constant of first group	0.024	s^{-1}
30	β_2	second group delayed neutron fraction	.00364	
31	λ_2	decay constant of second group	0.15	s^{-1}
32	V	volume of vapour in steam drum	1350	ft^3
33	M_{wd}	mass of water in steam drum	32900	lb
34	z	percentage of saturated water in drum	0.2	

Parameters 16, 17 and 27-34 affect the dynamics of the reactor only, other parameters affect dynamics and steady state.

APPENDIX 2 (1)

List of the S.G.H.W.R. design variables. The number in the first column is the subscript which identifies the variable in the variable arrays of the computer programs.

No.	Symbol	Description	Ref. value	Units
1	$\bar{f}$	average channel voidage	0.204	
2	T_f	inner zone fuel temperature	1514	°F
3	T_f	outer zone fuel temperature	953.6	°F
4	n	normalised neutron flux	1	
5	p_c	channel pressure	977.6	lb/in^2
6	Q	total heat flux	23063	Btu/s.ft
7	W_w	water mass circulation rate	4174	lb/s
8	Δh_o	total enthalpy rise of coolant in core	66.30	Btu/lb
9	Δh_b	enthalpy rise due to boiling	47.28	"
10	h_d	enthalpy of water leaving drum	519.9	"
11	x_c	channel exit dryness	0.0723	
12	f_b	average voidage in boiling region	0.2866	
13	K_c	effective density factor in channel	12.43	
14	p_d	drum pressure	941.6	lb/in^2
15	Δp_r	riser pressure drop	26.25	"
16	Δp_c	channel pressure drop	19.46	"
17	Δp_w	downcomer pressure drop	13.91	"
18	x_r	riser exit dryness	0.0801	
19	W_{sd}	steam demanded by turbine	334.5	lb/s
20	W_{wr}	liquid mass flow rate in riser	3840	"

APPENDIX 2 (2)

S.G.H.W.R. variables

No.	Symbol	Description	Ref. value	Units
21	K_r	effective density factor in risers	13.0	
22	ρ_w	density of water	47.00	lb/ft^3
23	q	volumetric circulation rate	88.81	ft^3/s
24	δk	excess reactivity	0	
25	C_1	first group delayed neutron concentration	161.7	
26	C_2	second group delayed neutron concentration	60.66	
27	T_c	coolant temperature	540	°F
28	h_{sc}	subcooled enthalpy at channel inlet	19.02	Btu/lb
29	h_i	channel inlet enthalpy	519.9	"
30	α	variables introduced to simulate	0	
31	β	downcomer delay	0	
32	Δp_{dc}	pressure drop between channel and drum	35.98	lb/in^2
33	Δp_p	circulating pump pressure rise	59.62	"
34	W_r	mass flow in riser	4174	lb/s
35	M	mass of fluid in core and risers	24100	lb
36	W_{sr}	vapour mass flow in riser	334.5	lb/s
37	W_{fw}	feedwater mass flow rate	334.5	"
38	W_b	drum evaporation/condensation rate	0	"
39	$\bar{T}_f$	average fuel temperature	1234	°F
40	H_w	enthalpy of saturated water	534	Btu/lb
41	H_{ws}	enthalpy of evaporation	648.9	"

APPENDIX 2 (3)

S.G.H.W.R. variables

No.	Symbol	Description	Ref. value	Units
42	ρ_s	density of vapour	2.194	lb/ft^3
43	W_g	mass of saturated vapour in drum	1960	lb
44	W_f	mass of saturated liquid in drum	28680	"
45	E	drum pressure rate coefficient	0.1712	in^{-2}
46	B	drum evaporation rate coefficient	2.643	in^2
47	k_c	control reactivity	0	
48	y_t	turbine stop valve position	0.8	

Variables 47 and 48 are inputs to the system.

APPENDIX 3 (1)

Non linear dynamic model equations for the S.G.H.W.R.

NEUTRONICS AND REACTIVITY

$$1 \quad \frac{dn}{dt} = \frac{\delta k - \beta_1 - \beta_2}{l} \cdot n + \lambda_1 C_1 + \lambda_2 C_2$$

$$2 \quad \frac{dC_1}{dt} = \frac{\beta_1}{l} \cdot n - \lambda_1 C_1$$

$$3 \quad \frac{dC_2}{dt} = \frac{\beta_2}{l} \cdot n - \lambda_2 C_2$$

$$4 \quad \delta k = K_v \bar{f} + K_t \bar{T}_f + K_{tc} T_c + \delta k_c - K_o$$

FUEL ELEMENT THERMAL

$$5 \quad \frac{dT_{f1}}{dt} = \frac{Rn}{C_f} - \frac{32 K_f}{d^2 C_f \rho_f} \left\{ T_{f1} - T_{f2} \right\}$$

$$6 \quad \frac{dT_{f2}}{dt} = \frac{Rn}{C_f} + \frac{32 K_f}{d^2 C_f \rho_f} \left\{ T_{f1} - T_{f2} \right\} - \frac{128 K_f h d}{d^2 C_f \rho_f (16 K_f + h d)} \left\{ T_{f2} - T_c \right\}$$

$$7 \quad Q = \frac{16 \pi n_b N_b K_f h d}{16 K_f + h d} \left\{ T_{f2} - T_c \right\}$$

$$8 \quad \bar{T}_f = 0{\cdot}5 (T_{f1} + T_{f2})$$

BOILING CHANNELS

$$9 \quad \Delta h_o = \frac{Q l_c}{W_w}$$

APPENDIX 3 (2)

Non linear dynamic model equations for the S.G.H.W.R.

10 $h_{sc} = H_w - h_i$

11 $\Delta h_b = \Delta h_o - h_{sc}$

12 $x_c = \frac{\Delta h_b}{H_{ws}}$

13 $f_b = 1 - \frac{\log_e (1+K_c x_c)}{K_c x_c}$

14 $\bar{f} = \frac{\Delta h_b}{\Delta h_o} \cdot f_b$

RECIRCULATION HYDRAULICS

15 $h_i = h_d e^{-s\tau_D}$

16 $p_c = p_d + \Delta p_{dc}$

17 $\Delta p_{dc} = \Delta p_r + 0{\cdot}5 \Delta p_c$

18 $\Delta p_c = 0{\cdot}347\, l_c (1-\bar{f}) + F_1 q^2 (1+1{\cdot}3\, \gamma_c K_c x_c)$

19 $\Delta p_r = \frac{0{\cdot}347\, l_{rv}}{1+K_r x_r} + F_2 q^2 (1+\gamma_r K_r x_r)$

20 $\Delta p_w = -11{\cdot}16 + F_3 q^2$

APPENDIX 3 (3)

Non linear dynamic model equations for the S.G.H.W.R.

21 $$\Delta p_p = \Delta p_c + \Delta p_r + \Delta p_w$$

22 $$\Delta p_p = P_1 + P_2 q - P_3 q^2$$

23 $$K_c = \frac{\rho_w}{\gamma_c \rho_s} - 1$$

24 $$W_w = q \rho_w$$

25 $$\rho_w = 51{\cdot}8(1 - 7{\cdot}72 \times 10^{-4}[h_d - 400])$$

26 $$x_r = \frac{(h_i + \Delta h_o) e^{-s\tau_R} - H_w}{H_{ws}}$$

27 $$W_r = W_w - \frac{dM}{dt}$$

28 $$M = \frac{V \rho_w}{1 + \frac{\rho_w x_r}{\gamma_r \rho_s}}$$

29 $$W_{sr} = x_r W_r$$

30 $$W_{wr} = W_r - W_{sr}$$

STEAM DRUM

31 $$\frac{dp_d}{dt} = E\left\{W_{sr} - W_{sd} - \frac{\rho_s}{\rho_w}\left[W_w - W_{wr} - W_{fw}\right]\right\}$$

APPENDIX 3 (4)

Non linear dynamic model equations for the S.G.H.W.R.

32 $$W_b = -B \frac{dp_d}{dt}$$

33 $$\frac{dh_d}{dt} = \frac{1}{M_{wd}}\left\{W_{wr}(H_w - h_d) + W_{fw}(h_{fw} - h_d) - W_b(H_w + H_{ws} - h_d)\right\}$$

34 $$\frac{dM_{wd}}{dt} = W_{wr} + W_{fw} - W_w - W_b$$

35 $$B = \frac{1}{H_{ws}}\left\{W_g \frac{d(H_w + H_{ws})}{dp_d} + W_f \frac{dH_w}{dp_d} - \frac{V_s}{J}\right\}$$

36 $$E = \frac{1}{\rho_s}\left\{B\left[\frac{1}{\rho_s} - \frac{1}{\rho_w}\right] - W_g \frac{d\left(\frac{1}{\rho_s}\right)}{dp_d} + W_f \frac{d\left(\frac{1}{\rho_w}\right)}{dp_d}\right\}^{-1}$$

37 $$W_f = z M_{wd} + \frac{V_s \rho_w (1 - x_r)}{1 + \left(\frac{\rho_w}{\rho_s} - 1\right) x_r}$$

38 $$W_g = \frac{V_s \rho_w x_r}{1 + \left(\frac{\rho_w}{\rho_s} - 1\right) x_r}$$

FEEDWATER CONTROLLER

39 $$\Delta W_{fw} = -\Delta M_{wd}\left\{g_c + \frac{g_c}{s\tau_c}\right\}$$

STEAM FLOW TO TURBINE

40 $$W_{sd} = 0{\cdot}444\, p_d\, y_t$$

APPENDIX 3 (5)

Non linear dynamic model equations for the S.G.H.W.R.

Coolant temperature T_c is a function of channel pressure. H_w, H_{ws}, ρ_w, ρ_s and their derivatives with respect to pressure may be a function of channel pressure p_c or drum pressure p_d depending upon the equation in which they occur. All the above variables are determined by interpolation from steam tables.

Certain coefficients in the above equations have no been defined, these are functions of design parameters as follows, the reference value is given after the definition -

CHANNEL FRICTION FACTOR

$$F_1 = \frac{l_c(d_c+(n_b+1)d)}{N_b^2(d_c^2-(n_b+1)d^2)^3} \times 1{\cdot}617\times10^{-4} \quad = 7{\cdot}05\times10^{-4} \quad (lb/in^2)/(ft^3/s^2)$$

RISER FRICTION FACTOR

$$F_2 = \frac{l_r}{d_r^5\, N_b^2} \times 11{\cdot}15 \quad = 1{\cdot}085\times10^{-3} \quad ''$$

DOWNCOMER FRICTION FACTOR

$$F_3 = \frac{l_d}{d_d^5} \times 3{\cdot}179\times10^{-3} \quad = 3{\cdot}179\times10^{-3} \quad ''$$

DOWNCOMER TRANSPORT DELAY

$$\tau_D = \frac{l_d\, d_d^2}{W_w} \times 2{\cdot}6\times10^{4} \quad = 6{\cdot}229 \quad s$$

RISER TRANSPORT DELAY

$$\tau_R = \frac{V\,\rho_w}{W_w\left(1+\frac{\rho_w X_r}{\gamma_r \rho_s}\right)} \quad = 5{\cdot}572 \quad s$$

RISER VOLUME

$$V = l_r\, d_r^2\, N_b \times 10{\cdot}2 \quad = 1050 \quad ft^3$$

APPENDIX 4 (1)

Linearised S.G.H.W.R. dynamic model equations.

Variables in these equations refer to perturbations from the initial equilibrium. S = Laplace Operator.

NEUTRONICS AND REACTIVITY

$$1 \quad sn = -\frac{n}{\tau_1} + G_1 \delta k + \frac{C_1}{\tau_2} + \frac{C_2}{\tau_3}$$

$$2 \quad sC_1 = G_2 n - \frac{C_1}{\tau_2}$$

$$3 \quad sC_2 = G_3 n - \frac{C_2}{\tau_3}$$

$$4 \quad \delta k = G_4 \bar{f} + G_5 T_{f1} + G_5 T_{f2} + G_{55} T_C + k_c$$

FUEL ELEMENT THERMAL

$$5 \quad sT_{f1} = G_6 n - \frac{T_{f1}}{\tau_4} + \frac{T_{f2}}{\tau_4}$$

$$6 \quad sT_{f2} = G_6 n + \frac{T_{f1}}{\tau_4} - \frac{G_7 T_{f2}}{\tau_4} + \frac{G_8}{\tau_4} \cdot T_C$$

$$7 \quad Q = G_8 G_9 T_{f2} - G_8 G_9 T_C$$

$$8 \quad \bar{T}_f = 0{\cdot}5\, T_{f1} + 0{\cdot}5\, T_{f2}$$

BOILING CHANNELS

APPENDIX 4 (2)

Linearised S.G.H.W.R. dynamic model equations.

9 $$\Delta h_o = G_{10}Q - G_{11}W_w$$

10 $$h_{sc} = G_{12}p_c - h_i$$

11 $$\Delta h_b = \Delta h_o - h_{sc}$$

12 $$x_c = G_{13}Q - G_{14}W_w + G_{15}h_i - G_{16}p_c$$

13 $$K_c = G_{17}p_c$$

14 $$f_b = G_{18}x_c + G_{19}p_c$$

15 $$\bar{f} = G_{20}\Delta h_b - G_{21}\Delta h_o + G_{22}f_b$$

16 $$T_c = G_{23}p_c$$

RECIRCULATION

17 $$h_i + \frac{\tau_5}{2}\alpha + \frac{\tau_5^2}{12}s\alpha = h - \frac{\tau_5}{2}\beta + \frac{\tau_5^2}{12}s\beta$$

18 $$\alpha = s h_i$$

19 $$\beta = s h_d$$

APPENDIX 4 (3)

Linearised S.G.H.W.R. dynamic model equations.

$$20 \quad p_c = p_d + \Delta p_{dc}$$

$$21 \quad \Delta p_{dc} = \Delta p_r + 0{\cdot}5 \Delta p_c$$

$$22 \quad \Delta p_c = -G_{24} \bar{f} + G_{25} q + G_{26} x_c + G_{27} K_c$$

$$23 \quad \Delta p_r = G_{28} q + G_{29} x_r + G_{30} K_r$$

$$24 \quad \Delta p_w = G_{31} q$$

$$25 \quad \Delta p_p = \Delta p_c + \Delta p_r + \Delta p_w$$

$$26 \quad q = -G_{32} \Delta p_p$$

$$27 \quad x_r + \tau_6 s x_r = x_c - G_{33} \tau_6 s p_d$$

$$28 \quad K_r = G_{34} p_d$$

$$29 \quad \rho_w = -G_{35} h_d$$

$$30 \quad W_w = G_{36} q + G_{37} \rho_w$$

$$31 \quad W_r = W_w - s M$$

APPENDIX 4 (4)

Linearised S.G.H.W.R. dynamic model equations.

32 $$M = G_{38} p_d - G_{39} x_r$$

33 $$W_{sr} = W_r - W_{wr}$$

34 $$W_{wr} = G_{40} W_r - G_{41} x_r$$

STEAM DRUM

35 $$s p_d = G_{42} W_r + G_{43} x_r - G_{44} W_{sd} - G_{45} W_w + G_{45} W_{fw}$$

36 $$W_b = -G_{46} s p_d$$

37 $$s M_{wd} = W_{fw} + W_{wr} - W_b - W_w$$

38 $$h_d (1 + s\tau_7) = G_{47} p_d + G_{48} W_r - G_{49} x_r + G_{50} h_f - G_{51} W_{fw} - G_{52} W_b$$

FEEDWATER CONTROLLER

39 $$W_{fw} = -G_{56} \left(1 + \frac{1}{s\tau_8}\right) M_{wd}$$

TURBINE STEAM FLOW

40 $$W_{sd} = G_{53} p_d + G_{54} y_t$$

APPENDIX 4 (5)

Definitions of gains for the linear dynamic model equations.

No.	Derivation	Equation	Reference value
1	n/l	1	2500
2	β_1/l	2	3.9
3	β_2/l	3	9.1
4	K_v	4	-0.02
5	$K_{t/2}$	4	-5×10^{-6}
6	R/C_f	5,6	72.0
7	$1+G_s$	6	3.721
8	$\frac{4hd}{16K_f+hd}$	6,7	2.721
9	$4\pi n_b N_b K_f$	7	20.58
10	l_c/W_w	9	2.875×10^{-3}
11	$\Delta h_b/W_w$	9	1.588×10^{-2}
12	$\frac{\partial H_w}{\partial p_c}$	10	0.1558
13	$l_c/W_w H_{ws}$	12	4.4×10^{-6}
14	$\Delta h_o/W_w H_{ws}$	12	2.4×10^{-5}

APPENDIX 4 (6)

Definitions of gains for the linear dynamic model equations.

No.	Derivation	Equation	Reference value
15	$1/H_{ws}$	12	1.53×10^{-3}
16	$\frac{1}{H_{ws}}\left\{\frac{\partial H_w}{\partial p_c}+x_c\frac{\partial H_{ws}}{\partial p_c}\right\}$	12	2.17×10^{-4}
17	$\frac{\partial K_c}{\partial p_c}=-\frac{\rho_w}{\gamma_c\rho_s^2}\cdot\frac{\partial \rho_s}{\partial p_c}$	13	-1.54×10^{-2}
18	$\frac{\partial f_b}{\partial x_c}=\frac{\log_e(1+K_cx_c)}{K_cx_c^2}-\frac{1}{x_c(1+K_cx_c)}$	14	2.582
19	$\frac{\partial f_b}{\partial p_c}=\frac{x_c}{K_c}G_{17}G_{18}$	14	-2.31×10^{-4}
20	$f_b/\Delta h_o$	15	4.32×10^{-3}
21	$\bar{f}/\Delta h_o$	15	3.083×10^{-3}
22	$\Delta h_b/\Delta h_o$	15	0.7132
23	$\frac{\partial T_c}{\partial p_c}$	16	0.1232
24	$0{\cdot}347\,l_c$	22	4.164
25	$2F_1q(1+1{\cdot}3\gamma_cK_cx_c)$	22	0.3637
26	$1{\cdot}3F_1q^2\gamma_cK_c$	22	145.5
27	$1{\cdot}3F_1q^2\gamma_cx_c$	22	0.8467
28	$2F_2q(1+\gamma_rK_rx_r)$	23	0.4536

APPENDIX 4 (7)

Definitions of gains for the linear dynamic model equations.

No.	Derivation	Equation	Reference value
29	$K_r(F_2 q^2 \gamma_r - \frac{0.347 l_{rv}}{1+K_r x_r})$	23	156.1
30	$\frac{x_r}{K_r} G_{29}$	23	0.9621
31	$2 F_3 q$	24	0.5648
32	$-(P_2 - 2qP_3)^{-1}$	26	1.427
33	$\frac{1}{H_{ws}} \left\{ \frac{\partial H_w}{\partial p_d} - \frac{H_w}{H_{ws}} \cdot \frac{\partial H_{ws}}{\partial p_d} \right\}$	27	4.75×10^{-4}
34	$\frac{\partial K_r}{\partial p_d} = - \frac{\rho_w}{\gamma_r \rho_s^2} \cdot \frac{\partial \rho_s}{\partial p_d}$	28	-1.64×10^{-2}
35	$\frac{\partial \rho_w}{\partial h_d}$	29	3.98×10^{-2}
36	ρ_w	30	47.0
37	q	30	88.8
38	$\frac{x_r}{\rho_s} \cdot \frac{\partial \rho_s}{\partial p_d} G_{39}$	32	14.39
39	$\frac{M^2}{\gamma_r \rho_s V}$	32	1.535×10^{5}
40	$1 - x_r$	34	0.9199
41	W_r	34	4174
42	$E\left\{(1 - \frac{\rho_s}{\rho_w}) x_r + \frac{\rho_s}{\rho_w}\right\}$	35	2.075×10^{-2}

APPENDIX 4 (8)

Definitions of gains for the linear dynamic model equations.

No.	Derivation	Equation	Reference value
43	$W_r E (1 - \frac{\rho_s}{\rho_w})$	35	682.9
44	E	35	0.1712
45	$E \frac{\rho_s}{\rho_w}$	35	7.644×10^{-3}
46	B	36	2.643
47	$\frac{\partial H_w}{\partial p_d}(1-x_r)$	38	0.1455
48	$\frac{(H_w - h_d)(1-x_r)}{W_w}$	38	2.945×10^{-3}
49	$H_w - h_d$	38	13.36
50	x_r	38	8.01×10^{-2}
51	$\frac{h_d - h_f}{W_r}$	38	3.675×10^{-2}
52	$\frac{H_w + H_{ws} - h_d}{W_r}$	38	0.1615
53	$0{\cdot}444 y_t$	40	0.3552
54	$0{\cdot}444 p_d$	40	418.1
55	K_{tc}	4	2.78×10^{-5}
56	g_c	39	0.1

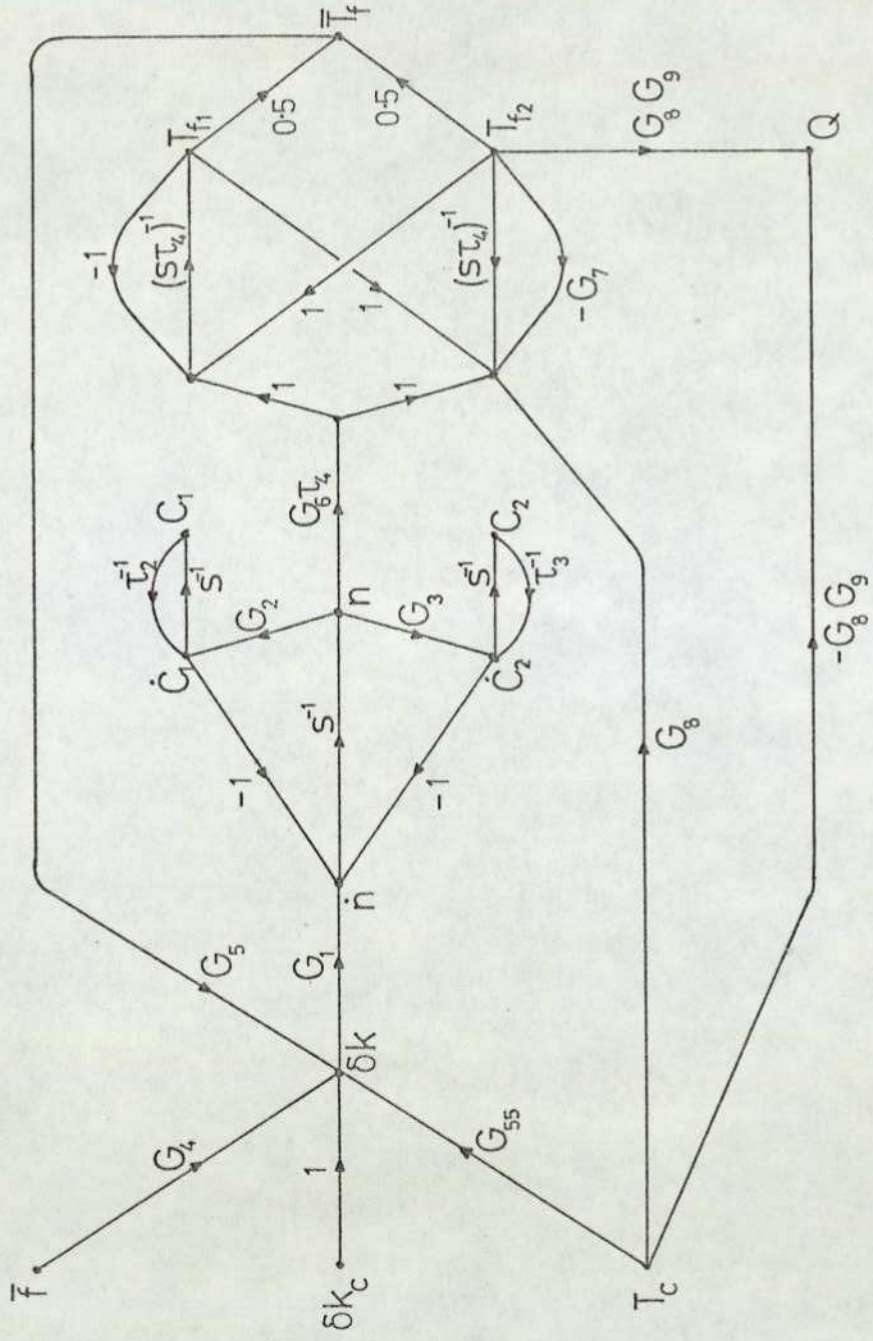
APPENDIX 4 (9)

Definitions of time constants for the linear dynamic model equations.

No.	Derivation	Equation	Reference value
1	$\frac{1}{\beta_1 + \beta_2}$	1	0.07692
2	λ_1^{-1}	1,2	41.67
3	λ_2^{-1}	1,3	6.667
4	$\frac{d^2 C_f \rho_f}{32 K_f}$ fuel time constant	5,6	7.782
5	τ_D	17	6.229
6	τ_R	27	5.572
7	$\frac{M_{wd}}{W_r}$ drum mixing time constant	38	7.882
8	τ_C	37	100

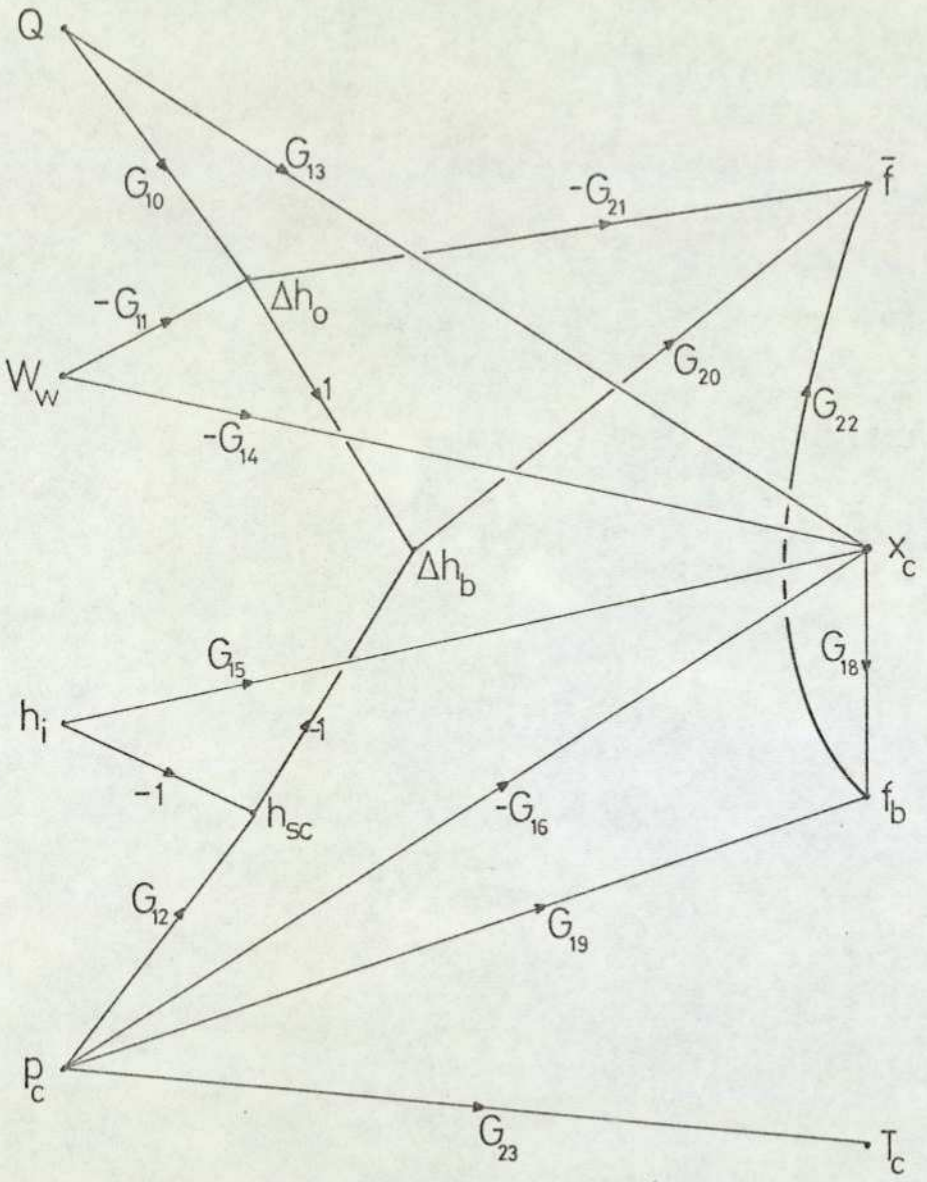
Variables referenced in the above tables are the steady state equilibrium values for the reference design.

Signal flow graphs of the S.G.H.W.R. linear dynamic model.



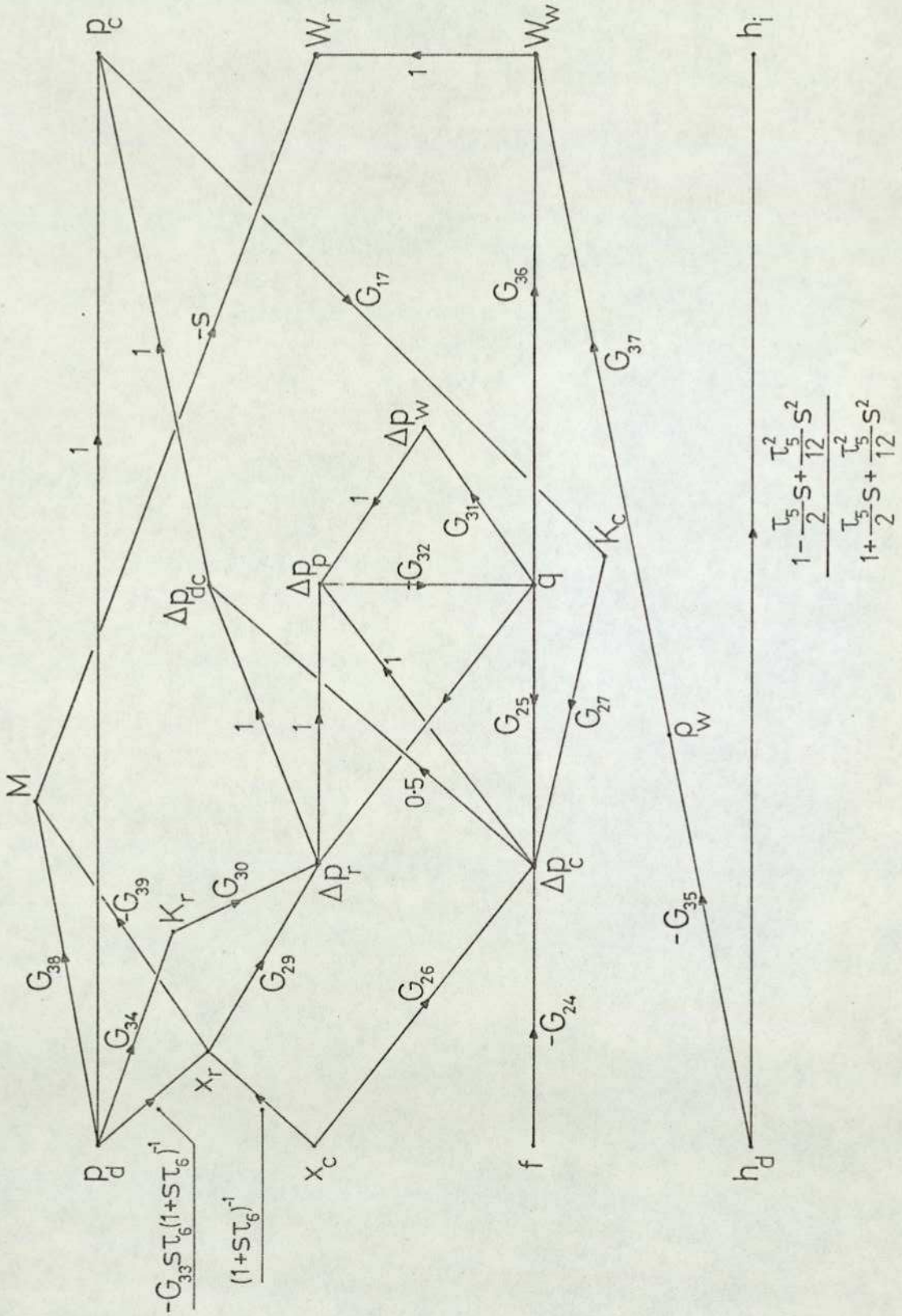
Neutronics, Reactivity and Fuel Element

Signal flow graphs of the S.G.H.W.R. linear dynamic model.

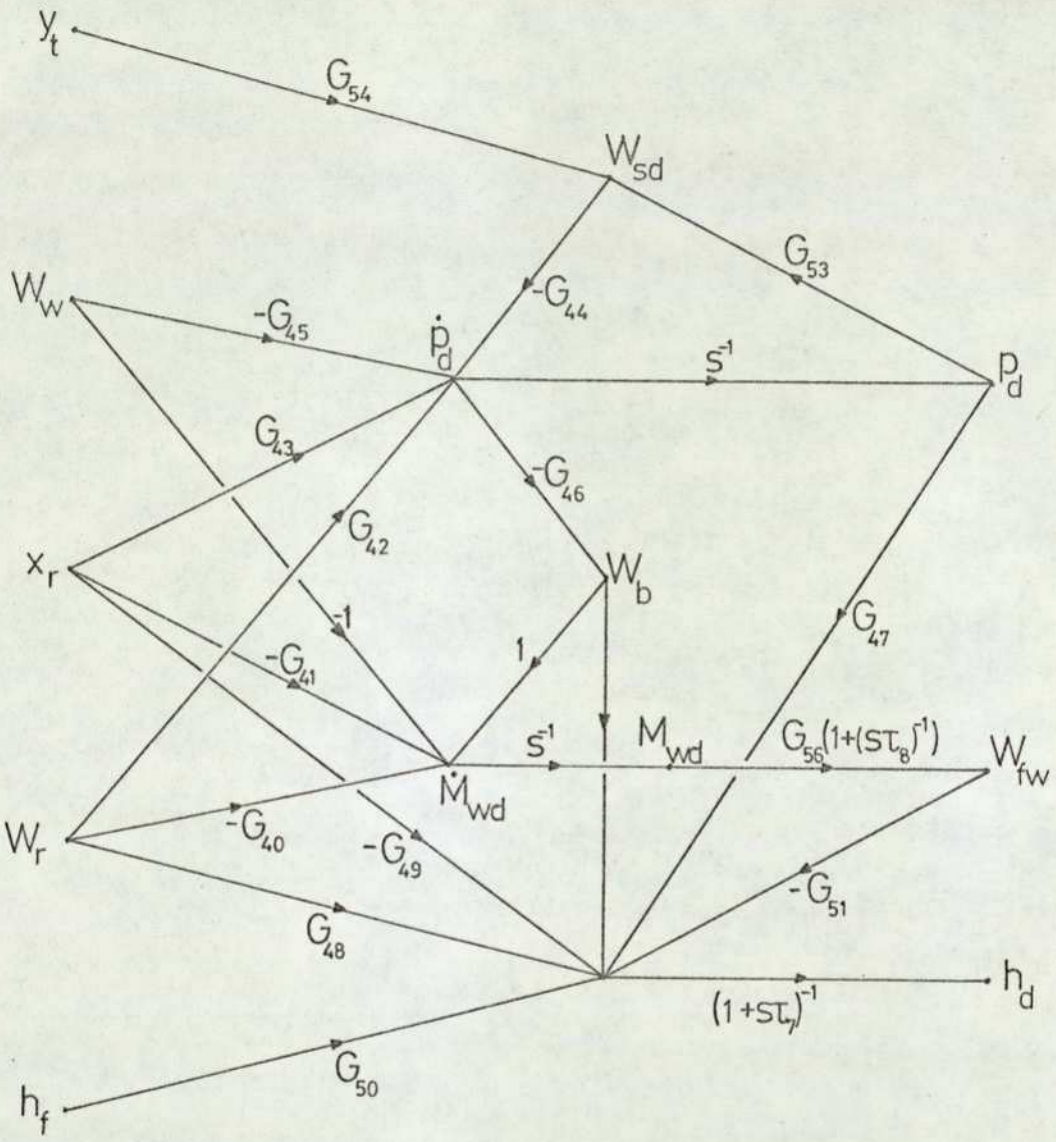


Boiling Channels

Signal flow graphs of the S.G.H.W.R. linear dynamic model.



Signal flow graphs of the S.G.H.W.R. linear dynamic model.



Steam Drum, Feedwater Controller and Steam Flow to Turbine

APPENDIX 5 (1)

Static Model of the S.G.H.W.R.

The static model consists of the equations of Appendix 3 with time derivatives set to zero, plus the following equations defining the reactivity surplus or deficit.

1 $$k = \varepsilon p f \eta (1-l)$$

FAST FISSION FACTOR ε

2 $$\varepsilon = 1{\cdot}03$$

RESONANCE ESCAPE PROBABILITY p

3 $$p = e^{-A'/5{\cdot}457 N_m}$$

4 $$A' = 11{\cdot}5\,(1+2{\cdot}1(M/S+0{\cdot}0826)^{-1})$$

5 $$M/S = 2{\cdot}625\,d \quad [\times 12 \times 2{\cdot}54]$$

6 $$N_m = 12{\cdot}9 \times 0{\cdot}1394\,(1-2{\cdot}5d_c^2)\,(n_b d^2)^{-1}$$

THERMAL UTILISATION FACTOR f

7 $$f = V_f (V_f + 0{\cdot}0880 V_m + 0{\cdot}0272 V_{zr} + 0{\cdot}0169 V_{al} + 0{\cdot}0601 V_c + 0{\cdot}0222)^{-1}$$

8 $$V_m = 0{\cdot}001381\, l_c N_b (1-2{\cdot}5d_c^2)$$

9 $$V_f = 0{\cdot}00992\, l_c n_b N_b d^2$$

10 $$V_{zr} = 0{\cdot}00487 d_c^2 N_b l_c$$

APPENDIX 5(2)

S.G.H.W.R. static model, equations defining reactivity surplus or deficit.

11 $V_{al} = 0{\cdot}0199 d_c N_b l_c$

12 $V_c = 0{\cdot}00985 N_b (d_c^2 - (n_b+1)d^2) l_c$

NEUTRON MULTIPLICATION FACTOR η

13 $\eta = 1430\, e\, (691{\cdot}3e+3{\cdot}66)^{-1}$

14 $e = 0{\cdot}003705 R$

ESCAPE PROPORTION l

15 $l = 0{\cdot}04 A/V$

16 $A = 0{\cdot}001532 (2N_b+3{\cdot}67 l_c)\sqrt{N_b}$

17 $V = 0{\cdot}00081 N_b l_c$

Effects due to change in the steady state equilibrium conditions resulting from parameter changes.

18 $$\begin{aligned} \delta k = & -0{\cdot}004085 K_v' \\ & -0{\cdot}01234 K_t' \\ & +0{\cdot}00566 K_f' \; -0{\cdot}0057 K_f'^2 \\ & +0{\cdot}00599 n_b' \; -0{\cdot}0093 n_b'^2 \\ & +0{\cdot}00733 N_b' \; -0{\cdot}0133 N_b'^2 \end{aligned}$$

APPENDIX 5(3)

S.G.H.W.R. static model, equations defining reactivity surplus or deficit.

$$-0{\cdot}00447\,l'_c + 0{\cdot}0035\,l'^2_c$$

$$+0{\cdot}00063\,d'_d$$

$$-0{\cdot}01507\,K'_{tc}$$

where $K'_v = \dfrac{K_v}{K^o_v} - 1$

and K^o_v is the reference value of K_v , etc.

APPENDIX 6

Cost Model Equations for the S.G.H.W.R.

The figure preceeding the leading bracket is the cost of the subsystem concerned as a percentage of the total station cost. The equations give the marginal costs of the subsystem, primed parameters are the normalised incremental values, i.e.-

$$d' = \frac{d}{d^\circ} - 1 \quad \text{where } d^\circ \text{ is the reference value of } d.$$

STEAM DRUM

$$1 \quad C'_{dr} = 0{\cdot}7\left\{43{\cdot}7\left[M'_{wd}+V'\right]\right\}$$

RISERS

$$2 \quad C'_{r} = 0{\cdot}3\left\{19{\cdot}65\,l'_{r}+5{\cdot}60\,d'_{r}+12{\cdot}4\,N'_{b}\right\}$$

DOWNCOMERS

$$3 \quad C'_{d} = 2{\cdot}2\left\{12{\cdot}0\,d'_{d}+165{\cdot}0\,l'_{d}\right\}$$

CORE

$$4 \quad C'_{c} = 11{\cdot}4\left\{22{\cdot}8\,l'_{c}+20{\cdot}6\,N'_{b}+20{\cdot}35\,d'_{c}\right\}$$

FUEL

$$5 \quad C'_{f} = 14{\cdot}6\left\{n_b(5{\cdot}42-172d+2450d^2)(1+N'_{b})(1+0{\cdot}1\,l'_{c})-100\right\}$$

APPENDIX 7 (1)

SENSITIVITY CHART

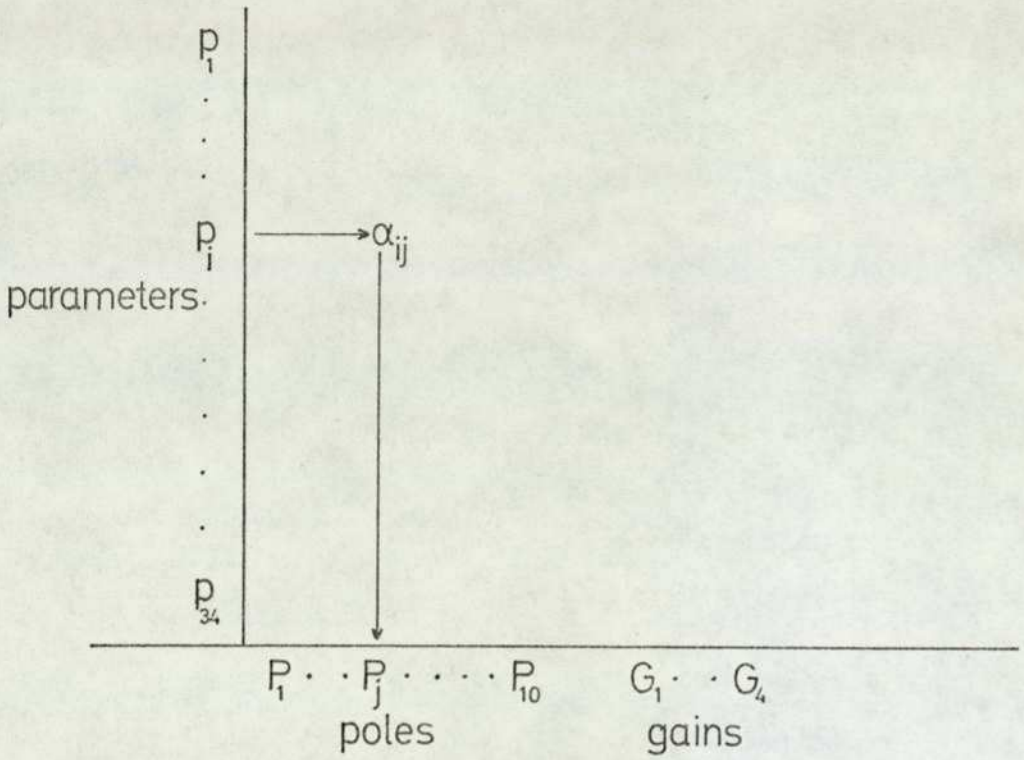
The Chart shows the sensitivity coefficients of the system poles and the static and dynamic gains of some transfer functions to the design parameters. Parameters are listed on the left followed by their reference values. Poles and gains are listed along the bottom of the Chart as follows:

Columns 1 - 10	System Poles, complex pairs are linked below and an R or I indicates the real or imaginary part of the pairs. Reference values are again given.
Columns 11 - 14	Static gains of the transfer functions indicated with reference values.
Columns 15 - 38	Dynamic gains of the transfer functions indicated in columns 11 - 14. The dynamic gains corresponding to the mode defined by a pole or pair of poles are given as a multiple of the static gain for the transfer function.

Sensitivity coefficients relate the normalised poles or gains to the normalised parameters as indicated by the diagram on the following page. Values of magnitude less than 0.1 are omitted for clarity.

APPENDIX 7 (2)

SENSITIVITY CHART



$$\frac{\delta P_j}{P_j} = \alpha_{ij} \frac{\delta p_i}{p_i}$$

APPENDIX 8(1)

COMPUTER PROGRAMS

Listed below are the computer programs developed during the S.G.H.W.R. study. They are divided into two sections, those applicable to general problems and those specific to the S.G.H.W.R. problem. The former group is as follows -

1.1	CHIC	which uses	SEARCH, STEP, CF
1.2	GAINS		
1.3	GAINI		
1.4	SRESP		
1.5	RRESP		
1.6	IRESP		
1.7	RELPZ		
1.8	RELGS		
1.9	ROOTS	which uses	FAC, BAIR, MAXE
1.10	INTERP		
1.11	NONLIN2	which uses	MAT, LHS, F4ACSL
1.12	SENSITIVITY		

The first of these is the optimising routine, numbers 1.2-1.9 are used in the generation of responses and dynamic utility from sensitivity coefficients and 1.10 - 1.12 are used in the solution of the non linear static model and the calculation of sensitivity coefficients.

The latter group is as follows -

2.1	CF	which calls	CUTE, DUTE, SUTE
2.2	CUTE		
2.3	DUTE	which calls	MWL, PCENT
2.4	SUTE		
2.5	GAIN	which calls	NONLIN2, INTERP
2.6	LHS		
2.7	ZIPE	which calls	GAIN

Routines 2.1 - 2.4 are used in generating the utility function used for optimising the S.G.H.W.R. design (by CHIC). Routines 2.5 & 2.6 are used in solving the non linear static model and in generating the linear dynamic model. ZIPE (2.7) prepares data for the ZIP pole-zero solving program at Winfrith.

1. FORTRAN IV routines written in a general form for use on any problem.

1.1 Subroutine CHIC, an optimising program for non linear utility functions with independent constraints on the parameters. CHIC predicts a search direction and then

calls subroutine SEARCH which makes a linear search along that direction until a maxima is encountered. If a constraint is reached during the search the search direction is projected onto the constraint. A step doubling (or halving) technique is used during the search and a quadratic fit made through these points straddling the peak to estimate the true peak co-ordinates and magnitude. CHIC uses n + 1 estimations of the utility function at the starting point to estimate the search direction by a quadratic fit method similar to that described in (6.). Modifications to the basic method are introduced if the predicted peak position violates a constraint, if the surface is convex with respect to some parameters at the starting point, or if the parameter increments used to estimate derivatives are too small or too large. Subroutines CHIC and SEARCH call a user function CF which defines the funtion to be maximised. The predict and search technique is repeated until successive optima are within a limit specified by the user.

Call statement

CALL CHIC (X, N, E, M, FP, XP, XN, ICON)

where arguments are as follows -

X(N) on entry the initial values of the parameters
on exit the optimum values of the parameters

N the number of parameters

E the required relative error in the optimum value of the utility function.

M on exit the number of iterations required to reach an optima

FP on exit the optimum value of the utility function

XP(N) the upper constraint on parameters

XN(N) the lower constraint on parameters

ICON(N) an integer array indicating the constraints

ICON(I) = 0 i^{th} parameter unconstrained

ICON(I) = 1 i^{th} parameter has lower constraint

ICON(I) = 2 i^{th} parameter has upper constraint

ICON(I) = 3 i^{th} parameter has upper and lower constraint

For unconstrained problems an alternative subroutine FLAP without arguments XP, XN, ICON is available. The user must supply

the utility function in the form -

FUNCTION CF(X, N)

where X and N are as defined above.

1.2 Subroutine GAINS, given the poles and zeroes of a transfer function this routine evaluates the gains and phase angles of the various modes in the response to a step input. Gains are given relative to the static gain of the transfer function.

Call statement

CALL GAINS (P, NP, Z, NZ, G, ID)

where the arguments are as follows -

P(NP) a complex array of the system poles, in any order but complex pairs must be adjacent.

NP the number of Poles

Z(NZ) a complex array of the zeroes, in any order but complex pairs must be adjacent.

NZ the number of zeroes NZ NP

G(NP) a real array containing on exit the gains and phase angles of the mode corresponding to a pole or complex pair of poles.

If P(I) is real then G(I) is the gain of the i^{th} mode. If P(I) and P(I+1) are complex, then G(I) is the gain and G(I+1) the phase angle of the mode defined by the i^{th} and $(i+1)^{th}$ poles in the form -

$G(I)e^{-at}\cos(bt+G(I+1))$

ID error flag identifier set by user. Error print out occurs on peripheral No. 2 if complex pairs of poles and zeroes are not conjugate or are not entered in adjacent locations.

Program will STOP after an error printout.

1.3 Subroutine GAINI, as subroutine GAINS but gives the gains and phase angles of the response of a transfer function to an impulse.

1.4 Subroutine SRESP, gives the poles and zeroes of a transfer function and the results of subroutine GAINS this routine evaluates the response of the transfer function to a step input.

Call statement

CALL SRESP (P, Z, NP, NZ, G, T, R)

where the arguments are as follows -

P(NP) a complex array containing the poles of the transfer function, poles may be in any order but complex pairs must be adjacent.

Z(NZ) a complex array containing the transfer function zeroes in any order but complex pairs must be adjacent.

NP the number of poles

NZ the number of zeroes NZ NP

G(NP) an array containing the gains and phase angles produced by subroutine GAINS.

T the time at which the response is required

R the system response as a multiple of the steady state response.

1.5 Subroutine RRESP, given the poles and zeroes of a transfer function and the results of subroutine GAINS this routine evaluates the response of the transfer function to a ramp input. Call statement is as for subroutine SRESP.

1.6 Subroutine IRESP, given the poles and zeroes of a transfer function and the results of subroutine GAINI this routine evaluates the impulse response of the transfer function. Call statement is as for subroutine SRESP except that -

G(NP) an array containing the gains and phase angles produced by subroutine GAINI.

1.7 Subroutine RELPZ calculates the shift in the position of a pole or zero due to parameter changes given the sensitivity matrix and parameter values.

Call statement

CALL RELPZ (P, PR, DVR, N, M, PSEN, K)

where arguments are as follows -

P(M) a complex array containing the shifted poles or zeroes.

PR(M) a complex array containing the reference poles or zeroes.

M the number of poles

N the number of parameters

DVR(N) the normalised change in parameter values

PSEN(N,M) the sensitivity matrix relating normalised pole or zero shift to normalised parameter change.

K(M) an integer array defining poles as singles or complex pairs as follows -

K = 1 a single pole

K = 2 the first of a complex pair

K = 0 the second of a complex pair

1.8 Subroutine RELGS, calculates the values of transfer function gains given the reference condition gains, the parameter changes and the gain-parameter sensitivity matrix.

Call statement.

CALL RELGS (GS, DVR, N, M, GSR, GSEN)

with arguments as follows -

GS(M) the transfer function gains

DVR(N) the normalised change in parameters

N the number of parameters

M the number of gains

GSR(M) the reference condition gains

GSEN(M,N) the normalised gain - normalised parameter sensitivity matrix.

1.9 Subroutine ROOTS, determines the roots of a polynomial using Bairstow's method. If convergence fails the polynomial is inverted and the procedure repeated to find an inverse root. If convergence again fails an error flag is set. The subroutine calls subroutines FAC, BAIR and MAXE.

Call statement.

CALL ROOTS (N, A, J, E, R, NR, L)

where the arguments are

N the order of the polynomial

A the coefficients of the polynomial in the form -

$$x^N + A(1)x^{N-1} + A(2)x^{N-2} + \ldots + A(N-1)x + A(N) = 0$$

J the number of roots required

E the maximum relative error of the solution

R(N) complex array containing the roots

NR the number of roots found

L error flag

L = 0 no error

L = 1 convergence failure

1.10 Subroutine INTERP, a third order interpolation and derivative interpolation procedure using Bessel's algorithm.

Call statement

CALL INTERP (X, Y, DY, XINT, YINT, K, J, KK, JJ)

with arguments as follows -

X	the input value of the independent variable
Y	the output value of the interpolated dependent variable
DY	the output value of the interpolated derivative of the dependent variable.
XINT(20,K)	an array defining 20 discrete values of K independent variables, note XINT(2,K) X XINT(19,K)
YINT(20,J)	an array defining 20 discrete values of J dependent variables.
KK	an integer defining which independent variable is to be used.
JJ	an integer defining which dependent variable is required.

1.11 Subroutine NONLIN2, solves a set of nonlinear algebraic equations using a multivariable Newton's method. The routine starting from initial values entered applies the algorithm iteratively using Matrix inversion until successive values are within a prescribed limit. The Matrix is generated by subroutine MAT which is called from NONLIN2 and MAT in turn calls subroutine LHS which defines the non linear equations. The Matrix inversion is carried out by an ICL library subroutine F4ACSL.

Call statement

CALL NONLIN2 (N, NI, E, XO, A, B)

with arguments as follows -

N	the number of variables and equations
NI	the number of iterations required to achieve a solution
E	the maximum error in any variable at solution
XO(N)	on entry the initial estimate of the solution on exit the solution

A(N,N))
) the matrix and vector which give the
B(N)) solution from the linear equations -

$$A.\underline{X} = B$$

the user must supply subroutine LHS defining the non linear equations in the form -

SUBROUTINE LHS (X, FX)

with arguments -

X(N) the current value of the system variables

FX(I) = $f_I(X(N))$ for I = 1,N

where the solution is given by

$f_I(X(N)) = 0$ I = 1,N

1.12 Subroutine SENSITIVITY, calculates the sensitivity of a variable, gain or pole to a parameter change.

Call statement

CALL SENSITIVITY (A, B, C, D, E, N)

where the arguments are

A(N) the values of variables, poles or gains with a positive parameter change.

B(N) the values of variables, poles or gains with a negative parameter change.

C(N) the reference values of variables, poles or gains.

D(N) the sensitivity coefficients

N the number of parameters, poles or gains

E the relative size of the parameter change.

2. Programs specific to the S.G.H.W.R. problem

2.1 Function CF, defines the utility function for the S.G.H.W.R. problem. The function calls subroutine CUTE, DUTE and SUTE described below and generates an overall utility value from a weighted sum of their outputs.

2.2 Subroutine CUTE, generates a cost utility value based on the cost model equations of Appendix 6.

2.3 Subroutine SUTE, generates a static performance utility value based on the equations of Appendix 5.

2.4 Subroutine DUTE, generates a dynamic performance utility value from the reference pole-zero positions and the sensitivity coefficients. The routine calls some or all of the routines 1.2-1.9 (depending upon the dynamic performance criteria used) and also subroutines PCENT and MWL. PCENT estimates the maximum step input of power demand size that the S.G.H.W.R. can accommodate (based on a simplified model with dominant poles and zeroes only). MWL calculates the annual Megawatt hours that the grid system cannot supply based on the step size estimated by PCENT and the proportion of S.G.H.W.R.s in the plant mix.

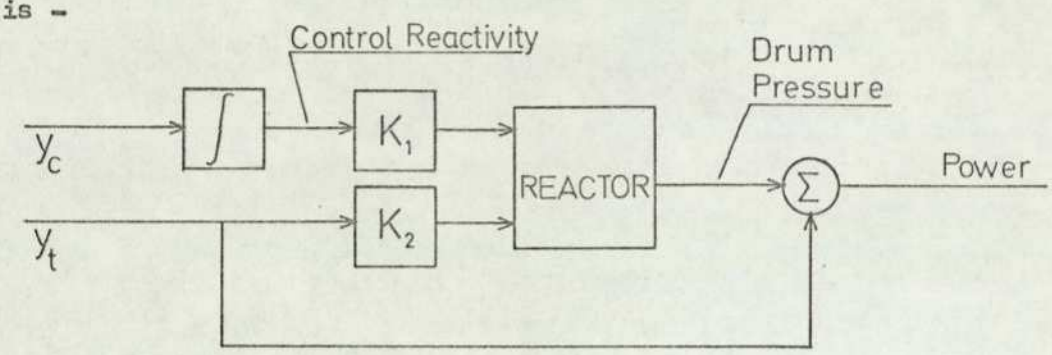
2.5 Subroutine GAIN, generates the gains and time constraints of the linear dynamic model (Appendix 4). Calls are made to NONLIN2 to solve the non linear static model and to INTERP to evaluate the steam table data.

2.6 Subroutine LHS, a routine (called by NONLIN2) which defines the non linear static model equations (Appendix 3 with time derivation set to zero).

2.7 Subroutine ZIPE, uses subroutine GAIN to generate the linear dynamic model equations for the reference condition and with perturbed parameter values. The results are printed out in a form suitable for input to the Winfrith pole-zero routine ZIP.

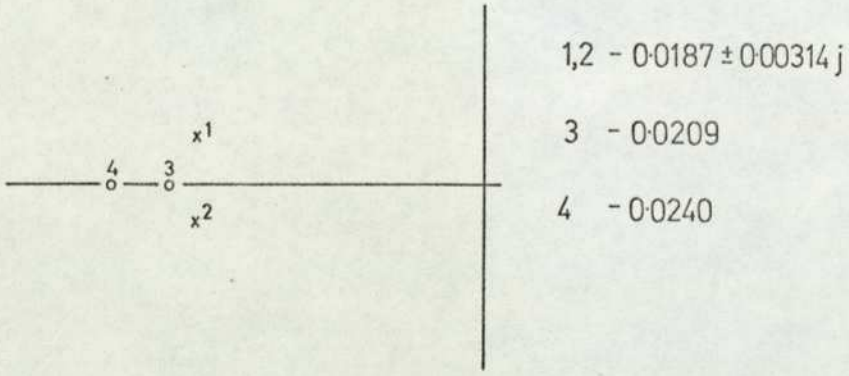
OPTIMAL CONTROL ACTIONS FOR THE S.G.H.W.R.

An insight into the control actions necessary to give a power response with a minimum integral of error may be gained by an analysis using Pontryagin's maximum principle on a simplified model of the reactor. The controls available are the turbine stop valve position y_t, and the moderator valve position y_c. A block diagram of the system is -

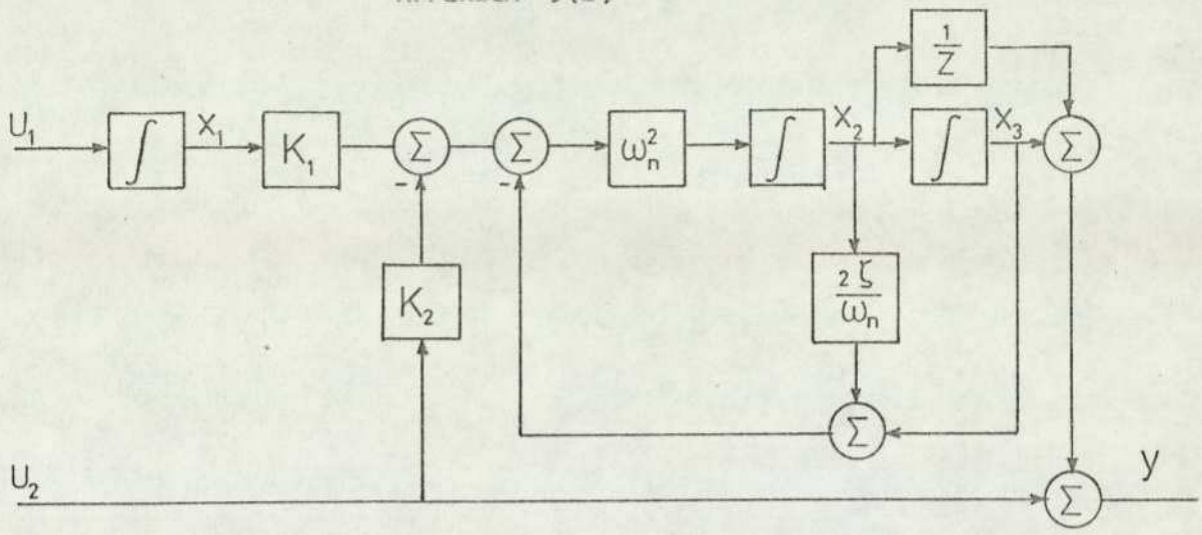


All variables are normalised

The dominant poles and zeroes for the responses of turbine stop valve and control reactivity for the reference design are shown on the diagram below -



Zero 3 refers to the turbine valve transfer function and zero 4 to the control reactivity transfer function. If these two zeroes are represented by a single zero at their mid point, the following block diagram results.



where -

U_1 = moderator control valve position and has a range +1 to -1.

U_2 = turbine stop valve position and has a range 0 to +1.

y = power output of the reactor.

K_1, K_2 = normalised gains, for the reference condition. $K_1 = 0.00282$ and $K_2 = 1.018$

Z = the position of the zero = 0.0222 for the reference condition.

State equations for the reduced system (which predicts power response to within 5% of that given by the complete model at all times, and after 20 seconds errors are virtually zero for step inputs) are then -

$$\dot{x}_1 = U_1$$

$$\dot{x}_2 = w_n^2 \left\{ K_1 x_1 - K_2 U_2 - \frac{2\zeta}{w_n} x_2 - x_3 \right\}$$

$$\dot{x}_3 = x_2$$

$$y = U_2 + x_3 + \frac{1}{Z} x_2$$

For a reactor operating at 75% full power, being asked to supply 100% full power it is assumed that y must be increased from 0 to 1. Following such a demand then the power error will be (1-y). Formulating an optimal control problem in Mayer form then gives -

$$\dot{x}_o = 1-y = 1-U_2 - x_3 - \frac{1}{Z} x_2$$

where x_{oT} is to be minimised.

This will lead to a control action which minimises integral power error, which as shown in section 5.3 minimises the grid frequency error

following a power demand.

The Hamiltonian for the reduced system is then -

$$H = p_o(1-U_2-x_3-\frac{1}{Z}x_2) + p_1U_1+p_2w_n^2\ (K_1x_1-K_2U_2 - \frac{2\zeta}{w_n}x_2-x_3) + p_3x_2$$

i.e.

$$H = p_1U_1 + U_2(-K_2p_2w_n^2 - p_o) + \ .....$$

$$\dot{p}_i = -\frac{\partial H}{\partial x_i}$$

i.e. $\dot{p}_o = 0$ $\qquad p_{oT} = -1$ $\qquad \therefore \quad p_o = -1$

$\dot{p}_1 = -p_2w_n^2 K_1$ $\qquad p_{1T} = 0$

$\dot{p}_2 = \frac{p_o}{Z} + p_2\frac{2\zeta}{w_n} - p_3$ $\qquad p_{2T} = 0$

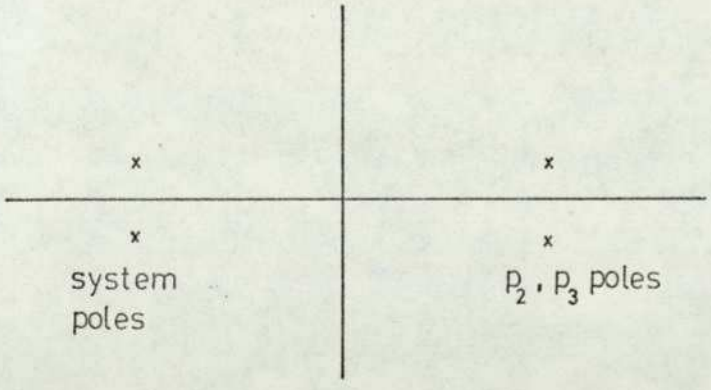
$\dot{p}_3 = p_2w_n^2 + p_o$ $\qquad p_{3T} = 0$

The equations in $\dot{p}_2$ and $\dot{p}_3$ may be combined to give -

$$\ddot{p}_2 - 2\zeta w_n\dot{p}_2 + w_n^2p_2 = 1$$

and $$\ddot{p}_3 - 2\zeta w_n\dot{p}_3 + w_n^2p_3 = 2\zeta w_n - \frac{w_n^2}{Z}$$

The poles of p_2 and p_3 are therefore seen to be reflections in the imaginary axis of the poles of the reduced system -



This applies whether the system is overdamped or oscillatory since no assumption has been made regarding the damping ratio. p_2 then is an expanding sinewave about $\frac{1}{w_n^2}$ —

$$p_2 = \frac{1}{w_n^2} + Ae^{\zeta w_n t} \sin (w_d t + B)$$

where A and B are constants. Boundary conditions are given by $p_{2T} = 0$, and from the equation for $\dot{p}_2$ above $\dot{p}_{2T} = -\frac{1}{Z}$

since $p_o = -1$, $p_{2T} = 0$ and $p_{3T} = 0$. Applying these condition gives -

$$Ae^{\zeta w_n T} \sin (w_d T + B) = -\frac{1}{w_n^2}$$

and $$w_n Ae^{\zeta w_n T}\left\{ \sqrt{1-\zeta^2} \cos (w_d T + B) + \zeta \sin (w_d T + B)\right\} = -\frac{1}{Z}$$

or putting $v = \sin (w_d T + B)$

$$Ae^{\zeta w_n T} v = -\frac{1}{w_n^2}$$

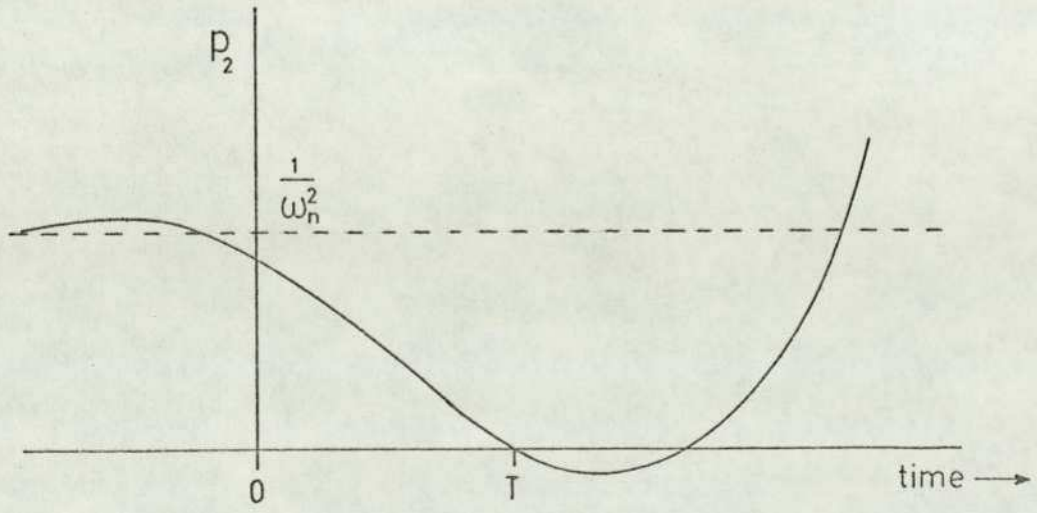
$$w_n Ae^{\zeta w_n T}\left\{ \sqrt{(1-\zeta^2)(1-v^2)} + \zeta v \right\} = -\frac{1}{Z}$$

These equations can be solved for the specific conditions applying to the S.G.H.W.R. reference design, but in order to preserve generality it is sufficient to say -

$$Ae^{\zeta w_n T} \simeq -\frac{1}{w_n^2}$$

$$v \simeq 1$$

p_2 may now be plotted -



For all T occurring before power crossover p_2 is positive and less than $\frac{1}{w_n^2}$ in the range t = 0-T. Referring to the Hamiltonian equation, the coefficient of U_2 is -

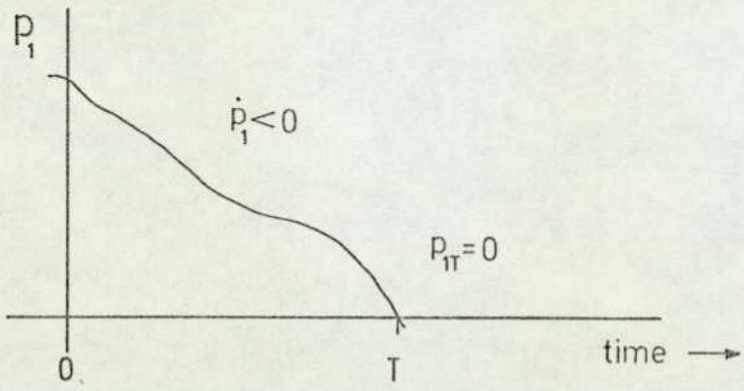
$$- K_2 p_2 w_n^2 - p_o$$

or $$1 - K_2 p_2 w_n^2$$

Since K_2 is only slightly greater than unity, the second term in this expression will always be less than unity for the time range of interest. To maximise the Hamiltonian (minimise x_{oT}) U_2 must be set to +1. p_1 is defined by the expression -

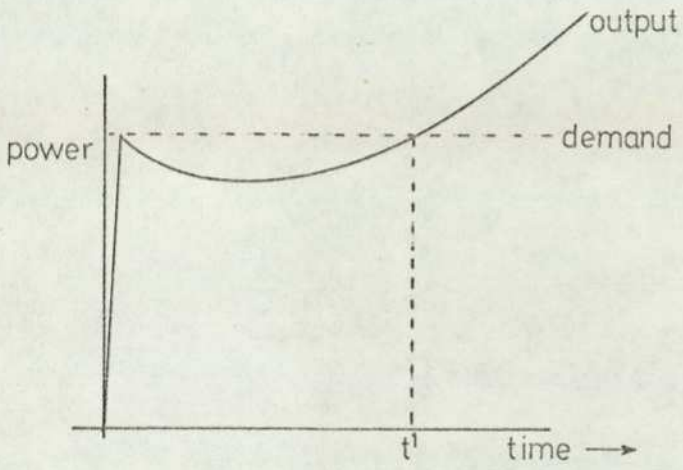
$$p_1 = - p_2 w_n^2 K_1$$

and since p_2 is positive for $t < T$, p_1 has a negative slope in this region. Also $p_{1T} = 0$ and these conditions demand that $p_1 > 0$ for $t < T$.



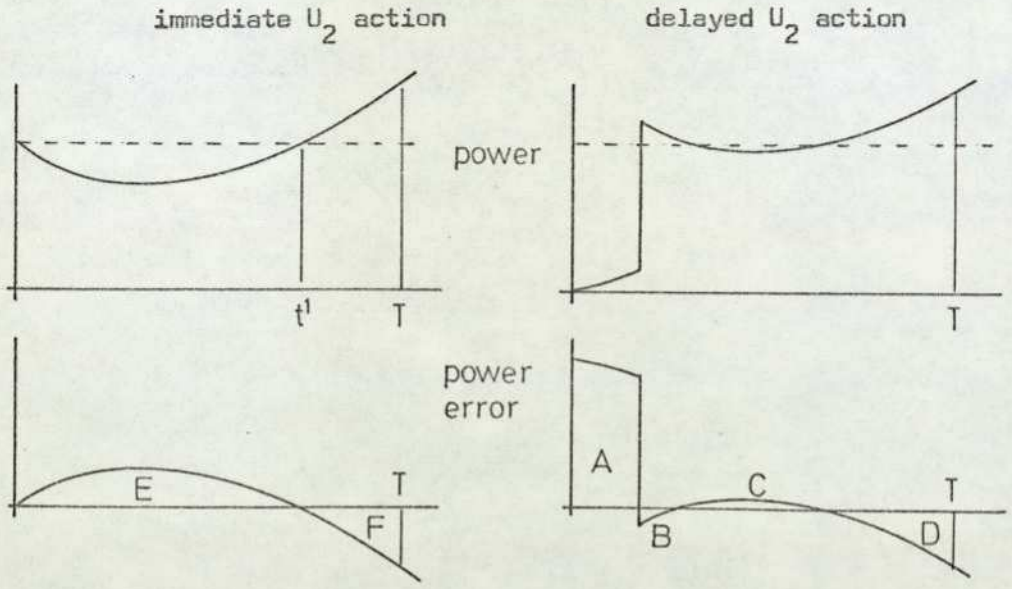
Referring again to the Hamiltonian equation, it may be seen that U_1 must be set to +1 to maximise the Hamiltonian.

For small values of T then the optimal control action is to open the turbine stop valve to its full extent and to insert reactivity at the maximum rate. For large T the analysis is not valid since the integral of error was specified as the performance index. The system will tend to an infinite power surplus as indicated by the following response -



Integral of power deficit will tend to $-\infty$ for $T > t'$

For $T > t^1$ (i.e. after crossover of output and demand) the analysis is invalid. Examination of the p_2 transient for large T would indicate that U_2 (the stop valve position) should not be set to +1 immediately. The reason for this is apparent from examination of transients and error integrals for immediate and delayed U_2 action -



In the delayed action case U_2 is switched to + 1 when $K_2p_2w_n^2$ becomes less than 1. For large T, $K_2p_2w_n^2$ is greater than 1 initially, but as explained above this case is of academic interest only.

$$D + B - A - C > F - E$$

To optimise control action after an excess of power is available it would be necessary to maximise $(1 - y)$ since what effectively is required is a minimum absolute integral of error. If this is attempted, however, the method breaks down as the error integral before crossover is maximised, instead of that after crossover being minimised. The use of integral of absolute error as a performance index overcomes this difficulty, but is not an ideal function since many small positive and negative errors have a cancelling effect on grid frequency change but accumulate in the performance index. An integral of error squared criteria would overcome this to some extent, but then the functional would not be related to grid frequency variations, and the equations become too complicated for analytical solution. Using an integral of absolute error criteria the system equations are -

$$\dot{x}_1 = U_1$$

$$\dot{x}_2 = w_n^2 \left(K_1 x_1 - K_2 U_2 - \frac{2\zeta}{w_n} x_2 - x_3\right)$$

$$\dot{x}_3 = x_2$$

$$\dot{x}_o = \left|1 - U_2 - x_3 - \frac{1}{Z} x_2\right|$$

and it is required to minimise x_{oT}

The Hamiltonian is now

$$= p_o \left|1 - U_2 - x_3 - \frac{1}{Z} x_2\right| + p_1 U_1 + p_2 w_n^2 \left(K_1 x_1 - K_2 U_2 - \frac{2\zeta}{w_n} x_2 - x_3\right) + p_3 x_2$$

and the differential equations in p are -

$$\dot{p}_o = 0 \qquad p_{oT} = -1$$

$$\dot{p}_1 = -K_2 p_2 w_n^2 \qquad p_{1T} = 0$$

$$\dot{p}_2 = \frac{p_o}{Z} \operatorname{sgn}\left(1 - U_2 - x_3 - \frac{1}{Z} x_2\right) + p_2 \frac{2\zeta}{w_n} - p_3 \qquad p_{2T} = 0$$

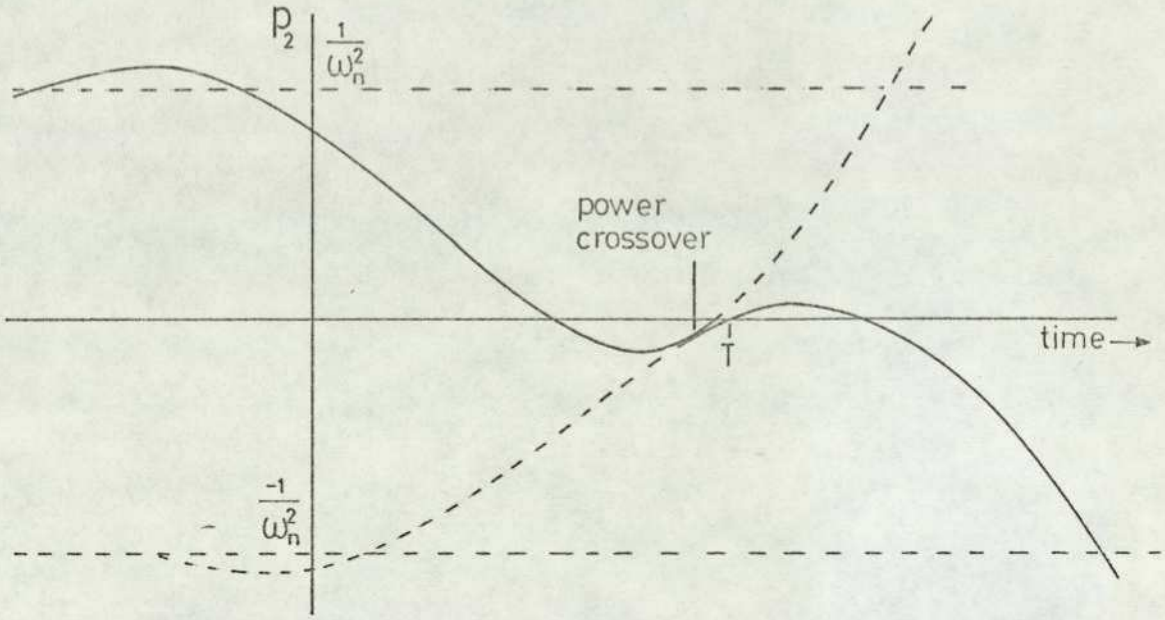
$$\dot{p}_3 = p_o \operatorname{sgn}\left(1 - U_2 - x_3 - \frac{1}{Z} x_2\right) + p_2 w_n^2 \qquad p_{3T} = 0$$

which may be arranged to give -

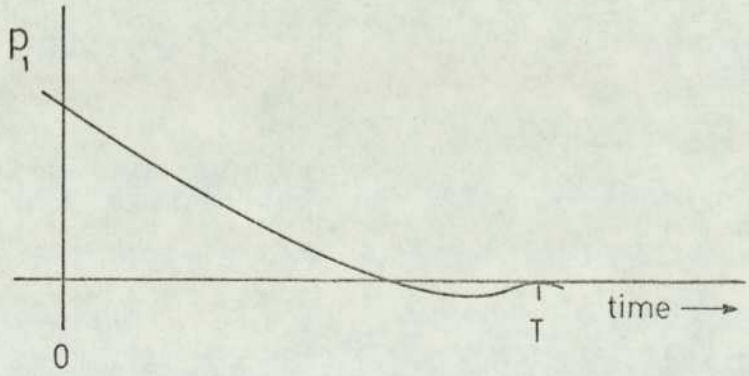
$$\ddot{p}_2 - 2\zeta w_n \dot{p}_2 + p_2 w_n^2 = \operatorname{sgn}\left(1 - U_2 - x_3 - \frac{1}{Z} x_2\right)$$

p_2 is therefore an expanding sinewave as before, but about $\frac{1}{w_n^2}$ or $-\frac{1}{w_n^2}$ depending upon $\operatorname{sgn}\left(1 - U_2 - x_3 - \frac{1}{Z} x_2\right)$ or the sign of

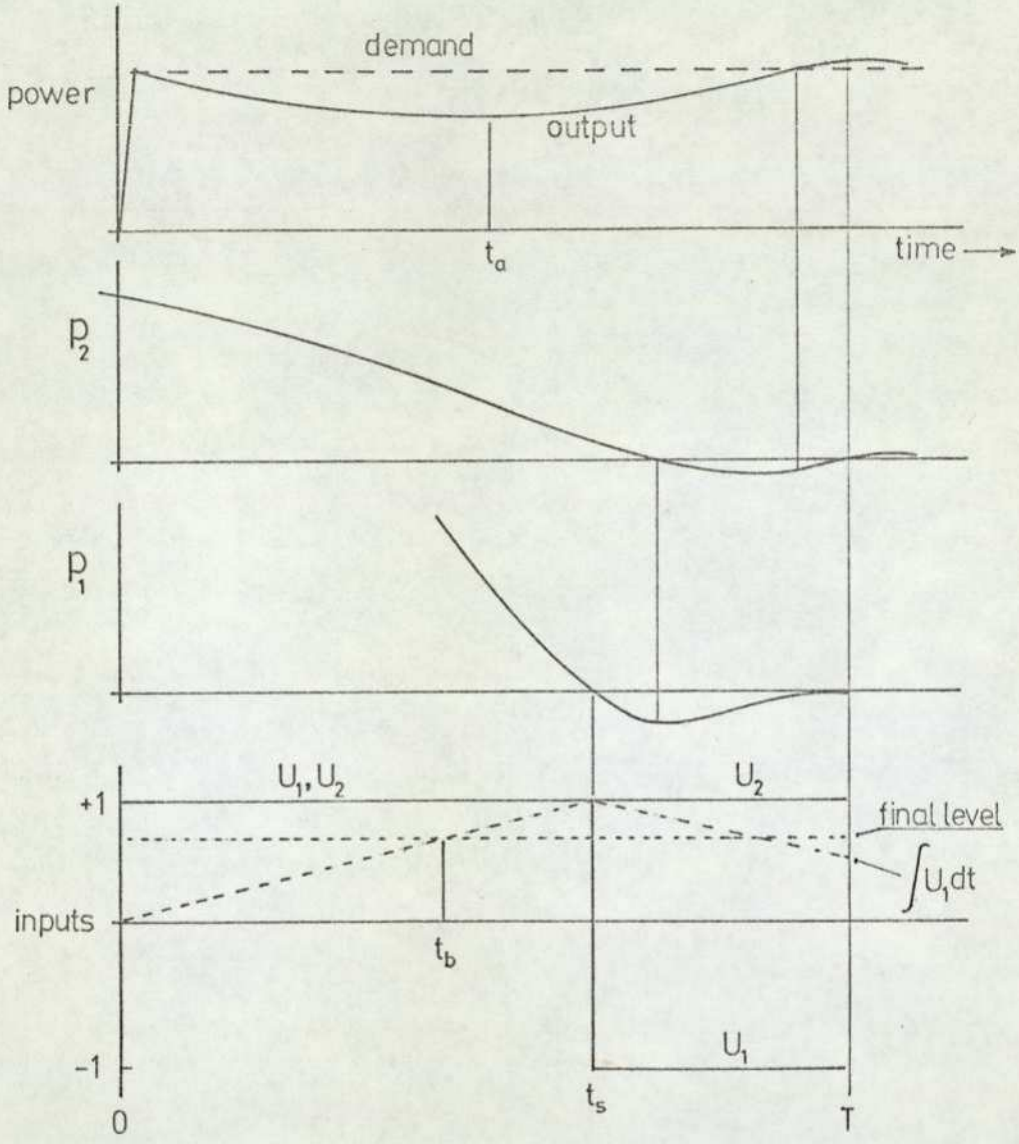
power error. Assuming that T occurs sometime after the first power crossover, p_2 will then be of the form -



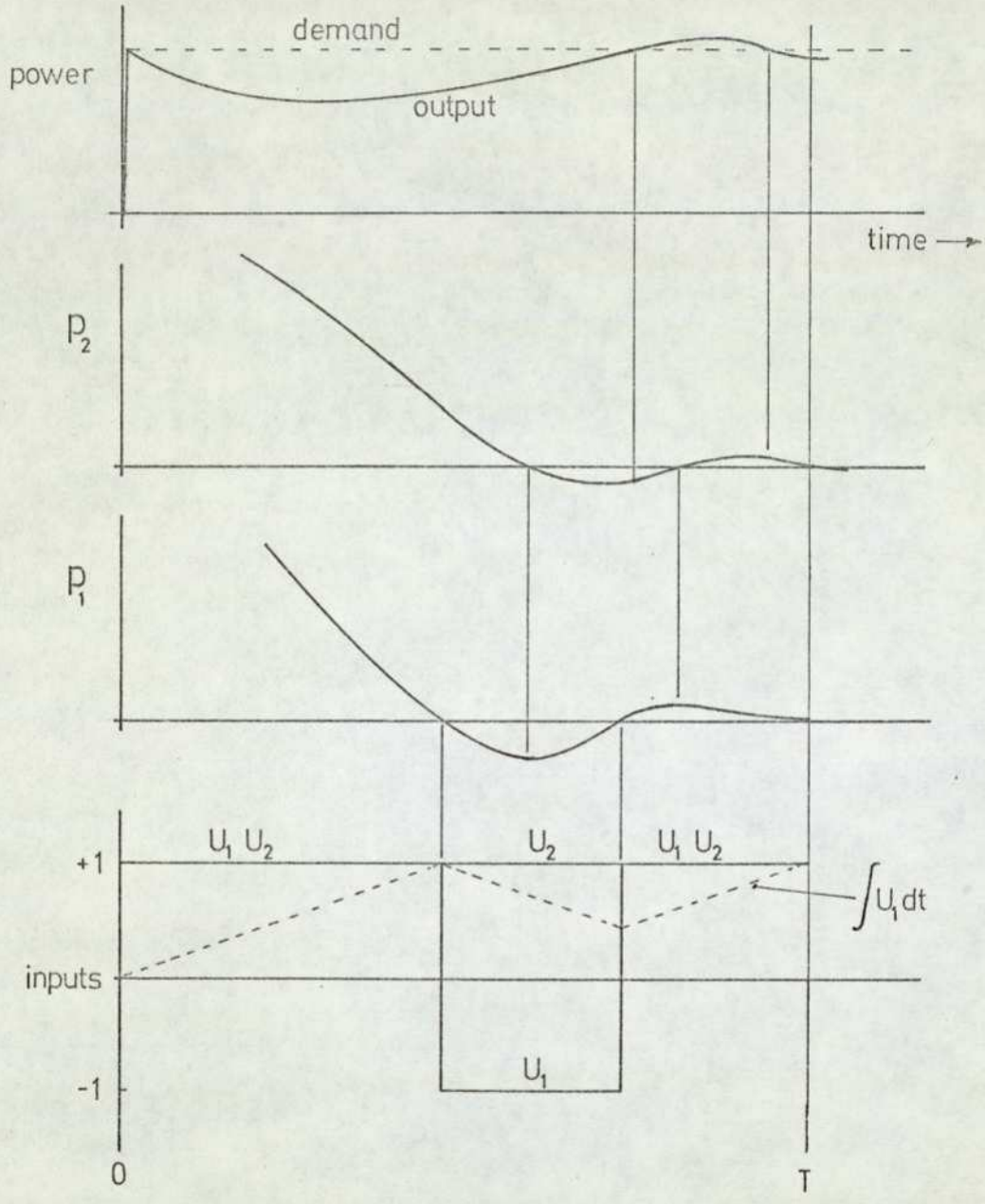
Once again in the range t = 0 - T, p_2 is always less than $\frac{1}{w_n^2}$ and referring to the Hamiltonian this gives U_2 = +1 for a maximum. p_1 is given again by the integral of $-p_2 w_n^2 K_1$ with $p_{1T} = 0$, p_1 is of the form -



indicating that U_1 should be set to +1 initially and switched to -1 at some time during the transient. The set of curves for input, power response, p_1 and p_2 are as follows -



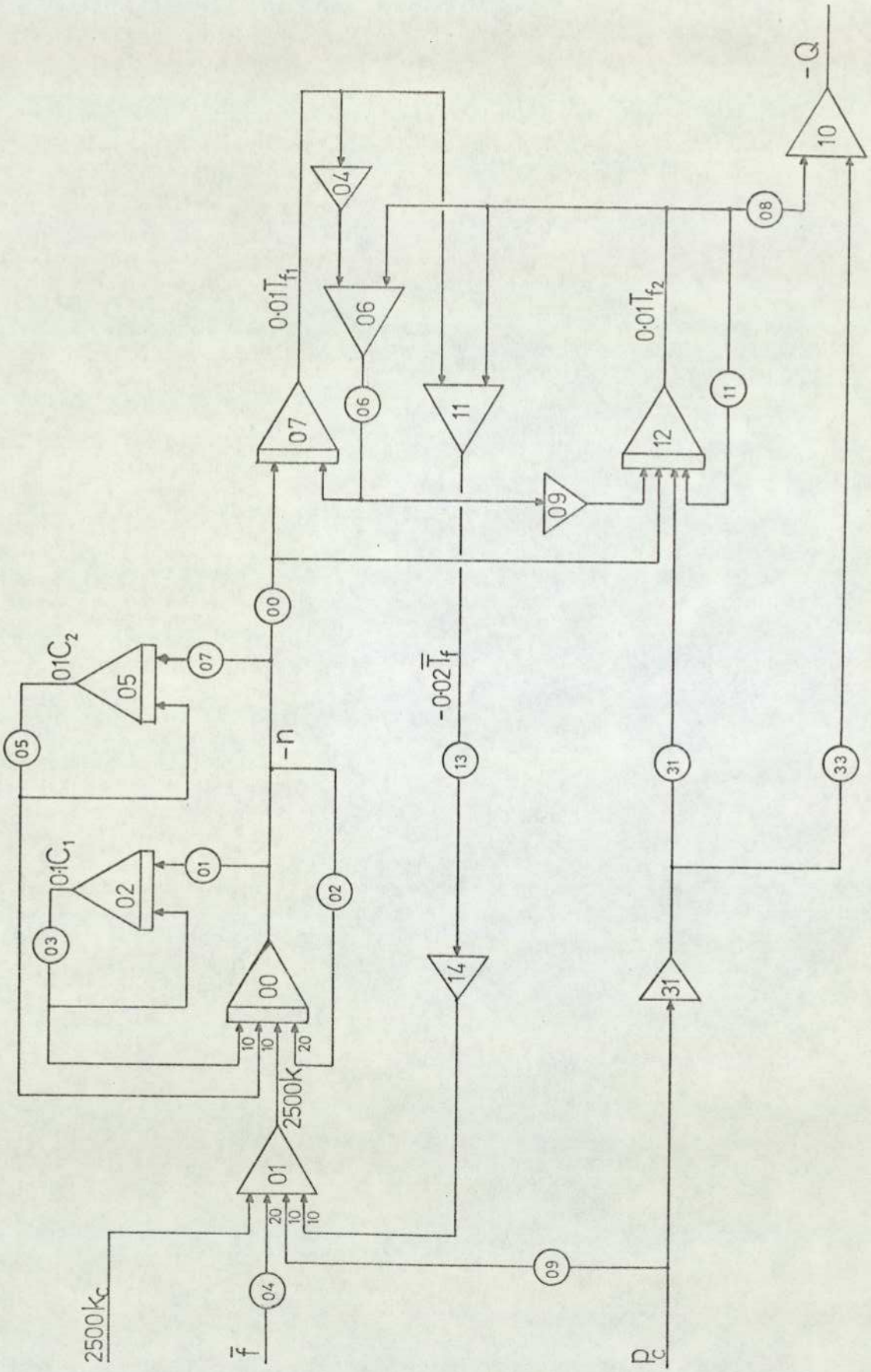
It should be noted that T can occur only slightly beyond the power crossover since the control action initiated to keep power error down will cause a second crossover shortly after the first. Analysis for a larger number of crossovers gives a control action in which U_2 remains at 1 and U_2 switches between +1 and -1. Thus the responses for two power crossovers are-



Referring to the single crossover case, it is found that the switching point for the moderator valve input U_1 occurs somewhat after drum pressure and power recovery, and also after a reactivity level equivalent to the final state power has been reached. These points are referred to by t_a, t_b and t_s on the diagram.

APPENDIX 10 (1)

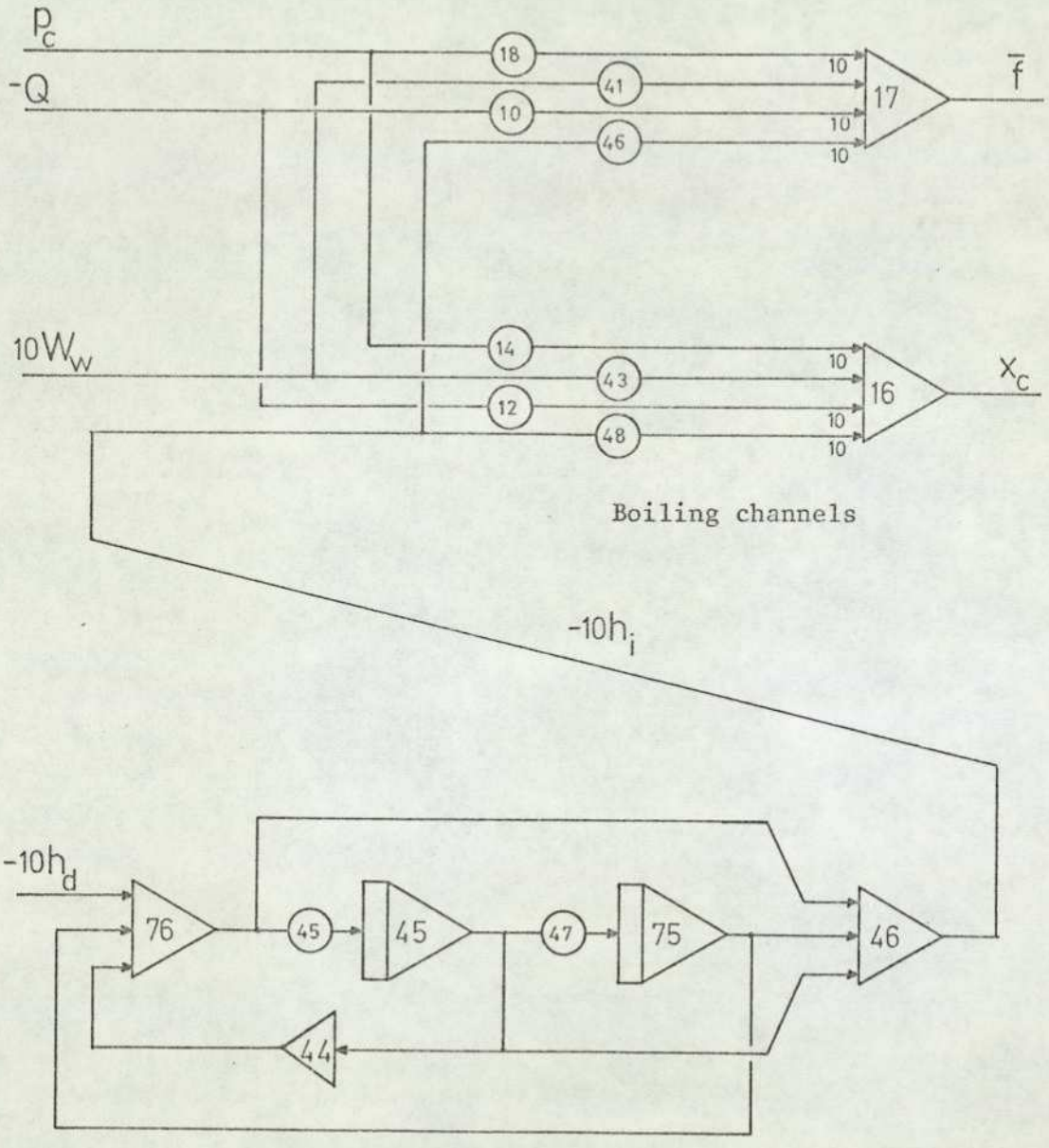
Analog patching diagram for the S.G.H.W.R. linear dynamic model.



Neutronics, Reactivity and Fuel Element

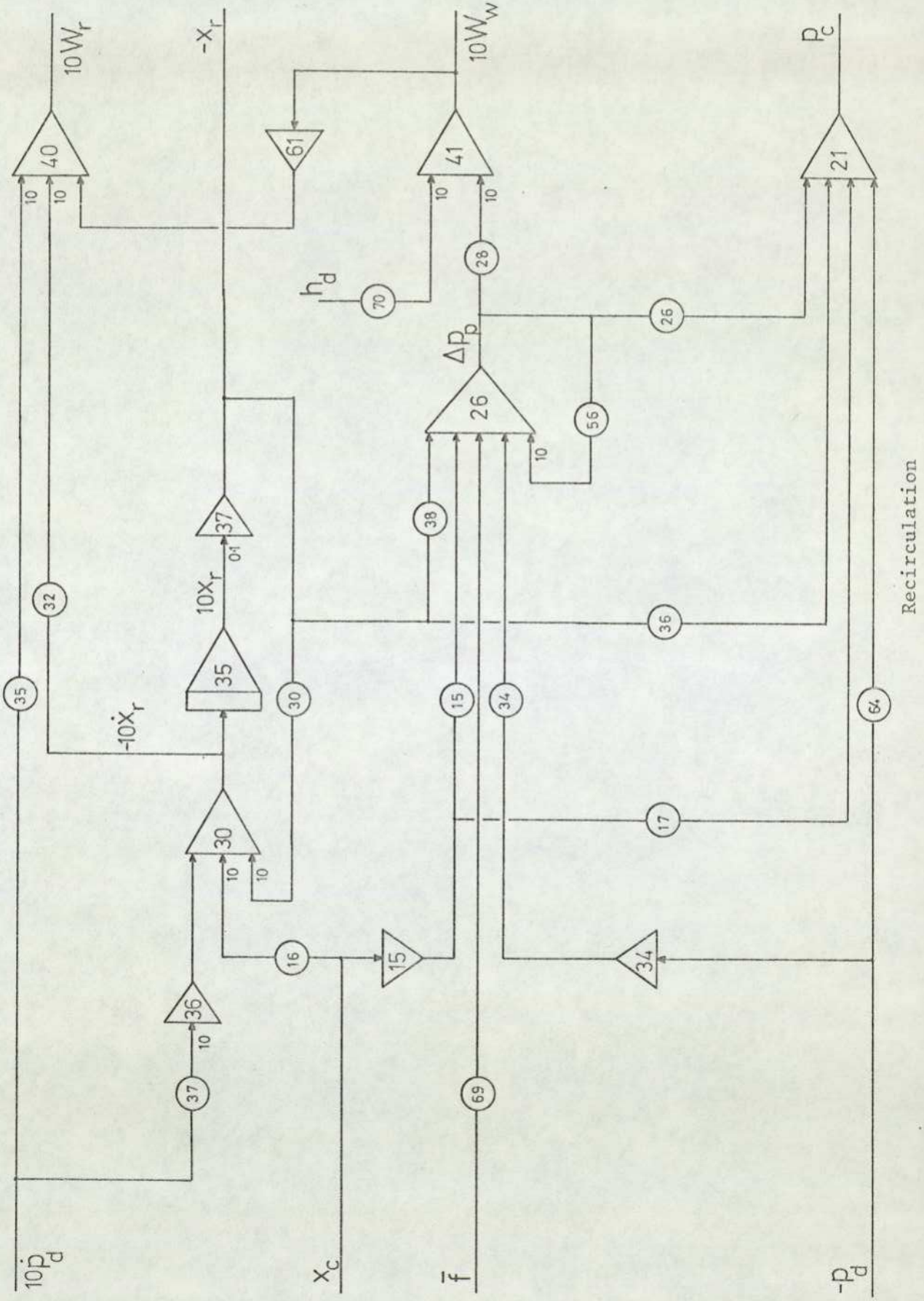
APPENDIX 10 (2)

Analog patching diagram for the S.G.H.W.R. linear dynamic model



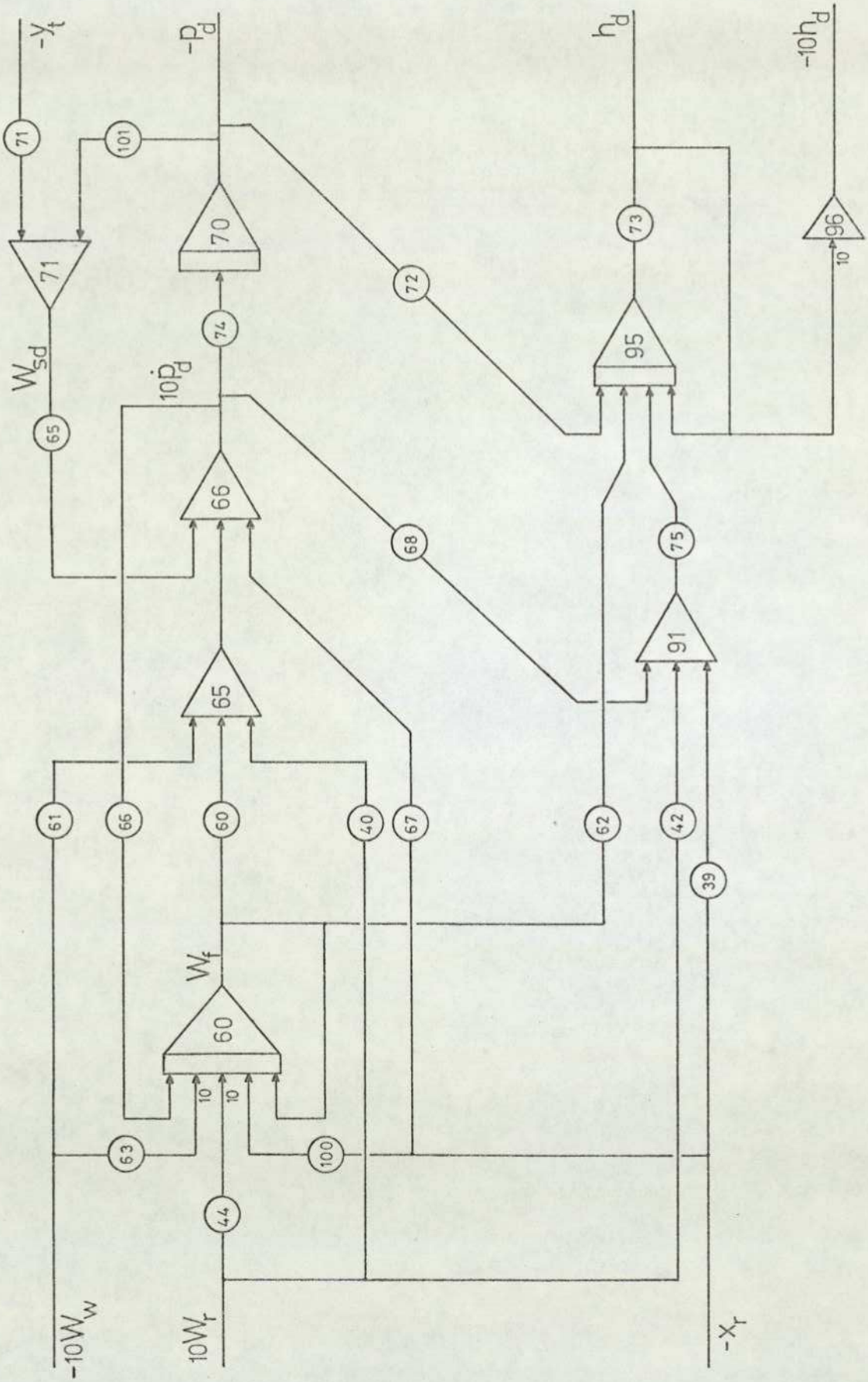
Downcomer Delay

Analog patching diagram for the S.G.H.W.R. linear dynamic model.



APPENDIX 10 (4)

Analog patching diagram for the S.G.H.W.R. linear dynamic model.



Steam Drum, Feedwater Controller and Steam Flow to Turbine

APPENDIX 10 (5)

Analog computer model of the S.G.H.W.R.

Potentiometer coefficients.

No.	Sect.	Derivation	Basic value	Factors N.F.	S.F.	I.G.	Scaled value
0	F	G_6	72.0		0.01		0.72
1	F	G_2	3.9		0.1		0.39
2	F	$\frac{1}{\tau_1}$	13.0			20	0.65
3	F	$\frac{1}{\tau_2}$	0.024				0.024
4	F	$-G_1 G_4$	50.0	$\bar{f}$		20	0.51
5	F	$\frac{1}{\tau_3}$	0.15				0.15
6	F	$\frac{1}{\tau_4}$	0.1284				0.1284
7	F	G_3	9.1		0.1		0.91
8	F	$G_8 G_9$	65.0	$\frac{1}{Q}$	100		0.2425
9	F	$G_1 G_{23} G_{55}$	8.57×10^{-3}	p_c		10	0.837
10	C	$G_{10}(G_{20}-G_{21}) + G_{13} G_{18} G_{22}$	1.17×10^{-5}	$\frac{Q}{\bar{f}}$		10	0.1317
11	F	$\frac{G_8}{\tau_4}$	0.3495				0.3495
12	C	G_{13}	4.4×10^{-6}	$\frac{Q}{x_c}$		10	0.1408
13	F	$-G_1 G_5$	0.0125		100	10	0.125
14	C	G_{16}	2.17×10^{-4}	$\frac{p_c}{x_c}$		10	0.2935
15	R	G_{26}	145.5	$\frac{x_c}{\Delta p_p}$			0.1764
16	R	$\frac{1}{\tau_6}$	0.1792	$\frac{x_c}{x_r}$	10	10	0.1619
17	R	$\frac{G_{26}}{2}$	72.75	$\frac{x_c}{p_c}$			0.0054

APPENDIX 10 (6)

Analog computer model of the S.G.H.W.R.

Potentiometer coefficients.

No.	Sect.	Derivation	Basic value	Factors N.F.	S.F.	I.G.	Scaled value
18	C	$G_{22}(G_{16}G_{18}-G_{19})+G_{12}G_{20}$	1.24×10^{-3}	$\frac{p_c}{\bar{f}}$		10	0.5920
26	R	$G_{32}(G_{28}+0{\cdot}5G_{25})$	0.906	$\frac{\Delta p_p}{p_c}$			0.0553
28	R	$G_{32}G_{36}$	67.1	$\frac{\Delta p_p}{W_w}$	10	10	0.958
30	R	$\frac{1}{\tau_6}$	0.1796		10	10	0.1796
31	F	$\frac{G_8 G_{23}}{\tau_4}$	0.0431	p_c	0.01		0.421
32	R	G_{39}	1.54×10^{5}	$\frac{x_r}{W_r}$		10	0.2942
33	F	$G_8 G_9 G_{23}$	6.89	$\frac{p_c}{Q}$			0.292
34	R	$G_{30}G_{34}+0{\cdot}5G_{17}G_{27}$	2.23×10^{-2}	$\frac{p_d}{\Delta p_p}$			0.3515
35	R	G_{38}	14.39	$\frac{p_d}{W_r}$		10	0.3242
36	R	G_{29}	156.1	$\frac{x_r}{p_c}$			0.0128
37	R	G_{33}	4.75×10^{-4}	$\frac{p_d}{x_r}$		10	0.5590
38	R	G_{29}	156.1	$\frac{x_r}{\Delta p_p}$			0.2096
39	D	G_{49}	13.36	$\frac{x_r}{h_d}$	10		0.0206
40	D	G_{42}	2.08×10^{-2}	$\frac{W_r}{p_d}$			0.0920
41	C	$G_{11}(G_{20}-G_{21})+G_{14}G_{18}G_{22}$	6.5×10^{-5}	$\frac{W_w}{\bar{f}}$	0.1		0.1330
42	D	G_{48}	2.95×10^{-3}	$\frac{W_r}{h_d}$			0.0236
43	C	G_{14}	2.4×10^{-5}	$\frac{W_w}{x_c}$	0.1		0.1386
44	D	G_{40}	0.9199	$\frac{W_r}{W_{fw}}$	0.1	10	0.1146

APPENDIX 10 (7)

Analog computer model of the S.G.H.W.R.

Potentiometer coefficients.

No.	Sect	Derivation	Basic value	Factors N.F.	S.F.	I.G.	Scaled value
45	T	$\frac{6}{\tau_5}$	0.9640				0.9640
46	C	$G_{20}+G_{15}G_{18}G_{22}$	7.14×10^{-3}	$\frac{h_j}{\bar{f}}$	0.1	10	0.1816
47	T	$\frac{2}{\tau_5}$	0.3213				0.3213
48	C	G_{15}	1.53×10^{-3}	$\frac{h_j}{x_c}$	0.1	10	0.1100
56	R	$G_{32}(G_{25}+G_{28}+G_{31})$	1.973			10	0.1973
58							
60	D	G_{45}	7.64×10^{-3}	$\frac{W_{fw}}{P_d}$	10		0.0272
61	D	G_{45}	7.64×10^{-3}	$\frac{W_w}{P_d}$			0.0339
62	D	G_{51}	0.0368	$\frac{W_{fw}}{h_d}$			0.0237
63	D		1.0	$\frac{W_w}{W_{fw}}$	0.1	10	0.1250
64	R	$1+G_{30}G_{34}$	0.984	$\frac{P_d}{P_c}$		10	0.0947
65	D	G_{44}	0.1712	$\frac{W_{sd}}{P_d}$		10	0.6090
66	D	G_{46}	2.643	$\frac{P_d}{W_{fw}}$	0.1		0.7440
67	D	G_{43}	682.9	$\frac{x_r}{P_d}$	10		0.5810
68	D	$G_{46}G_{52}$	0.427	$\frac{P_d}{h_d}$			0.7750
69	R	G_{24}	4.163	$\frac{\bar{f}}{\Delta P_p}$			.0.0142
70	R	$G_{35}G_{37}$	3.535	$\frac{h_d}{W_w}$	10	10	0.4400
71	D	G_{54}	418.1	$\frac{y_t}{W_{sd}}$			1.0

APPENDIX 10 (8)

Analog computer model of the S.G.H.W.R.

Potentiometer coefficients.

No.	Sect	Derivation	Basic value	Factors N.F.	S.F.	I.G.	Scaled value
72	D	G_{47}	0.1455	$\frac{P_d}{h_d}$			0.2635
73	D	$\frac{1}{\tau_7}$	0.1268				0.1268
74	D		1.0		0.1		0.1
75	D		1.0		0.1		0.1
76							
77							
100	D						1.0
101	D						1.0

The column headed sect. indicates the section of the nodel in which the potentiometer occurs as follows:

F neutronics-reactivity-fuel element

C boiling channel

R recirculation

D steam drum

T downcomer time delay

The factors' columns are as follows:

N.F. Normalising factor, given as the ratio of two steady state equilibrium variables.

S.F. Scaling factor

I.G. Input gain of the amplifier following the potentiometer.

Blanks in the factors' columns indicate a value of unity.

APPENDIX 11 (1)

Limits on the estimation of pole or zero shifts by sensitivity coefficients.

Consider the second order system defined by the equations -

$$\begin{bmatrix} \dot{x}_1 \\ \dot{x}_2 \end{bmatrix} = \begin{bmatrix} A_{11} & A_{12} \\ A_{21} & A_{22} \end{bmatrix} \begin{bmatrix} x_1 \\ x_2 \end{bmatrix} \qquad \text{A 11.1}$$

The poles of the system are given by the eigenvalues of the A matrix, i.e. by -

$$\begin{vmatrix} A_{11} - \lambda & A_{12} \\ A_{21} & A_{22} - \lambda \end{vmatrix} = 0 \qquad \text{A 11.2}$$

This will be considered the reference condition with poles λ_{10} and λ_{20} given by -

$$\left.\begin{matrix} \lambda_{10} \\ \lambda_{20} \end{matrix}\right\} = \frac{A_{11} + A_{22}}{2} \pm \frac{\sqrt{(A_{11} + A_{12})^2 - 4(A_{11}A_{12} - A_{12}A_{21})}}{2} \qquad \text{A 11.3}$$

For convenience in the following development the first term of A 11.3 is referred to as the 'real' part and the second term as the 'imaginary' part although it may, in fact, be real.

If a small change δ occurs in one of the diagonal elements of A (say A_{11}) then the system poles are shifted to λ_{11} and λ_{21} given by -

$$\left.\begin{matrix} \lambda_{11} \\ \lambda_{21} \end{matrix}\right\} = \frac{A_{11} + \delta + A_{22}}{2} \pm \frac{\sqrt{(A_{11} + \delta + A_{22})^2 - 4(A_{22}(A_{11}+\delta) - A_{12}A_{21})}}{2} \qquad \text{A 11.4}$$

$$= \frac{\lambda_{10} + \lambda_{20} + \delta}{2} \pm \frac{\sqrt{(\lambda_{10} - \lambda_{20})^2 + 2\delta(A_{11} - A_{22}) + \delta^2}}{2} \qquad \text{A 11.5}$$

$$= \frac{\lambda_{10} + \lambda_{20} + \delta}{2} \pm \frac{\lambda_{10} - \lambda_{20}}{2} \sqrt{1 + \frac{2\delta(A_{11} - A_{22})}{(\lambda_{10} - \lambda_{20})^2} + \frac{\delta^2}{(\lambda_{10} - \lambda_{20})^2}} \qquad \text{A 11.6}$$

Binomial expansion of the square-rooted term gives -

$$\left.\begin{matrix} \lambda_{11} \\ \lambda_{21} \end{matrix}\right\} = \frac{\lambda_{10} + \lambda_{20} + \delta}{2} \pm \frac{\lambda_{10} - \lambda_{20}}{2} \left\{ 1 + \left[\frac{\delta(A_{11} - A_{22})}{(\lambda_{10} - \lambda_{20})^2} + \frac{\delta^2}{2(\lambda_{10} - \lambda_{20})^2} \right] - \right. \qquad \text{A 11.7}$$

$$\left.\frac{1}{2}\left[\quad\right]^2 + \frac{1}{4}\left[\quad\right]^3 \text{-------}\right\} \qquad \text{A 11.7 (cont.}$$

A 11.8

$$\left.\begin{matrix}\lambda_{11}\\ \lambda_{21}\end{matrix}\right\} = \left.\begin{matrix}\lambda_{10}\\ \lambda_{20}\end{matrix}\right\} + \frac{\delta}{2} \pm \frac{\lambda_{10}-\lambda_{20}}{2}\left\{\frac{(A_{11}-A_{22})\delta}{(\lambda_{10}-\lambda_{20})^2} + \frac{\delta^2}{2(\lambda_{10}-\lambda_{20})^2}\right.$$

$$\left. - \frac{(A_{11}-A_{12})^2\delta^2}{2(\lambda_{10}-\lambda_{20})^4} + \text{--------}\right\}$$

Terms following the $\pm$ sign in equation A 11.8 are all imaginary if the reference poles are complex as the denominators of all terms within brackets contain $(\lambda_{10}-\lambda_{20})^n$ where n is even. From equation A 11.8 it may be seen that the 'real' parts of the poles shift linearly with the diagonal matrix elements, whereas the 'imaginary' shift (the part following the $\pm$ sign) is a power series in δ. The sensitivity coefficients are defined as the relative shift of a pole divided by the relative change of a matrix element. For the present case the relative change of the matrix element is -

$$\Delta = \frac{\delta}{A_{11}} \qquad \text{A 11.9}$$

and the relative imaginary pole shift comes from the first term within the brackets of equation A 11.8, and is -

$$\frac{(A_{11} - A_{22})\delta}{(\lambda_{10}-\lambda_{20})^2} \qquad \text{A 11.10}$$

The sensitivity coefficient for imaginary pole shift due to a change in A_{11} is then -

$$S = \frac{A_{11}(A_{11}-A_{22})}{(\lambda_{10}-\lambda_{20})^2} \qquad \text{A11.11}$$

The imaginary pole shift $\delta\lambda_i$ from equation A 11.8 may be expressed in terms of the relative matrix element shift by substituting from A 11.9 -

A 11.12

$$\delta\lambda_i = \pm \frac{\lambda_{10}-\lambda_{20}}{2}\left\{\frac{A_{11}(A_{11}-A_{22})}{(\lambda_{10}-\lambda_{20})^2}\Delta + \right.$$

$$\left.\frac{A_{11}^2\Delta^2}{2(\lambda_{10}-\lambda_{20})^2} - \frac{A_{11}^2(A_{11}-A_{22})^2\Delta^2}{2(\lambda_{10}-\lambda_{20})^4} + \text{-------}\right\}$$

The term preceding the brackets is the reference value of the imaginary pole position. Sensitivity coefficients may be introduced into A 11.12 from A 11.11 to give -

A 11.13

$$\delta\lambda_i = \pm \frac{\lambda_{10} - \lambda_{20}}{2} \left\{ s\Delta + \frac{A_{11}^2 \Delta^2}{2(\lambda_{10}-\lambda_{20})} - \frac{s^2\Delta^2}{2} + \cdots\cdots \right\}$$

The second order term in the power series defining the imaginary pole shift is then -

$$\frac{s^2\Delta^2}{2} \left\{ \frac{A_{11}^2}{s^2(\lambda_{10}-\lambda_{20})^2} - 1 \right\} \qquad \text{A 11.14}$$

Which is appreciable only when the relative linear imaginary pole shift ($s\Delta$) is not substantially less than unity (if $[\lambda_{10}-\lambda_{20}] \rightarrow 0$, then $s^2 \rightarrow \infty$ at a faster rate - see equation A 11.11).

For a change δ in an off diagonal element A_{12} a similar binomial expansion leads to an expression for the shifted pole positions as -

A 11.15

$$\left.\begin{matrix}\lambda_{11}\\ \lambda_{21}\end{matrix}\right\} = \left.\begin{matrix}\lambda_{10}\\ \lambda_{20}\end{matrix}\right\} \pm \frac{\lambda_{10}-\lambda_{20}}{2} \left\{ -\frac{2A_{21}\delta}{(\lambda_{10}-\lambda_{20})^2} + \frac{2A_{21}^2\delta^2}{(\lambda_{10}-\lambda_{20})^4} + \cdots\cdots \right\}$$

In this case the real pole positions are unaffected and other terms are imaginary if reference poles are complex as in the diagonal element case. The sensitivity coefficient from off diagonal element to imaginary pole shift is given as before -

$$s = -\frac{2A_{12}A_{21}}{(\lambda_{10}-\lambda_{20})^2} \qquad \text{A 11.16}$$

and the imaginary pole shift is given by -

$$\delta\lambda_i = \pm \frac{\lambda_{10}-\lambda_{20}}{2} \left\{ s\Delta - \frac{s^2\Delta^2}{2} + \cdots\cdots \right\} \qquad \text{A 11.17}$$

Once again the second order contribution is not significant if the linear relative shift is substantially less than unity. Equations A 11.14 and A 11.17 show the effect of second total derivatives on shifted pole accuracy, similar binomial expansions may be used to show that second partial derivative terms are also insignificant if linear pole shifts are kept small. The second order effects may be alternatively analysed with similar results by a Taylor expansion of equation A 11.3 with respect to the matrix elements.

It will be noted that sensitivity coefficients become very large as the 'imaginary' part of the reference poles approaches zero, i.e. the poles become coincident, equations A11.11 and A 11.16 (the sensitivity of the absolute shift also becomes large and the effect is only in part due to the zero reference value). Sensitivity coefficients also change rapidly in this region, which means that only small shifts may be made before the linearity constraints are violated.

Analytical treatment of pole shift errors is not possible for higher order systems, as poles cannot be explicitly expressed in terms of the matrix elements. In applying the sensitivy method to larger systems one has to rely on experience which indicates that the same general rules apply, i.e. that errors are small so long as relative shifts are restricted and that sensitivity coefficients are large and changeable when a complex pair becomes two real poles. Errors may be larger than indicated if several matrix elements are changed such that first order effects cancel and higher order effects accumulate.

The matrix element to pole error is only part of the problem, since matrix elements are not necessarily linear functions of the design parameters. Limits here are imposed by conventional linearisation considerations, which again in general conclude that errors are small if changes are small.

APPENDIX 12

Nuclear properties of materials used in the S.G.H.W.R.

Material	Symbol	Neutron Cross Sections Barns			Logarithmic energy decrement per collision	No.of atoms per cc $\times 10^{-24}$
		Thermal Absorption	Scattering			
			Thermal	Average		
		σ_a	σ_{st}	σ_{se}	ξ	N
Hydrogen	H	0.332	38	20.4	1.0	
Deuterium	D	0.00046	7.0	3.4	0.7261	
Oxygen	O	0.00019	4.2	3.75	0.1209	
Aluminium	Al	0.230	1.4	1.4	0.0730	0.0603
Zirconium	Zr	0.180	8.0	6.2	0.0220	0.0425
Boron	B	755.0	4.0	3.7	0.1756	0.1411
Xenon	Xe_{135}	2.7×10^6	4.3		0.0153	
Uranium	U_{235}	694	8.3		0.0084	0.0473
	U_{238}	2.73	8.3		0.0084	0.0473

Where no atomic weight is specified, the figures are for the naturally occuring distribution of isotopes.

The average scattering cross section σ_{se} is an effective value for neutrons being slowed from high to thermal energies.